



HAL
open science

Hybrid voxels 4D printing based on topologically interlocked multi-material assembly

Kheira Benyahia

► **To cite this version:**

Kheira Benyahia. Hybrid voxels 4D printing based on topologically interlocked multi-material assembly. Other. Université Bourgogne Franche-Comté, 2023. English. NNT : 2023UBFCA026 . tel-04587593

HAL Id: tel-04587593

<https://theses.hal.science/tel-04587593>

Submitted on 24 May 2024

HAL is a multi-disciplinary open access archive for the deposit and dissemination of scientific research documents, whether they are published or not. The documents may come from teaching and research institutions in France or abroad, or from public or private research centers.

L'archive ouverte pluridisciplinaire **HAL**, est destinée au dépôt et à la diffusion de documents scientifiques de niveau recherche, publiés ou non, émanant des établissements d'enseignement et de recherche français ou étrangers, des laboratoires publics ou privés.



THÈSE DE DOCTORAT DE L'ÉTABLISSEMENT UNIVERSITÉ BOURGOGNE FRANCHE-COMTÉ
PRÉPARÉE À L'UNIVERSITÉ DE TECHNOLOGIE DE BELFORT-MONTBÉLIARD

École doctorale n°37

SPIM - Sciences Pour l'Ingénieur et Microtechniques

Doctorat en Sciences pour l'Ingénieur

**Hybrid Voxels 4D Printing Based On Topologically Interlocked Multi-Material
Assembly**

présentée et soutenue publiquement à Sevenans, France, le "21/12/2023"

par

Mme. Kheira BENYAHIA

Ingénieure en Matériaux et Structures pour l'Aéronautique et le Spatial UPS3

devant le jury composé de :

Président de jury:	Prof. Gaël CHEVALLIER	Université de Franche-Comté
Rapporteurs :	Prof. Jean-Philippe PERNOT	Arts et Métiers Aix-en-Provence
	Dr. Pierre-Jean COTTINET	INSA Lyon
Examineurs :	Prof. Olivier KERBRAT	École Normale supérieure de Rennes
	Prof. H. Jerry QI	Georgia Institute of Technology
Directeur de thèse :	Prof. Frédéric DEMOLY	Université de Technologie de Belfort-Montbéliard
Encadrant :	Prof. Samuel GOMES	Université de Technologie de Belfort-Montbéliard
Co-Encadrant :	Dr. Jean-Claude ANDRÉ	Université de Lorraine

To my tiny little baby Kye... Because we wrote this thesis together...

سيرني ببطء، يا حياة! لكي أراك بِكاملِ النقْصانِ
وكلّما أدركت سرّاً منطقت بقسوة: ما أجهلاً!

Translation: “Walk slowly, Ô life! So that I can see you with all your missing laws, and whenever I grasped one of your secrets, you would starkly say how ignorant I am!”.

By Mahmoud DERWICH

Remerciements

*"Gratitude is not only the greatest of virtues, but
the parent of all others."*

- Marcus Tullius Cicero -

In embarking on this academic endeavor, the journey was marked not only by intellectual growth but also by the invaluable support of those who played instrumental roles in shaping this thesis. I extend my sincere gratitude to the individuals and institutions whose contributions have made this scholarly pursuit possible.

First of all, I express my heartfelt gratitude to my thesis advisor, Prof. Frédéric Demoly, Professor at the Université de Technologie Belfort-Montbéliard (UTBM) and Director of the Interdisciplinary Carnot de Bourgogne Research Laboratory - Conception Optimization and Modeling in Mechanics (ICB-COMM). His unwavering support throughout these three years and his commitment to pushing people around him to become the best version of themselves have been instrumental in my research journey. I am also thankful for the considerable time he dedicated to me. His energy and confidence served as driving forces for my growth.

I extend my sincere appreciation to my colleague, Hichem Seriket, whose continuous assistance significantly contributed to the depth of this research. I am grateful not only for his professional support but also for his genuine friendship and positive energy.

Warm thanks go to my co-advisors, Prof. Samuel Gomes (UTBM) and Prof. Emérite Jean-Claude André (University of Lorraine), a CNRS research director. Their guidance and valuable advice, though few in number, were rich in quality.

I acknowledge the members of my thesis jury: Prof. Gaël Chevallier (Université de Franche-Comté), Prof. Jean-Philippe Pernot (Arts et Métiers Aix-en-Provence), Dr. Pierre-Jean Cottinet (INSA Lyon), Prof. Olivier Kerbrat (École Normale Supérieure de Rennes), and Prof. H. Jerry Qi (Georgia Institute of Technology) for accepting the responsibility of evaluating my work.

Special thanks are due to my colleagues and friends who made the years of working together enjoyable: Monzer, Hadrien, Louise, Luca, Laura, Fattah, Darshan, Thomas, Judice, Garcia, Pushkar, Aswin, as well as Sophie and Philippe from the COMM laboratory. I also express gratitude to the French 'Investissements d'Avenir' program and the EUR-EIPHI Graduate School (contract ANR-17-EURE-0002) for funding this thesis over three years.

To my cherished family—my mom, my husband, my sister, and my brothers—your unconditional love and precious support were a pillar throughout this journey. A special note of admiration for my mother, who sacrificed significantly while raising five children all on her own.

Abstract

4D printing is considered a disruptive manufacturing technology for creating innovative devices able to evolve in their usage environment. By coupling additive manufacturing (AM) processes and active/passive materials, objects can change properties, shapes, or even functionalities under the effect of an energy stimulation. To achieve a desired shape-change, recent advances in computational design around digital materials require tackling multi-material 4D printing. However, the deposition of active and passive materials in a single run remains difficult due to the limited compatibility of existing printers with smart materials (SMs) possessing the necessary properties. To overcome this limitation in the context of complex materials distributions, an original approach is to address multi-material 4D printing from the perspective of interlocking blocks assembly. These types of assemblies have gone through a long journey of evolution and attracted various applications. They have been investigated as a solution to the assembly challenges of large and complex parts. Therefore, the main objective of this thesis is to propose a computational design approach that converts a multi-material 4D object with a computed digital materials distribution into suitable interlocking blocks. The latter can be printed separately using single material AM and then assembled to achieve the targeted shape change. This thesis will unfold in three major contributions. First and foremost, a contribution will cover the sequence of steps used to develop the interlocking assembly generation algorithm. Moving on, another proposed contribution will deepen the approach of interlocking blocks assembly by investigating their effect on the behavior of multi-material 4D printed structures, the study in focus will compare structures printed in a single run versus interlocking ones. Mechanical/stimulation tests and numerical simulations will be conducted to demonstrate that interlocking structures exhibit relevant mechanical performance while enhancing better actuation response than multi-material structures within a single print. A final contribution will be dedicated to generalizing the applicability of the interlocking blocks assembly approach by improving the uniformity of shape/property changes in a 4D multi-material interlocked structure. Besides, this contribution also aims at addressing limitations that can occur due to the interlocking blocks' interfaces such as lack of deformation and contact continuity. Thus, it will be a question of proposing customized interlocking blocks concept that takes into account SMs and their potential transformations. In order to highlight their relevance and practical use, case studies will be included alongside the proposed contributions.

Keywords: Design for AM, interlocking assemblies, 4D printing, smart materials, assembly characterization

Résumé

L'impression 4D est considérée comme une technologie de fabrication prometteuse pour créer des dispositifs innovants capables d'évoluer dans leur environnement d'utilisation. En couplant les processus de fabrication additive (FA) avec des matériaux actifs/passifs, les objets peuvent changer de propriétés, de formes ou même de fonctionnalités sous l'effet d'une énergie de stimulation. Pour réaliser un changement de forme souhaité, les récents progrès en conception informatique autour des matériaux numériques nécessitent de s'attaquer à l'impression 4D multi-matériaux. Cependant, la déposition de matériaux actifs et passifs en une seule structure reste difficile en raison de la compatibilité limitée des imprimantes existantes avec les matériaux intelligents possédant les propriétés nécessaires. Pour surmonter cette limitation dans le contexte de la distribution de matériaux complexe, une approche originale consiste à aborder l'impression 4D multi-matériaux du point de vue de l'assemblage de blocs imbriqués. Ces types d'assemblages ont parcouru un long chemin d'évolution et ont suscité diverses applications. Ils ont été étudiés comme une solution aux défis d'assemblage des pièces grandes et complexes. Par conséquent, l'objectif principal de cette thèse est de proposer une approche de conception informatique qui transforme un objet 4D multi-matériaux avec une distribution de matériaux numériques calculée en blocs imbriqués appropriés. Ces derniers peuvent être imprimés séparément en utilisant la FA à matériau unique, puis assemblés pour atteindre le changement de forme ciblé. Cette thèse se déroulera en trois contributions majeures. Tout d'abord, une contribution couvrira la séquence des étapes utilisées pour développer l'algorithme de génération d'assemblage imbriqué. Ensuite, une autre contribution proposée approfondira l'approche de l'assemblage de blocs imbriqués en étudiant leur effet sur le comportement des structures imprimées en 4D multi-matériaux. L'étude en question comparera les structures imprimées en une seule opération à celles qui sont imbriquées. Des tests mécaniques/de stimulation et des simulations numériques seront effectués pour démontrer que les structures imbriquées présentent des performances mécaniques pertinentes tout en améliorant la réponse à l'activation par rapport aux structures multi-matériaux imprimées en une seule fois. Une contribution finale sera consacrée à la généralisation de l'applicabilité de l'approche d'assemblage de blocs imbriqués en améliorant l'uniformité des changements de forme/de propriété dans une structure 4D multi-matériaux assemblée. De plus, cette contribution vise également à résoudre les limitations qui peuvent survenir en raison des interfaces des blocs imbriqués, telles que le manque de continuité du contact et de déformation. Ainsi, il s'agira de proposer un concept de blocs imbriqués personnalisés prenant en compte les matériaux actifs et leurs transformations potentielles. Pour souligner leur pertinence et leur utilisation pratique, des cas d'études seront inclus en parallèle des contributions proposées.

Mots-clés :

Conception pour FA, assemblage entremêlés, impression 4D, matériaux intelligents, caractérisation des assemblages.

Table of Contents

Remerciements.....	vii
Abstract.....	ix
Résumé	xi
Table of Contents.....	xiii
List of Figures	xvii
List of Tables	xxiii
List of Acronyms.....	xxv
Chapter 1: Introduction and Research Context	1
1.1. Introduction	3
1.2. Evolution In Mankind Craft and Manufacturing Processes	3
1.3. Evolution In Objects Capabilities.....	6
1.4. 4D Printing Origins	8
1.4.1. Additive Manufacturing/3D Printing	9
1.4.2. Smart Materials	11
1.4.3. Brief Introduction To 4D Printing	12
1.5. General Context for This Ph.D.....	15
1.6. Motivations & Objectives	18
1.7. Thesis Structure.....	22
Chapter 2: State of the Art and Related Scientific Questions	25
2.1. Preface.....	27
2.2. 4D Printing	27
2.2.1. Related Additive Manufacturing Technologies	29
2.2.2. Smart Materials	33
2.2.3. Stimuli	36
2.2.4. Materials Distribution and Transformations Classification.....	40
2.2.5. Applications.....	45
2.3. Research in Design.....	47
2.3.1. Design for Additive Manufacturing.....	47
2.3.2. Design for 4D Printing	48
2.4. Evolution in Assemblies/Interlocking Assemblies	53
2.5. Key Research Question	56
Chapter 3: A Computational Design Approach For Multi-material 4D Printing Based On Interlocking Blocks Assembly	59
3.1. Introduction	61
3.2. Computational Design Approach for Multi-material 4D Printing.....	62
3.2.1. Digital Material partitioning (step 1 of Figure 39).....	63

3.2.2. Blocking Relations Modeling (step 2 of Figure 39).....	64
3.2.3. Interlocking Blocks Assembly Computation (step 3 of Figure 39).....	66
3.2.4. Interlocking Parts Assembly Planning (step 4 of Figure 39).....	72
3.3. Results & discussion	75
3.3.1. Interlocking Assembly Computation Add-on.....	77
3.3.2. Simulation	77
3.4. Conclusion.....	81
Chapter 4: Influence of Interlocking Blocks Assembly on the Actuation Time, Shape Change, and Reversibility of Voxel-Based Multi-Material 4D Structures.....	83
4.1. Introduction	85
4.2. Materials and Methods	86
4.2.1. Materials.....	86
4.2.2. Printing Parameters	86
4.2.3. Interlocking Assembly Generation.....	87
4.2.4. Test Before Stimulation.....	89
4.2.5. Test under Stimulation.....	90
4.3. Results & Discussion.....	92
4.3.1. Analysis Before Actuation.....	93
4.3.2. Actuation Performance.....	94
4.4. Conclusion.....	102
Chapter 5: A Customized Interlocking Assembly blocks for Improved Multi-Material 4D Printing Structures Performances	105
5.1. Introduction	107
5.2. Materials & Methods.....	109
5.2.1. Materials.....	109
5.2.2. Printing parameters.....	110
5.2.3. Interlocking assembly generation approaches.....	110
5.2.4. Assembly stability	114
5.2.5. Actuation simulation	114
5.2.6. Actuation process	114
5.3. Results & Discussion.....	115
5.3.1. Interlocking assembly generation with customized interlocking blocks results	115
5.3.2. Assembly stability	117
5.3.3. Actuation simulation	120
5.3.4. Actuation process	124
5.4. Conclusion.....	126
Chapter 6: Conclusions and Perspectives	129
6.1. Conclusions	131

6.2. Perspectives	132
Research Work Publications	135
References	137

List of Figures

Figure 1: Industry revolutions through the time [7]	6
Figure 2 : Example of convertible objects from antiquity vs. today, (a) an ancient roman Triclinium, (b) a multi-configuration chair.	7
Figure 3 : Heat-Sensitive wall. It changes its color when exposed to heat. People can draw figures using their warm bodies temperature.	8
Figure 4 : Le Méhauté on the left & J.C. André on the right with 3D printed objects	9
Figure 5: 3D printed metallic parts with complex geometries.	10
Figure 6: Generic process main steps of 3D Printing technology	10
Figure 7: The seven existing 3D Printing processes.....	11
Figure 8: Examples of shape-changing structures. (A) from flat strip to wavy structure, (B) from a flat ring to a wavy structure, (C) from flat strip to curly structure, (D) from a collapsed to a deployed lattice, (E) from a collapsed structure to a bending lattice, (F) from a flat star-shaped structure to a 3D dome, (G) blooming flower upon heating, extracted from [37].	14
Figure 9: A 4D printed stent for heart surgery. (a) 2D view of the stent, (b) perspective view [38].	15
Figure 10: Evolution of product categories and their main scientific issues, results, and maturity levels [39].	16
Figure 11: Hype cycle for emerging technologies and research domains as expected in 2018. 4D printing is highlighted in a red dashed rectangular. [40].....	17
Figure 12: Ph.D. dissertation outline	23
Figure 13: 4D printing existing papers breakdown by year, extracted from [50].	27
Figure 14: A self-Bending 4D Structure from 1D line to MIT form [34].....	28
Figure 15: The general concept of 4D printed object dynamic [58].....	28
Figure 16: An illustration of a 4D printed shape-changing orchid made of hydrogel, extracted from [55].	29
Figure 17: Smart materials classification according to their active function [2,39,59].....	33
Figure 18: Stimuli illustration	36
Figure 19: Constrained-thermo mechanism [56,97].....	37
Figure 20: Different stimulation mechanisms illustration, extracted from [56-97].....	39
Figure 21: A beam structure with different printing paths. (a) Examples of segment compositions; (b) Possible bending transformations. A helix can be created by applying heat to a straight line through the combination of various bending directions in different segments. [92]	41
Figure 22: Multi-material distribution categories [139].	42

Figure 23: Example of an active multi-material structure using PolyJet® technique. (a) The patterns, (b) moisture-based stimulation, (c) the multi-material section structures printed using DIW and responsible of (d) bending orientation in 2D-to-3D transformation lattice-based applications [39].....	43
Figure 24: Smart bending hook [142]	44
Figure 25: Self-folding structure [34]	44
Figure 26: Hydrogel sample states [30].....	44
Figure 27: Example of helixing behavior [143]	45
Figure 28: Curling behavior [34].....	45
Figure 29: multiple curving behavior [34]	45
Figure 30: General design for 4D printing technology framework [39]	50
Figure 31: VoxSmart modelisation tool for 4D printing. (a) Different components of the plugin, (b) An example of a determined distribution, (c) the deformation of the wing when the magnetostrictive materials reach saturation.....	51
Figure 32: Full design process schematic flowchart of the driven by an EA in [181]	52
Figure 33: Design for X (DFX) approaches involved in our thesis work	53
Figure 34: Examples of bio-inspired interlocking assemblies. (a) elbow joint anatomy, (b) interlocking feature inspired from mangrove roots, and (c) assembly using interlocking nacreous features.....	54
Figure 35: Action figure anatomy. (a) the interlocking parts, and (b) the assembly [199].....	55
Figure 36: Interlocking 3D puzzles. Different figures from left to right: BUNNY, MUG, DUCK, SHARK, CACTUS, PIGGY, CHAIR, WORK PIECE, ISIDORE HORSE, TEAPOT [212].....	56
Figure 37: Digital (or computed) material distribution illustration.....	61
Figure 38: A set of different shapes of polyvoxels	Erreur ! Signet non défini.
Figure 39: Flowchart of the computational design for multi-material 4D printing based on interlocking blocks assembly computation.....	64
Figure 40: (a) Directed blocking graph $DBG_d = (P, R)$ and (b) its adjacency matrix M according to a specific direction	65
Figure 41: Example of a (a) 2D assembly of three interlocked parts, with its (b) DBGs along the directions $+x$ and $+y$, and (c) the related adjacency matrices. The dashed red circle and rectangle highlight the key part along the $+y$ direction.....	65
Figure 42: Insight of the computational approach to generate a multi-material interlocking assembly leaning on DBGs and adjacency matrices: (a) the input structure is of 10×10 voxel-based representation of a random digital material distribution, (b) neighboring voxels of mobile part highlighted in red, (c) selection of the most suitable candidate to generate the key part, (d) key part redesign, (e) voxels blocking P_2 toward $+y$ direction in red, (f) P_4 cannot be inserted into the assembly (not suitable as a solution), (g) generation of a suitable interlocking part.	70
Figure 43: DBGs and M on $+x$ and $+y$ directions related to cases a, d, f, and g of Fig. 4. The dashed red circle in the DBGs and rectangle in matrices refer to key parts in the specific direction.....	71

Figure 44: Illustrative case showing $6 \times 6 \times 6$ voxelized multi-material cube (1) the interlocking parts computation: (a) input structure, each voxel color refers to a type of material/property, (b) to (d) key part generation, (e) and (f) refer to fixed interlocking parts generation. (2) Assembly sequence planning of the generated interlocking parts: (a) insertion direction of each interlocking part, (b) the assembly order, (c) a multi-material interlocking assembly..... 73

Figure 45: Illustration of a $18 \times 18 \times 126 \text{ mm}^3$ multi-material structure interlocking assembly generation steps: (a) initial structure, (b) initial distribution, (c) homogeneous subassemblies after material distribution partitioning, and (d) design program flow within the VoxSmart add-on in Grasshopper for the interlocking computatio..... 76

Figure 46: Simulation of the original distribution deformation (A) and the interlocked distribution (B): (a) VoxSmart program flow for voxelization, materials assignment (inert material: Agilus30; active material: hydrogel), and SM simulation, (b) A and B distributions before thermal stimulation (at 25°C) and after stimulation (at 40°C)..... 79

Figure 47: Numerical simulation with VoxSmart plugin of the initial distribution (A) and adjusted distribution (B) at 25°C , 30°C , 40°C , and 80°C 80

Figure 48: Multi-material 4D printing via interlocking blocks: (a) thermo-responsive hydrogel blocks printed with DIW technique, (b) Agilus30 blocks printed with MJ (PolyJet technique), (c) manual assembly of the interlocking blocks by following the assembly sequence generated by the developed VoxSmart component , (d) deformed structure after stimulation at 40°C in water, (e) interlocking assembly deformation zooming in (Focus x5). 81

Figure 49: Multi-material distribution categories. The special pattern is considered in this study to further master the fabrication of computed materials distributions..... 85

Figure 50: Study to investigate the effects of (a) interlocking blocks assembly on multi-material 4D printing versus (b) multi-material 4D objects printed in one go. 86

Figure 51: Rhinoceros3D/Grasshopper® program flow to determine the interlocked blocks assembly of a $62 \times 10 \times 5 \text{ mm}^3$ multi-material sample: (a) initial geometric structure highlighting the distribution of active/inert materials, (b) voxelization of the materials distribution, (c) homogeneous subassemblies after material distribution partitioning, (d) design program flow dedicated to the interlocking computation, (e) generated interlocking parts, and (f) final assembled structure. 87

Figure 52: Description of the assembly sequence of the multi-material 4D printed sample using interlocking blocks. (a) 23 blocks have been determined by the software tool, (b) the assembly sequence operation of the interlocking blocks, and (c) Assembly step by step..... 89

Figure 53: Three-point bending test procedure: (a) the multi-material structure printed in one go, (b) the interlocked structure configuration, and (c) LLOYD Instruments LR 50K Universal tester. 90

Figure 54: measurement of curvatures 91

Figure 55: 4D printing process to achieve a shape change on a structure composed of Agilus30™ and VeroWhite™ materials. The specimens are 3D printed via the PolyJet™ technique, solvent stimulated

at room temperature (RT) for 1 h enabling the swelling of the elastomer, then thermally stimulated at 60°C for 5 min enabling the shape change of the whole structure. The specimens are finally cooled down at 10°C for 1 min to ensure the shape fixity. The shape recovery stage consists in drying the specimens at RT for 12 h and then heating up them at 60°C for 5 min. 92

Figure 56: Fabrication of the multi-material samples via material jetting (PolyJet™ technique) with the Objet260 Connex3 printer and VeroWhite™ and Agilus30™ materials: (a) the interlocking blocks printed separately then manually assembled, (b) the multi-material structure printed in a single operation..... 93

Figure 57: The plot of deflection against average time as 3pts-bending test results. The results of the multi-material structure printed in one go are presented in blue color, the results of the multi-material structure made of interlocked blocks are presented in orange color 94

Figure 58: Simulation of the interlocked structure deformation (A) and the printed structure in a single operation (B), within the process flow of the VoxSmart software tool for voxelization, materials assignment, and simulation of the energy stimulation. A and B are represented before stimulation (at 25°C) and after stimulation at 30°C, 40°C, and 60°C..... 95

Figure 59: (a) Illustration of the deformation of both structures in hot bath water (60°C) during 5 min time-lapse, and (b) related graph of curvature against time. The fully printed structure is represented in blue color, while the interlocked structure is in orange color. the interlocked structure showing curvature at an earlier stage compared to the fully printed structure. In the interlocked structure, hot water can easily access the interfaces, allowing the entire structure to be heated rapidly above the transition material T_g . This results in the assembled structure relieving stored stress and bending more quickly. The fully printed structure takes longer to achieve a temperature higher than the T_g of the VeroWhite™ material, thus explaining the slower deformation. All scale bars: 10 mm..... 97

Figure 60: Comparison of the samples performance: (a) experimental curvature radius (experiments outcome) vs. the theoretical curvature radius (from simulation results), (b) time spent to achieve the experimental curvature by both interlocked and fully printed structures, (c) experimental stimulated structures once cooled down in water bath, (d) voxel-based simulations, and (e) local view of the interlocked structure after actuation. All scale bars: 10 mm. 99

Figure 61: Reversibility cycles of both interlocked structure samples and fully printed ones. The samples bend in the programming phase, then return to their straight shape after the shape recovery phase. Four completed cycles are presented. All scale bars: 10 mm. 100

Figure 62: Curvature measurements of four completed reversibility cycles of both interlocked structure samples and fully printed ones. 101

Figure 63: The stimulated samples of both interlocked and fully printed structures are bearing weight once are cooled down and the transition material gains its glassy state after the actuation phase. (a) the specimens as fabricated, (b) the specimens as actuated, (c) the actuated specimens bearing a load of 200 g..... 102

Figure 64: illustrating limitations of interlocking blocks assembly concerning the contact and deformation continuity, a) illustration scheme after multiple cycles of stimulation, b) case of a shrinking hydrogel demonstrating the un-uniform overall deformation of the structure. 108

Figure 65: Illustrative case studies. Starting from (A) as an initial digital materials distribution, (B) is the interlocking assembly generated from the previous interlocking approach developed in chapter 3 (without customized interlocking blocks), and (C) is the interlocking assembly generated using customized interlocking blocks. 109

Figure 66: Rhinoceros3D/Grasshopper® program flow to determine the interlocked blocks assembly of an 80 x 30 x 18 mm³ multi-material sample: (a) initial geometric structure highlighting the distribution of active/inert materials, (b) voxelization of the materials distribution, (c) homogeneous subassemblies after material distribution partitioning, (d) design program flow dedicated to the interlocking computation. 111

Figure 67 : Actuation and recovery procedures of the interlocking assembly case studies 115

Figure 68: Rhinoceros3D/Grasshopper® program flow to determine the interlocked blocks assembly of the 80 x 30 x 18 mm³ multi-material sample, the red color refers to the hydrogel and the grey color to the inert material: (a) voxelization of the remaining space component initial geometric structure highlighting the distribution of active/inert materials, (b) the interlocking assembly generator component, at the end of the process, it generates the interlocking blocks as well as their related assembly sequence, (c) the customized interlocking blocks involved in this case of study. 116

Figure 69: Multi-material interlocking assembly generated using a customized interlocking blocks. (a) description of the assembly sequence of the multi-material 4D printed sample, 6 blocks have been determined by the software tool in addition to the customized blocks, (b) the direct blocking graph of the final interlocking assembly, the nodes represent the 9 blocks of the assembly, an ordered pair (arrow) between *P1* and *P2* means that *P1* is blocked by *P2* along a direction *d*, the dashed red circles illustrate the key parts in the direction *d*, and (c) related adjacency matrices. 117

Figure 70: Printed interlocking blocks and related assemblies. (a) Assembly B, (b) Assembly C 118

Figure 71: Shaking test protocol. (a) the shaking test machine, (b) Assembly B and (c) Assembly C on the vibration tray. 119

Figure 72: Shaking test results summary. The blue graph refers to the Assembly B performance and the orange graph refers to the Assembly C performance. (a) first Assembly C part separation, (b) first Assembly B part separation. 119

Figure 73: Simulation of multi-material 4D printed structures using the VoxSmart add-on simulator within the Rhinoceros3D/Grasshopper® environment, (A) initial distribution, (B) the interlocking assembly without using customized blocks, distribution (C) the interlocking assembly using a customized blocks. The different structures are represented before stimulation (at 25°C) and after stimulation at 40°C. 121

Figure 74: Shape-changing simulation of (A) initial distribution, (B) the interlocking assembly without using a customized blocks, distribution (C) the interlocking assembly using a customized blocks. Simulations were performed before stimulation at 25°C and after stimulation at 30°C, 35°C, 38°C, and 40°C..... 123

Figure 75: Multi-material 4D printed interlocking assembly without customized blocks (Assembly B) : (a) manual assembly of the interlocking blocks by following the assembly sequence generated by the developed VoxSmart component , (b) deformed structure after stimulation at 40°C for 30 min, (c) Hydrogel Block 1 deformation zooming in (Focus x20), (d) Hydrogel Block 2 deformation zooming in (Focus x10). Scale bars: 10 mm. 124

Figure 76: Multi-material 4D printed interlocking assembly with customized blocks (Assembly C) : (a) manual assembly of the interlocking blocks by following the assembly sequence generated by the developed VoxSmart component , (b) deformed structure after stimulation at 40°C for 30 min, (c) Hydrogel Block 1 deformation zooming in (Focus x24), (d) Hydrogel Block 2 deformation zooming in (Focus x10). Scale bars: 10 mm. 125

Figure 77: Gap measurements at hydrogel block 1&2 interfaces results. Blue color refers to Assembly B while the orange color refers to Assembly C. 126

List of Tables

Table 1: AM processes used in 4D printing technology. Extracted from [39].	30
Table 2: SMs strengths, weaknesses, and potential applications.	35
Table 3: Stimulation mechanisms with involved materials and their potential applications.	40
Table 4: 4D printing transformations and examples of applications	44
Table 5: A suggested roadmap of design for 4D printing technology, extracted from [39].	49
Table 6: interlocking assemblies characteristics, examples, and applications.	56
Table 7 : Illustrations of various possibilities of interlocking assembly generations based on different choices of blocking the key part P_1 along different directions	74
Table 8: Calculation of the maximum and average distances between voxels' positions in the initial distribution (A) and adjusted one (B) at 25°C, 30°C, 40°C, and 80°C	80
Table 9: Calculation of the maximum and average distances between voxels' positions in the interlocked structure (A) and the fully printed structure (B) at various temperatures.	96
Table 10: Customized interlocking blocks (examples of blocks according to SM Iso/anisotropic behavior and SMs location).	112
Table 11: Calculation of the maximum and average distances between voxels' positions in (B) the interlocking assembly without using a customized blocks, distribution (C) the interlocking assembly using a customized blocks at 25°C, 30°C, 35°C, 38°C, and 40°C.	123

List of Acronyms

Term	Definition
AM	Additive Manufacturing
CAD	Computer-Aided Design
CAE	Computer-Aided Engineering
CNC	Computer Numerical Control
JIT	Just-In-Time
IoT	Internet of Things
AI	Artificial Intelligence
SM(s)	Smart Material(s)
DFX	Design For X
DFAM	Design For Additive Manufacturing
DFA	Design For Assembly
FFF	Fused Filament Fabrication
DIW	Direct Ink Writing
MJ	Material Jetting
SLA	Stereolithography
DLP	Digital Light Processing
SLM	Selective Laser Melting
SMA	Shape Memory Alloy
SMP	Shape Memory Polymer
SME	Shape Memory Effect

TO	Topology Optimization
EAP	Electro-active Polymer
FEM	Finite Element Method
DOF	Degree Of Freedom
DBG	Directed Blocking Graph
LCST	Lower Critical Solution Temperature
LCE	Liquid Cristal Elastomer

Chapter 1: Introduction and Research Context

“A problem well stated is a problem half-solved.”

Charles Kettering

“Unravel the knot to find the key,

Understanding the problem is the way to be free.”

Rumi

Chapter 1: Introduction and Research Context	1
1.1. Introduction	3
1.2. Evolution In Mankind Craft and Manufacturing Processes	3
1.3. Evolution In Objects Capabilities.....	6
1.4. 4D Printing Origins	8
1.4.1. Additive Manufacturing/3D Printing	9
1.4.2. Smart Materials	11
1.4.3. Brief Introduction To 4D Printing	12
1.5. General Context for This Ph.D.	15
1.6. Motivations & Objectives	18
1.7. Thesis Structure	22

1.1. Introduction

"Every generation sees in the past not merely a vanished world but also the dim outlines of its own. We are all Greeks already, and the Hellenistic age belongs to us as much as to the Alexandrians of that time. The same holds true of the Renaissance, of the Enlightenment, and of the industrial revolution. These were not simply occurrences of the past; they are part of our present inheritance. To be sure, each generation modifies this inheritance, but it modifies it by adding to it, not by subtracting from it." - Lewis Mumford, "The Myth of the Machine", 1967.

Manufacturing is not just about making things, but about continuously improving the process of making things in order to create better products and services that enhance our lives. Craft and manufacturing have been central to human civilization since the dawn of time. From early primitive tools made of stone to modern-day technologies like additive manufacturing (AM) and 4D printing, the evolution of manufacturing has been marked by an ongoing quest for better ways to create and shape materials. This chapter will take a closer look at the history of mankind's craft and manufacturing processes and explore how AM and 4D printing are shaping the future of manufacturing.

1.2. Evolution In Mankind Craft and Manufacturing Processes

The history of craft and manufacturing goes back to the earliest days of human civilization. Archaeological evidence shows that our ancestors were already crafting tools from stone, bone, and other materials as far back as 3.3 million years ago to support their survival needs. These early tools were simple and made by hand, but they represented a significant step forward in the development of human technology. The reason behind that development is that human needs have expanded beyond mere survival to encompass a wide range of pursuits such as economics, competition, entrepreneurship, science, finance, research, and more [1]. The progress that we observe today can be traced back to the primitive ages of pre-history:

- **The Stone Age:** Began around 3.3 million years ago and ended around 3300 BCE, where stone tools were used by early human societies. During this time, humans were primarily hunter-gatherers, and their tools were used for tasks such as hunting, butchering animals, and preparing food.
- **The Neolithic Age:** Also known as the New Stone Age, began around 10,000 BCE and lasted until around 4000 BCE. characterized by the development of agriculture, the domestication of animals, the use of fire for pottery, weaving, and the use of polished stone tools.

- **The Bronze Age:** 3000 BCE, marked by the beginning of metalworking techniques to craft metal tools and weapons. Bronze, a combination of copper and tin, was the primary metal used during this time.
- **Iron Age:** Around 1200 BCE, marked by the widespread use of iron tools and weapons. The development of ironworking techniques, such as forging, casting, and welding allowed humans to create even stronger and more durable tools, which had a significant impact on warfare, trade, and agriculture.

Towards the end of these epochs, human has already become familiar with a range of manufacturing techniques. These included coating, which involves applying a layer to the surface of an object; molding, like shaping a strip of wood as a decorative architecture; forming, cutting, and joining, which refer to techniques for shaping and attaching materials to create objects such as knives and scrapers made from flint or obsidian and attached to wooden handles using resin or sinew [2]. As time progressed beyond the prehistoric ages, generations kept evolving and paving the way for further technological innovations in manufacturing that would shape the world for centuries to come. The succeeding eras are as follows:

- **The Middle Ages:** Spanned from the 5th to the 15th century, were marked by significant advancements in agriculture, architecture, and the arts. During this time, new technologies like the printing press, water-powered and wind-powered mills, the Blast Furnace, gunpowder, and the compass were developed, which had a significant impact on society and helped to pave the way for the Renaissance. While there were some instances of mechanization and automation during the Middle Ages, many manufacturing processes were still primarily handcrafted. It was not until the Industrial Revolution in the 18th and 19th centuries that manufacturing processes became more heavily mechanized and automated.
- **The Industrial Revolution:** was a period of rapid industrialization that began in Britain in the late 18th century and spread to other parts of Europe and North America in the 19th century and marked a major turning point in the history of manufacturing. During this time, factories began to replace traditional craft methods, and machines were developed to automate many manufacturing processes. This led to significant increases in productivity and efficiency, and it allowed manufacturers to produce goods on a much larger scale than ever before. The Industrial Revolution was fueled by several key inventions and innovations, including the steam engine (Thomas Newcomen, 1712), the spinning jenny (James Hargreaves, 1764), and the power loom (Edmund Cartwright, 1784). The Industrial Revolution was also fueled by several manufacturing techniques such as rolling in 1783 (the process of passing metal through rollers to flatten and shape it into uniform sheets or plates), puddling in 1784 (a method of melting iron and stirring it to remove impurities, resulting in a stronger and more malleable metal), turning in 1752 (a subtractive manufacturing technique using a lathe to shape and cut material into a desired form), and milling in 1816 (another subtractive manufacturing method that uses moving

cutters to remove material from a workpiece and create complex shapes and designs). These technologies revolutionized the production, allowing the creation of textiles, iron, glass, and other goods on a massive scale. The development of new transportation technologies, such as the steam-powered locomotive and the steamship, also made it easier and more efficient to transport goods and people over long distances [3].

- **The Digital Age:** which began in the late 20th century, marked the widespread use of digital technologies like computers, the internet, and mobile devices. These technologies have had a significant impact on every aspect of society, from business and commerce to entertainment and communication. The rise of automation made machines capable of operating independently. In the 1950s, the development of Computer Numerical Control (CNC) merged, and machines were monitored to allow more precise and efficient manufacturing processes. Later, the 1970s saw the development of Just-In-Time (JIT) manufacturing, which allowed companies to reduce inventory costs by only producing goods as they were needed. In 1984, the 3D printing technology consisting in using a computer-aided design (CAD) model to build a 3D object, has been developed [4]. This technology has revolutionized manufacturing by allowing the production of complex geometries and reducing the need for expensive tooling. These advances have not only improved efficiency, but also increased the speed and accuracy of manufacturing, enabling companies to produce goods on a larger scale and with higher quality.
- **Industry 4.0:** refers to the current trend of automation and data exchange in manufacturing and other industries. It is a new era of industrial revolution (see Figure 1) characterized by the integration of advanced technologies such as the Internet of Things (IoT), artificial intelligence (AI), and robotics into manufacturing processes [5]. Industry 4.0 aims to create "smart factories" that are fully connected and can operate autonomously with minimal human intervention. First, with the help of IoT sensors, machines and equipment in the factory can be monitored in real-time to optimize production, reduce downtime, and improve quality control. Then, AI and machine learning algorithms can analyze vast amounts of data to predict equipment failure or identify areas where efficiency can be improved. Besides, robotics and automation can perform repetitive tasks, freeing up workers to focus on higher value-added activities.
- **Industry 5.0:** is a term that has emerged more recently and represents a shift away from the hyper-automation of Industry 4.0 towards a more human-centered approach. Industry 5.0 is focused on creating a closer collaboration between humans and machines, with the goal of creating more customized, flexible, and sustainable products. This is done by leveraging the unique skills of human workers alongside advanced technologies such as robotics and AI [6].

If one takes a step back to better observe these progresses, one can realize that each new era has brought with it new challenges and new opportunities, and has helped to shape the way we live, work, and interact with the world around us today. Besides, all the aforementioned technologies have involved a

process of experimentation, refinement, and formalization to our understanding of materials, processes, and design principles, leading to the creation of highly complex and sophisticated manufacturing processes. 4D printing builds upon this foundation, pushing the boundaries of what is possible in terms of adaptive and responsive manufacturing.

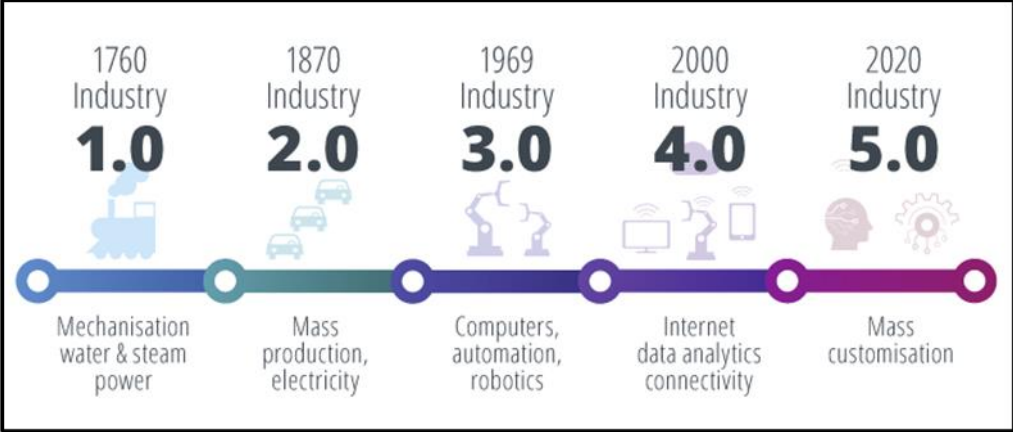


Figure 1: Industry revolutions through the time [7].

1.3. Evolution In Objects Capabilities

The evolution of object capabilities has been a continuous process throughout human history, with each era introducing new and innovative ways to enhance the functionality of objects and meet the changing needs of consumers and businesses. As technology continues to advance, products will continue to evolve and integrate even more features and capabilities [8]. From communication devices to home appliances, the possibilities are endless, and the future looks exciting. For instance, with the advent of digital technology, the integration of connectivity, and data analysis, products have become much more sophisticated and dynamic. They are now able to interact with users in new and innovative ways leading to more personalized and effective experiences. Let’s bring up light bulbs for example! Traditional incandescent light bulbs are static objects that emit light at a fixed brightness level. However, with the development of LED lights and smart bulbs, light bulbs can now adjust their brightness, color, and even respond to voice commands or motion sensors [9].

In a matter of a fact, transformability in objects is not a recent innovation. This concept has been around for centuries, dating back to antiquity. In ancient times, transformable objects were often designed for practical purposes, such as to accommodate different numbers of diners or to provide a multi-functional piece of furniture for outdoor events. These objects were typically designed with simple mechanisms, such as collapsibility or reconfigurable parts for easy transformations [10-13]. One of the most well-known examples of convertible objects in antiquity is the Roman triclinium, a dining room that could be arranged in different configurations to accommodate different numbers of diners (see Figure 2.a).

The couches were also designed to be collapsible for easy storage. In ancient Greece, the klinē was a couch that could be used for sleeping or reclining during meals and was often designed to be collapsible for easy transportation. Convertible objects were also used for religious purposes. In ancient Egypt, for example, the benben was a type of altar that could be reconfigured into a statue of a god or goddess.

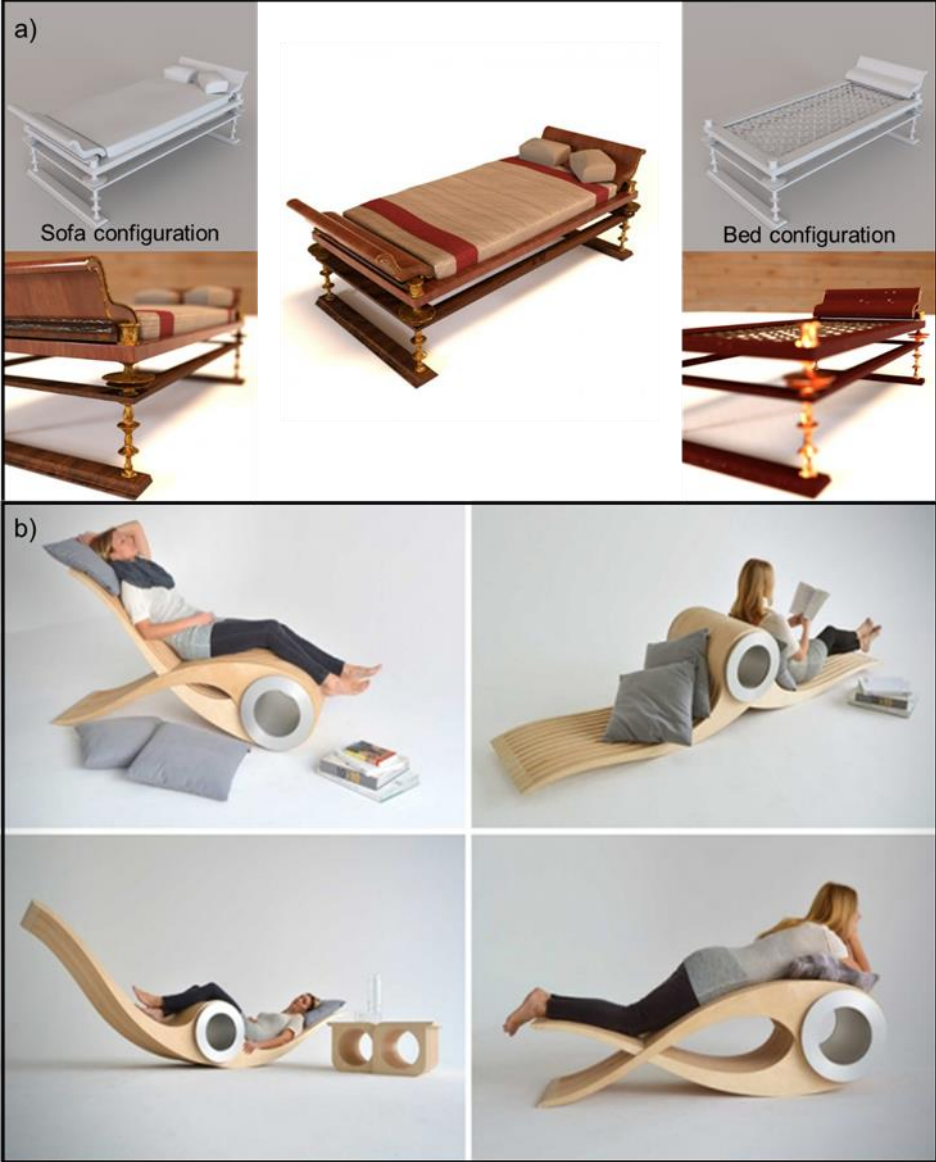


Figure 2: Example of convertible objects from antiquity vs. today, (a) an ancient roman Triclinium, and (b) a multi-configuration chair.

Today, the concept of transformability has been taken to new heights due in large part to advancements in materials, manufacturing, nanotechnology, and design. Contemporary designers and engineers are exploring new materials and manufacturing methods to incorporate transformability into objects and products to increase functionality, sustainability, and user experience. One of the most significant related advancements is the development of state-shifting objects with unique capabilities, such as self-healing, shape memory, and self-assembly properties [14-16]. These objects can shift between different states or

configurations and change their physical properties in response to different stimuli, such as temperature or other environmental factors.

State-shifting objects are becoming increasingly popular and potentially attracting fields such as medicine, electronics, and environmental sustainability. As technology continues to advance, it is likely that we will see even more innovative and sophisticated state-shifting objects in the future. By automatically adjusting their behavior based on user needs or environmental conditions, state-shifting objects offer many advantages that one can enumerate as follows:

- Personalization, by adapting to the needs and preferences of individual users, providing a personalized experience that can enhance usability and user satisfaction.
- Reduce waste, energy consumption and environmental impact, by reducing the need for disposable objects and materials.
- Storage space saving, based on their environment or user actions, a single state-shifting object can serve multiple purposes.
- Improved safety, by alerting users when responding to potential dangers in their environment.

In addition to practical purposes, transformable objects today are also being dedicated for artistic and aesthetic purposes by providing endless possibilities for industrial designers and artists (see Figure 3). In brief, an object that can change its shape or properties in a controlled manner has numerous benefits. There are various methods of incorporating this functionality into objects, and the emergence of 4D printing as a manufacturing breakthrough is likely to be a significant one. In the following section, we will begin by introducing this technology.



Figure 3: Heat-Sensitive wall. It changes its color when exposed to heat. People can draw figures using their warm bodies temperature.

1.4. 4D Printing Origins

The term "4D printing" was coined in 2013 by Skylar Tibbits, an architect at the Massachusetts Institute of Technology (MIT). 4D printing technology is a relatively new technology that involves AM processes/techniques and smart or active materials (SMs) to build innovative objects. Let's give a brief overview of AM, SMs, and 4D printing.

1.4.1. Additive Manufacturing/3D Printing

AM, also known as 3D printing, has a complex history with multiple inventors and milestones. The earliest forms of AM date back to the 1980s, but the technology didn't become widely known until the late 1990s. The first French patent related to 3D printing was filed by Alain Le Méhauté, Olivier de Witte, and Jean Claude André in 1986 (see Figure 4). The patent, titled "Process for Rapid Prototyping of Solid Models," describes a method for producing three-dimensional models' layer by layer using a laser to selectively solidify a liquid polymer. This method is now commonly known as stereolithography (SLA), and the patent played a key role in the development of the technology [17,18]. The patent was filed with the French National Industrial Property Institute (INPI) on June 16, 1986, and was published as FR2585667A1 on December 24, 1986. The inventors went on to fund the company CILAS (Compagnie Industrielle des Lasers) to commercialize their technology. However, Le Méhauté (and de Witte) employers abandoned the patent a few years later as they did not recognize potential possibilities offered by the invention.



Figure 4: Alain Le Méhauté on the left & Jean-Claude André on the right with 3D printed objects

On the other hand, and around the same time, Chuck Hull across the Atlantic in the USA, used a laser to selectively solidify a liquid resin layer by layer to create a three-dimensional object. He filed his first patent for the technology in 1986 and went on to found 3D Systems Corporation, which became one of the leading producers of 3D printing technology. While Alain Le Méhauté and his colleagues were among the early pioneers of 3D printing, Chuck Hull is generally credited with inventing the technology

because he developed a commercially viable system and became more widely known and used. It is worth noting that the development of 3D printing was a collaborative effort involving many researchers and inventors, both Hull and Le Méhauté played important roles in the development of 3D printing and helped lay the foundation for the field as it exists today.

Unlike traditional subtractive manufacturing, which involves removing material to create a final product, AM builds a product layer by layer using a digital design. This process has several advantages over traditional manufacturing, including faster production times, reduced waste, and the ability to create complex geometries that are impossible to achieve using traditional methods (see Figure 5). It is fair to say that this innovation has introduced a completely new perspective on the approach to design and fabrication, creating a whole new realm of possibilities [19].



Figure 5: 3D printed metallic parts with complex geometries.

The generic process of AM involves several steps, as presented in Figure 6. First, a digital 3D model of the desired product is created using computer-aided design (CAD) software. The model is then sliced into thin cross-sections, which are used to guide the 3D printer. The machine then builds the product layer by layer using a variety of materials, such as plastics, metals, ceramics, or even biological materials [2].

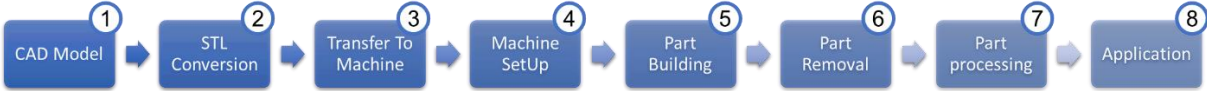


Figure 6: Main steps of 3D printing technology

There are seven main categories of additive manufacturing, as shown in Figure 7. vat photopolymerization, material extrusion, powder bed fusion, material jetting, binder jetting, sheet lamination, and directed energy deposition. It is worth noting that these categories are not mutually

exclusive, and some 3D printing technologies can fall into multiple categories depending on their specific process [20].



Figure 7: The seven existing 3D printing processes

1.4.2. Smart Materials

Smart materials are a class of materials that possess unique properties that enable them to change their behavior in response to external stimuli, such as temperature, moisture, pressure, light, electrical or magnetic fields [21,22]. They have gained significant attention in recent years due to their potential to revolutionize numerous industries, including healthcare, automotive, aerospace, and energy, among others.

As John Muir said: *“In every walk with nature one receives far more than he seeks”* ... One of the key inspirations behind the development of smart materials is nature itself [23]. Many organisms have evolved over millions of years to possess unique adaptive and responsive materials, allowing them to survive in challenging environments. For instance, spider silk is an exceptionally strong and tough material that can also be stretched and contracted in response to changes in humidity, making it an ideal material for use in responsive textiles. The skin of the chameleon changes color to blend into its surroundings, and the wings of the butterfly reflect light in a way that makes them appear iridescent. SMs have been found in various biological systems, such as the muscles of squid and the beaks of birds, and have been used in a variety of applications, including orthodontic braces and stents for blood vessels. Another example is self-healing materials, which have the ability to repair damage to themselves without human intervention. These materials have been inspired by biological systems such as the ability of

some plants to repair damage to their leaves. Self-healing materials have found applications in a variety of fields, including construction and electronics. Other examples of SMs inspired by nature include materials with variable stiffness, inspired by the structure of plant stems, and materials with reversible adhesion, inspired by the structure of gecko feet [24].

By studying and emulating these natural designs, scientists have been able to create new materials with unprecedented properties, such as self-healing polymers, shape-memory alloys, and biomimetic nanomaterials. This approach, known as biomimicry, has opened up exciting new avenues for material innovation, with the potential to transform the way we interact with the world around us.

1.4.3. Brief Introduction To 4D Printing

Although it has existed since the 1980s, AM is still considered a relatively new manufacturing method that has not yet been fully adopted. However, it has given rise to another disruptive technology known as 4D printing. This method strives to incorporate transformative capabilities in 3D printed objects by involving the deposition of multiple materials, including SMs [21]. These objects have the ability to alter their properties, such as their shape and physical characteristics, and potentially their functionality after being printed. There are numerous definitions of 4D printing in the literature, some of them describe 4D printing in such a philosophical way as:

"Bringing objects to life: the magic of 4D printing technology..." [25];

"From static to dynamic: how 4D printing breathes life into objects..." [26];

"Transforming objects through time: the life-giving potential of 4D printing..." [27].

Some other definitions are more common such as:

"a manufacturing approach that uses smart materials and digital fabrication techniques to create objects that can change shape or function in response to specific stimuli, such as heat, moisture, light, or other environmental cues..." [2];

"a new approach for printing three-dimensional objects that can self-transform or adapt their shape or properties when subjected to an external stimulus such as heat, water, or light, through the integration of smart materials and additive manufacturing techniques..." [28];

The 4th temporal dimension is made possible and is described in the literature as:

"4D printing: exploring the fourth dimension of time to create dynamic structures that can change their shape, properties, or functionality over time in response to external stimuli." [29];

"The fourth dimension of 4D printing: how time is used to create objects that can change shape and function by leveraging the properties of smart materials that can respond to external stimuli in a predictable and controllable manner. By programming these materials to change their shape, size, or properties over time, 4D printed objects can perform a range of functions, from shape-memory materials that can revert to their original shape to biomimetic structures that can mimic the behavior of living organisms." [30];

"From 3D to 4D printing: how the fourth dimension of time adds a new level of complexity and functionality to printed objects." [31];

Responsive transformation is at the heart of the emerging technology of 4D printing, which involves the creation of objects that are not only three-dimensional, but also have the ability to transform in response to various stimuli. This transformation can take many forms, including changes in shape, texture, color, and even functionality [32]. The key to this technology is the use of SMs, which can respond to external stimuli such as heat, light, or moisture, and undergo reversible changes in their physical or chemical properties. For instance, the shape-changing ability of 4D printed objects is typically achieved by designing the object to have certain programmed shape changes, and then using a SM or structure that responds to the stimuli to drive those shape changes [33-36]. The deposition of materials in 4D printing can play a crucial role in determining the shape-changing behavior of the printed object. For example, as shown in Figure 8, the orientation and distribution of the printed material can influence the anisotropy of the object, which can affect its mechanical behavior [3,37]. In addition, the amount and distribution of the SM or structure within the printed object can also influence its shape-changing behavior.

One of the most promising applications of responsive transformation in 4D printing is in the field of healthcare, where it has the potential to revolutionize the way medical devices and implants are designed and manufactured [38]. For example, a 4D-printed stent could be designed to expand or contract in response to changes in blood flow, reducing the risk of blockages or other complications (see Figure 9). Similarly, a 4D-printed orthotic device could adjust its shape to provide the optimal level of support for a patient's changing needs over time.

In conclusion, responsive transformation is a key feature of 4D printing, which is poised to revolutionize the way we design and manufacture objects in a wide range of industries. By harnessing the power of SMs and advanced manufacturing techniques, we can create highly adaptive systems that can respond to changing conditions and user needs in real-time. As this technology continues to evolve, it is likely to open up new possibilities for innovation and efficiency, transforming the way we live, work, and interact with the world around us. In recent times, the idea of creating a 4D printing Society in 2021 has gained the interest of researchers globally.

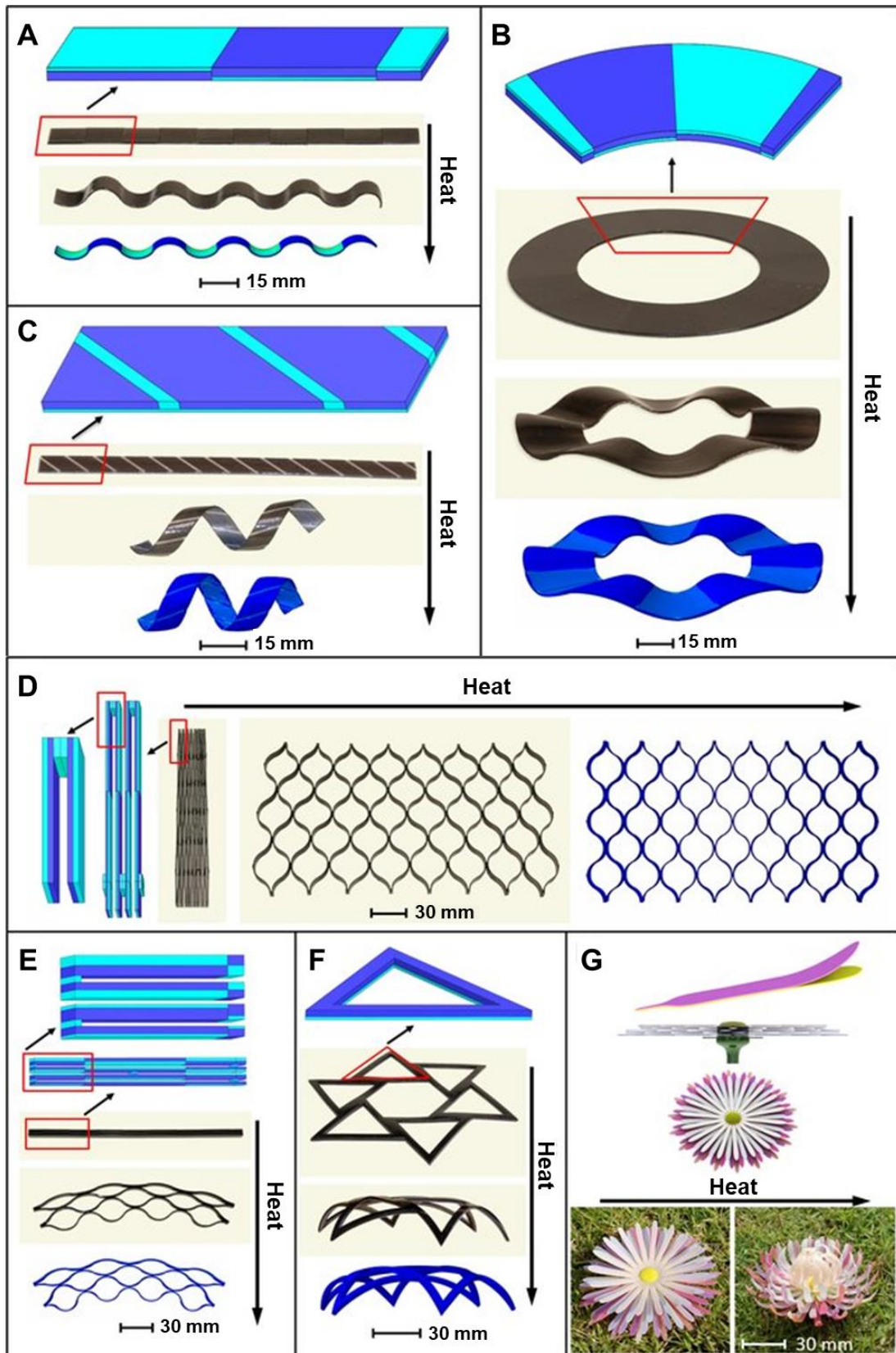


Figure 8: Examples of shape-changing structures. (A) from flat strip to wavy structure, (B) from a flat ring to a wavy structure, (C) from flat strip to curly structure, (D) from a collapsed to a deployed lattice, (E) from a collapsed structure to a bending lattice, (F) from a flat star-shaped structure to a 3D dome, (G) blooming flower upon heating (extracted from [37]).

This 4D printing society aims to bring together scientists and engineers from different fields to discuss and explore the potential of this emerging technology for commercialization. UTBM is one of the members of this society, along with other universities such as Georgia Institute of Technology, Concordia University, Deakin University, Singapore University of Technology and Design, among others.

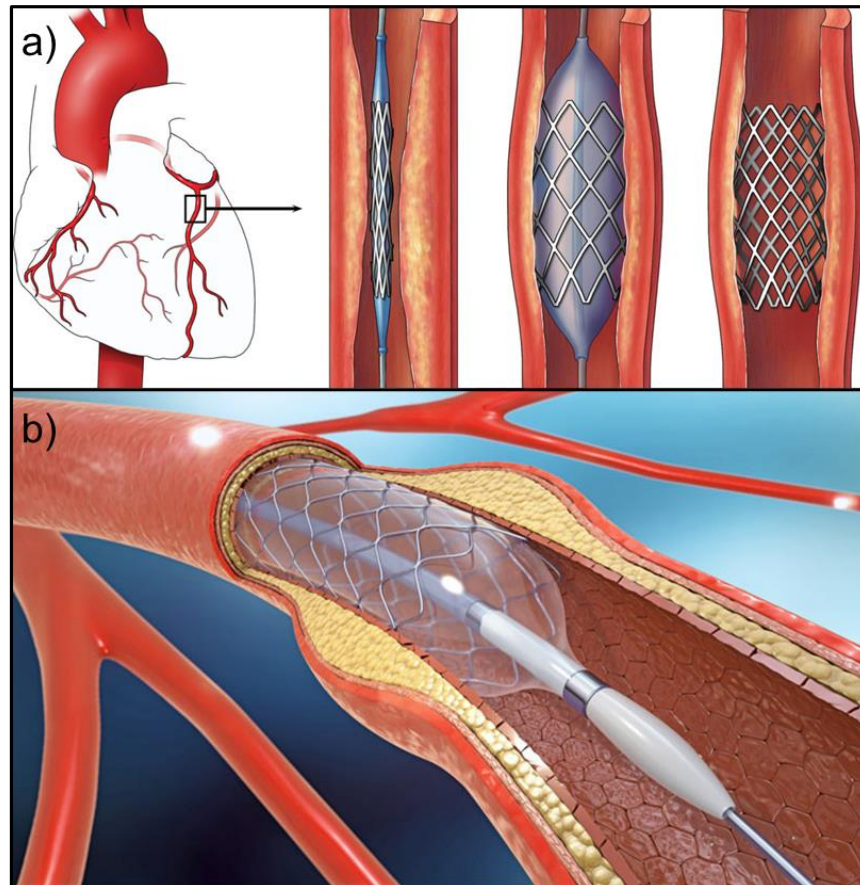


Figure 9: A 4D printed stent for heart surgery. (a) 2D view of the stent, (b) perspective view [38].

1.5. General Context for This Ph.D.

The advancements in technology have led to significant changes in various aspects of the manufacturing industry [39]. From the development of conventional mechanical products, we have now progressed towards more versatile and autonomous products, as shown in Figure 10. These products consist of mechatronic products, connected products, and smart systems that are designed to adapt and evolve according to their environment. Along with changes in products, there has been a shift in manufacturing processes as well [2,39]. Conventional manufacturing processes have been replaced by AM processes, which enable the creation of complex and intricate designs. Additionally, there has been a shift in materials used in manufacturing, with a move from conventional materials to programmable or

intelligent materials. The goal of this vision is to create products that can meet the evolving needs of users throughout their lifecycles.

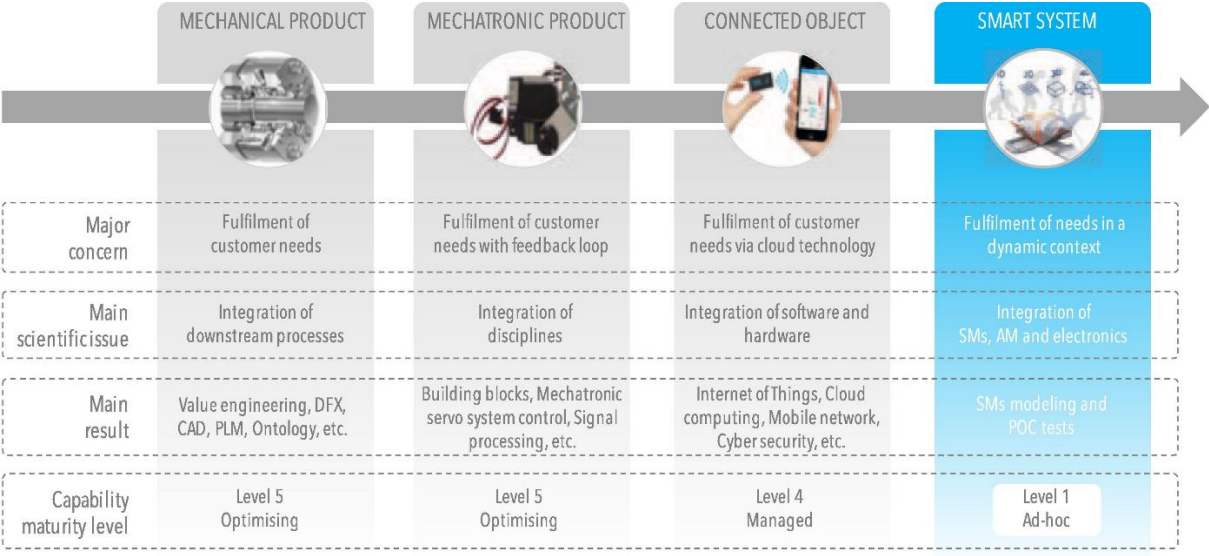


Figure 10: Evolution of product categories and their main scientific issues, results, and maturity levels [39].

As time progresses, the potential for programmable products becomes more and more promising. With the ability to change their state, kinematics, and form, these products have the potential to revolutionize the way we interact with our environment. The shift towards programmable products also has significant implications for sustainability. By postponing obsolescence and reducing waste, these products could help us create a more sustainable future. As we continue to push the boundaries of what is possible with programmable materials and manufacturing processes, the possibilities for new and innovative products are truly endless [39].

The emergence of 4D printing appears to be in line with these developments. The increasing demand for adaptable products and advancements in AM have led to the exploration of integrating SMs. Although this promising technology is still in the innovation trigger stage according to the latest Hype cycle (see Figure 11) [40], both governments and companies have recognized the potential of this technology and have decided to keep up with these advancements to remain competitive and profitable [41]. A number of companies have already begun investing in 4D printing to embrace this evolution. For instance, Airbus is exploring the use of 4D printing technology to create self-assembling aircraft parts. They are hoping to reduce the weight and complexity of their planes [42]. 4D printing has also attracted BMW company. This German manufacturer has developed the Vision Next 100 model with 4D capabilities, BMW envisions the outer shell to change shape in response to airflow and wheel arches in response to steering movement. [43]. Their platform, called the 4D Additive Experience, allows designers to create parts that can change their shape or properties over time. Remaining ahead of the

game in a constantly changing environment involves more than just investing in new technologies. It also requires a complete reevaluation of the product development processes. In simpler terms, successfully adopting a new technology means introducing new design approaches, methodologies, and tools.

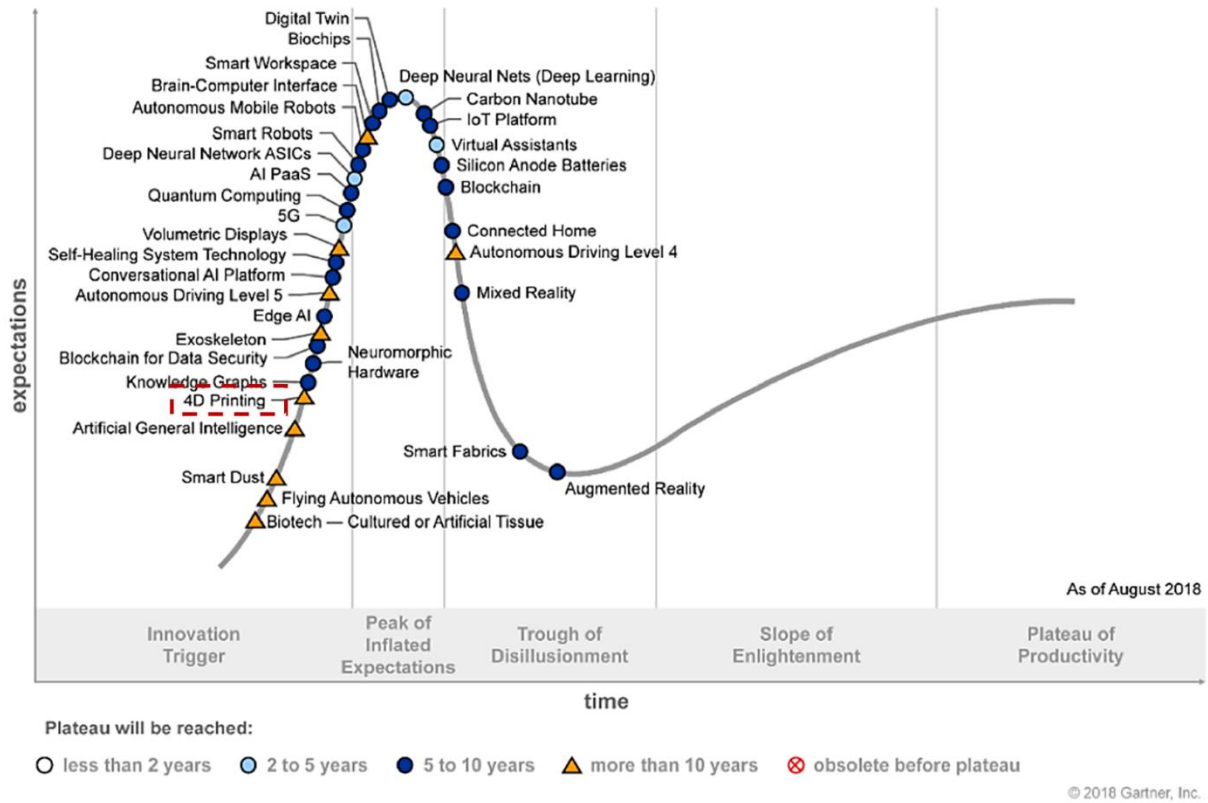


Figure 11: Hype cycle for emerging technologies and research domains as expected in 2018. 4D printing is highlighted in a red dashed rectangular [40].

In such a large-scale research interdisciplinary field, this Ph.D. thesis aims at investigating an original way of designing and fabricating stimulus-responsive objects, in order to rightly deliver behavior and multi-physics properties on demand. Designing 4D printing-friendly solutions, therefore, requires a high degree of flexibility from the conceptual design stage to the manufacturing stage. The objective is to assist designers in comprehending this innovative mindset and creating products that align with this groundbreaking manufacturing technology while also adapting to their evolving usage. Funded by the French ‘Investissements d’Avenir’ program, and the EUR-EIPHI Graduate School (contract ANR-17-EURE-0002), this Ph.D. thesis is carried out at the CO2M (Design, Optimization, and Mechanical Modeling) department at the ICB UMR 6303 CNRS laboratory (Belfort, France). This research work is also associated with the LRGP UMR 7274 CNRS at the University of Lorraine (Nancy, France). The next section will lay out the related motivations and objectives.

1.6. Motivations & Objectives

Winston Churchill once said: "*Success is not final, failure is not fatal... It is the courage to continue that counts...*". The challenges that a technology faces on the path to maturity can be significant. Successful technologies are those that are able to embrace these challenges as opportunities for growth and innovation and navigate them to evolve over time from the research and development stage, through prototype development, pilot testing, and commercialization, until maturity. It appears that 4D printing technology is also subject to this innate inclination. While the potential applications of 4D printing are vast, there are still several challenges that need to be addressed for this technology to be widely adopted, and to expand the knowledge of designers to gain greater profit from it. One can notice that 4D printing limitations can be categorized into two main dimensions -scientific and engineering- as outlined hereafter:

On one hand, some of the scientific challenges of 4D printing include:

- Materials selection, development, and control:

One of the main scientific challenges of 4D printing is identifying the right materials that can respond to environmental stimuli, such as temperature, humidity, or light. The materials used in 4D printing must be able to deform and transform into specific shapes and sizes when triggered by an external stimulus. Currently, only a limited number of materials are available and suitable for 4D printing, and more research is needed to identify and develop new materials. Besides, the properties of the materials used in 4D printing, such as the combination between both stiffness and elasticity, must be precisely controlled in order to achieve the desired transformation behavior. This requires a deep understanding of the material properties and their response to different stimuli. Furthermore, it seems to be important to mention -Durability- as one of the scientific challenges related to materials development. The materials used in 4D printing must be durable and able to withstand repeated cycles of deformations and transformations without losing their functionality. Thus, one can state that the materials in 4D printing still require full attention in order to push this technology steps further [39,44,45].

- Stimulus design and control:

The stimuli that trigger the shape or property change of 4D printed objects need to be precisely designed and controlled. Achieving this requires a deep understanding of the physical and chemical mechanisms that occur within the materials. Yet, the underlying mechanisms of stimuli-responsive materials are still complex and not well understood. Besides, stimuli need to be tailored to specific applications. Different applications require different stimuli, and it can be challenging to identify the optimal stimulus for a particular application. The choice of stimulus must be carefully considered based on factors such as the desired transformation behavior, the properties of the material, and the environmental conditions. It is also worth pointing out that the design and integration of stimuli with other components such as inert/

active materials, sensors, actuators, and electronics to work together seamlessly is a significant scientific challenge. Therefore, this indicates a gap in the current knowledge that needs to be addressed as well. [39,46].

- Reversibility programming:

Reversibility is an important aspect of 4D printing, as it enables structures to be repeatedly transformed between different configurations. However, the majority of materials used in 4D printing today lack the autonomy to return to their initial state after undergoing a transformation. This limits the practical applications of 4D printed structures, as they cannot be reconfigured or reused once they have undergone a transformation. To address this challenge, researchers need to explore new approaches to build active structures and control the transformation behavior of existing materials. This will aim to expand the capabilities of 4D printing and enable the development of more advanced and versatile structures. [39,47].

On the other hand, the engineering challenges related to 4D printing encompass, without being restricted to:

- Design and Assembly:

Designing and assembling 4D printed structures that can change their shape and functionality in a controlled manner requires advanced engineering skills and expertise. Engineers need to develop new design tools and methods that can account for the dynamic behavior of the printed structures, such as using computer simulations to predict the shape change and optimize the design. Assembly of the printed structures requires precise alignment and integration of multiple components, such as sensors and actuators, which may require novel fabrication techniques [21,39].

- Integration with existing systems:

Integration with existing systems is a key challenge for 4D printing because it requires coordination between different technologies and processes to enable mass production and practical applications. For example, 4D printed objects may need to be assembled or integrated with other components in a larger system, such as a building or a vehicle. This requires careful consideration of the design and engineering requirements of different systems, as well as the compatibility of materials and processes. One approach to addressing this challenge is to develop standards and guidelines for 4D printing technology, similar to those that exist for other manufacturing and construction processes. This would help ensure that 4D printed objects can be integrated into existing systems with minimal modifications or disruptions [21,39,48].

- Scaling up:

4D printing is currently limited to small-scale production due to the complexity of the structures and the variability of the printing process. Researchers need to develop new methods for 4D printing on a larger scale, while maintaining the quality, functionality, and precision of the printed structures. Developing new methods, such as using robotic assemblies, may be a highly effective means of driving progress in the field of 4D printing technology [34].

- Modeling and Simulation:

Developing accurate models and simulations that can predict the behavior of 4D printed structures under different conditions is essential for designing and optimizing the printing process and the final products. However, this task is challenging due to the complex and nonlinear behavior of smart materials and requires advanced computational techniques and reliable experimental data. Therefore, researchers need to explore new models and simulation tools that can account for the dynamic behavior of the printed structures and allocate the appropriate inert/smart material at the right place to ensure the optimal interaction between the latter and the stimuli [49].

- Printing Process Optimization:

The 4D printing process involves several steps, including printing, shaping, and activation, each with its own challenges and requiring coordination of various parameters. For example, printing SMs necessitates precise control of the printing parameters such as temperature, pressure, and deposition rate (sometimes even controlling the light in the laboratory room might be necessary to properly tune certain light-responsive SMs), to ensure the quality and integrity of the printed structure. Shaping the printed structure requires careful manipulation and control of the stimuli, such as heat or light, to induce the desired shape change. Activation of the printed structure requires selecting the appropriate stimulus and controlling its intensity, duration, and durability. Developing such efficient and reliable 4D printing processes that can produce complex and functional structures is still a major engineering challenge, despite this, it should not hinder the evolution of 4D printing [21].

In a nutshell, 4D printing is a highly interdisciplinary field that requires collaboration between scientists and engineers from various disciplines, including materials science, physics, mechanics, design, and computer science. This collaboration is essential to overcome the scientific and engineering challenges and realize the full potential of this technology that can transform various industries, such as healthcare, aerospace, robotics, among others.

The main emphasis of this Ph.D. thesis is addressing some of the intangible issues mentioned earlier by investigating an original way of designing and fabricating stimuli-responsive products and delivering multi-physics properties properly. One can state that fulfilling this task requires a high degree of flexibility from the conceptual design stage to the manufacturing stage. One novel concept that considers digital materials/manufacturing seems very promising to tackle 4D printing challenges. Referred as

voxel-based modeling, where the allocation of different physical properties within the structure geometry can be controlled to achieve desired 4D transformations. Voxel-based models can also cover multi-material (inert/smart materials), multi-scale (e.g., nano, micro, macro, etc.), multi-function (e.g., sensor, actuator, structural, etc.), and multi-structure (solid, lattice, etc.) modeling, which exposes us to hybrid voxels 4D printing.

In this thesis work, we will consider voxel-based modeling from an assembly perspective by espousing partitioning approaches, in order to build multi-material voxel-based 4D printed structures. In such a way, voxels should be physically printed individually or grouped based on their nature and then assembled. To secure the voxels assembly, topological interlocking assembly techniques need to be explored such as bio-inspired interlocking techniques, mechanical interlocking techniques, or computational interlocking techniques to name a few. Such efforts will reinforce ongoing research works on Design For 4D Printing and extend current computational mechanisms and 4D printing knowledge. The primary focus of this thesis is to tackle the previously mentioned issues by developing a design approach for hybrid voxels 4D printing, based on topologically interlocked multi-material assembly. Therefore, the tangible objectives can be outlined as follows:

- O₁** Propose a computational design approach for multi-material 4D printing. It enables the interlocking blocks (individual or polyvoxels) assembly computation by analyzing the distribution of the digital materials on a voxel basis in a given structure. This approach is general and efficient and allows exploring new types of complex assemblies that are impossible to be printed using a unique AM technique in a single run, such as combining solid voxels/lattices or metals/polymers in the same assembly. This deals with most, if not all, of the aforementioned scientific and engineering concerns.
- O₂** Further explore the approach of interlocking blocks assemblies by investigating their impact on the behavior of multi-material 4D printed structures. This involves analyzing various parameters such as the actuation time, shape change, and reversibility of 4D printed structures through a combination of mechanical/stimulation tests and numerical simulations. The ultimate aim is to demonstrate the relevance of the computational design approach, and most of all, tackle the previously stated challenges, notably the second and the third scientific challenge.
- O₃** Generalize the applicability of the developed computational design approach. This will be achieved by improving the uniformity of shape/property(ies) changing in a 4D multi-material interlocked assembly and addressing the limitations associated with the interfaces between blocks. It is thus a question of customizing the shapes of the blocks in the early stages of development when generating the assembly, taking into account the available smart materials and their potential transformations. This will mainly address the first scientific challenge (i.e.,

materials selection, development, and control) and the first engineering challenge (i.e., design and assembly).

1.7. Thesis Structure

The diagram labeled as Figure 12 illustrates the structure of the Ph.D. dissertation, detailing how the state of the art, research questions, and contributions are addressed. Once the research context and objectives have been introduced in this chapter, the thesis structure can be outlined as the following:

- Chapter 2: Surveys the existing landscape of research in 4D printing, design for AM and 4D printing, and multi-material assemblies. The research questions that guide the thesis are then formulated based on the gaps identified in the literature.
- Chapter 3: Puts forward a method of designing a computational approach for multi-material 4D printing based on interlocking blocks assembly.
- Chapter 4: Studies the impact of interlocking blocks assembly on the actuation time, shape change, and reversibility of voxel-based multi-material 4D structures.
- Chapter 5: Introduces a customized interlocked assembly blocks library for improved multi-material 4D printing structures performances.
- Chapter 6: Summarizes the findings, evaluates the proposed contributions, and highlights the potential prospects arising from the present research work. In addition, outlines future work to be done.

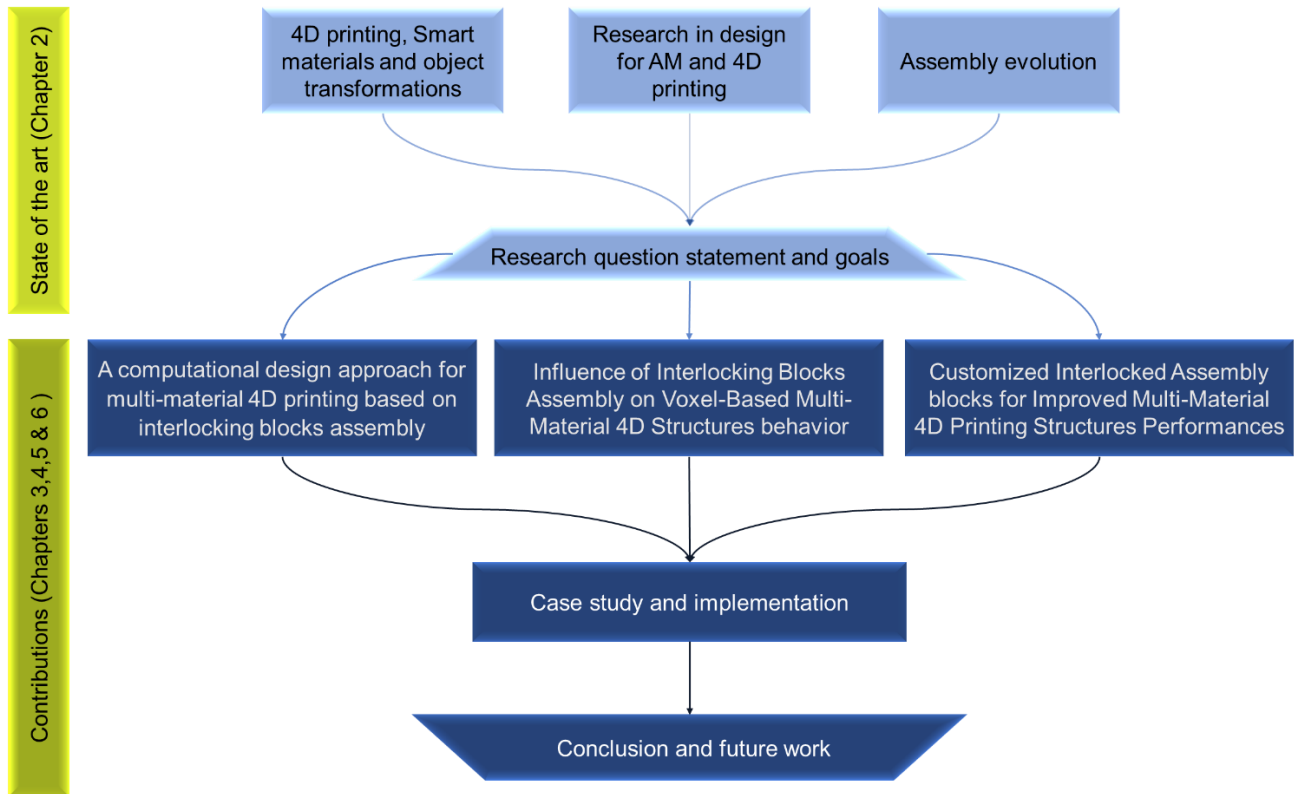


Figure 12: Ph.D. dissertation outline

Chapter 2: State of the Art and Related Scientific Questions

*“So, seek out those who differ,
And those who are the same.
For in learning from each other,
Our world will never be the same.”*

Anonymous

*“But inspiration can come from afar,
A whisper, a word, a shining star.
From the tales of others, we can learn,
And to new heights, we can yearn.”*

Anonymous

Chapter 2: State of the Art and Related Scientific Questions	25
2.1. Preface.....	27
2.2. 4D Printing	27
2.2.1. Related Additive Manufacturing Technologies	29
2.2.2. Smart Materials	33
2.2.3. Stimuli	36
2.2.4. Materials Distribution and Transformations Classification.....	40
2.2.5. Applications.....	45
2.3. Research in Design.....	47
2.3.1. Design for Additive Manufacturing.....	47
2.3.2. Design for 4D Printing	48
2.4. Evolution in Assemblies/Interlocking Assemblies	53
2.5. Key Research Question	56

2.1. Preface

After briefly introducing the concept of 4D printing in the previous chapter and discussing the historical development of manufacturing techniques. We hereby delve deeper into the topic by providing background information on the main pillars of 4D printing, namely related AM techniques, smart materials, and stimuli, with the aim of further comprehending the concept of this technology. It is worth mentioning that the purpose of the thesis is not primarily focused on manufacturing but rather on design and assembly methodologies. Therefore, once the background information has been established, this chapter will proceed by laying out the important advancements in engineering design research and design for X, in order to address 4D printing technology not only in terms of manufacturing but also from a design methodology perspective. Furthermore, this chapter will also highlight critical studies in multi-material assemblies to tackle 4D printing current limitations. The body of literature covering 4D printing is massive, and significantly growing since the appearance of the term by Skylar Tibbits (Massachusetts Institute of Technology) in 2013 (see Figure 13). Let us now analyze these existing findings from a design and assembly-related point of view, identify gaps, and clearly state the key research question that motivates this Ph.D., along with an outline of the proposed solution.

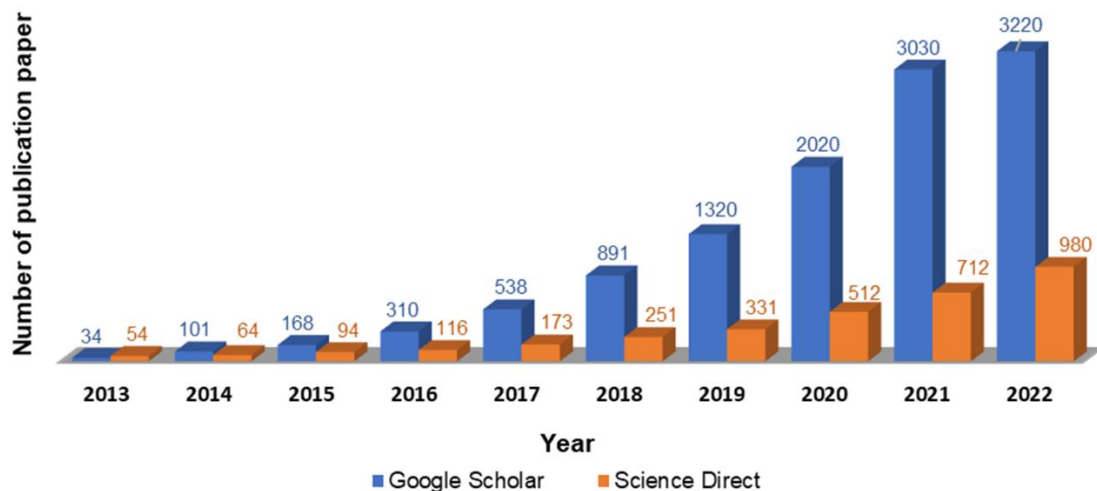


Figure 13: 4D printing existing papers breakdown by year, extracted from [50].

2.2. 4D Printing

In April 2013, Skylar Tibbits hosted a Ted X Talk and presented his proof-of-concept of a self-bending structure [51]. Tibbits is a well-known figure in the field of 4D printing, and his work has been instrumental in advancing the technology. The self-bending structure he demonstrated was created using a combination of 3D printing and SMs, and it was designed to be able to change its shape to MIT form

in response to external stimuli (see Figure 14). This work has been widely recognized as a breakthrough in the field of self-assembly and programmable materials, and it has inspired numerous researchers and engineers to explore the possibilities of 4D printing, marking the beginning of a new era of research and innovation in this field.



Figure 14: A self-bending 4D structure from 1D line to MIT form [34].

In fact, 4D printing defines the fact of combining AM processes and SMs through the use of external or internal stimuli, such as heat, electric current, magnetic field, light, or chemical solvent. This technology introduces a temporal dimension - the fourth dimension of time- to structures and objects, allowing transformability and evolution (see Figure 15) [52]. With this temporal dimension, objects gain the ability to change their shape, properties, functionalities, and states, ultimately leading to increased performance [33,39,53]. Therefore, 4D printing offers greater design flexibility and cost efficiency by expanding the design space. This technology enables multiple transformation scenarios between two states of objects, with various methods of stimulation and selected materials (see Figure 16 for an example of a printed orchid-shaped structure made of a hydrogel composite ink containing aligned cellulose fibrils. These fibrils swell when moisturized) [54-57]. The following sub-sections will provide a more detailed overview of the essential elements of 4D printing: AM processes, SMs, and stimuli.

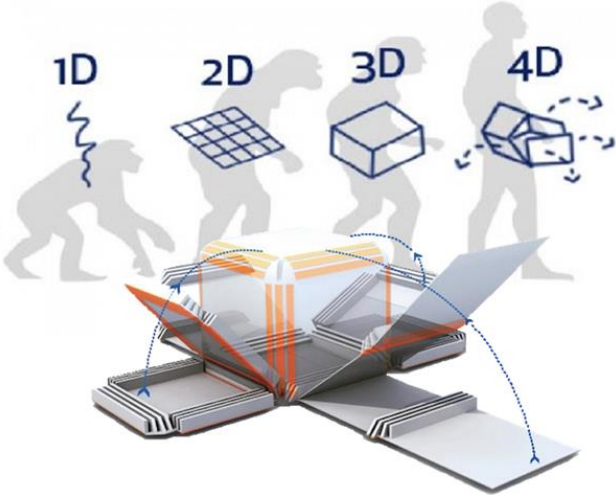


Figure 15: The general concept of 4D printed object dynamic [58].

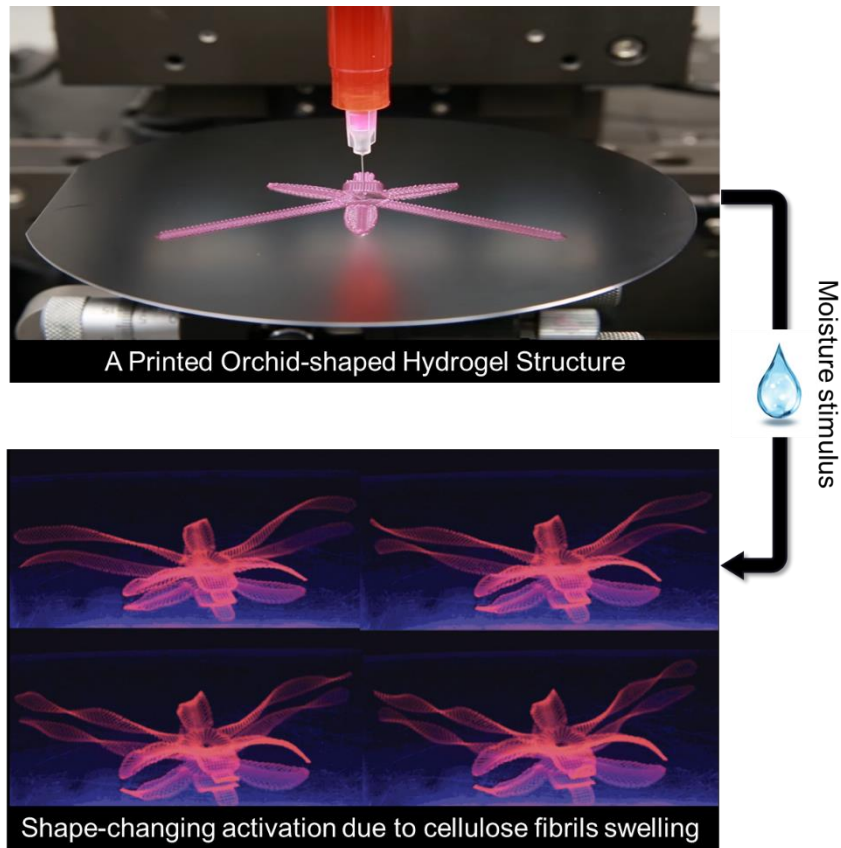


Figure 16: An illustration of a 4D printed shape-changing orchid made of hydrogel, extracted from [55].

2.2.1. Related Additive Manufacturing Technologies

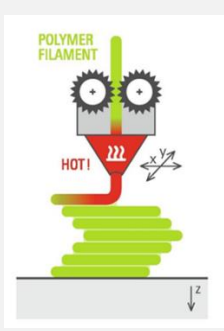
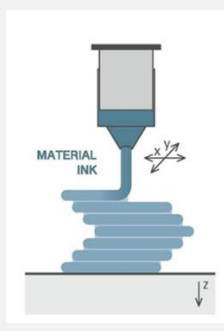
Since its appearance, 3D printing technology has been opening up new possibilities in various industries including medicine, robotics, jewelry, soft sensors, and actuators, automotive, and aerospace engineering [19,21,33]. It is however unattainable to discuss AM without considering the various AM processes involved. AM processes enable the creation of intricate structures that are difficult or impossible to fabricate using traditional manufacturing techniques. Each AM process offers various advantages, such as high precision and accuracy, efficient use of materials, and printing volume to cite a few [2]. Among all the existing AM processes, only a few are used for 4D printing [39,57]. Some of the most commonly used AM processes in 4D printing include Fused Filament Fabrication (FFF) [59,60], Direct Ink Writing (DIW) [2,61], Material Jetting (MJ) [62], Stereolithography (SLA) [63], Digital Light Processing (DLP) [59,64], and Selective Laser Melting (SLM) [39,65]. Their corresponding illustrations are shown in Table 1. Each of these processes has unique features that make them suitable for specific applications. For instance, FFF is commonly used to print large, low-resolution parts, while MJ is ideal for creating intricate designs with high accuracy. From a material deposition capacity perspective, these processes can also be classified into two categories [2,39]: processes that are

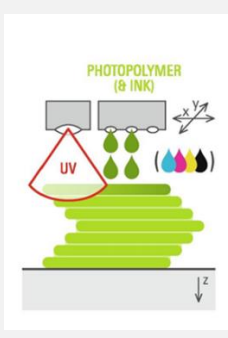
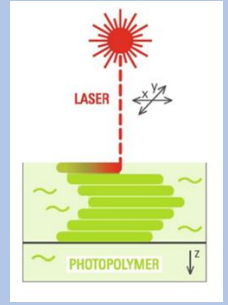
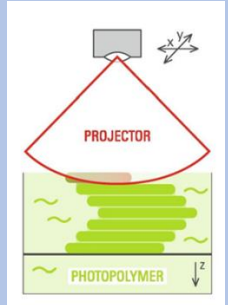
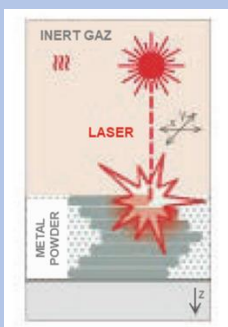
capable of single printing and processes with multi-material printing capacity (see Table 1). AM processes that have the ability to print multiple materials simultaneously offer several advantages over single-material printing techniques leading to improved performances and functionalities [65-71], such as:

- The creation of complex and heterogeneous objects.
- The combination of different materials with varying properties, such as stiffness, elasticity, and transparency, in a single object.
- The ability to create custom-tailored materials with specific properties for particular applications.
- Reducing the need for post-processing to assemble parts, which can save time and reduce production costs.

AM processes are a crucial component of 4D printing technology. The following subsections describe some of the processes used in 4D printing, including MJ, extrusion-based processes, and photopolymerization.

Table 1: AM processes used in 4D printing technology. Extracted from [39].

	AM Process	Description	Typical Processed Materials	Typical Techniques	Illustration
Multi-material capacity	FFF (Fused Filament Fabrication)	Extrudes a continuous filament of thermoplastic material from a nozzle that moves along a predetermined path, building the object layer by layer.	Thermoplastics such as PLA, ABS, PETG, Nylon	Desktop FFF, Large Scale FFF	
	DIW (Digital Light Processing)	A liquid resin is selectively cured using a light source (usually a projector or a laser) that illuminates the entire build platform at once.	Photopolymers	Vat Polymerization	

	MJ (Material Jetting)	Droplets of a material (or a mix of two materials) are selectively deposited in thin layers from a print head and cured either by a source of energy or by environmental conditions.	Photopolymers, wax, polymers	Multi-Jet Modeling (Drop-On-Demand), PolyJet	
Single material capacity	SLA (Stereolithography)	A liquid photopolymer is selectively cured by a UV laser that traces a cross-section of the object onto the surface of a liquid resin.	Photopolymers	Vat Polymerization	
	DLP (Digital Light Processing)	Similar to SLA, but instead of a laser, a digital projector is used to selectively cure the liquid resin.	Photopolymers	Vat Polymerization	
	SLM (Selective Laser Melting)	A high-power laser selectively melts and fuses metal powder or wire, building up the object layer by layer.	Metals and alloys such as titanium, aluminum, stainless steel, nickel alloys	Powder Bed Fusion	

2.2.1.1. Material Jetting Processes

Material jetting involves depositing droplets of a material or a mix of materials in precise locations to build up a part in a layer-by-layer fashion. The process is similar to inkjet printing, where ink droplets are deposited onto paper to create text or images. In material jetting, a print head containing multiple nozzles is used to selectively deposit droplets of material onto a build platform with automatically generated sacrificial support materials to support overhanging structures [72]. The material is typically in a liquid or semi-liquid form, such as a polymer or wax, and is heated or cooled to achieve the desired

viscosity. As the droplets are deposited, they are cured or solidified either by exposure to a source of energy, such as UV light or by environmental conditions, such as air or heat. One example of a material jetting printer is the PolyJet technology from Stratasys, which uses a print head to jet tiny droplets of liquid photopolymer onto a build tray layer by layer. The droplets are immediately cured by UV light, producing fully cured parts with fine details and smooth surfaces. Another example is the Drop-on-Demand (DOD) inkjet printing technology, which is used by the 3D Systems ProJet line of printers. These printers can use a range of materials including plastics, ceramics, metals, and wax, and can produce high-resolution parts with excellent surface finish. By using a print head with multiple nozzles or multiple print heads with different materials, it is possible with this process to print parts with different properties like color, stiffness, and melting point, in a single build. This makes the process particularly useful in applications that require complex geometries or multi-functional parts like 4D printing [73].

2.2.1.2. Material Extrusion-Based Processes (FFF/DIW)

This process involves the extrusion of material through a nozzle during the printing process. Extrusion-based AM techniques have certain distinguishing characteristics, including the loading of material, material liquefaction, the method of pressure applied to move the material through the nozzle, the deposition strategy, the ability to create support structures, and bonding between layers. FFF and DIW are two examples of extrusion-based AM processes [74]. FFF involves the deposition of melted filament material in a predetermined pattern on a build platform to create a three-dimensional object [75-77]. The melted filament is deposited through a nozzle onto the platform, where it solidifies and forms a layer. The platform then lowers, and a new layer is deposited on top of the previous layer until the object is completed. FFF printers can use a variety of thermoplastic filaments of different colors and material properties, including flexible and conductive materials. DIW is a process similar to FFF, but instead of using a solid filament, it uses liquid ink or a paste that is extruded through a nozzle. The ink or paste is typically a mixture of a polymer precursor and a solvent, which are deposited onto the build platform and cured using a UV light or a chemical reaction. DIW is commonly used to print soft materials such as hydrogels and elastomers, which are not compatible with FFF printers. Both FFF and DIW offer advantages in terms of their simplicity, versatility, and low cost. They are widely used in prototyping, small-scale production, and education due to their ease of use and accessibility. However, they are limited in terms of the resolution and precision that can be achieved, making them less suitable for high-precision or high-performance applications [59,78].

2.2.1.3. Photopolymerization-Based Processes (SLA/DLP)

This process works by selectively exposing liquid photopolymer resin to light, causing it to solidify and bond to the previous layer. There are two main types of photopolymerization: Stereolithography (SLA) and Digital Light Processing (DLP) [2]. In SLA, a laser or a UV light source is directed onto a vat of liquid photopolymer, causing the liquid to solidify at the desired locations. The solidified part is then

lifted out of the vat, and the excess liquid is drained away. The process is repeated for each layer until the entire object is created. The process is highly accurate, can produce parts with high resolution and surface quality, and is suitable for creating complex geometries. A newer version of SLA, known as micro-Stereolithography (μ SLA), has been developed that uses a higher resolution laser to produce even finer intricate parts that are less than a millimeter in size. In DLP, a projector is used to project an image of the object onto the surface of the photopolymer, causing it to solidify at the desired locations. This method is similar to SLA, but the entire layer is cured at once, making it faster than SLA. However, it can result in lower resolution and surface quality than SLA. One advantage of photopolymerization is the ability to print with a wide range of materials, including resins that have different properties such as color, flexibility, and strength [59,79]. However, the process is limited to materials that can be cured with light, and the final parts can be brittle and susceptible to breaking under stress. Some examples of photopolymerization printers include Formlabs Form 3 and EnvisionTEC Perfactory.

2.2.2. Smart Materials

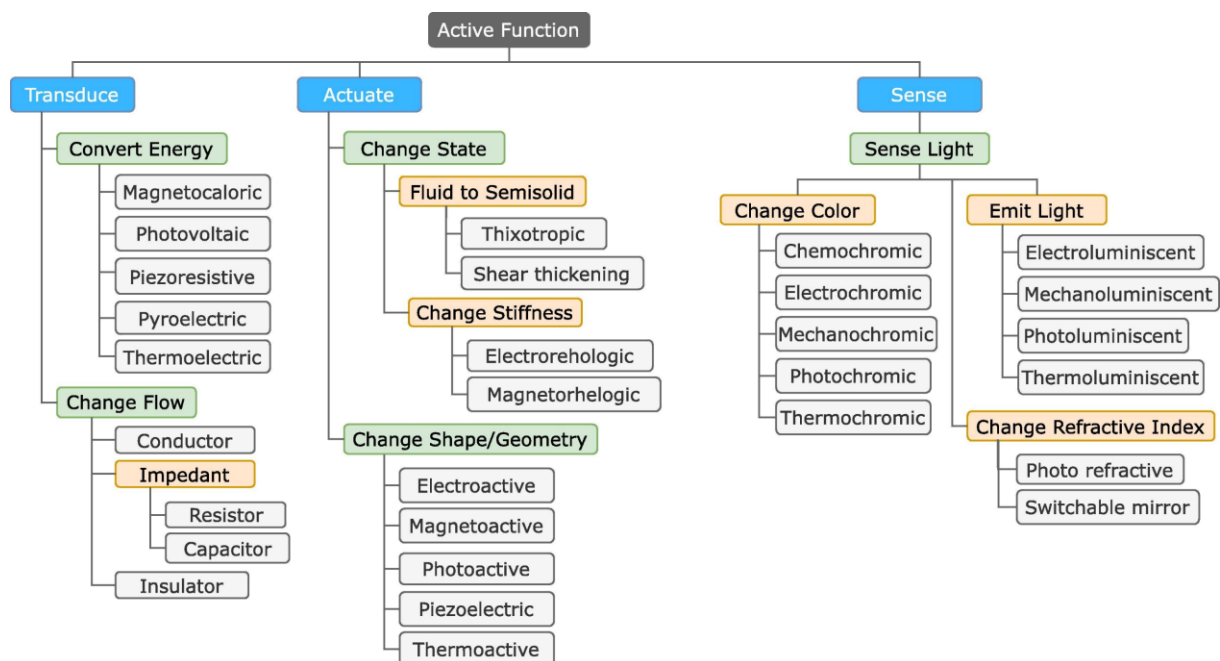


Figure 17: Smart materials classification according to their active function [2,39,59].

The development of SMs can be traced back to research on shape morphing and artificial muscles. In the 1950s and 60s, researchers began exploring the idea of creating materials that could change shape in response to an external stimulus, such as heat or electricity [59,70,80]. This research led to the development of shape-memory alloys (SMA) and shape-memory polymers (SMP), which can "remember" their original shape and return to it when heated [81,82]. In the 1970s and 80s, research into piezoelectricity - the ability of certain materials to generate an electric charge when subjected to mechanical stress - paved the way for the development of piezoelectric sensors and actuators [83]. In

the 1990s, researchers began to explore the use of electroactive polymers (EAPs) as artificial muscles, capable of contracting and expanding in response to an electric field. This research, along with advances in nanotechnology and materials science, has paved the way for the development of a wide range of SMs with unique and useful properties [84,85].

In this section, we will briefly review the realm of SMs. While there are many definitions of SMs in the literature, they all agree that SMs are materials whose physical or chemical properties are altered in response to a specific change, or stimulus, in their environment [86-88]. The goal behind incorporating these properties is to add intelligence to matter, so that it can behave autonomously by sensing, reacting, and adapting to the environment, much like a biological system [21,66,85]. Based on their response to an energy stimulus, SMs can be categorized into the following families (see Figure 17):

- Energy converters: These SMs are capable of converting one form of energy into another. For example, piezoelectric materials can convert mechanical stress into an electrical charge, while thermoelectric materials can convert heat into electricity.
- State changers: These SMs can change their physical state in response to an external stimulus, such as a change in temperature or pressure. Examples include thermochromic materials, which change color in response to a change in temperature.
- Flow changers: These SMs can act as valves or pumps, by altering the flow of an energy. They may be conductors (control electrons flow), impeding (control electricity flow), or insulators (do not easily transmit an energy flow)
- Light sensors: These SMs are sensitive to light and can be used in a variety of applications, including optical switches and displays. Examples include photochromic materials, which change color in response to light, and liquid crystals, which can change their optical properties in response to an electric field [86].
- Shape changers: These SMs are capable of changing their shape in response to an external stimulus such as heat, light, or electricity [87-92]. Besides SMPs and SMAs [93-96], this category includes the following subgroups:
 - Hydrogels: can swell or shrink in response to changes in temperature, pH, or the presence of certain chemicals. They are commonly used in biomedical applications such as drug delivery and tissue engineering [57,70,92].
 - Piezoelectric materials: such as quartz and some ceramics, can change their shape when an electric field is applied to them. Conversely, when they are subjected to mechanical stress, they generate an electric charge. These materials are used in sensors, actuators, and energy-harvesting devices.
 - Electrostrictive materials: such as barium titanate and lead magnesium niobate, can change their shape in response to an electric field. They are used in sensors, actuators, and microelectromechanical systems (MEMS).

- Magnetostrictive materials: such as iron-gallium alloys and Terfenol-D, can change their shape in response to a magnetic field. They are used in sensors, actuators, and vibration-damping systems [59].
- Photostrictive materials: such as some glasses and crystals, can change their shape in response to light. They are used in optical switches, light shutters, and image stabilization systems [70].

It is worth noting that some shape-changers can automatically change their form once subjected to a stimulus. They can either return to their permanent shape or not when the stimulus is removed, depending on their shape memory effect (SME) [93]. However, other materials require additional steps to program their shape permanent configurations and make the material “remember” them. SME can be categorized as either a single-way or multi-way SME [2,94]. The single-way SME refers to the classic where a material changes in form after a stimulus is applied. However, unidirectional SME materials have the significant disadvantage of irreversibility. On the other hand, a multi-SME material has one permanent form and multiple temporary [95]. Speaking of the irreversibility, Table 2 will provide an overview of the strengths, other weaknesses, and potential applications of each shape-changing SM.

Table 2: SMs strengths, weaknesses, and potential applications

Smart Material	Strengths	Weaknesses	Potential Applications
SMP	-Good shape recovery -Easily processed -Potential for biocompatibility	-Limited strength and stiffness -Long response time	Biomedical devices, self-healing materials, soft robotics, aerospace, automotive
SMA	-High strength and stiffness -Fast actuation speed -Elasticity -Resistance to fracture -Good thermal and mechanical memory	-Limited recoverable strain -High cost -Rapid defects formation	
Hydrogel	-Potential for biocompatibility -Good swelling and responsiveness to stimuli	-Weak mechanical properties -Slow response time	Tissue engineering, drug delivery, sensors
Piezoelectric Material	-Fast and precise actuation -High energy conversion efficiency	-Brittle -Limited strain and temperature range -Not common in 4DP	Sensors, energy harvesting, actuators
Electrostrictive Material	-High energy density -Fast response time	-High driving voltage -Limited strain	Actuators, micro-robotics
Magnetostrictive Material	-High energy density -Good durability -High resistance to temperature	-Limited strain -Limited printing volume	Actuators, sensors, energy harvesting

Photostrictive Material	-High sensitivity to light -Fast response time	-Limited actuation force - Not very used in 4DP	Optical switches, sensors, micromechanical systems
--------------------------------	---	--	--

2.2.3. Stimuli

4D printing refers to a technology that involves the creation of 3D printed objects that can change their shape/property over time in response to energy stimulation [96]. A diverse array of stimuli has been exposed in the literature, such as heat, light, or moisture (see Figure 18) [97-99]. These stimuli trigger the programmed material to transform from its initial shape/property into a new, pre-designed shape/property [100-105].

There are different mechanisms involved in 4D printing [2,56,97]. Thermomechanical and hydromechanical mechanisms are two of the most common mechanisms used in this technology. There exist other mechanisms that will be discussed in the following subsections, including the unconstrained hydro-thermo-mechanism, unconstrained pH mechanism, unconstrained thermo-photo mechanism, dissolution mechanism, and osmosis mechanism. These mechanisms can be used individually or in combination to achieve the desired transformation [2,106,107].

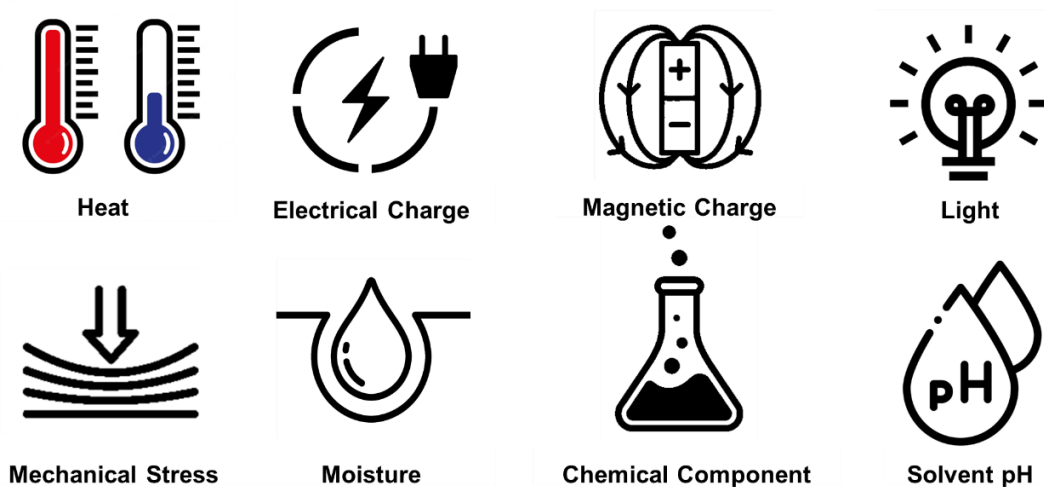


Figure 18: Stimuli illustration

2.2.3.1 The Constrained-Thermo-Mechanism

It is a type of stimuli-response mechanism used in 4D printing that involves the use of heat as the external stimulus. With this mechanism, the smart printed structure is composed of two materials: a rigid material and a thermally responsive active material. When subjected to a specific temperature, the active material undergoes a transition phase, which results in a change in its shape. The shape change is driven by the difference in thermal expansion coefficients between the two materials, which generates a force that leads to the shape change. The magnitude and direction of the shape change depend on the spatial

arrangement of the two materials [56,97]. This mechanism has potential applications in various fields, including medicine, aerospace, and robotics. For example, in medicine, constrained-thermo-mechanisms can be used to create implants or prosthetics that can change shape to conform to the surrounding tissues or organs [108]. Figure 19 illustrates an example of a constrained-thermo-mechanism.

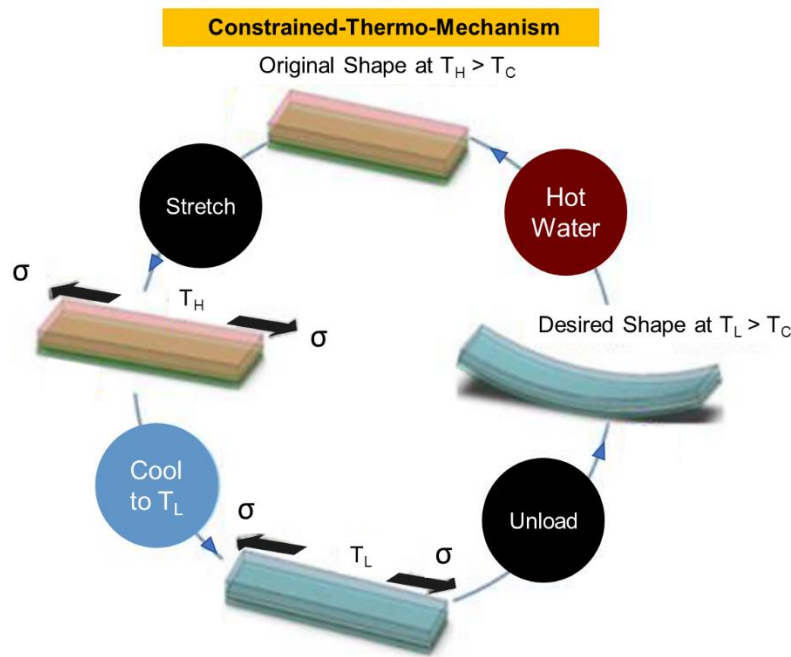


Figure 19: Constrained-thermo mechanism [56,97].

2.2.3.2. The Unconstrained-Thermo-Mechanism

The unconstrained-thermo-mechanism is a variant of the thermo-mechanical mechanism in which the shape-shifting behavior of the printed structure is not restricted by external stresses during the cooling process. With this mechanism, the printed structure is heated above its glass transition temperature to allow it to deform freely and then cooled to a temperature below its glass transition temperature to lock in the temporary shape. Unlike the constrained-thermo-mechanism, the cooling process is not controlled, and the printed structure is free to deform spontaneously. The structure can then be reheated above its glass transition temperature to recover its initial shape, and the cycle can be repeated. In some cases, this mechanism is combined with other stimuli, such as pH or light, to achieve multi-responsive behavior. Compared to constrained-thermo-mechanism, the unconstrained-thermo-mechanism offers more flexibility and spontaneity in shape-shifting but may also lead to less predictable and less controlled behavior [56,109].

2.2.3.3. Unconstrained-Hydro Mechanism

In this context, a smart structure is composed of two materials: a rigid material and a hydrophilic active material. The goal is to create a shape-shifting structure that can change its shape when placed

underwater and return to its original shape when dried [110]. This mechanism is based on the difference in swelling ratios between the active and rigid materials, which creates a force that leads to the shape change. To achieve complex shape-shifting behaviors, the SMs must be arranged in a specific pattern with other rigid materials. The magnitude and direction of the shape change depend on the spatial arrangement of the two materials. This mechanism is naturally reversible, meaning that drying the smart structure will recover its original shape (see Figure 20 for an illustration).

2.2.3.4. Other Mechanisms

There are also other composed mechanisms that can be used in 4D printing, such as unconstrained hydro-thermo-mechanisms, unconstrained pH mechanisms, unconstrained thermo-photo mechanisms, dissolution mechanisms, and osmosis mechanisms (see Figure 20). Unconstrained hydro-thermo-mechanisms use water as a stimulus to trigger the shape-shifting behavior. The printed structure consists of a hydrogel that can absorb water and a rigid material. The swelling of the hydrogel generates a force that leads to shape change. Heating the structure can fix the temporary shape and cooling it to room temperature will recover the original shape [97-111].

While unconstrained pH mechanisms use changes in the pH level of the surrounding environment to cause the material to change shape. Unconstrained thermo-photo mechanisms, on the other hand, use a combination of heat and light to trigger the transformation of the printed material. When the structure is exposed to light, the polymer undergoes a conformational change, leading to shape change. The shape change can be fixed by heating the structure, and the original shape can be recovered by cooling it down.

As for dissolution mechanisms, they work by printing the object with two or more materials, one of which can dissolve in a specific solvent. Once the printed object is exposed to the solvent, the dissolved material is removed, causing a change in the structure and shape of the object.

Finally, osmosis mechanisms involve the diffusion of a solution across a semi-permeable membrane to induce shape change. The printed structure consists of a hydrogel and an inert material. When the hydrogel is exposed to a solution with a different concentration, it swells or shrinks, leading to shape change. The shape change can be fixed by drying the structure, and the original shape can be recovered by exposing it to the original solution [112-114].

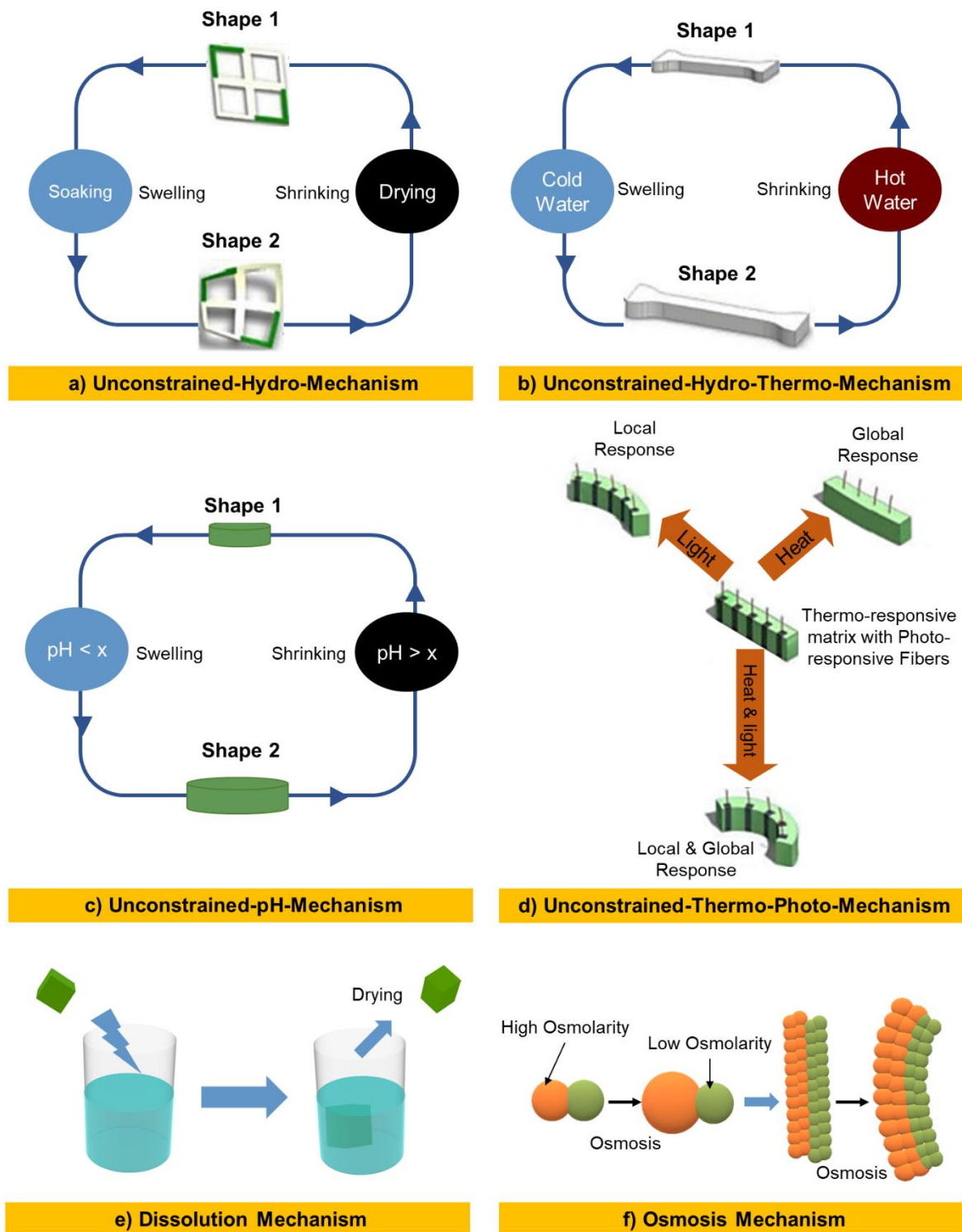


Figure 20: Different stimulation mechanism illustrations, extracted from [56-97]

Each of these mechanisms has unique advantages and disadvantages, depending on the intended application of the 4D printed object (see Table 3). For example, hydromechanical mechanisms are highly responsive to changes in moisture levels and can be used for biomedical applications, while thermomechanical mechanisms are highly precise and can be used in engineering applications.

However, some mechanisms may also have limitations, such as the irreversible nature of shape changes in some materials, or the slow response times of others.

Table 3: Stimulation mechanisms with involved materials and their potential applications.

Stimulation Mechanism	Involved Materials	Potential Applications
Constrained-Thermo-mechanisms	Thermoset polymer and rigid filler materials	Multi-shape memory structures
Unconstrained-Thermo-mechanisms	Thermoplastic polymer and filler materials, typically elastomers	Self-folding objects, soft robotics, morphing aircraft wings
Unconstrained Hydro-mechanisms	Hydrogels and water	Drug delivery, tissue engineering, sensors
Unconstrained-Hydro-Thermo-mechanisms	Hydrogels and temperature changes with water	Drug delivery, tissue engineering, sensors
Unconstrained-pH mechanisms	Polymers sensitive to pH changes and water	Controlled drug delivery, smart packaging, soft robotics
Unconstrained-Thermo-Photo mechanisms	Photo-responsive polymers and temperature changes	Self-assembling structures, soft robotics, sensors
Dissolution mechanisms	Water-soluble polymers and water	Controlled drug delivery, self-destructing devices
Osmosis mechanisms	Semi-permeable membranes and osmotic pressure changes	Water filtration, energy harvesting

2.2.4. Materials Distribution and Transformations Classification

2.2.4.1. Materials Distributions

Material distribution in 4D printing refers to the way different materials are arranged within a printed structure to achieve desired shape/property-changing behavior. There are two main categories of material distribution: homogenous and heterogeneous distributions:

- **Homogeneous material distributions:** In 4D printing, they refer to the uniform distribution of materials throughout the 3D printed object. It can be achieved either by mixing the materials before printing or using a printing process that ensures even distribution. One should comprehend that the printing process parameters are highly important, even when one material is used for printing [92]. As depicted in Figure 21, it is feasible to control the transformation by modifying the path of the nozzle and the induced stresses during the material deposition phase. Homogeneous material distribution can improve the performance and functionality of 4D printed objects, reducing the risk of defects and

inconsistencies. However, it may also limit the ability to create complex structures with varying properties, as the entire object will have the same material composition.

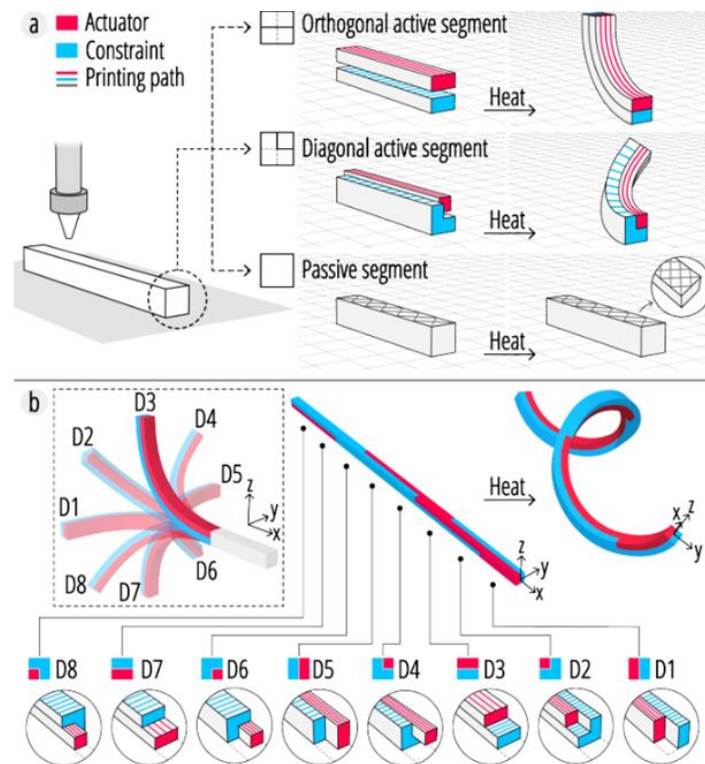


Figure 21: A beam structure with different printing paths. (a) Examples of segment compositions; (b) Possible bending transformations. A helix can be created by applying heat to a straight line through the combination of various bending directions in different segments [92].

- **Heterogeneous material distributions:** Multi-material distributions involve arranging different materials in distinct regions or patterns, resulting in a more complex and tailored shape/property-changing behavior [115-119]. When the structure is composed of more than one material, it can either be a blend of different SMs or a combination of SMs and passive materials in a single printed object [120-126]. These types of distributions can lead to various transformations, including bending and twisting beyond linear expansion and contraction, depending on the specific combination of the involved materials [126-128]. Here are the different categories of multi-material distributions in 4D printing (see Figure 22):

- **Multilayer distributions:** In this category, materials are layered one over the other to achieve the desired functionality.
- **Gradient distribution** involves arranging different materials in a gradual manner, resulting in a gradient of properties, such as stiffness or swelling behavior, across the structure.
- **Special pattern distributions:** In this category, materials are distributed in a specific pattern to achieve a desired function [56,129,130].
- **Digital distributions:** The idea of digital conceptualization can be applied to material structures as well. In this approach, the basic building block that occupies a 3D physical space is called a

voxel and it allows for a shift from analog to digital materials [131-134]. Therefore, a digital material is essentially a voxel. Physical voxels, or printed voxels, can serve as building blocks for 4D printed objects in multi-material structures where materials are distributed using computer algorithms [135-138]. The temporal arrangement of these voxels plays a crucial role in defining the final shape and behavior of the 4D printed structure [134]. Nonetheless, the utilization of AM processes and machines that can accommodate digital materials is imperative for achieving this distribution category [59,70,71,86].

Multi-material distribution allows for the creation of complex and functional objects that cannot be achieved with a single material (see Figure 22).

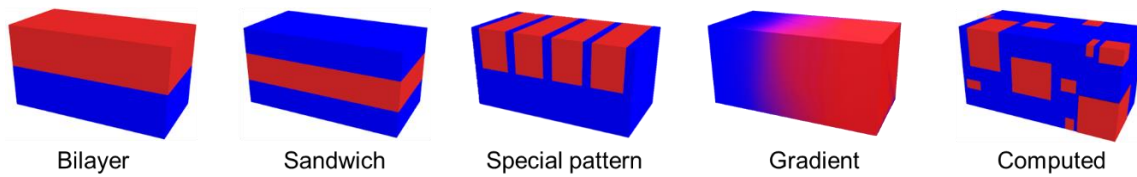


Figure 22: Multi-material distribution categories [139].

2.2.4.2. Transformations Classification

Besides the energy stimulation, shape or property transformations are directly influenced by the material distributions in the printed structure (refer to Figure 23). For instance, if a 4D printed object has a non-uniform material distribution, the resulting property transformations may be localized to specific regions of the object. In this section, we will focus on the transformations from a shape behavior perspective. Each transformation can manifest in different dimensions, such as converting a 2D origami structure into a 3D cube or transforming a 1D line into a 3D spatial structure. The following enumerations will highlight 4D transformations in terms of shape-changing:

- **Bending** (see Figure 24): Bending transformation involves the curving of a 3D printed object along specific axes, creating an obtuse angle (less than 180°). The process relies on the orientation and distribution of the printed material to achieve the desired curvature [140]. Bending can be achieved by controlling the stiffness of the material and the magnitude of the curvature [2,34,59].

- **Folding** (see Figure 25): Folding is a transformation that involves the creation of a crease or folds in a 3D printed object, which allows it to collapse into a more compact form. This transformation can be achieved through the use of special hinge-like structures that can be incorporated into the design [70,141].

- **Expansion/contraction** (see Figure 26): These transformations involve linear changes in the dimensions of a 3D printed object, either by increasing or decreasing its size. For instance, this

transformation can be achieved through the use of materials with different coefficients of thermal expansion, which respond differently to changes in temperature [2,34].

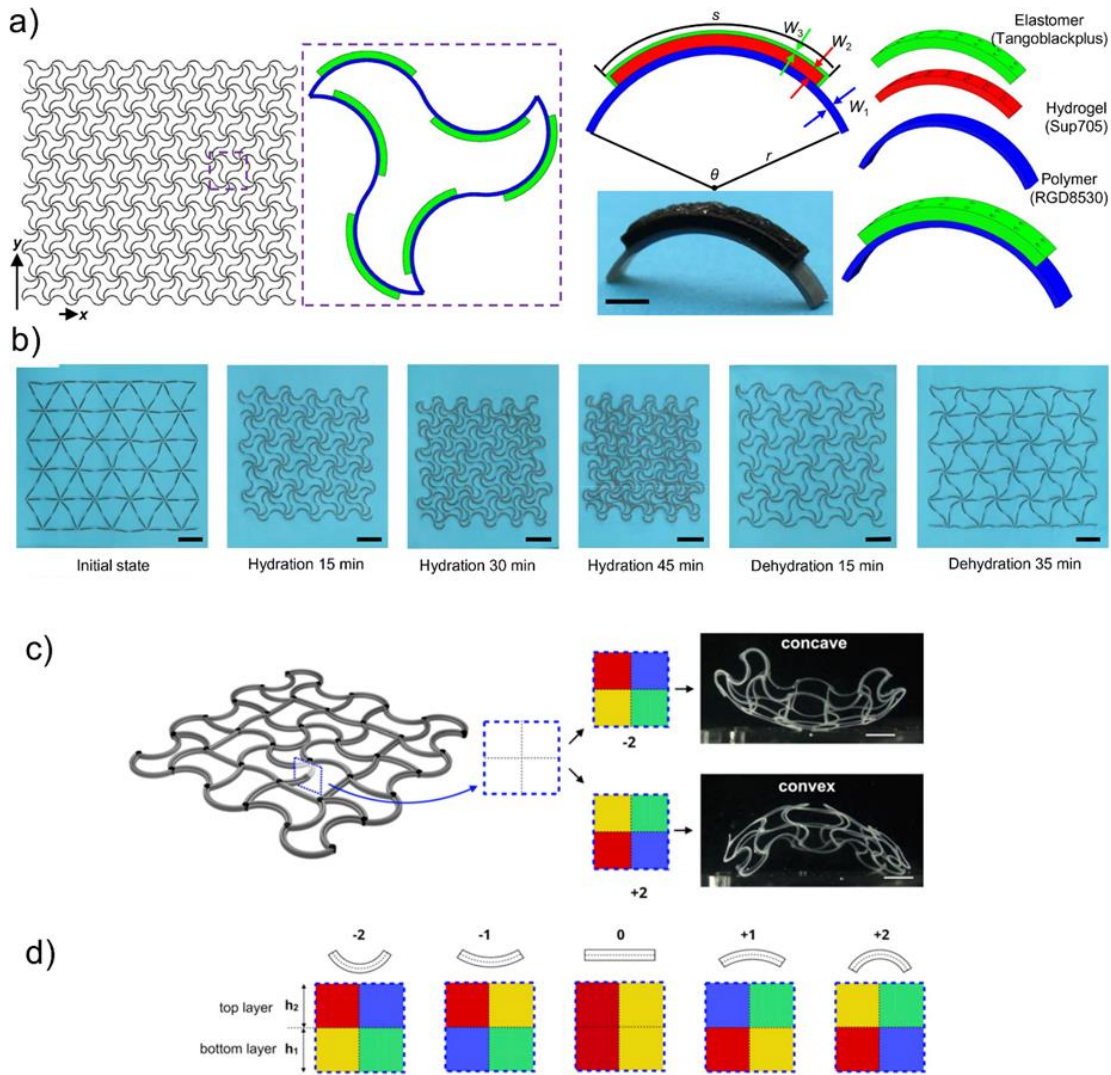


Figure 23: Example of an active multi-material structure using PolyJet® technique. (a) The patterns, (b) moisture-based stimulation, (c) the multi-material section structures printed using DIW and responsible of (d) bending orientation in 2D-to-3D transformation lattice-based applications [39].

- Twisting/helixing/waving (see Figure 27): These transformations involve the creation of helix-like or wave-like structures in a 3D printed object along different axes. This can be achieved through the use of materials with different mechanical properties, which respond differently to external stimuli such as heat or light [34,132].

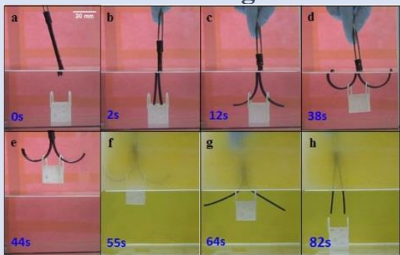
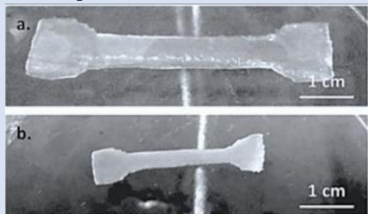
- Surface curling (see Figure 28): It involves the deformation of the printed object's surface into a curled shape, shifting the object from a 2D to a 3D configuration. This can be achieved through the

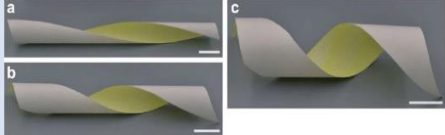
use of materials with different thermal expansion coefficients or through the application of heat or moisture [39,70].

- Surface topographical change (see Figure 29). This transformation involves the creation of 3D surface patterns on a 3D printed object. It is enabled by pressure discrepancies resulting from the differential stretching properties of stiff and active materials when submerged. This can be achieved through the use of materials with different mechanical properties or through the application of heat or light. The resulting patterns can be used for a variety of applications, such as creating textures or controlling fluid flow [34].

Table 4 gathers such information and adds potential applications for each 4D transformation. Note that these applications are not exhaustive and may be overlapped between different transformations and their applications.

Table 4: 4D printing transformations and examples of applications.

Transformation	Description	Applications
<p style="text-align: center;">Bending</p>  <p>Figure 24: Smart bending hook [142]</p>	<p>Curving or flexing of the printed object along one or more axes</p>	<p>Medical implants, soft robotics, deployable structures, morphing aerospace structures, architecture</p>
<p style="text-align: center;">Folding</p>  <p>Figure 25: Self-folding structure [34]</p>	<p>Creasing or curvature change along multiple axes, resulting in a flat-to-3D transformation</p>	<p>Self-assembling furniture, origami-inspired structures, packaging, medical devices</p>
<p style="text-align: center;">Expansion/Contraction</p>  <p>Figure 26: Hydrogel sample states [30]</p>	<p>Changing of dimensions of the printed object along one or more axes, usually due to changes in environmental conditions</p>	<p>Smart textiles, biomedical devices, energy harvesting, soft robotics, actuators</p>

<p>Twisting/Helixing/Waving</p>  <p><i>Figure 27: Example of helixing behavior [143]</i></p>	<p>Rotational or twisting movement of the printed object along its length or width</p>	<p>Robotics, sensors, aerospace</p>
<p>Surface Curling</p>  <p><i>Figure 28: Curling behavior [34]</i></p>	<p>Localized curling or bending of the surface of the printed object to create complex textures or shapes</p>	<p>Wearable technology, optics, architectural facades, consumer products</p>
<p>Surface Topographical Change</p>  <p><i>Figure 29: multiple curving behavior [34]</i></p>	<p>Alteration of the surface texture or shape of the printed object</p>	<p>Sensors, biomedical devices, soft robotics, adaptive surfaces.</p>

2.2.5. Applications

The ability to create objects that can change their shape or properties over time is what makes 4D printing unique and promising [125-128]. Self-assembly, self-adaptability, time gain, medical devices, pH-response, adaptive metamaterials, soft robotics, and active origami boxes are just a few of the applications of 4D printing [21]. Here are some illustrating examples:

- **Medical devices:** are an area where 4D printing is gaining popularity. The technology can be used to create customized implants and prosthetics that adapt to the patient's body over time. For example, 4D printed stents can expand and contract to fit the shape of blood vessels, reducing the risk of complications [126-127]. A 4D printed stent can also change its shape to fit the arc patterns and cartilaginous rings after insertion into the body. For example, researchers at the University of Texas at Austin have developed a 4D printed stent that can change its shape in response to the patient's body temperature, allowing for a better adaptation [144-146]. Additionally, in [147], a highly responsive and reversible skeletal muscle-like actuator was proposed, which was employed in a smart valve to regulate water flow. The actuator was capable of opening the valve in cold water and closing it in hot water, indicating the potential of 4D printing in creating smooth mechanical actuators.

- Soft robotics: is another field that is gaining popularity due to its potential to revolutionize many industries such as healthcare, manufacturing, and space exploration. 4D printing can be used to create soft robots that are flexible, adaptable, and can change their shape or properties in response to external stimuli. Researchers in [148] have developed a 4D printed soft robot that can crawl and change its shape under light and magnetic field. This source [121-125] demonstrated the lateral movement of a caterpillar, which can be useful for developing intelligent components in advanced systems.

- Self-Assembly: refers to the ability of printed objects to assemble themselves into a desired shape without the need for external manipulation. With the potential use in both micro- and macro-scale devices, these objects have the capability of revolutionizing many fields, including medical care, construction, manufacturing, and robotics to name a few [143]. At the small scale, for instance, researchers at MIT have developed a 4D printed strand that can be programmed to fold itself into a specific shape when exposed to water [34]. At the macro-scale, these objects also offer multiple possibilities. For example, structures can be printed using specific AM machines and then activated into larger or smaller systems such as satellites, antennas, and spacecrafts. This approach is relatively simple, cost-effective, and easy for transport and store purposes [123].

- Self-adaptability: refers to the ability of printed objects to change their shape or properties in response to external stimuli. For example, 4D printed materials can change their stiffness or flexibility, making them useful for soft robotics and prosthetics. This has potential applications in fields such as aerospace, where structures can adapt to different airflow conditions, or in prosthetics, where the device can adapt to the shape and movement of the user's body. For example, a team at the University of Wollongong in Australia has developed a 4D printed hand prosthetic that can change its shape to adapt to the user's grip [149]. Another example is the use of 4D printing in the textile industry. In contrast to fabrics made of stretchable fibers, intelligent textile designs with self-adaptive features can be resized without the need for any stretching force. These smart textiles have multiple functions such as regulating body moisture and temperature, monitoring wounds, providing skin care, offering protection against severe weather conditions, and even changing clothing color [150].

- Adaptive metamaterials: are another area where 4D printing is showing great possibilities. Metamaterials are materials with properties that are not found in nature [151-154], such as negative refractive index or acoustic cloaking, making them useful for a variety of applications such as soundproofing, energy absorption, and stealth technology. For example, two studies [104,143] involved lattice designs that could be reconfigured in a reversible manner, with heat serving as an external stimulus. These metamaterials can have mechanical properties that depend on their geometric architecture instead of their chemical composition [154-156].

- Time gain: 4D printing can save time and resources in manufacturing by allowing for objects to be printed in their final shape. Certain structures can be modified to eliminate the need for external electromechanical devices. With 4D printing, sensors, and actuators can be integrated directly into the product, which reduces the number of components required for design, installation time, equipment, and

power costs. This can be particularly useful in fields such as aerospace, where complex and customized parts can be printed on demand [19,21].

- pH-Response materials: can be used for drug delivery, where the drug is released only when the pH level reaches a specific threshold. For example, researchers at the University of Portsmouth in the UK have developed a 4D printed pH-responsive hydrogel that can change its shape in response to changes in pH, allowing for controlled drug release [157]. These types of materials can also serve as an important platform for pH-responsive membranes and photonic gels [158]. For instance, in [159], a valve was 3D printed which displays a responsive behavior of swelling and shrinking and is capable of regulating the flow rate based on the pH levels.

- Active origami: can fold and unfold themselves, making them useful for storage, transportation, and packaging. For example, researchers at Georgia Institute of Technology have developed a 4D printed origami box that can fold and unfold in response to changes in temperature. In [140], an origami layout algorithm for freeform surfaces was proposed. Additionally, self-bending bio-origami structures were suggested and created for use in tissue engineering in [123].

2.3. Research in Design

From the preceding sections, one can comprehend that the key factors that contribute to 4D printing technology are stimuli, geometry, AM processes/techniques, SMs, and transformation functions. It is also clear that it requires a combination of science and engineering studies to enhance this technology's applications and overcome related obstacles regarding the quality and efficiency of the AM processes and SMs/AM techniques combinations. These obstacles become even more crucial when dealing with multi-material setups and complex printed structures. Therefore, looking at 4D printing technology from a design perspective is also important in the process of establishing and adopting it in the industry. The next subsections will focus on reviewing the existing literature on this topic. First, design for additive manufacturing will be addressed, then, design for 4D printing will follow.

2.3.1. Design for Additive Manufacturing

The introduction of AM has necessitated a paradigm shift in designing objects for manufacturing, as it eliminates many of the constraints associated with traditional subtractive manufacturing processes. AM offers various freedoms, including the ability to produce complex shapes, hierarchical and functional assemblies of parts, and multi-material parts [21]. However, there are also constraints, such as minimum/maximum achievable dimensions, anisotropy, intern constraints, and the need for support materials, that must be considered during the design process to ensure the manufacturability of the part [160]. Effective design for AM (DFAM) should balance these constraints with the opportunities offered

by the process to maximize the performance of the part. DFAM should also consider the layer-by-layer nature of AM in order to take full advantage of the capabilities of AM processes [160-162].

Many studies have been conducted to develop design rules specific to the various AM processes (such as designing specific software that can effectively consider the unique characteristics of AM to replace software packages used in traditional manufacturing), top-down design approaches, and re-design approaches. These approaches provide recommendations on geometry and materials, global design methods, and the integration of functions and part consolidation, respectively [163,164].

There are several existing literature and case studies concerning DFAM that demonstrate how it can be used to optimize the design and production of a wide range of products, from aerospace components to medical implants. One such example is Airbus, which used AM to create a 3D printed titanium bracket for the A350 XWB aircraft [165-166]. The bracket was designed using DFAM principles, which reduced the weight of the part by 40% compared to the conventional manufacturing method.

Another example is the use of DFAM in the production of custom-made implants in the medical industry. By using AM, it is possible to produce implants with complex geometries that are specific to the individual patient's requirements. For instance, King Saud university has produced cranial implants using AM that are tailored to each patient's needs, resulting in faster recovery times and better outcomes [167].

In addition to aerospace and medical applications, DFAM has also been used to produce unique consumer products, such as the Adidas Futurecraft 4D shoe. The shoe's midsole is made using a process called Digital Light Synthesis (DLS), which combines AM with liquid polymer. The DFAM principles used in the production of the Futurecraft 4D midsole ensure that the shoe is both lightweight and comfortable while providing the required support [168].

While these approaches have shown the functional role of DFAM, their material considerations are purely structural and based on conventional materials. To account for the use of SMs in 4D printing, it may be necessary to extend these approaches by including SMs properties in order to cover design for 4D printing similarly.

2.3.2. Design for 4D Printing

In order to effectively design for 4D printing, a comprehensive understanding of various aspects of the technology is essential. This includes knowledge of the materials, the printing processes, and the potential applications of 4D printed objects [169-170].

For instance, to formalize 4D printing knowledge, a domain ontology called HERMES has been built in [171] using basic formal ontology (BFO) and underpinning theories like 3- and 4-dimensionalisms. The

approach required a strong knowledge base of stimuli, SMs, product, and manufacturing/stimulation/actuation process models. First, the authors have developed a domain ontology that collects and formalizes scattered 4D printing knowledge for use in the conceptual design stage. Secondly, they defined a multi-representation of a 4D printed object in the conceptual design stage. Finally, they built a recommendation system that assists the designer in selecting the material distribution according to the specific requirements in the conceptual design stage. Additionally, a design for 4D printing roadmap has been developed in [39], taking into account the challenges and opportunities associated with the technology. The roadmap aimed at mapping out all aspects of 4D printing in order to deliver functional and practical products and systems, including short to long-term objectives. Table 5 and Figure 30 respectively provide an overview of the roadmap highlighting the complexity and challenges associated with 4D printing, as well as the suggested design for 4D flowchart.

Table 5: A suggested roadmap of design for 4D printing technology, extracted from [39].

	Achieved Today	Short-Term	Mid-Term	Long-Term
Tools & Equipment	-Voxel-based modeling tool -DLP, SLA, DIW, FFF, SLM, PolyJet 3D printers	-Computational design tool -Multi-technique 3D printer	-Extension of 3D/4D printing capabilities over multiple scales, multiple techniques, and digital tools	-Products that make sense -Products that meet the use -Products that live
Methods & Processes	-Origami-based design -SM simulation -AI-based SMs distribution	-Prediction with machine learning -Metamaterials patterns discovery -Generative design of Solid/latticed structures	-Augmentation in AI-based generative design, multi-material optimization, Multiphysics simulation, biomimetic computing, and symbolic AI reasoning	
Models	-Laws of 4D printing -Voxel-based model -Euler-Bernoulli beams	-Multi-scale voxel-based model -SMs distribution patterns -4D printing data representation format	-Augmentation in terms of geometric and structural complexities, Multiphysics models, and data representation	
Knowledge	-4D printing ontology at part design level	-Profiled knowledge -Distribution and recommendations	-Extension to the system and materials levels	

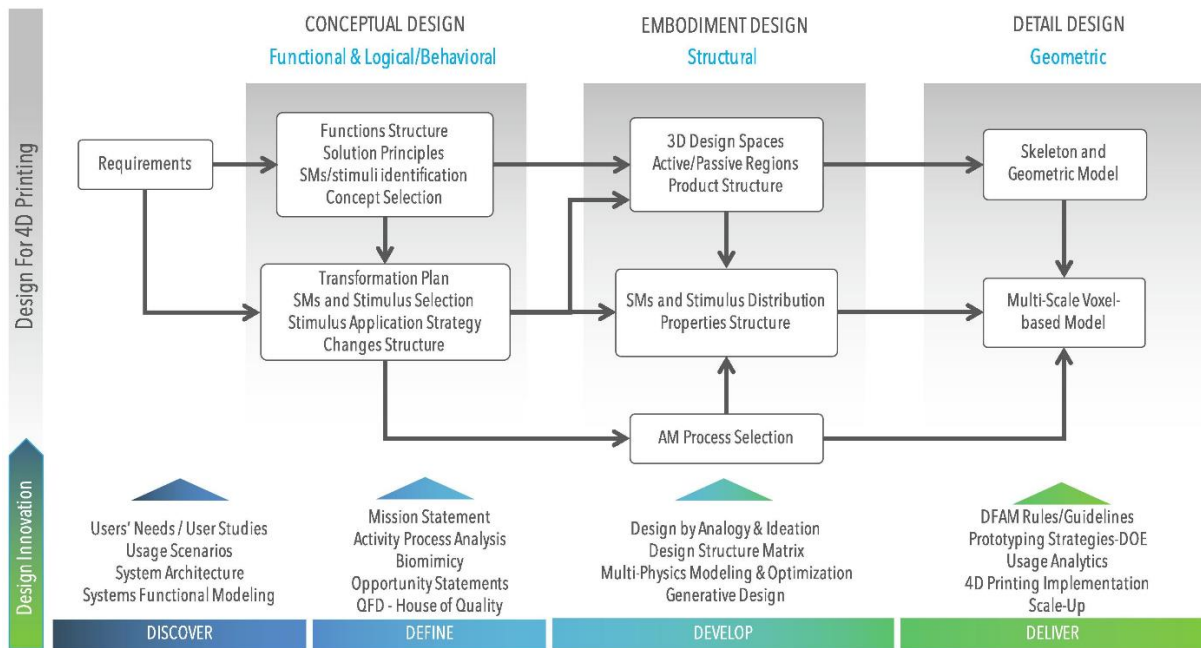


Figure 30: General design for 4D printing technology framework [39].

Besides research that explored the connection between materials, stimuli, and AM processes, designers should also have access to software and simulation tools that enable them to model and simulate the behavior of 4D printed objects [172-174]. These tools can help designers identify potential issues early in the design process and make adjustments accordingly. It is worth mentioning that simulating the behavior of structures that include SMs requires addressing the factors governing their smartness in preliminary design phases [175].

Efforts have been made to develop selection tools and design aid tools for designers to use SMs effectively. TechOptimizer™ provides a set of tools, including a library of SM effects, advantages, and limitations [175]. On a principle similar to that of Ashby's graphs, SMA performance indicators and selection graphs based on these indicators have been proposed in [176]. A team of German researchers has developed the K&M-based SMA tool, which is a design support tool with SMAs for designers [177]. The tool provides knowledge on SMA effects, solution principles, material properties, design rules, and other quantitative and qualitative information. However, these tools only provide formulas and do not enable making innovative 4D printed designs.

In recent years, researchers have used connectionist AI techniques to explore the distribution of multiple materials in 4D printing. Figure 31 illustrates a tool developed by Sossou et al. that uses a genetic algorithm to allocate materials in a voxel-based representation of a 4D printed part [66,70]. This helps enhance shape and form morphing by predicting materials distribution in the design phase, giving designers predictable recommendations. A Grasshopper plugin called VoxSmart has been developed to enable voxel based SMs modeling and simulation in the Rhinoceros3D environment. The developed

tool can simulate heterogeneous objects with any materials distribution, including SMs and inert materials, in real time.

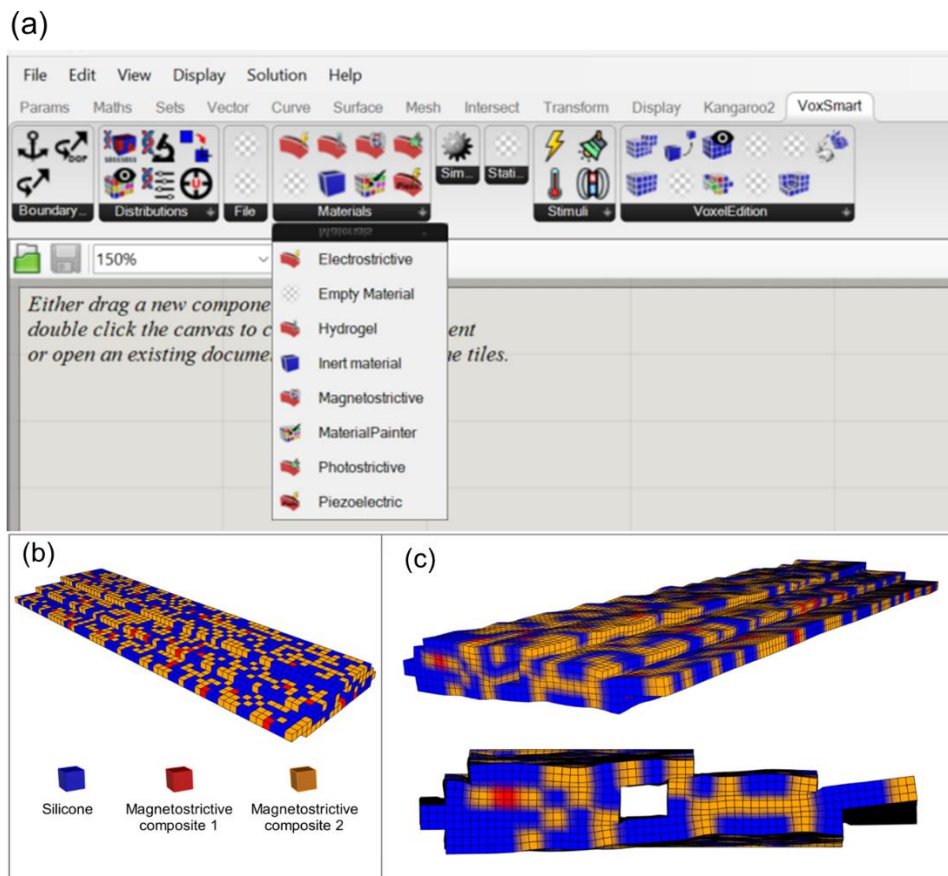


Figure 31: VoxSmart design, modeling, and simulation tool for 4D printing. (a) Different components of the plugin, (b) An example of a determined distribution, (c) the deformation of the wing when the magnetostrictive materials reach saturation.

Another study was carried out to optimize the design of 4D printed parts in [178]. The authors have used parametric optimization techniques such as the Kriging meta-model and genetic algorithms to find the optimal combination of design variables. This approach aimed at reducing weight and manufacturing costs while using shape-changing printed parts made of SMPs. In [179-180], a fuzzy model and a discrete stiff finite element method (FEM) were created to estimate the bending time of porous polyelectrolyte hydrogel actuators that were 3D printed in response to a given applied voltage. Meanwhile, [46] proposed a distribution optimization of two materials, active and passive, based on an evolutionary algorithm and finite element (FE) analysis. Their model consisted of identically sized voxel units, and a genetic encoding was used to spatially split the functional composite structure. Additionally, in [181], the authors have undertaken a study aiming at finding the best material distribution in a voxel structure using a finite element analysis-based evolutionary algorithm. Their approach incorporated topology optimization and void voxels integration to achieve a target shape change of 4D-printed active composites (see Figure 32).

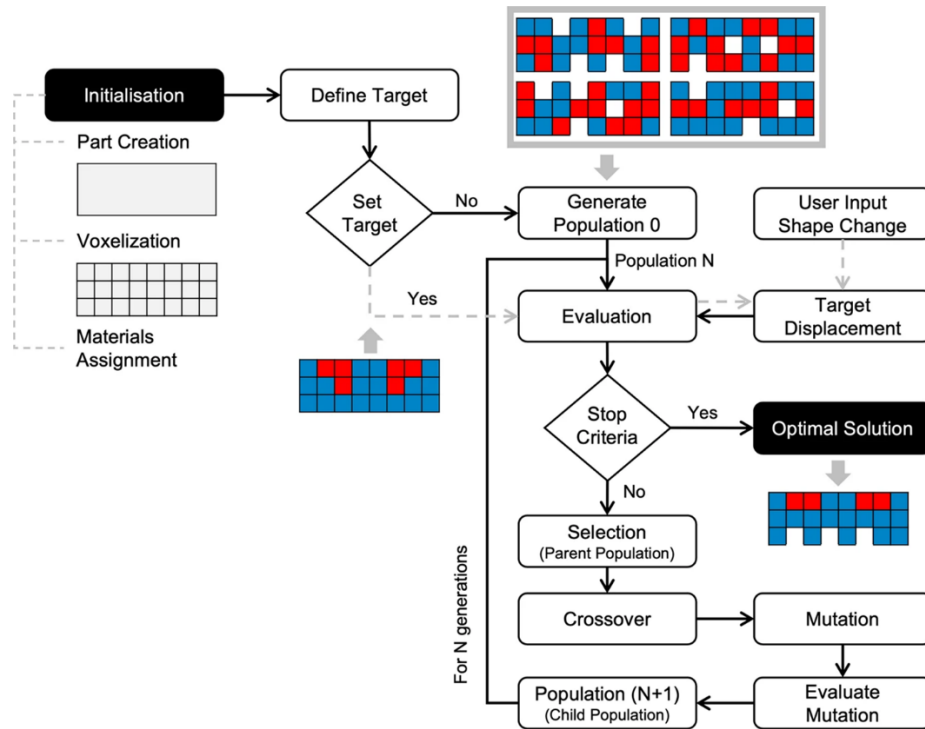


Figure 32: Full design process schematic flowchart of the driven by an EA in [181].

Although numerous research works and multiple software tools exist in the literature regarding design for 4D printing, there is no single software that encompasses all aspects such as design, simulation, modeling, slicing, firmware, monitoring, and printing planning. Therefore, efforts to facilitate designing with SMs remain insufficient. Research should focus on developing more tools and methods that would allow using 4D printing effectively in their designs, particularly when it comes to multi-material active structures.

As our thesis focuses on the design for multi-material 4D printing from an assembly perspective, it is also important to consider the principles of design for assembly (DFA), besides design for AM and design for 4D printing (see Figure 33).

Design for Assembly (DFA) is a methodology used in manufacturing to improve the ease of assembly of products, reduce the time required for assembly, and lower manufacturing costs [182]. DFA involves designing products with assembly in mind from the very beginning of the design process, with the goal of minimizing the number of components and fasteners, reducing the complexity of assembly operations, and ensuring that parts are easy to handle and orient correctly during assembly [183]. There have been numerous studies on DFA, with a focus on different aspects of the design process. Some studies have focused on developing methods and tools for evaluating the ease of assembly of different product designs [59,71,184], while others have looked at how to incorporate DFA principles into the early stages of the design process [185-186].

As for our research study, DFA will be combined with design for AM and 4D printing to tackle multi-material 4D printing challenges regarding distinct SMs and inert materials behaviors, available SMs, and compatible AM processes/techniques. The following section will discuss the state of the art in terms of assemblies.

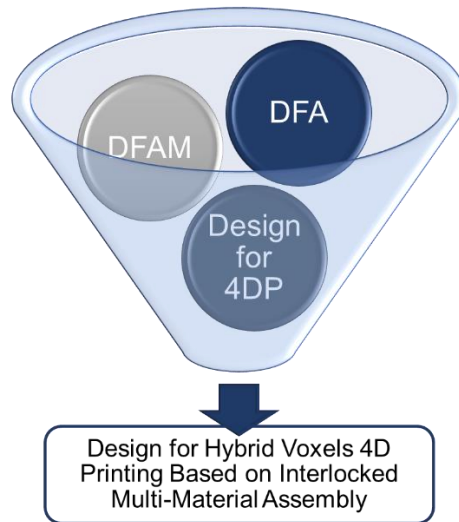


Figure 33: Design for X (DFX) approaches involved in our thesis work.

2.4. Evolution in Assemblies/Interlocking Assemblies

Assemblies are used in almost all aspects of our lives, from everyday objects to complex structures. They have gone through a long journey of evolution and innovation to achieve their current form. This section will briefly explore the evolution of assemblies and interlocking assemblies in particular. Then, it will discuss the different categories of interlocking assemblies, ranging from bio-inspired, mechanical, and computational interlocking assemblies.

An assembly can be defined as a group of interrelated parts that work together to form a complex product or system. Assemblies have been around for centuries, with evidence of interlocking joints found in ancient structures such as the pyramids of Egypt [187]. Over time, the technology of assembly has evolved, with the introduction of new materials, tools, and techniques. In the industrial revolution (18th and 19th centuries), assembly line production became popular, leading to the mass production of standardized parts that could be easily assembled [188]. With the advent of computer-aided design and manufacturing (CAD/CAM), assembly design has become more sophisticated, with the ability to model and simulate complex assemblies before they are built [57,71]. Interlocking assemblies, on the other hand, are a specific type of assembly where the parts are connected using interlocking joints, rather than fasteners such as screws or bolts [57]. Interlocking assemblies can provide several benefits, such as

increased strength, rigidity, and ease of assembly. There are several categories of interlocking assemblies, including bioinspired, mechanical, and computational interlocking assemblies.

- **Bioinspired Interlocking Assemblies:** Bioinspired interlocking assemblies take inspiration from nature, where organisms have evolved interlocking structures that provide strength and flexibility [189-190]. Examples include the interlocking scales of pangolins, the shells of turtles, the spines of sea urchins, and the elbow joint to cite a few (see Figure 34.a). Studies have shown that bioinspired interlocking assemblies can provide superior strength and flexibility compared to traditional assemblies. For example, in Shaokang Cui et al. (2019), Yuming Zhang et al. (2012), and Lee Djumas et al. (2016) [191-193], fundamental insight studies on mechanical properties of the interlocked nacreous composites were provided to effectively strengthen the mechanical junction at the composite interfaces (see Figure 34.c). Other bio-inspired interlocking features were suggested in Alshegri et al. (2018) to improve metal/polymer interfacial strength in dental and orthopedic prostheses [194]. They suggested a Y-shape assembly design, which was similar to mangrove tree roots (see Figure 34.b).

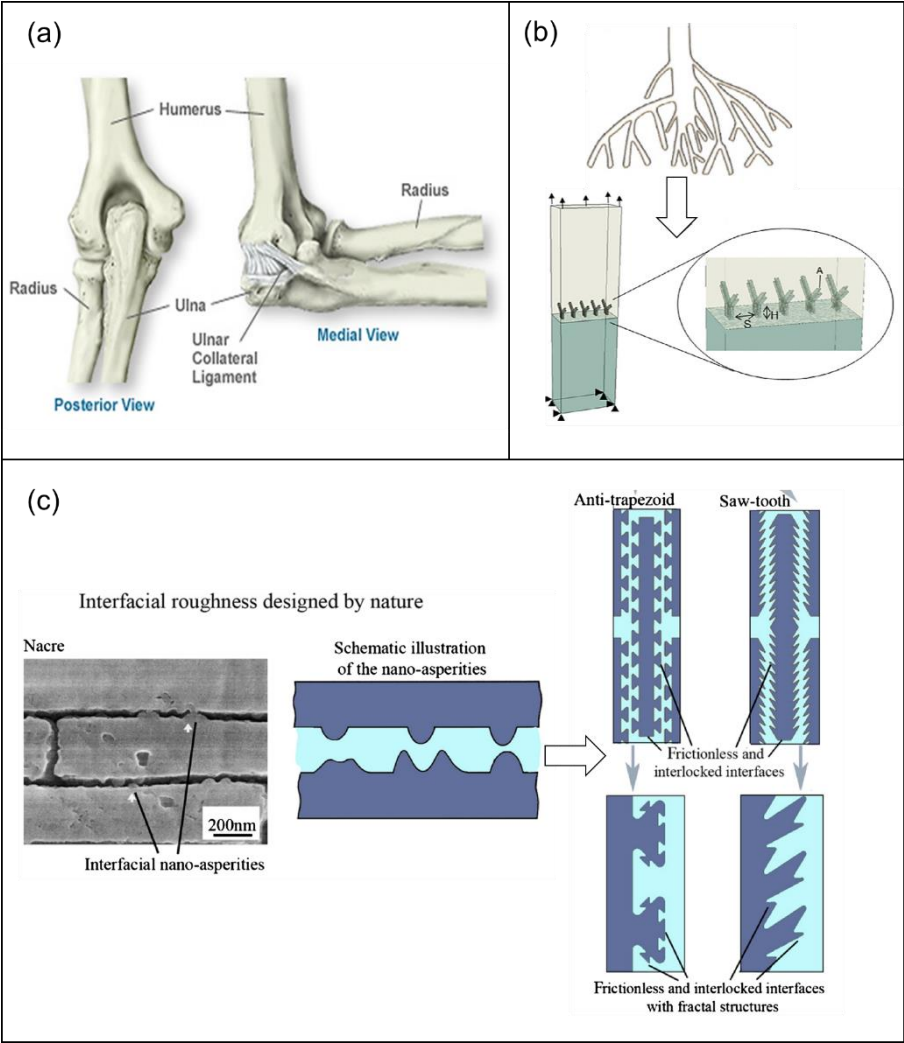


Figure 34: Examples of bio-inspired interlocking assemblies. (a) elbow joint anatomy, (b) interlocking feature inspired from mangrove roots, and (c) assembly using interlocking nacreous features.

- Mechanical Interlocking Assemblies: Mechanical interlocking assemblies use physical mechanisms to connect the parts, such as grooves, tabs, or hooks [195-198]. Mechanical interlocking assemblies have been used in many applications, including furniture, automotive, and aerospace industries. As an example, a study in [195] explored the use of mechanical interlocking snap fits to improve the strength and durability of composite materials. Another study carried in [199] used mechanical snap-fits for articulation joints to create toys that can move closer to actual human beings (see Figure 35).

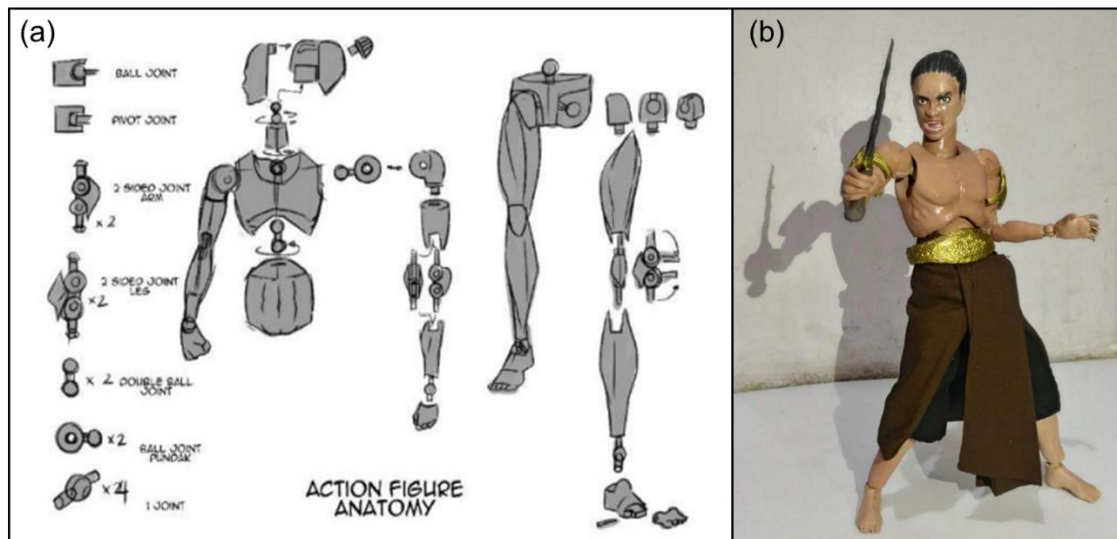


Figure 35: Action figure anatomy. (a) the interlocking parts, and (b) the assembly [199].

- Computational Interlocking Assemblies: Computational interlocking assemblies employ computer algorithms and simulations to divide a given 3D model into puzzle-like interlocking parts [200-203]. The parts can be firmly joined then by their own geometry [204-207]. Several innovative interlocking research works can be found in the literature. By utilizing these interlocking designs, it becomes feasible to create objects larger than the printing volume of an AM printer (see Figure 36). Besides, these parts can be disassembled and reassembled repeatedly without compromising the physical or structural properties of the assembly [200-212], as occurs in conventional assembly methods where features like nails or screws are used.

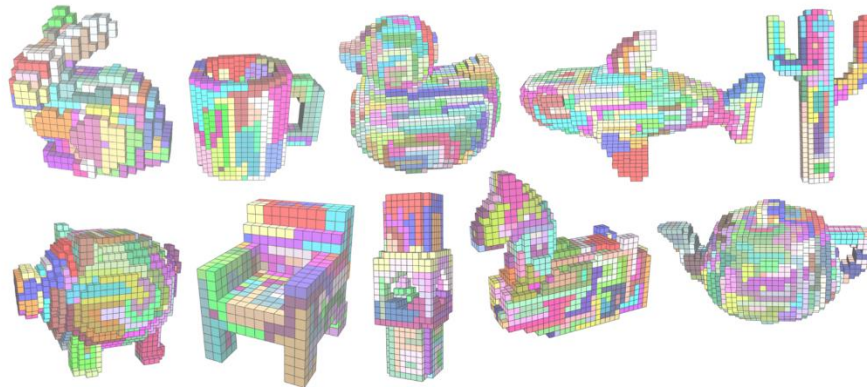


Figure 36: Interlocking 3D puzzles. Different figures from left to right: BUNNY, MUG, DUCK, SHARK, CACTUS, PIGGY, CHAIR, WORK PIECE, ISIDORE HORSE, TEAPOT [212].

Table 6 hereafter, provides additional examples of potential applications of the aforementioned assembly methods.

Table 6: Interlocking assemblies characteristics, examples, and applications.

Category	Characteristics	Examples	Potential Applications
Bio-inspired interlocking Assemblies	Inspired by natural structures and systems	-nacre structures -Bird beaks -Sea urchin spines	-Beetle-inspired locking mechanism for joining components in aerospace and automotive industries
Mechanical interlocking Assemblies	Based on physical locking mechanisms	-Snap-fit joints -Tongue and groove joints -Dovetail joints	-Snap-fit connectors in consumer electronics such as mobile phones and laptops -Joints in furniture assembly, such as cam and dowel fittings -Zippers and Velcro fasteners in clothing and accessories
Computational interlocking Assemblies	Designed using computational tools and generative algorithms	-Custom-designed interlocking mechanisms	-Puzzle-like assemblies in toys -Wooden interlocked construction and architecture

2.5. Key Research Question

Through the literature review conducted in this chapter, it has become evident that 4D printing is a multidisciplinary field that requires collaboration among various disciplines, including materials science, mechanics, design, and computer science. It has also been found that none of the design for 4D printing approaches addresses challenges in terms of a concrete realization of multi-material 4D printed structures. This is due to the limited availability (or complete unavailability) of SMs that are compatible with the currently existing printers. Thus, and, in order to provide new design methods in this field, the main research question of this thesis work can be stated as follows:

In terms of the concretization of voxel-based hybrid structures that incorporate both passive and active materials, how to achieve this goal using the currently available AM techniques and processes, and overcome the challenge of the limited compatibility of existing printers with SMs that possess the necessary properties for realizing such structures?

Ultimately, the goal is to solve this question and achieve a high degree of flexibility from the conceptual design stage through to the manufacturing stage, using novel concepts such as voxel-based modeling and topologically interlocked multi-material assembly. Hence the concrete proposed contributions can be outlined in the following manner:

- Developing computational design approach dedicated to the realization of multi-material 4D printed structures based on interlocking blocks assembly;
- Investigating the impact of interlocking block assemblies on the behavior of multi-material 4D printed structures, by analyzing various parameters such as actuation time, shape change, and reversibility/repeatability cycles;
- Generalizing the applicability of the developed computational design approach by enhancing the uniformity of shape/property(ies) change in a 4D multi-material interlocked assembly by customizing the shapes of blocks in early development stages.

Chapter 3: A Computational Design Approach For Multi-material 4D Printing Based On Interlocking Blocks Assembly

“You can never cross the ocean if you do not have the courage to lose sight of the shore...”

Arabic saying

“We cannot solve our problems with the same thinking we used when we created them.”

Albert Einstein

Chapter 3: A Computational Design Approach For Multi-material 4D Printing Based On Interlocking Blocks Assembly	59
3.1. Introduction	61
3.2. Computational Design Approach for Multi-material 4D Printing.....	62
3.2.1. Digital Material partitioning (step 1 of Figure 39).....	63
3.2.2. Blocking Relations Modeling (step 2 of Figure 39).....	64
3.2.3. Interlocking Blocks Assembly Computation (step 3 of Figure 39).....	66
3.2.4. Interlocking Parts Assembly Planning (step 4 of Figure 39).....	72
3.3. Results & discussion	75
3.3.1. Interlocking Assembly Computation Add-on.....	77
3.3.2. Simulation	77
3.4. Conclusion.....	81

3.1. Introduction

Recent works in multi-material 4D printing have illustrated the opportunity to compute material distributions in three-dimensional structure with the support of AI-based techniques [66,70]. The resulting counter-intuitive distributions are promising to achieve a desired shape-changing behavior while ensuring good mechanical performance. At this stage, most of the numerical results remain difficult to print with the available multi-material AM processes and techniques. Thus, design computation with digital materials (see Figure 37) requires developing new multi-material AM strategies. An original way of bypassing the limitations of multi-material AM – in terms of AM processes and materials compatibility [213] – is to consider discrete assembly of interlocking blocks with different materials built from multiple AM processes and techniques. A few assembly methods have been investigated in the literature, ranging from bio-inspired interlocking techniques, mechanical interlocking features, and computational interlocking methods [191-201]. Among the approaches ensuring more freedom in terms of material combination, mechanical interlocking with the aid of computational procedures becomes a relevant strategy. It is thus a question of decomposing a 3D model into discrete elements like Lego-like blocks, whether to overcome large parts printing issue or multi-material AM [201-212]. Although significant research has been done in this field in terms of computational generation of interlocking 3D assemblies [208-212], a barrier still exists to tackle multi-material 4D printing from an assembly perspective. Here the starting point is a digital materials distribution – obtained from AI-based techniques like evolutionary and genetic algorithms [66-70] – to which a determination of interlocked blocks is sought in the embodiment design stage.

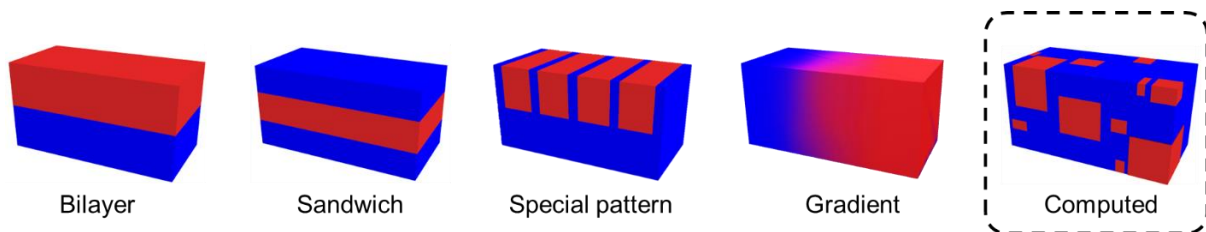


Figure 37: Digital (or computed) material distribution illustration

In such a context, the main objective of this chapter is to propose a computational design approach for multi-material 4D printing by considering the assembly of discrete 3D printed voxels (or blocks). Addressing such a way enable to build any voxel-based structures which includes either lattice and/or solid units, further falling under both design for 4D printing and design for assembly domains. The proposed approach consists in working with digital materials within a 3D/4D object or structure and determining subsets of polyvoxels (i.e., a solid figure similar to polycubes in discrete geometry formed by joining one or more equal cubes face to face). Polyvoxels are the three-dimensional counterparts of planar pixels (see Figure 38), intended to be printed separately and then assembled. The scientific originality lies in defining judicious interlocking arrangement of the polyvoxels, ensuring the assembly

and the maintenance of the structure, thus, providing more flexible and efficient interlocking methods that are not achieved yet by existing state-of-the-art approaches. For that very reason, we will adopt a voxel-based representation in CAD appropriate to multi-material design and 4D printing [33,70,214-215]. Such a representation provides advantages to (i) describe the overall geometry of the part, (ii) specify the active and inert regions, (iii) allocate properties having a role in transduction, sensing, and actuation, and (iv) distribute materials in the three-dimensional design space [39]. From this, it is then possible to address multi-scale modeling [135-137] with different voxel shapes and structures [138], whether solid, lattice, or even metamaterials [151-156]. The proposal extends prior work on interlocking assemblies [208-212,216] by considering as initial input a computed materials distribution in a 4D object via a dedicated CAD plugin [66-70].

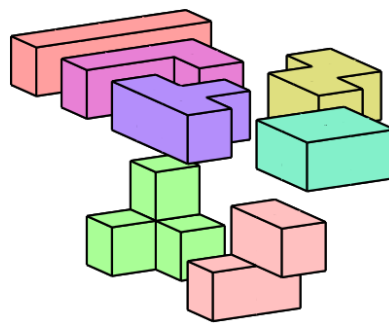


Figure 38: A set of different shapes of polyvoxels

The structure of the chapter is as follows. Section 2 presents the proposed computational design approach able to analyze digital materials distribution into interlocked blocks. In Section 3, an implementation of the reasoning mechanisms is made via a computational design plugin within a CAD environment, and a case study is introduced to illustrate the relevance of the proposal. Last, discussion and conclusion are provided.

3.2. Computational Design Approach for Multi-material 4D Printing

The proposed computational design approach, illustrated in Figure 39, is composed of four main steps. The first step consists in (i) analyzing the distribution of the digital materials on a voxel basis of a given structure (in the next section, we will use the work of Sossou et al. [66,70] to illustrate complex multi-material structures that are achieved with genetic algorithm), and in (ii) identifying the homogeneous (i.e., same material) set of voxels (also called polyvoxels). The voxels are then categorized according to the properties and/or materials. Afterward, Step 2 introduces the blocking relations modeling. It involves mathematical models to define blocking relations between the identified polyvoxels in Step 1 and determine their degree(s) of freedom (DOF). Step 3 focuses on the interlocking polyvoxels assembly computation and is two-fold: the key (i.e., mobile) interlocking polyvoxels are

firstly determined, then fixed interlocking polyvoxels are computed. The last step is dedicated to the interlocking polyvoxels assembly planning. In the following sections, each step is further detailed with an illustrative case.

3.2.1. Digital Material Partitioning (Step 1 of Figure 39)

This step starts then with the main hypothesis that a pre-computed materials distribution is available through a voxel-based representation. To achieve the desired transformation with a specific stimulation, materials are spatially arranged on a regular voxel grid in the three-dimensional space. At this stage, a partitioning is needed to identify homogeneous parts P_i (voxels or polyvoxels) in the structure (denoted A). This material partitioning represents the first reasoning step to which further analysis will be performed.

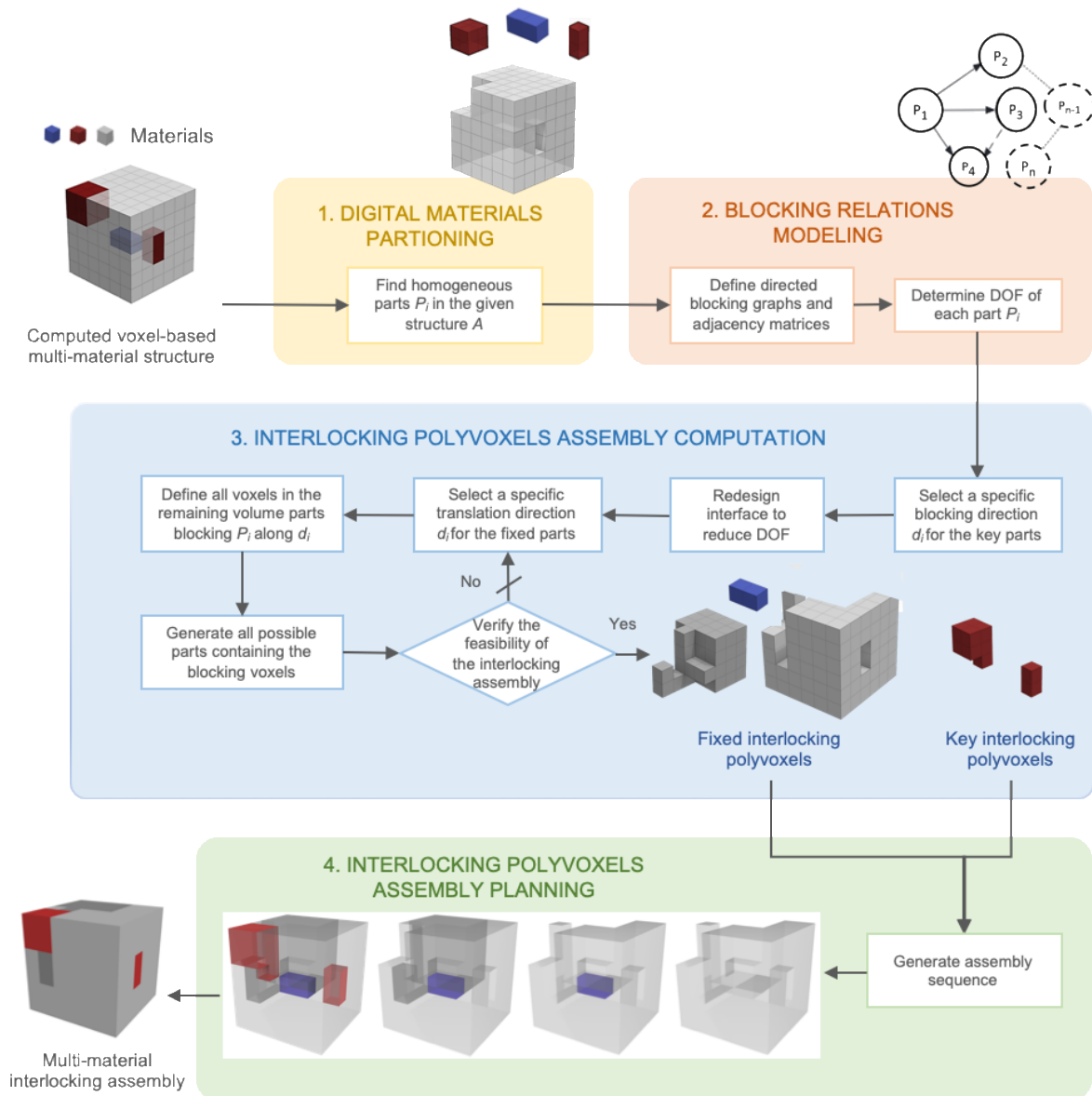


Figure 39: Flowchart of the computational design for multi-material 4D printing based on interlocking blocks assembly computation.

3.2.2. Blocking Relations Modeling (Step 2 of Figure 39)

Based on the identified homogeneous parts P_i , the next step consists in modeling blocking relations along the six directions $(\pm x, \pm y, \pm z)$. To do so, a directed graph – such as used in [211-212,216] – is adopted. Let a directed blocking graph, denoted $DBG_d = (P, R)$, where P is the set of homogeneous parts of the structure A , and R is the set of ordered pairs (arrows) of nodes describing the blocking relations between these parts along the direction $d (\pm x, \pm y, \pm z)$. Then, according to this modeling scheme, an ordered pair between P_1 and P_2 means that P_1 is blocked by P_2 along a direction d (see Figure 40a). The resulting DBGs are then converted into adjacency matrices, denoted M , for computation purposes,

as illustrated in Figure 40b. An adjacency matrix M is a square matrix, where entries can be defined as follows (Equation 1):

$$M = [m_{ij}]_{i,j \in \mathbb{N}^* \times \mathbb{N}^*} \quad (1)$$

with

$$\begin{cases} m_{ij} = 1 & \text{if } P_i \text{ is blocked by } P_j \text{ in a given direction} \\ m_{ij} = 0 & \text{if there is no blocking relation between } P_i \text{ and } P_j \text{ in a given direction} \end{cases}$$

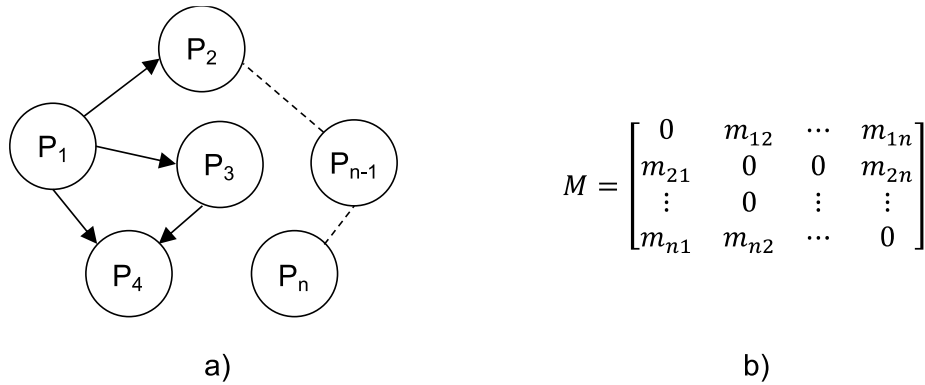


Figure 40: (a) Directed blocking graph $DBG_d = (P, R)$ and (b) its adjacency matrix M according to a specific direction.

Parts (voxels or polyvoxels) are assumed to be assembled through one single translational motion. In such a context, parts exhibiting mobility will be considered as “key” parts (i.e., parts ensuring the mechanical fastening of the assembly and eventually requiring an adhesive bonding operation). To illustrate the principle of modeling the blocking relations of the parts in an assembly, Figure 41 introduces a two-dimensional assembly composed of three interlocked parts, namely P_1 , P_2 , and P_3 , to which DBG on $+x$ and $+y$ directions (denoted DBG_{+x} and DBG_{+y}) and related adjacency matrices (denoted M_{+x} and M_{+y}) have been defined.

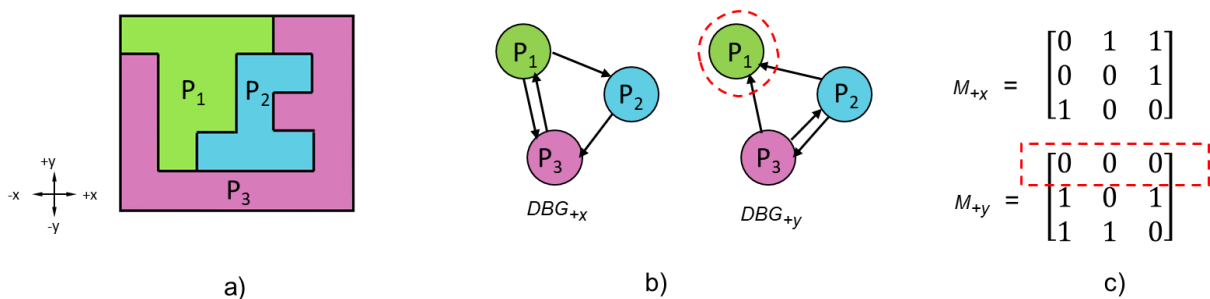


Figure 41: Example of a (a) 2D assembly of three interlocked parts, with its (b) DBGs along the directions $+x$ and $+y$, and (c) the related adjacency matrices. The dashed red circle and rectangle highlight the key part along the $+y$ direction.

An assembly A is deemed to be interlocked, if each of its single parts and subassemblies are blocked along all directions once positioned, except the key(s) part(s) that has(have) the freedom of moving on one imposed direction (see Figures 41.a&b). In order to determine the DOF of the parts P in the assembly A , the computation of blocking relations along all translation directions is required with the support of related adjacency matrices. For instance, if all the entries m_{ij} in a row i of an adjacency matrix M_d are equal to 0, then it indicates that the part P_i is mobile along the direction d (see P_1 in Figures. 41.a&c) and gains in this manner 1 DOF .

3.2.3. Interlocking Blocks Assembly Computation (Step 3 of Figure 39)

Built on this, a computation step is needed to determine interlocking parts (whether voxels or polyvoxels) to build the multi-material 3D/4D structure. The proposed Algorithm 1 (See Pseudo-code 1) aims to define judicious interlocking arrangement of homogenous polyvoxels intended to be printed separately using different AM processes and materials and then assembled. It exhibits two reasoning layers: (i) first, parts with $DOF > 1$ are redesigned to reduce their DOF and set as key parts subsequently (see Algorithm 1, lines 15-25); (ii) then, parts with $DOF = 0$ (i.e., embedded parts) are liberated to enable their assembly, through a generation of additional interlocking parts from the embodying volume. The computational iteration of these interlocking parts takes into account the aforementioned key parts and their insertion directions in the assembly (see Algorithm 1, lines 27-43). Parts with $DOF=1$ are automatically considered as key parts. The following will lay out the algorithm objectives with more details.

Algorithm 1: Interlocking parts assembly computation

Input: Set of homogeneous parts of the structure (see Figure 42a)

Output: Set of interlocking parts for multi-material assembly

```

01:   Set  $P$  the list of all parts
02:   Set  $MP$  the list of mobile parts
03:   Set  $L_{vm}$  the list of all voxels forming the mobile parts
04:   Set  $FP$  the list of fixed parts
05:   Set  $L_{rv}$  the list of voxels in the remaining volume
06:   Set  $DOF_{MP}$  list of  $DOF$  of mobile parts
07:   Set  $KP$  list of key parts
08:   Use the directed graphs and adjacency matrices to deduce  $DOF$  of each part  $MP_i$  in  $MP$ .
09:   foreach part  $MP_i$  in  $MP$  do
10:       Move  $MP_i$  toward all directions
11:       if move  $MP_i$  in  $d_i =$  not null then

```

```

12:          {DOFMPi + 1 in  $d_i$ }
13:          Deduce DOF of  $MP_i$ 
14:          end
15:      if DOFMPi > 1, then Define key parts
16:          Add  $MP_i$  to  $KP$  as a key part
17:          Decrease DOFMPi to 1
18:          Keep  $MP_i$  mobile toward one and only one random direction  $d_i$ , and block it
19:          toward the other directions (Condition 1)
20:          Set  $Lvn_1$  the list of all voxels from  $Lrv$  neighboring  $MP_i$  (see Figure 42b)
21:          foreach voxel  $Vn_{1i}$  from  $Lvn_1$  that fulfills (Condition 1) do
22:              Pick a random voxel  $Vn_{1i}$  (see Figures 42c,d)
23:              Add  $Vn_{1i}$  to  $MP_i$  (Figures 42c,d)
24:              Update  $MP_i, P, MP, KP, Lvm$  and  $Lrv$ 
25:              Rank the assembly of  $MP_i$  as a key part
26:          end
27:      else if DOFMPi = 0 then
28:          Set  $P_{DOF_0}$  list of parts with DOF = 0
29:          Increase DOF of parts in  $P_{DOF_0}$ 
30:          foreach part  $P_i$  in  $P_{DOF_0}$  do
31:              Add  $P_i$  to  $FP$ 
32:              Set  $d_i$  a random direction as the direction of the insertion of  $P_i$ 
33:              Set  $Lvn_2$  the list of all voxels  $Vn_{2i}$  from  $Lrv$  blocking  $P_i$  along  $d_i$  (Fig. 42e)
34:              Generate possible parts containing  $Vn_{2i}$ . The generated parts must have 1 DOF
35:              before the insertion of the key part, and DOF = 0 once the key parts are inserted
36:              (Condition 2) (see Figures. 42f,g)
37:              if there are possible solutions fulfilling (Condition 2) then
38:                  Set  $Lpg$  the list of all the generated parts
39:                  Pick a random part  $Lpg_i$  from  $Lpg$ 
40:                  Add  $Lpg_i$  to  $FP$ 
41:                  Update  $MP_i, P, FP, MP, Lvm$  and  $Lrv$ 
42:              else if there are no possible solutions fulfilling (Condition 2) then
43:                  Backtrack and change direction  $d_i$ 
44:              end
45:          end
46:      end

```

46: **Return** interlocking parts

47:

48:

Pseudo-code 1: Interlocking parts assembly computation pseudo-code

```
public (Polycube, Polycube, Polycube, double) DigPolycubeAlongAdirectionBis(Polycube
anchoredPolycube, Polycube movingPolycube, Vector3d direction)
{
    Polycube tempPolycube = new Polycube(movingPolycube);
    Polycube returnPolycube = new Polycube(anchoredPolycube);
    Polycube PolycubeRetire = new Polycube();
    List<Point3d> PolycubeRetirePoint = new List<Point3d>();
    int cntIterationsMaxi = 10;
    int cntIterations = 0;

    while (!PolycubeFreeAlongAdirection(anchoredPolycube, tempPolycube, direction))
    {

        if (cntIterations != cntIterationsMaxi)
        {
            tempPolycube = TransformPolycube.Trans_Abs(tempPolycube, direction);
            cntIterations++;
        }
        else if (cntIterations == cntIterationsMaxi)
        {
            break;
        }

        List<Point3d> listOfPointToRemove = tempPolycube.ListVoxels.Where(p =>
returnPolycube.ListVoxels.Contains(p)).ToList();
        PolycubeRetirePoint.AddRange(listOfPointToRemove);
        returnPolycube.ListVoxels.RemoveAll(p => tempPolycube.ListVoxels.Contains(p));
    }
    // Retirer les voxels de base non creusés
    PolycubeRetirePoint.RemoveAll(p => movingPolycube.ListVoxels.Contains(p));
    PolycubeRetire = new Polycube(PolycubeRetirePoint);
```

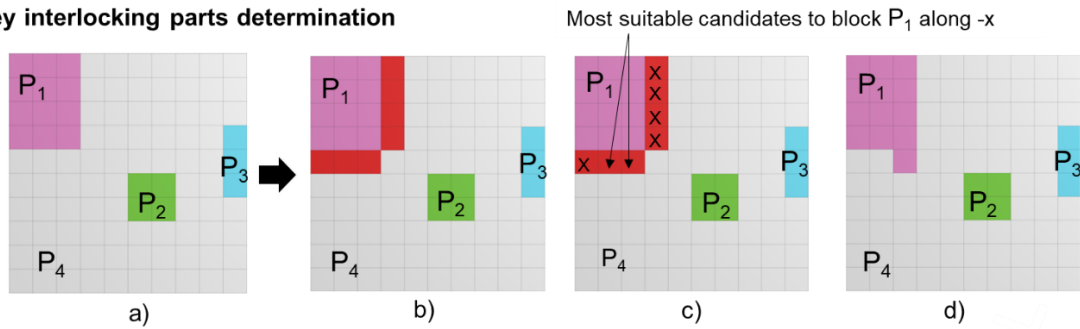
```
return (returnPolycube, tempPolycube, PolycubeRetire, cntIterations);  
}
```

By processing the above-described algorithm, iterative computations might be time-consuming due to the complexity of the imposed multi-material 3D/4D structure. To overcome this potential computational limitation, slight modifications in the digital material distribution are allowed while maintaining the desired shape-changing or property-changing behavior. Thus, to ensure the interlocking and the assemblability of the generated parts, the following conditions must be considered:

- 1) Slight modifications in the digital material distribution when required;
- 2) One and only one translation direction is allowed to insert each part in the assembly;
- 3) The sub-assembly $\{P_i, A\}$ is interlocking with the part P_{i-1} . In other words, P_{i-1} blocks the sub-assembly $\{P_i, A_i\}$ once assembled and so on until the key part(s) is(are) lastly inserted to secure the entire assembly;
- 4) P_{i-1} can be disassembled from $\{P_{i-1}, P_i, A\}$ along one translation direction (key part(s) is(are) the first to disassemble).

To illustrate this step, a two-dimensional assembly composed of four homogeneous parts is introduced in Figure 42. It shows a randomly computed distribution of materials through a voxel-based representation of the object. In this illustrative case, P_1 , P_2 , P_3 , and P_4 are respectively composed of a specific material (or bear a specific property). First the key parts are generated by reasoning on the related *DBGs* and adjacency matrices (see Figure 43), then the fixed interlocking parts determination is addressed.

1 Key interlocking parts determination



2 Fixed interlocking parts determination

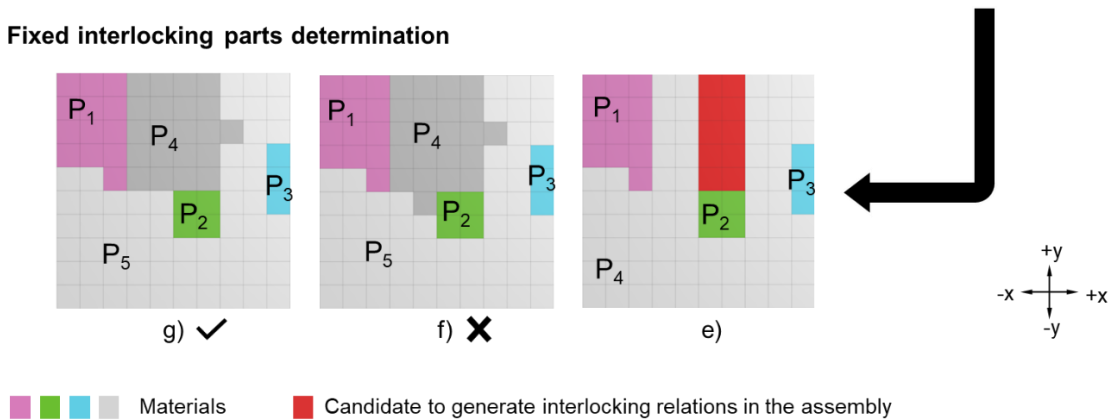


Figure 42: Insight of the computational approach to generate a multi-material interlocking assembly leaning on DBGs and adjacency matrices: (a) the input structure is of 10×10 voxel-based representation of a random digital material distribution, (b) neighboring voxels of mobile part highlighted in red, (c) selection of the most suitable candidate to generate the key part, (d) key part redesign, (e) voxels blocking P_2 toward $+y$ direction in red, (f) P_4 cannot be inserted into the assembly (not suitable as a solution), (g) generation of a suitable interlocking part.

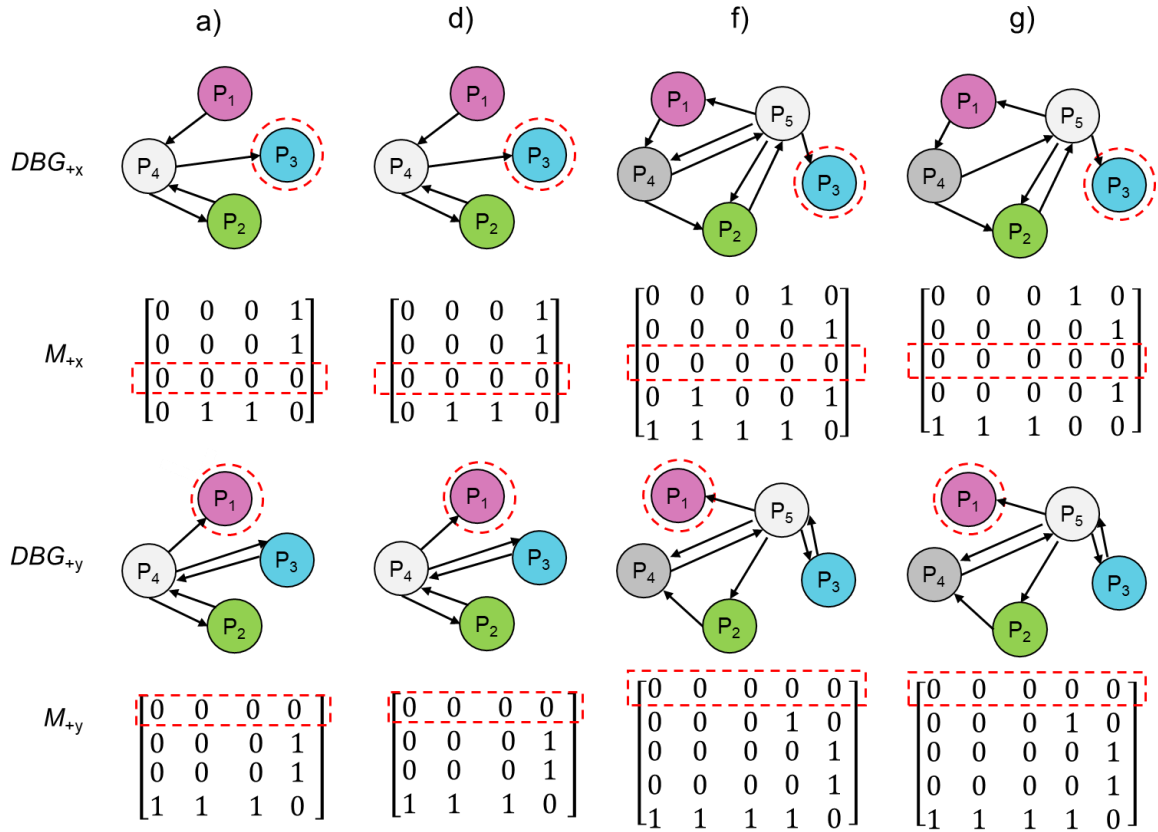


Figure 43: DBGs and M on $+x$ and $+y$ directions related to cases a, d, f, and g of Fig. 4. The dashed red circle in the DBGs and rectangle in matrices refer to key parts in the specific direction.

3.2.3.1. Key Interlocking Parts Determination

Since the key parts are the only mobile parts in the assembly, we will set them among parts with a $\text{DOF} \geq 1$, as illustrated with P_1 and P_3 in Figure 42a. As for parts exhibiting a $\text{DOF} > 1$, i.e., allowing more than one translation motion as P_1 in Figure 42a, a slight modification has to be made in the initial dissection in order to ensure its interlocking. Suppose that the key part (P_1 in the illustrate case), is movable along $-x$ and $+y$ directions and the objective is to block its motion in the $-x$ direction. To do so, all the neighboring voxels to the candidate key part are selected (i.e., they share one side with the key part), then a random candidate voxel fulfilling the blocking condition is picked. Once the candidate voxels are identified and selected, they are added to the key parts (as illustrated in Figure 42b,c,d). In such a way, the single translation of the key parts is ensured.

3.2.3.2. Fixed Interlocking Parts Determination

The illustrative case in Figure 42a shows one part (P_2) embedded in a larger one (P_4). In order to solve this dilemma, the following process can be applied as follows:

- 1) Pick a random direction d_i to insert the desired part (for instance in Figure 42, $+y$ direction is selected to insert P_2);

- 2) Select all the voxels blocking the motion of the desired part along d_i as candidate voxels of interlocking part generation (see Figure 42e);
- 3) Generate all possible parts containing the aforementioned candidate voxels (see Figures 42f,g for examples of generated part possibilities);
- 4) Pick a proper part among the generated interlocking parts. Considering that the key parts blocks $\{P_i, A\}$ once assembled, the generated part P_4 in Figure 42g needs to be inserted in the assembly A along one single translation direction ($+x$) and blocked along all direction once the key piece(s) is(are) assembled;

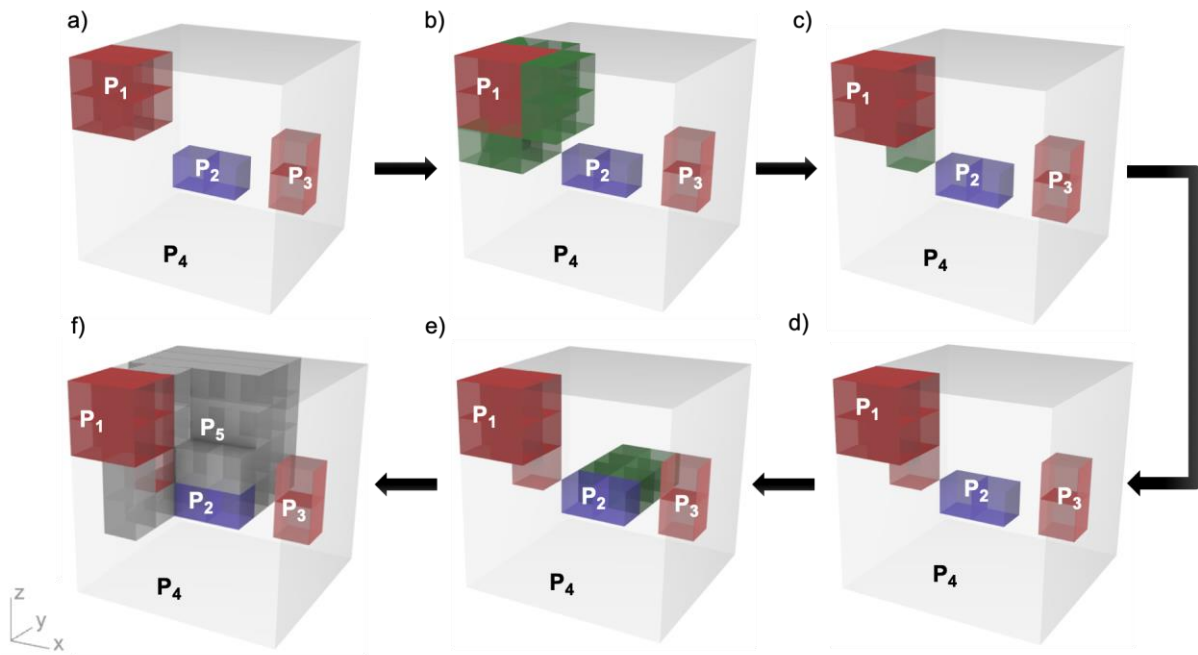
If there are no possible interlocking parts along the chosen direction, then we should backtrack and restart the above actions with a different direction.

3.2.4. Interlocking Parts Assembly Planning (Step 4 of Figure 39)

Following the computation of the interlocking parts, the last step addresses the assembly sequence planning. This critical step aims at determining the assembly order of the generated interlocking parts to build the multi-material 3D/4D structure. To do so, the blocking relations information are used as well as the reasoning layers of Algorithm 1. Once the interlocking parts are generated, they will be ranked according to their generation order. Afterward, we will reverse the order of interlocking parts computation to obtain the assembly sequence; in other words, the first generated parts (key parts) are the last to be inserted to the assembly, which is logically fitting since the key parts are the only mobile parts and block the remaining parts in the assembly. For example, if we follow the interlocking parts computation order in Figure 42g, P_3 , as key part, was firstly generated as it had only one DOF, then the creation of the second key part P_1 followed. Later, the extraction of P_4 took place to enable the insertion of P_2 into the remaining volume P_5 . Therefore, the assembly sequence of the case g in Figure 42 is as follows: $\{P_5, P_2, P_4, P_1, P_3\}$.

Figures 44 on the other hand, illustrates a 3D model of interlocking blocks assembly iteration and their assembly sequence. Starting from a voxelized multi-material/properties cube with an edge length of six voxels, the interlocking parts were generated successively. Thereafter, the assembly sequence has been determined to finally reach a multi-material/properties interlocking assembly.

1 Interlocking parts computation



2 Interlocking parts assembly planning

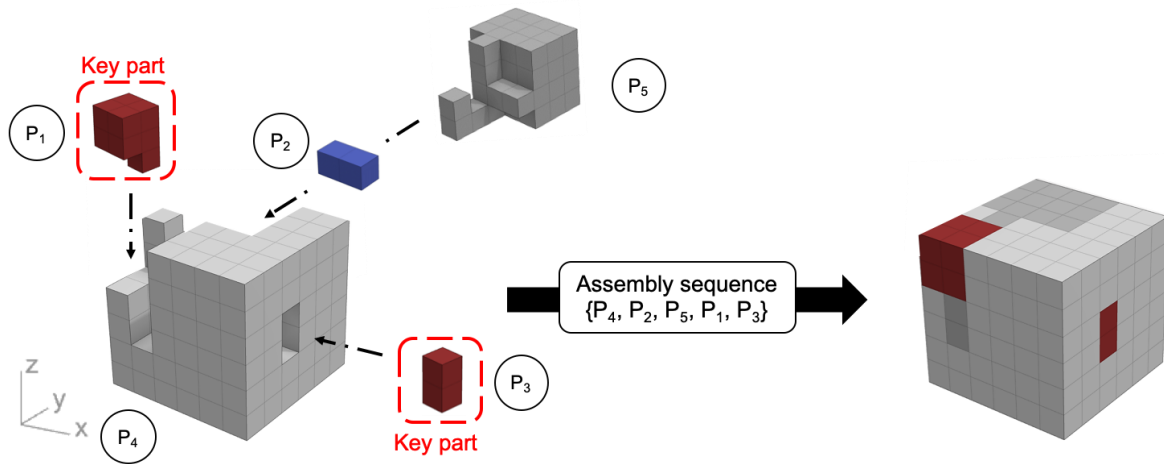
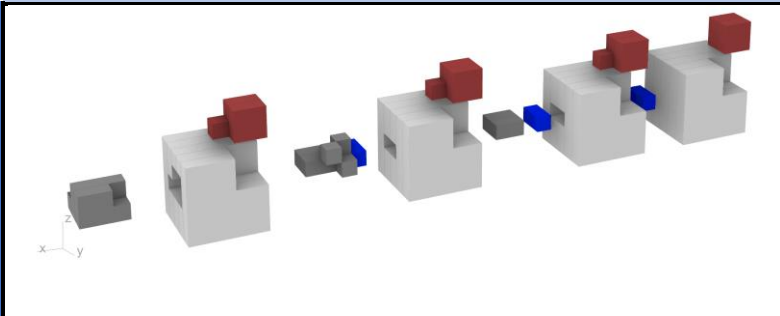
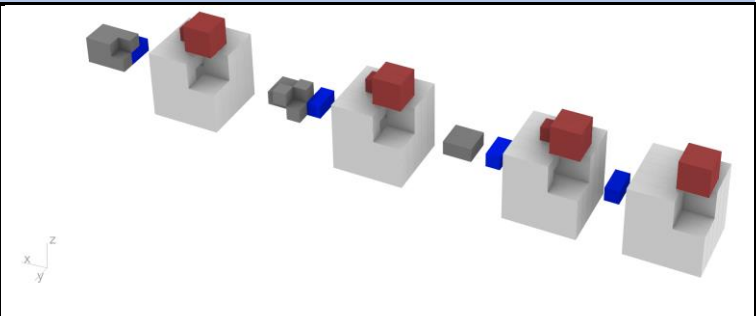
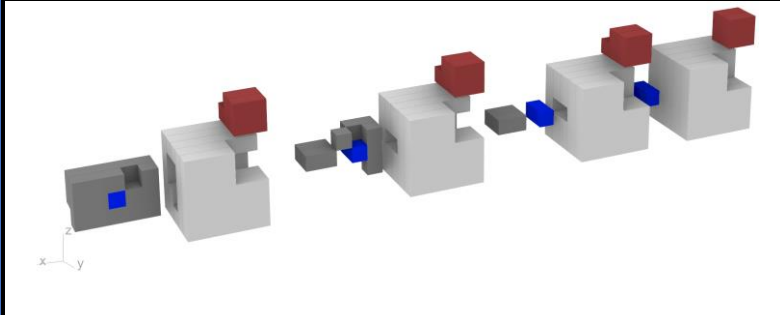
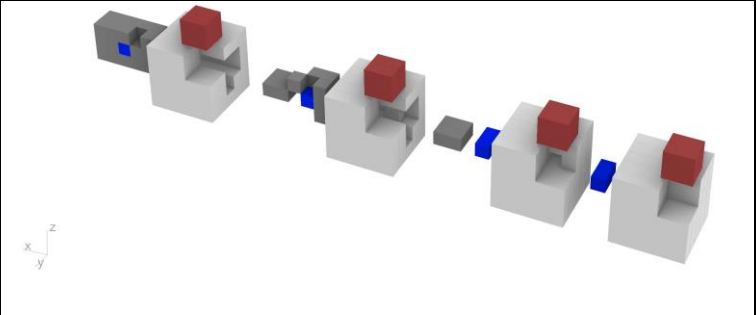
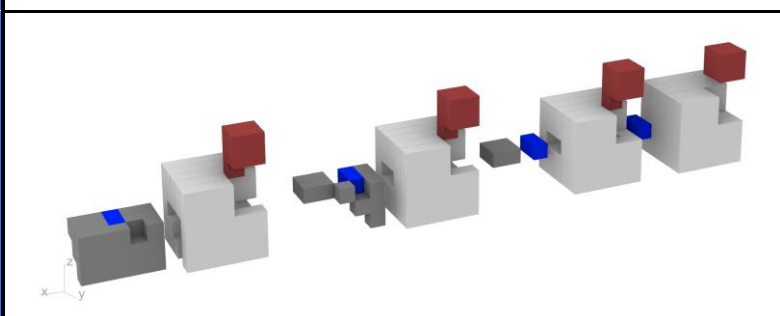
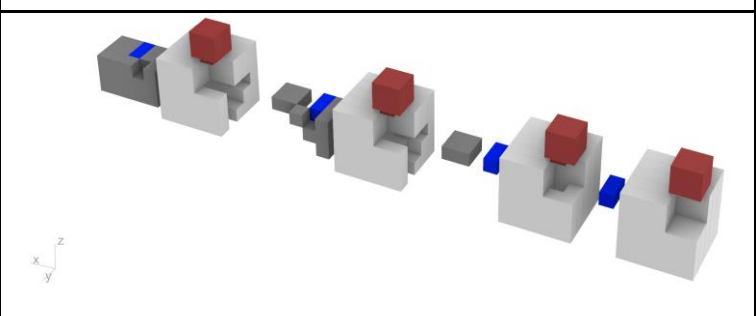


Figure 44: Illustrative case showing $6 \times 6 \times 6$ voxelized multi-material cube (1) the interlocking parts computation: (a) input structure, each voxel color refers to a type of material/property, (b) to (d) key part generation, (e) and (f) refer to fixed interlocking parts generation. (2) Assembly sequence planning of the generated interlocking parts: (a) insertion direction of each interlocking part, (b) the assembly order, (c) a multi-material interlocking assembly.

It is worth mentioning that there are multiple possibilities for generating interlocking block sets. These possibilities depend on the selection of voxel candidates along different directions. For instance, Table 7 below illustrates various possibilities of interlocking assembly generation based on different choices of blocking the key part P_1 in different directions.

Table 7 : Illustrations of various possibilities of interlocking assembly generations based on different choices of blocking the key part P_1 along different directions.

		Interlocking assembly generation	
		Perspective view n°1	Perspective view n°2
-x direction	-x direction		
	+y direction		
	+z direction		

3.3. Results & discussion

The proposed approach is dedicated to assembling 3D/4D structures with a pre-computed materials distribution addressed through a voxel-based representation. To do so, we use the work of Sossou et al. [66,70] to compute a preliminary materials distribution in the structure with the aid of genetic algorithms to fulfill a desired shape-changing behavior. Then, our computational design approach aims to determine the interlocking blocks to be 3D printed and assembled, therefore leading to a complex 3D/4D object achieving the desired shape change. In this section, the relevance and applicability of the proposed approach are illustrated, by introducing a case study covering 4D voxelized structures with computed material distributions.

The proposed case study is a beam with a specific shape change. The design of the beam is described with a voxel-based representation for materials distribution (a multi-shaped digital distribution of an inert material and an active material via VoxSmart add-on, a Grasshopper plugin in Rhinoceros3D environment [66,70] (Figures 45 a,b). The sample is $18 \times 18 \times 126 \text{ mm}^3$, containing 1512 voxels (3^3 mm^3 per each voxel). To design the shape-changing structure, we used a soft material (Agilus30, Stratasys, USA, tensile strength~2,4 MPa) printed with a Objet260 Connex3 machine (Stratasys Ltd., USA) as passive material. The machine leverages a MJ technique called PolyJet. A temperature-sensitive hydrogel is used as active material. The material has been printed by using DIW with a Hydra 16A machine (Hyrel3D, Norcross, USA) and a stepper-controlled EMO-25 extruder (Hyrel3D, Norcross, USA). To ensure the shaping of the hydrogel blocks, SUP706B™ (Stratasys, Rheinmüster, Germany) molds were built with the Stratasys PolyJet™ Objet260 Connex3 machine because of the ability of the material to be removed manually without damaging the hydrogel. This thermo-responsive hydrogel has been adopted due to its ease of formulation and extrusion with DIW, its non-toxicity and biocompatibility. This hydrogel shrinks when exposed to heat. The exhibited shape change is an isotropic shrinkage and there is lower threshold by which the dimension's change begins (usually referred to as lower critical solution temperature – LCST). Away from the critical temperature, the change stops, as the material reaches equilibrium collapsed state. The hydrogel was prepared according to the work of Lai et al. [217]. It is composed Alginate (Alg) and Methylcellulose (MC). First, Alg powder is added into a Calcium Chloride solution (0.075% w/v) to obtain a homogeneous 3% (w/v) Alg hydrogel. The solution is then heated to about 80°C and MC powder with 9% (w/v) is added to obtain Alg/MC hydrogel. The chemical mixture is magnetically stirred until the dissolution of MC powder to finally obtain a printable Alg3/MC9 hydrogel (viscosity $\sim 5 \cdot 10^3 \text{ Pa.s}$).

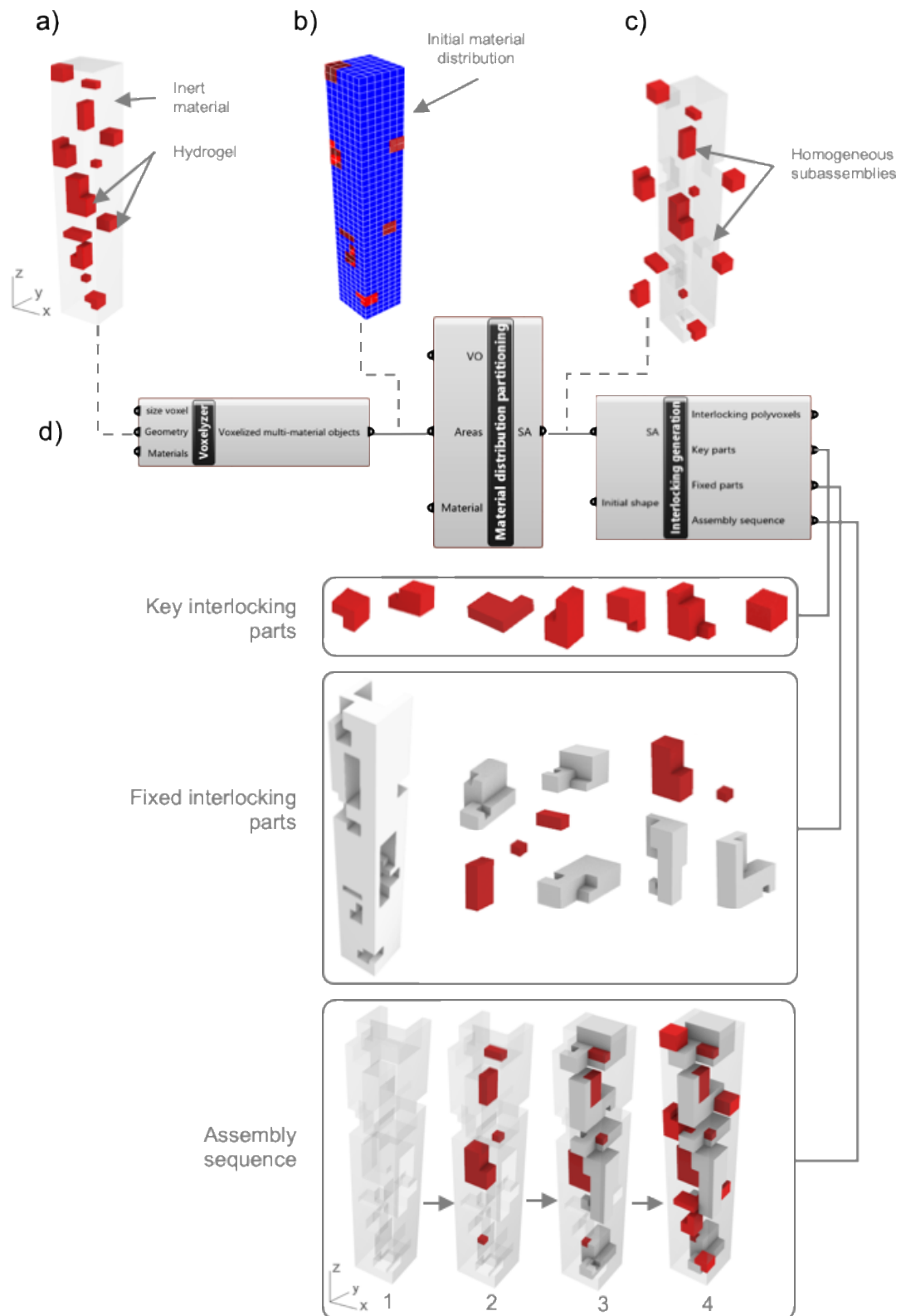


Figure 45: Illustration of a $18 \times 18 \times 126 \text{ mm}^3$ multi-material structure interlocking assembly generation steps: (a) initial structure, (b) initial distribution, (c) homogeneous subassemblies after material distribution partitioning, and (d) design program flow within the VoxSmart add-on in Grasshopper for the interlocking computation

3.3.1. Interlocking Assembly Computation Add-on

In this section, an implementation of the computational approach via new developed VoxSmart components within Rhinoceros3D/Grasshopper environment is presented. It consists in three dedicated components (refer to Figure 45): (i) the “Voxelyzer” component has been developed to obtain a voxel-based representation of the materials distribution, (ii) the “Material distribution partitioning” component to section the given structure into homogeneous parts, and (iii) the “Interlocking generation” component to generate a set of key parts and fixed parts with a proper assembly sequence. There is more than one possible solution that can be generated by the interlocking blocks assembly algorithm, since the directions of insertions are randomly chosen in each iteration, as well as the blocking voxels candidates. Here one possible interlocking assembly set is suggested to build the multi-material 4D structure. Figure 45 illustrates the case study results in terms of digital materials distribution partitioning, interlocking parts generation, and assembly sequence planning. Minor changes have been made in the digital materials distribution to ensure both the interlocking and assemblability of the blocks.

3.3.2. Simulation

As mentioned in Section 3.2.3, the digital materials distribution is considered as an imposed input, which may lead to complications at the interlocking computation step. Slight modifications of the digital materials distribution can then be allowed when necessary in order to overcome this limitation. The purpose of the simulation phase is to investigate the consequences of the changes regarding the physical behavior of the structure. We target a minor shape-changing difference between the original distribution and the adjusted one once stimulated, while maintaining the physical properties. Figures 46 and 47 highlight respectively the simulation of the distributions and the change calculation in physical deformations at multiple temperatures. The simulation of the considered case study was carried out using VoxSmart add-on [66-70].

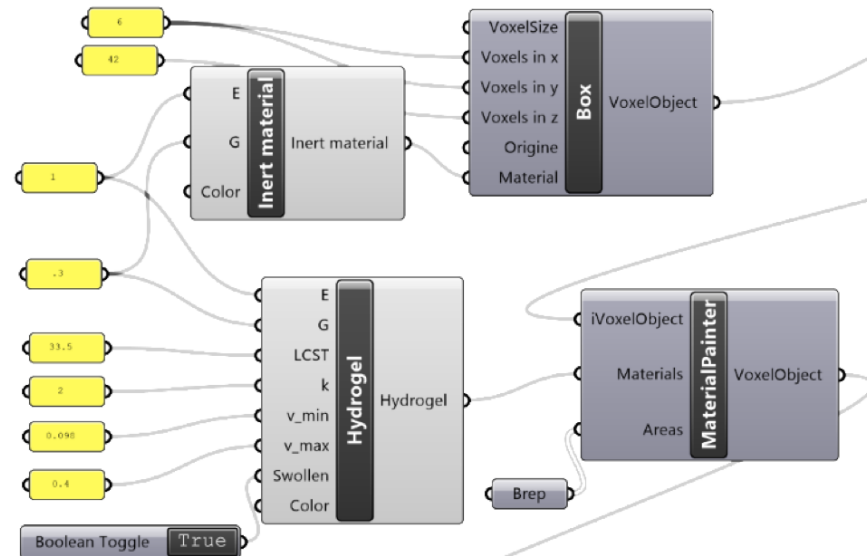
Once the simulation done, the designer will be able to access to detailed information about voxels displacements along x -, y -, and z - axis, via the simulator component (of the VoxSmart add-on) output U (i.e., the list of values showing all the DOFs in terms of displacements and rotations of the underlying truss’s nodes) as shown in Figure 46a. In order to compare both distributions in terms of physical behavior the computed displacements are used to measure the distance between the position of each voxel v_i in the original digital materials distribution and its position (v_i') in the adjusted one. To do so, vectors moduli are calculated using the following equation (2).

$$\| \overrightarrow{v_i'v_i} \| = \sqrt{(U_{xadjusted} - U_{xoriginal})^2 + (U_{yadjusted} - U_{yoriginal})^2 + (U_{zadjusted} - U_{zoriginal})^2} \quad (2)$$

Where:

$v_i = (U_{x_i \text{original}}, U_{y_i \text{original}}, U_{z_i \text{original}})$ and $v_i' = (U_{x_i \text{adjusted}}, U_{y_i \text{adjusted}}, U_{z_i \text{adjusted}})$ are the voxel displacements vectors in the original and adjusted distribution respectively.

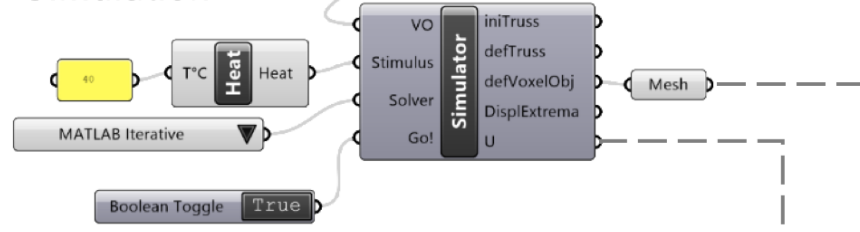
a) Voxelization and material assignment



Boundary conditions



Simulation



b)

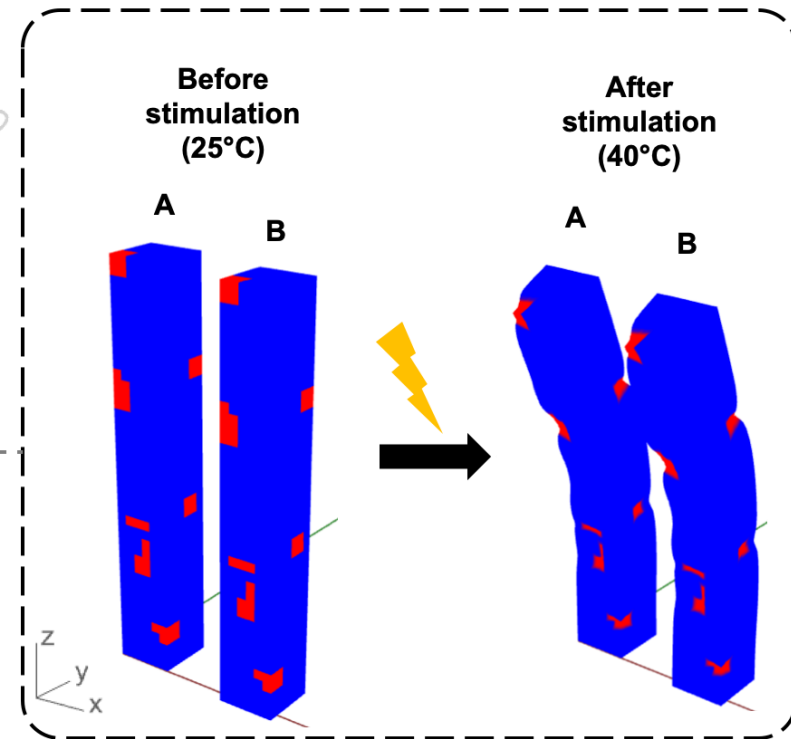


Figure 46: Simulation of the original distribution deformation (A) and the interlocked distribution (B): (a) VoxSmart program flow for voxelization, materials assignment (inert material: Agilus30; active material: hydrogel), and SM simulation, (b) A and B distributions before thermal stimulation (at 25°C) and after stimulation (at 40°C).

Taking into account VoxSmart simulation and distances measurement results, we demonstrate in Figure 47 and Table 8 that the difference in terms of deformation variation between both distributions is slightly different, or even non-existent, regarding displacements along $\pm x$, $\pm y$ and $\pm z$. The narrow modification that has been applied to the digital material distribution in order to generate the interlocking assembly, has not offended the physical properties of the original 4D structure. Therefore, the relevance and the applicability of the proposed approach is demonstrated.

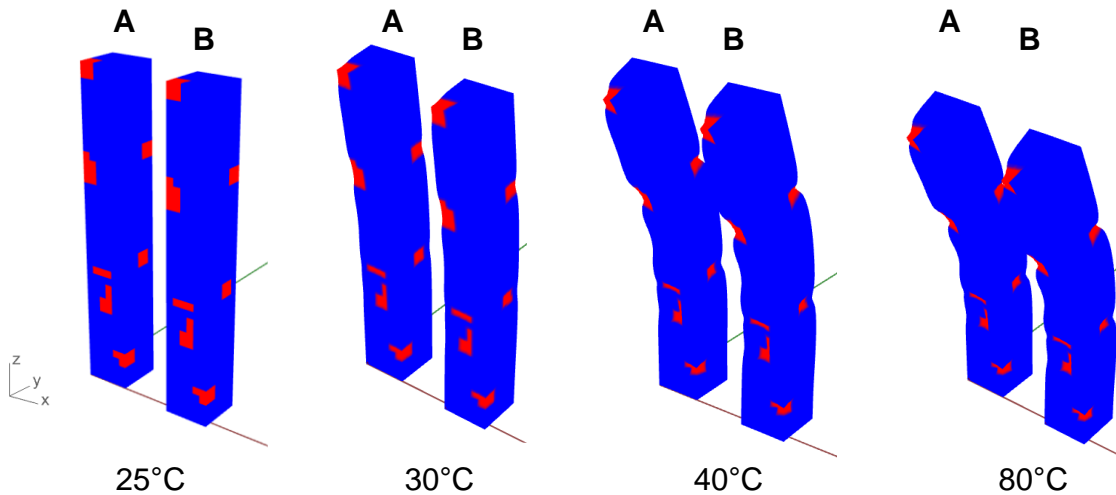


Figure 47: Numerical simulation with VoxSmart plugin of the initial distribution (A) and adjusted distribution (B) at 25°C, 30°C, 40°C, and 80°C.

Table 8: Calculation of the maximum and average distances between voxels' positions in the initial distribution (A) and adjusted one (B) at 25°C, 30°C, 40°C, and 80°C.

	25°C	30°C	40°C	80°C
Maximum Distance (10^{-2} mm ± 0.0001)	0	07.74	24.22	24.61
Average Distance (10^{-2} mm ± 0.0001)	0	01.79	05.58	05.68

Table 8 provides the maximum and the average distances between a voxel's position in the original materials distribution (A) and its positions in the adjusted one (B). For instance, the largest difference in displacements of a voxel between (A) and (B) at 40°C, was equal to 0.2422 mm which is fairly negligible. The physical shape change of the case study is illustrated in Figure 48 where the printed interlocking active and passive blocks (see Figures 48a&b) are laid out before the manual assembly, after the assembly and after the stimulation. This figure shows a shape change as expected in the design and simulation stages. The change is achieved when the multi-material structure is exposed during 3 min in water at 40°C. The shape recovery is achieved when water is progressively cooled down to room

temperature after 5 min. The shape fixity (i.e., the property of a material to stay at a specific shape once stimulated) is made possible when the object is constantly stimulated.

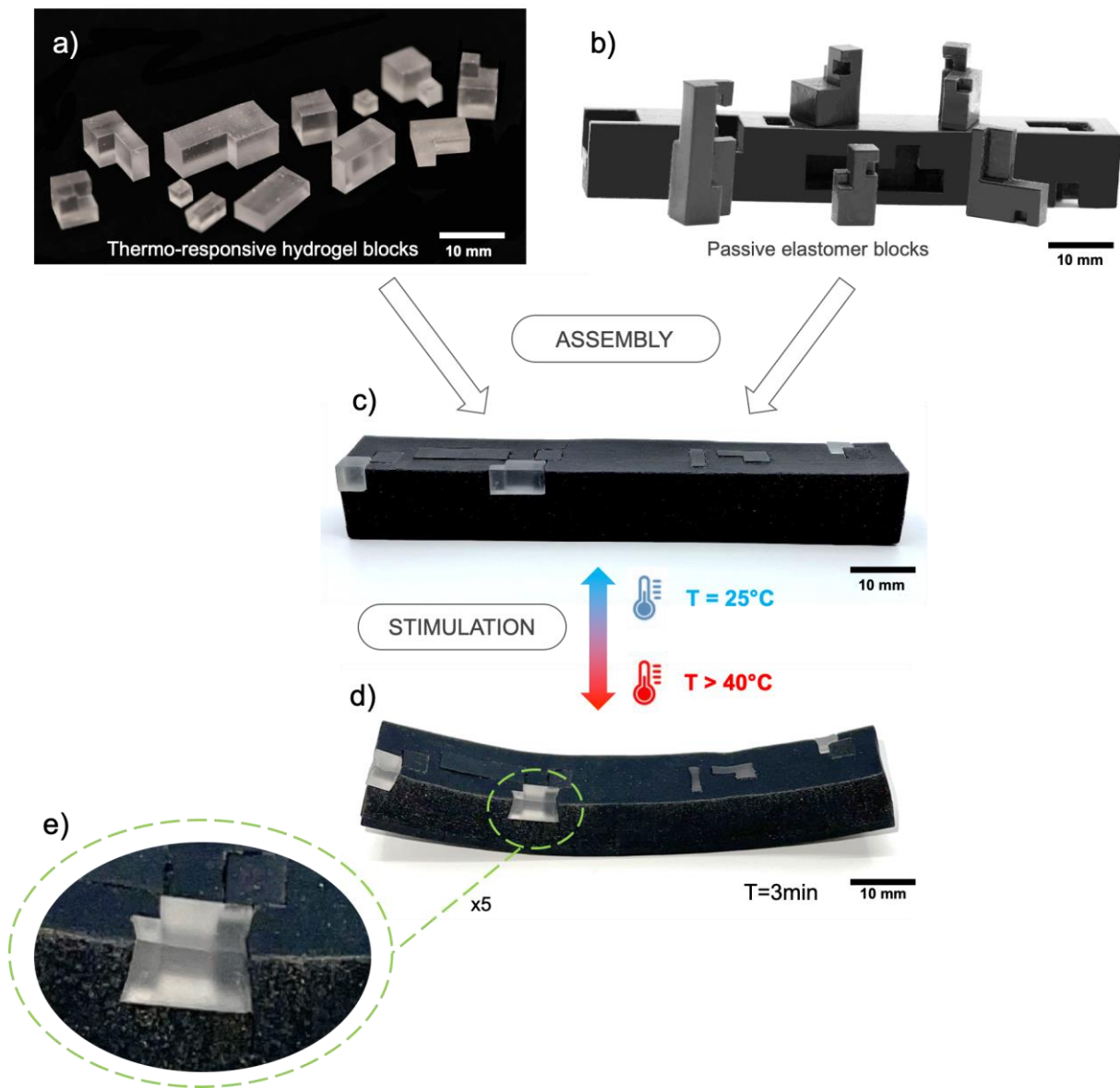


Figure 48: Multi-material 4D printing via interlocking blocks: (a) thermo-responsive hydrogel blocks printed with DIW technique, (b) Agilus30 blocks printed with MJ (PolyJet technique), (c) manual assembly of the interlocking blocks by following the assembly sequence generated by the developed VoxSmart component, (d) deformed structure after stimulation at 40°C in water, (e) interlocking assembly deformation zooming in (Focus x5).

3.4. Conclusion

This research work highlights a computational design approach for multi-material 4D printing. By considering a given digital materials distribution fulfilling a desired shape-changing behavior, the approach aims to generate interlocking blocks intended to be printed separately then assembled to build the multi-material 4D structure. On one hand, our computational design enables the creation of an

interlocking assembly automatically, rather than its creation by expensive assembly design methods. On the other hand, its generality and efficiency allow to explore new types of complex assemblies that are impossible to be printed via a unique AM technique in a single run, such as combining solid voxels/lattices or metals/polymers in the same assembly. Thus, it enables the integration of dissimilar materials in 4D printed structures such as for instance materials ensuring internal and local stimulation. The illustrative case study, exhibiting a specific shape-changing behavior, has shown the added value of the proposal in terms of computation and realization. The work done opens the door toward promising and innovative applications in multiple domains such as automotive, soft robotics, spatial structures, medical technologies to name a few.

It is worth mentioning that in this chapter, interlocking blocks are assumed to follow the same modeling scheme. However, it would be more realistic to integrate the mechanical behavior at the interfaces of the interlocking blocks. Another study should cover this avenue to predict the functional fatigue of the interlocking blocks assembly under the effect of multiple cycles of stimulation. This is going to be the subject of the next chapter.

Chapter 4: Influence of Interlocking Blocks Assembly on the Actuation Time, Shape Change, and Reversibility of Voxel-Based Multi-Material 4D Structures

“It doesn’t matter where you are in life, it really doesn’t matter! Because the great thing about life is always your next move!”

Chazz Palminteri

Chapter 4: Influence of Interlocking Blocks Assembly on the Actuation Time, Shape Change, and Reversibility of Voxel-Based Multi-Material 4D Structures.....	83
4.1. Introduction	85
4.2. Materials and Methods	86
4.2.1. Materials.....	86
4.2.2. Printing Parameters	86
4.2.3. Interlocking Assembly Generation.....	87
4.2.4. Test Before Stimulation.....	89
4.2.5. Test under Stimulation.....	90
4.3. Results & Discussion.....	92
4.3.1. Analysis Before Actuation.....	93
4.3.2. Actuation Performance.....	94
4.4. Conclusion.....	102

4.1. Introduction

Besides overcoming the current limitations of 4D printing technology regarding process compatibility and SMs availability, relying on computational interlocking mechanisms seems to be highly promising to offer more freedom in terms of design for multi-material assemblies in general (3D/4D printing). The previous chapter has proposed a computational design approach based on interlocking blocks assembly dedicated to multi-material 4D printing. The overall idea was to decompose a 4D voxel-based model with a multi-material digital distribution into subassemblies of voxels – blocks or parts in other terms which were intended to be printed separately and then assembled. Relying on a suitable interlocking arrangement and an appropriate assembly sequence of the printed blocks, building voxel-based structures including either lattice and/or solid units was enabled. This design approach was dedicated not exclusively to overcoming multi-material AM limitations, but also to addressing manufacturing 3D/4D large parts that exceed the building volume of existing printing machines.

In such a context, this chapter aims at investigating the effect of interlocking blocks assemblies on the actuation time, shape change, and reversibility of 4D printed structures to demonstrate the applicability of the computational design approach proposed in the previous chapter. Considering that the former approach was assigned exclusively to digital material distributions (see the computed category in Figure 49) resulting from voxel-based modeling, we hereby justify the relevance of the computational design approach and further expand its application by adopting special pattern distributions (as highlighted in Figure 49) as a starting point [129-130], for which a determination of interlocking blocks will be conducted to build a multi-material 4D assembly. To carry out this study, a comparison between both an interlocked 4D structure and a single print multi-material structure is made through a combination of numerical simulation and actuation tests. The related results will be then presented and discussed.



Figure 49: Multi-material distribution categories. The special pattern is considered in this study to further master the fabrication of computed materials distributions.

The proposed analytical study, illustrated in Figure 50, consists of mechanical and actuation tests associated with numerical simulations of a multi-material special pattern sample. Contrary to computed material distributions where the arrangement of voxels can be random and multi-scaled [65-66,70,181], special pattern distributions are more regular structures composed of a matrix and periodic

fiber-like arrangements of active/inert voxels enabling quick and reversible shape-shifting behaviors [218-219]. The analyses are performed on both assembled structures resulting from the interlocking blocks assembly approach as well as on 4D multi-material objects printed in one go to compare and further understand the effect of interlocking blocks assembly in 4D printing.

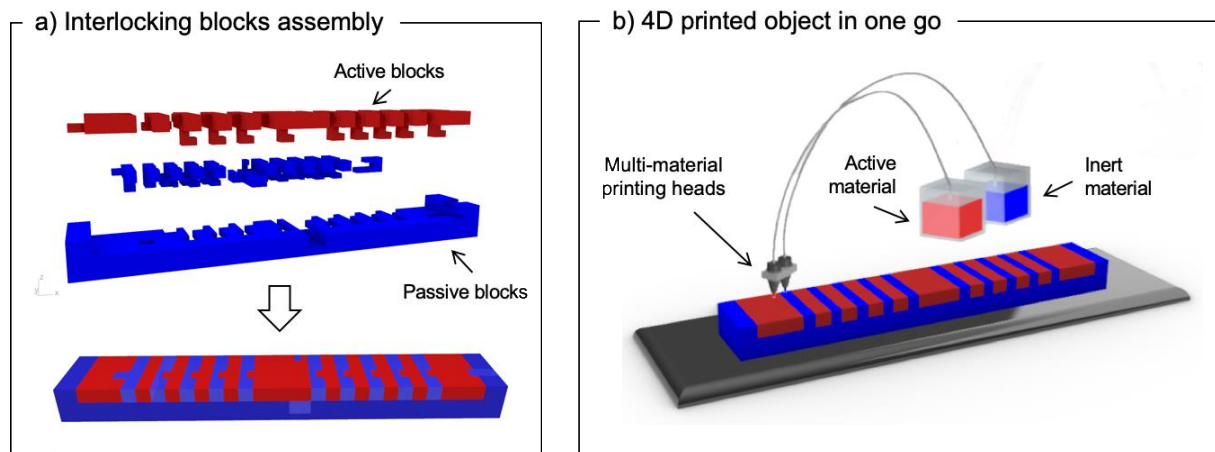


Figure 50: Study to investigate the effects of (a) interlocking blocks assembly on multi-material 4D printing versus (b) multi-material 4D objects printed in one go.

4.2. Materials and Methods

4.2.1. Materials

The fabrication of the samples was made on a PolyJet™ Objet260 Connex3 printer (Stratasys®, Ltd., USA). This machine combines Inkjet technology and the use of photopolymers. Two materials from Stratasys were utilized: Agilus30™ and VeroWhite™. At room temperature, the VeroWhite™ material is rigid with a glass transition temperature (T_g) of 56-58°C, while the Agilus30™ is a soft and rubber-like material with a T_g of -10°C. The VeroWhite™ liquid resin comprises a photoinitiator, urethane acrylate, epoxy acrylate, isobornyl acrylate, acrylic oligomer, and acrylic monomer. The Agilus30™ liquid resin is composed of a photoinitiator, exo-1,7,7-trimethylbicyclo(2.2.1)hept-2-yl acrylate, urethane acrylate oligomer, methacrylate oligomer, and polyurethane resin. Ethylic alcohol (96%) was used as a solvent (Arcane industries, France) with a boiling point of 78°C and a special gravity of 0.79 [218,220-222].

4.2.2. Printing Parameters

The samples were printed by applying the digital material mode at a resolution of 118 dpi.cm⁻¹ along the x - and y -directions. The parts were printed with a layer thickness of 30 μm and up to 85 μm for the x - and y -axes. The resins are polymerized by the ultraviolet light with a spectral range of 300-450 nm.

4.2.3. Interlocking Assembly Generation

Starting from a multi-material distribution in a 3D/4D structure defined or computed via machine learning and genetic algorithm [65-66,70,181], the computational design approach is applied to determine suitable interlocking patterns of homogenous blocks of voxels [53]. The approach is automated by utilizing a software tool within the Rhinoceros3D/Grasshopper® environment and a dedicated add-on, VoxSmart [66,70,181]. These blocks are intended to be printed separately using different AM processes and materials and then assembled. The application of the computational procedure is then made on a $62 \times 10 \times 5 \text{ mm}^3$ strip sample containing 3,100 voxels (the volume of a voxel is 1 mm^3) to an interlocking assembly. The software tool is composed of three components, as illustrated in Figure 51, such as (i) the ‘Voxelyzer’ component to obtain a voxel-based representation of the materials distribution within the 3D/4D structure (see Figure 51a,b), (ii) the ‘Material distribution partitioning’ component to divide the given structure into homogeneous parts (i.e., with same materials) (see Figure 51c), and (iii) the ‘Interlocking generation’ component to generate a set of interlocking blocks and the suitable assembly sequence (Figure 51e,f).

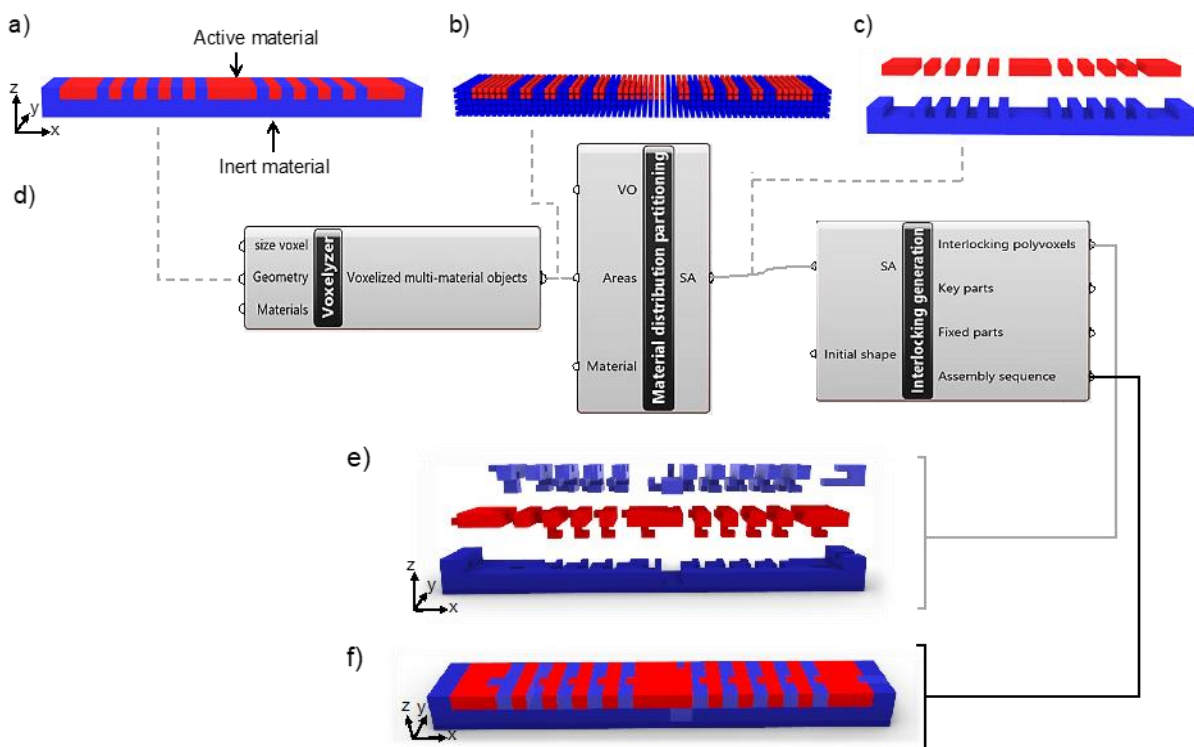


Figure 51: Rhinoceros3D/Grasshopper® program flow to determine the interlocked blocks assembly of a $62 \times 10 \times 5 \text{ mm}^3$ multi-material sample: (a) initial geometric structure highlighting the distribution of active/inert materials, (b) voxelization of the materials distribution, (c) homogeneous subassemblies after material distribution partitioning, (d) design program flow dedicated to the interlocking computation, (e) generated interlocking parts, and (f) final assembled structure.

To briefly summarize the rationale behind the computational design software tool to determine interlocking blocks assembly, converting a multi-material structure to an interlocked blocks assembly

will be carried out in four successive steps (see Figure 52). The first step is two-fold (i) analyzing the distribution of materials on a voxel basis, and (ii) finding homogeneous sets (single-material sets) of voxels (also called blocks) according to their properties and/or materials. Afterward, the second step involves mathematical models (directed blocking graphs and adjacency matrices) to interpret blocking relations between the previously identified blocks along all translation directions. Consequently, their degree(s) of freedom (DOF) are calculated. The third step consists of adopting the blocking relations to generate a set of interlocking blocks, designed to be printed independently and then assembled to build the 3D/4D multi-material structure. We assume that an assembly is interlocked or secured if each of its blocks is blocked along all directions once positioned, except for the part(s) ensuring the final securing of the assembly; they can be mobile along one imposed direction. In this study, we will adapt a slightly different strategy from the work of Benyahia et al. to achieve a more robust assembly [53], which requires the following algorithmic conditions:

- 5) All parts will be blocked in all directions. One and only one key part (mobile part) is accepted in the assembly configuration. To do so, we impose a single interlocking generation direction. For example, interlocking parts can be generated from left to right so only one key part could be generated.
- 6) The interlocking computation might be complex if not impossible because of the imposed material distribution at the starting point. To overcome this significant computational constraint, we allow slight modifications in the materials distribution when required. Thus, we ensure the assembly capability without offending the desired physical properties and shape-changing behavior.
- 7) Each block/part is inserted in the assembly along one and only one translation direction, i.e., blocks cannot be rotated to fit in the assembly.

The last step is related to the assembly sequence planning, where the assembly order of the generated interlocking blocks is computed to build the multi-material 3D/4D structure. This order will depend on the interlocking blocks' generation direction. If the interlocking blocks are generated from left to right, their assembly will occur in the opposite direction. The interfaces are then redesigned, and the interlocking parts/blocks are generated automatically by the VoxSmart software tool to fulfill the conditions.

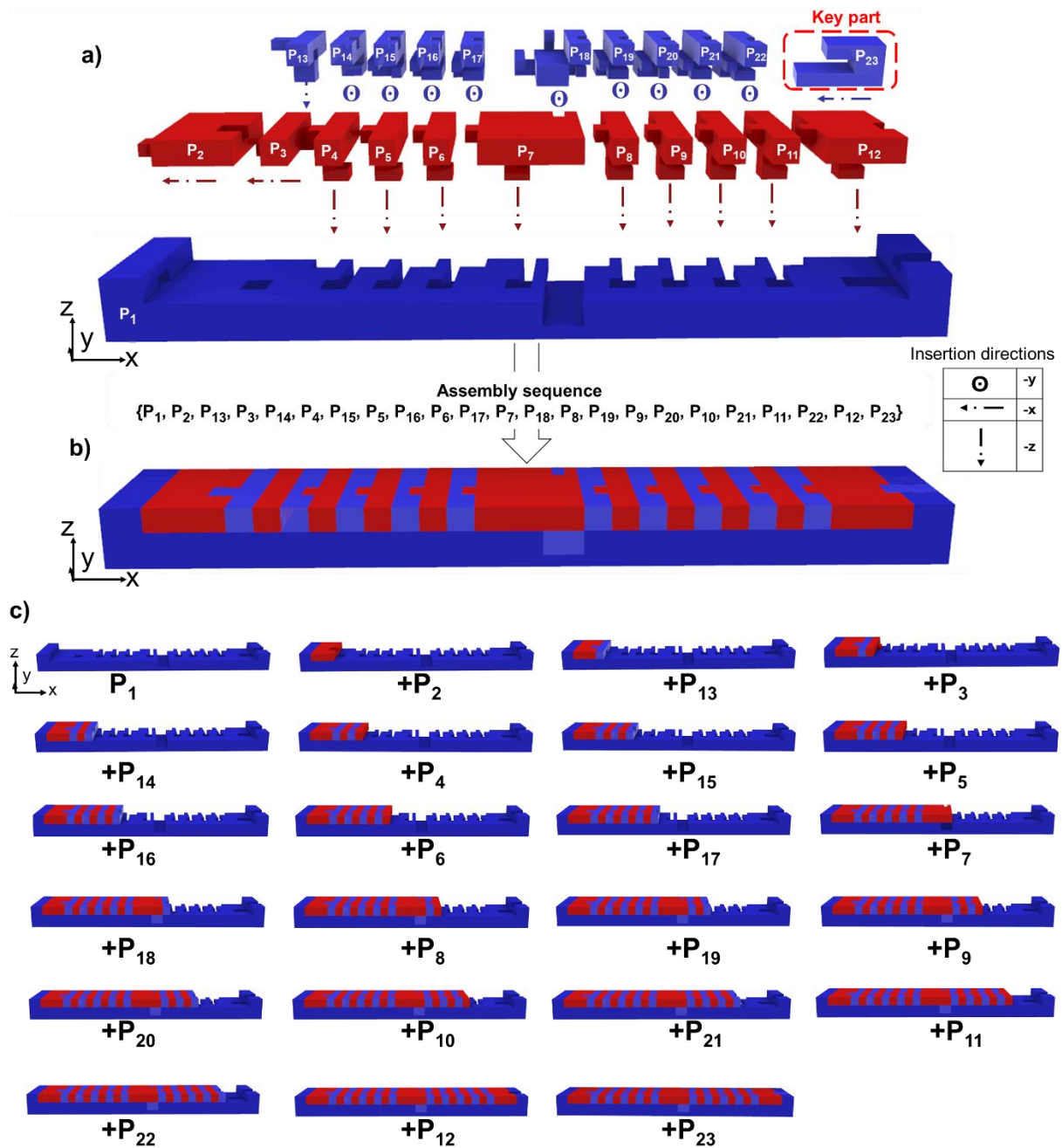


Figure 52: Description of the assembly sequence of the multi-material 4D printed sample using interlocking blocks. (a) 23 blocks have been determined by the software tool, (b) the assembly sequence operation of the interlocking blocks, and (c) Assembly step by step.

4.2.4. Test Before Stimulation

A three-point bending test was performed on 5 structure samples printed according to the interlocking blocks assembly and printing in one go strategies respectively. To do so, the LLOYD Instruments Ltd. (UK) LR 50K Universal Testing Machine was utilized at 90 N with the test procedure compliant with performance requirements and test methods amendment: 40/0678 (provided by LLOYD instruments LR

50K software) and ISO178. The samples were preloaded at 0.1 N (supporting span of 50 mm). The bending test was carried out to measure and compare the deflection rate of both structures (see Figure 53).

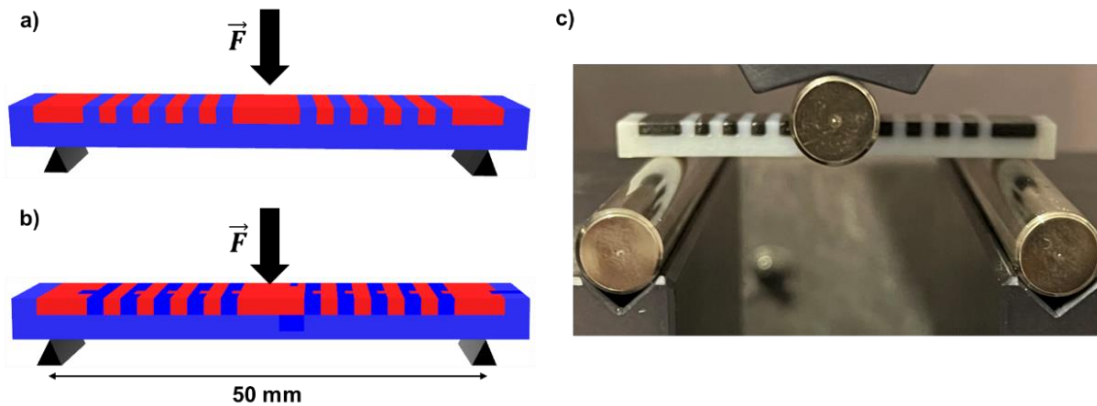


Figure 53: Three-point bending test procedure: (a) the multi-material structure printed in one go, (b) the interlocked structure configuration, and (c) LLOYD Instruments LR 50K Universal tester.

4.2.5. Test under Stimulation

4.2.5.1. Predictive Simulation Model

We referenced in Section 4.2.3, that special pattern materials distribution is an imposed input. It may involve complications in the interlocking blocks generation step. To overcome this potential constraint, slight modifications in the materials distribution are allowed when required. In order to assess the consequences of these adaptations, simulation of both structures and the change calculation in physical deformations at multiple temperatures are carried out using the VoxSmart add-on in the Rhinoceros3D/Grasshopper® environment. The latter will also provide a computational predictive model of the physical behavior in a presence of stimulation energy.

4.2.5.2. Stimulation

Here two stimuli are set up to achieve the actuation of the samples, i.e., exposure to heat and a suitable solvent (ethanol). The bi-material samples made of VeroWhite™ and Agilus30™ were exposed to ethanol at room temperature for 1 hour. In such an environment, the elastomer material (Agilus30™) will behave as a swelling hydrogel (i.e., it swells and increases in volume due to the absorption of the alcohol). Whereas as regards the transition material (VeroWhite™), it will not swell with solvent. The imbalance in strain will induce stress and create pressure that will force the VeroWhite™ material to bend. However, the created bending force is notably insufficient against the VeroWhite™ mechanical strength at room temperature, the latter transition material will then not bend. Therefore, the samples

are removed from the ethylic alcohol to be placed directly in a hot bath of water at 60°C for 5 min. In such a manner, the VeroWhite™ material is heated above its T_g , resulting in decreasing its stiffness and enabling its shape-changing ability. Thus, the samples will eventually be able to bend and release the stored stress. Finally, the specimens are placed in cold water for about 1 min to bring the temperature below the T_g of the VeroWhite™ and freeze its microstructure. Thus, the mechanical strength and stiffness of the VeroWhite™ are once again restored [52,218]. The structure can then take its second permanent shape (a stable configuration that can be maintained without further external stimuli).

4.2.5.3. Measurement of Curvature

Once the bi-material samples ($6.2 \times 1 \times 0.5$ cm³) are placed in the hot water bath at 60°C following an ethanol absorption, they will begin to bend evenly and continuously within a time-lapse of 5 min. In the meantime, we will compare the behavioral patterns of both structures. To do so, images were taken during the interval to determine the curvature of the samples every one minute while the latter are still soaked in the hot water bath. The CANON EOS 50D camera was placed at a right angle to the surface of the hot water bath while taking the pictures. The chord height and the cord length are then measured using an image processing software ImageJ (Version 1.54b) offering accurate measurements for very little effort. First, the radius is calculated according to Equation 3:

$$r = \frac{c^2}{8f} + \frac{f}{2} \quad (3)$$

where r is the curvature radius (cm), f is the chord height (cm), and c is the chord length (cm), see Figure 54.

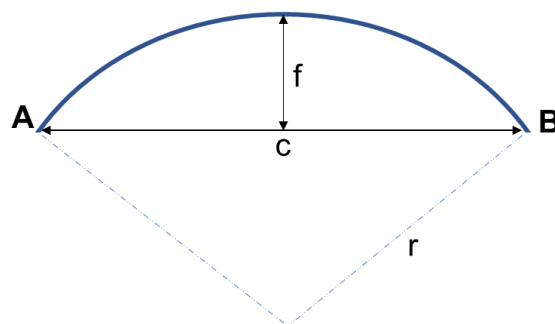


Figure 54: measurement of curvatures.

The curvature K (cm⁻¹) is the reciprocal of its radius, given in Equation 4:

$$K = \frac{1}{r} \quad (4)$$

Following the above procedure, the curvature will also be measured after removing the samples from the 60°C bath of water and directly placing them in cold water. These results will be later compared to the theoretical predictive model provided by the VoxSmart tool.

4.2.5.4. Shape Recovery and Reversibility Cycles

The reversibility cycle of both evaluated structures consists of two main phases: the actuation and the shape recovery phases. In the actuation phase, both ethanol and heat are used as stimuli to enable shape changing from the first permanent shape to the second one, as illustrated in Figure 55. However, only heat stimulus is applied in the shape recovery phase. In such a way, the transition material (VeroWhite™) will be once again heated above its T_g , and the sample will recover its first shape, and so on. In order to obtain meaningful and accurate results, we leave the samples to dry overnight, as a means to completely release the absorbed ethylic alcohol within the elastomer material (Agilus30™). The samples can be then placed once again in the hot water bath for shape recovery. In this study, the reversibility aspect will be considered as an additional perspective to add value to our interlocking assembly approach. The aim is that the interlocked blocks structure successfully completes reversibility cycles, as much as multi-material structure printed in one go.

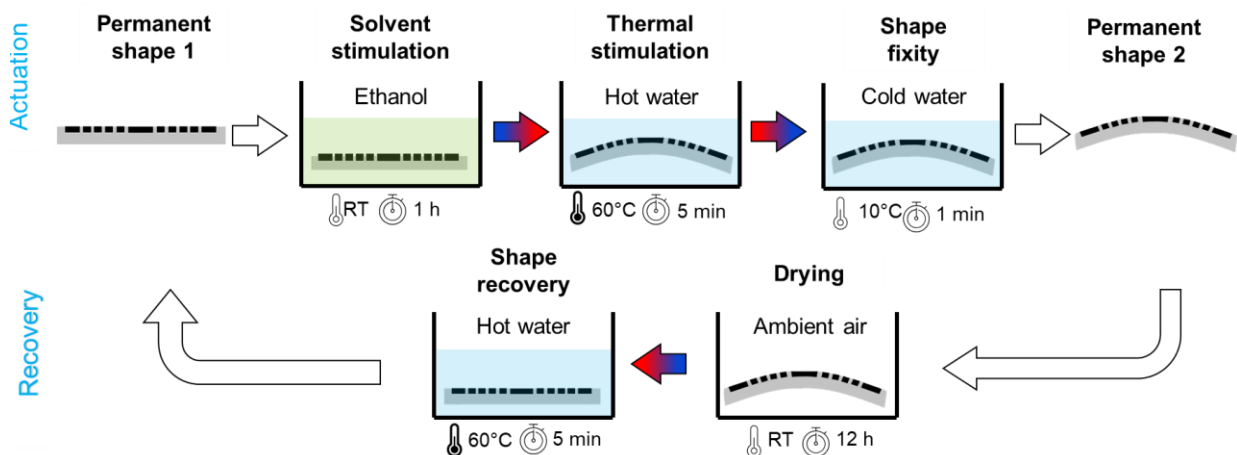


Figure 55: 4D printing process to achieve a shape change on a structure composed of Agilus30™ and VeroWhite™ materials. The specimens are 3D printed via the PolyJet™ technique, solvent stimulated at room temperature (RT) for 1 h enabling the swelling of the elastomer, then thermally stimulated at 60°C for 5 min enabling the shape change of the whole structure. The specimens are finally cooled down at 10°C for 1 min to ensure the shape fixity. The shape recovery stage consists in drying the specimens at RT for 12 h and then heating up them at 60°C for 5 min.

4.3. Results & Discussion

The study consists of a parallel investigation of the influence of interlocking blocks assembly on the actuation time, shape change, and reversibility of a multi-material special pattern sample. To demonstrate the performance of such structures, they have been compared to multi-material structures

printed in a single go with MJ. A combination of numerical simulation, mechanical tests, and physical stimulation results are presented to emphasize the feasibility of the computational design approach and related fabrication strategy. The samples are a strip measuring 6.2 cm long, 1 cm wide, and 0.5 cm thick (containing 3.100 voxels measuring 1 mm³ each) and are entirely printed with the Stratasys PolyJet™ printer using Agilus30™ and VeroWhite™ resins as shown in Figure 76a,b. To verify the reproducibility of the results, 5 samples were tested for each manufacturing strategy.

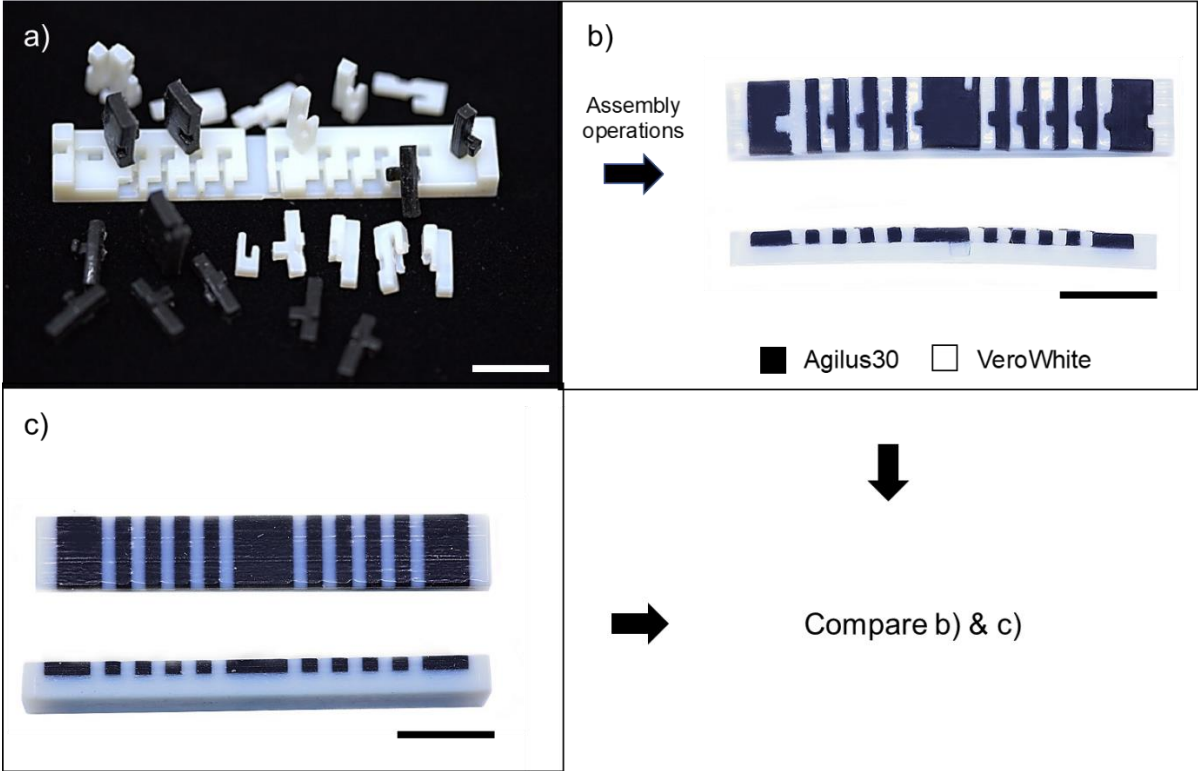


Figure 56: Fabrication of the multi-material samples via material jetting (PolyJet™ technique) with the Objet260 Connex3 printer and VeroWhite™ and Agilus30™ materials: (a) the interlocking blocks printed separately then manually assembled, (b) the multi-material structure printed in a single operation.

4.3.1. Analysis Before Actuation

A first test was carried out with three-point bending test to measure and compare the deflection rate of both structure samples. A graph of the deflection of the samples (in mm) against the average time spent in the bending (in seconds) is presented in Figure 57. While increasing the bending force continuously, the samples achieved a deflection of 14.5 mm. The figure demonstrates that both interlocked and fully printed structures kept pace and deformed almost perfectly at an even speed, in an interval of 17 seconds. One can deduce that from a mechanical perspective, the interlocking blocks assembly method did not

decrease the mechanical properties of the multi-material structure nor the deformation shape of the samples. These results then add value to interlocking assemblies from a mechanical point of view.

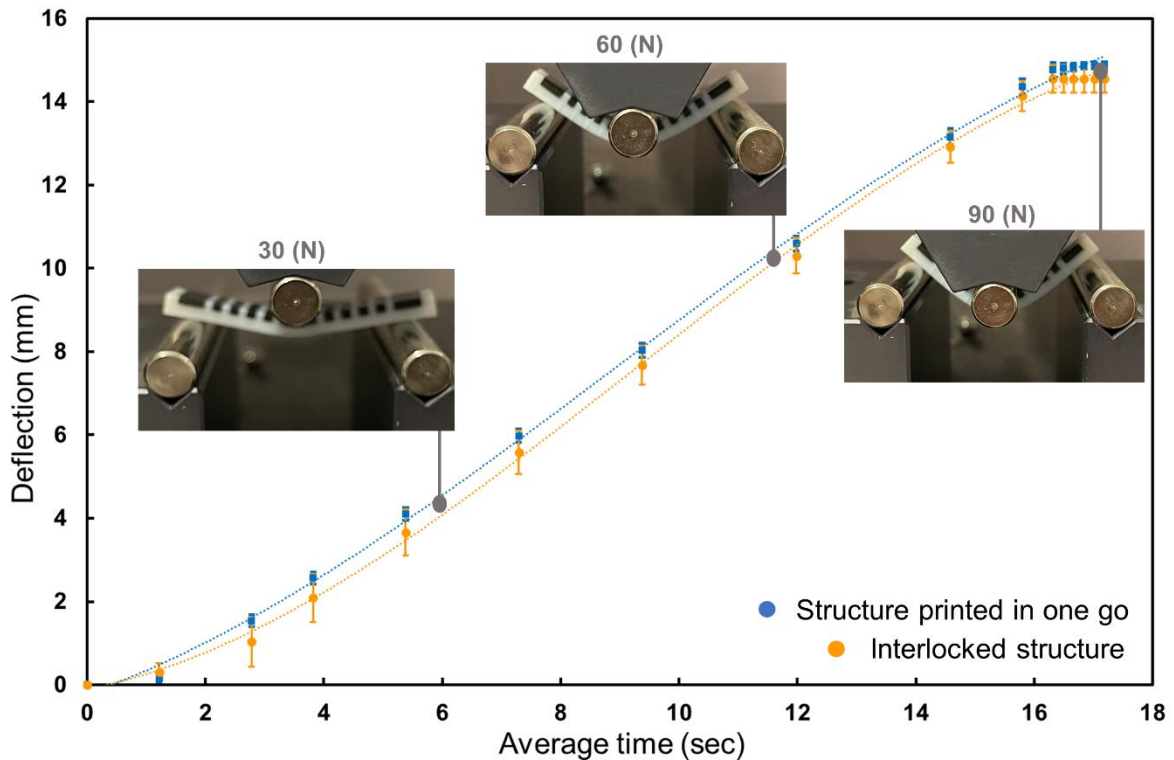


Figure 57: The plot of deflection against average time as 3pts-bending test results. The results of the multi-material structure printed in one go are presented in blue color, the results of the multi-material structure made of interlocked blocks are presented in orange color.

4.3.2. Actuation Performance

4.3.3.1. Simulation in a voxel-based computational design software

As previously stated in Section 4.2.3., narrow modifications in the materials distribution were carried out when necessary in order to create the conditions for the interlocking blocks generation. However, modifications in structural parts, regardless of their size, may be delicate and have a negative impact on physical behavior. Here is where the simulation phase plays a crucial role, aiming at investigating the consequences of the modifications regarding the physical characteristics of the structure. For a relevant study, we target minor or nonexistent differences during the simulation in terms of shape-changing and physical properties of the assembled structure compared to the multi-material structure printed in a single operation. The simulation results are highlighted in Figure 58, in which voxels displacements along the X, Y, and Z axis can be obtained, using the VoxSmart software tool (U output as highlighted in Figure 58). The computed displacements are then used to compare both structures regarding their physical behavior in a presence of energy.

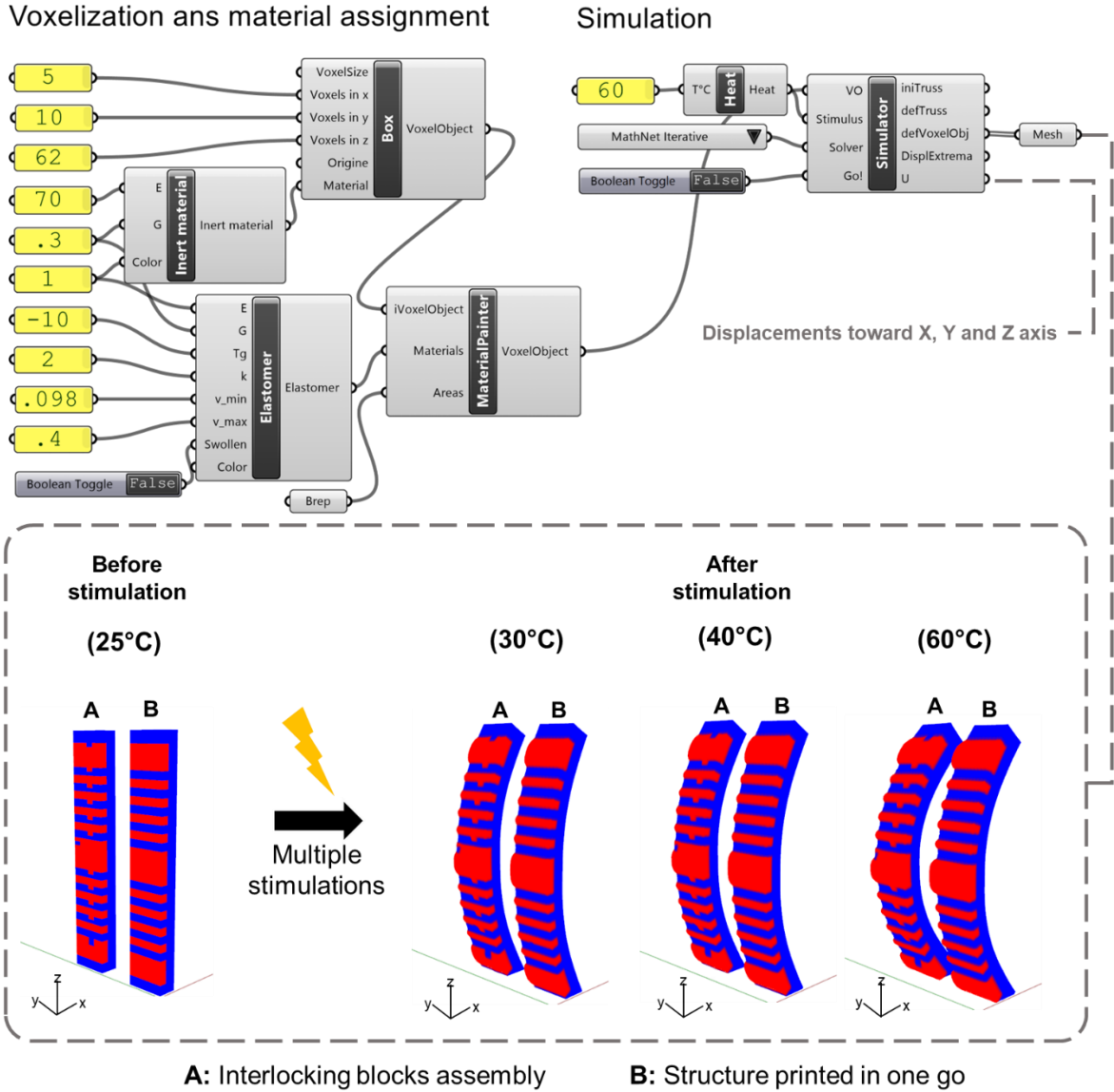


Figure 58: Simulation of the interlocked structure deformation (A) and the printed structure in a single operation (B), within the process flow of the VoxSmart software tool for voxelization, materials assignment, and simulation of the energy stimulation. A and B are represented before stimulation (at 25°C) and after stimulation at 30°C, 40°C, and 60°C.

To do so, we proceed by measuring vector moduli, referring to the distance between the position of a voxel v_B in the fully printed structure (B) and its position (v_A) in the interlocked one (A). The vector moduli are given as follows (Equation 5):

$$\| \vec{v_A v_B} \| = \sqrt{(U_{x_A} - U_{x_B})^2 + (U_{y_A} - U_{y_B})^2 + (U_{z_A} - U_{z_B})^2} \quad (5)$$

where $v_B = (U_{x_B}, U_{y_B}, U_{z_B})$ and $v_A = (U_{x_A}, U_{y_A}, U_{z_A})$ are displacements vectors of the voxels in the fully printed and the interlocked structures respectively.

Considering the simulations and distances calculation results, Figure 58 and Table 9 demonstrate that the variation of deformation between both structures is very little, either at 30°C, 40°C, or 60°C. For instance, Table 9 lays out the maximum and the average distances between a voxel's position in (A) and (B), indicates that at 60°C, the average distance between a voxel in (A) and its position in (B), corresponds to 1.065 mm, which is small against a sample measuring 62 mm long. Once again, the narrow modification that has been applied to the materials distribution to generate the interlocking blocks assembly, has not violated the physical properties of the 4D structure. Therefore, we further prove the relevance of the interlocking assembly method.

Table 9: Calculation of the maximum and average distances between voxels' positions in the interlocked structure (A) and the fully printed structure (B) at various temperatures.

	25°C	30°C	40°C	60°C
Maximum distance [mm ±0.01]	0	0.717	0.724	2.291
Average distance [mm ±0.01]	0	0.335	0.342	1.065

4.3.4.2. Deformation ratio and curvature measurements

As described in Section 4.2.5.2, both heat and ethanol are applied to the bi-material samples. Their actuation will take place in three main stages. In the first stage, The bi-material samples made of VeroWhite™ and Agilus30™, are immersed in ethanol at room temperature for 1hr. In such an environment, the small molecules of ethylic alcohol will diffuse in between the elastomer (Agilus30™) polymeric chains. The latter will behave as a hydrogel by swelling and increasing in volume due to the alcohol diffusion. Whereas as regards the transition material (VeroWhite™), it will not swell in the same environment, since the material is still stiff at room temperature. The imbalance in strain and volume will induce stress and create pressure that is notably very weak against the VeroWhite™ mechanical strength and stiffness at room temperature, the transition material ending will then not be witnessed. Therefore, we proceed to the second stage, where the samples are removed from the ethanol to be placed directly in a hot bath of water at 60°C for 5 min. In such a manner, the VeroWhite™ is heated above its T_g , resulting in significantly decreasing its stiffness and enabling its shape-changing ability. Thus, the samples will eventually be able to bend and relieve the stored stress. The third stage consists in placing the samples in cold water for about 1 min to cool down quickly and maintain the new shape after bending.

On one hand, Figure 59a shows pictures that were captured every minute during an interval of 5 min while the samples are still soaked in the hot water bath at 60°C. On the other hand, Figure 59b illustrates curvature measurements of the samples of both structures. If we gather the observations, one could deduce from the results that after 5 min, both structures have shown almost the same curvature (0.12 mm⁻¹ for the fully printed structure and 0.13 mm⁻¹ for the assembled structure). However, the structures

did not deform at the same speed. Figure 59a,b and Figure 60b demonstrate that the deformation of the interlocked structure was faster than the deformation of the fully printed structure. As a matter of fact, the interlocked structure presented the aforementioned curvature in an early stage (about 2 min), whereas the fully printed structure took about 5 min to achieve almost the same change. These results were quite expected since, in the interlocked structure, the hot water can easily access to the transition material interfaces. Thus, the entire structure can be heated above the transition material T_g rapidly. Therefore, the assembled structure can relieve the stored stress and bend more rapidly while in the fully printed structure, it takes time to achieve a temperature that is higher than the T_g of the VeroWhite™ material. An important observation that one can also make from the images in the assembled structure, is that parts maintained their positions while bending, i.e., the interlocked structure did not fall apart even though it has undergone a shape change. These observations are all promoting the multi-material interlocking assembly approach, which open the door of multi-material 4D printing through materials assembly.

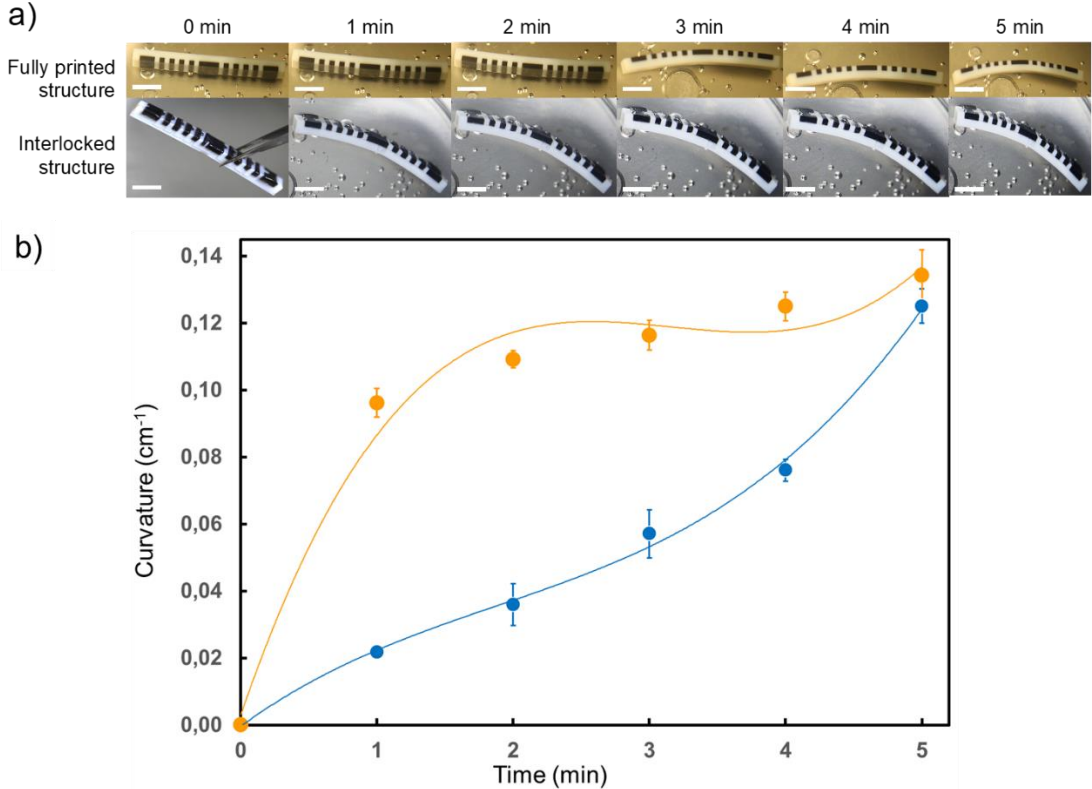


Figure 59: (a) Illustration of the deformation of both structures in hot bath water (60°C) during 5 min time-lapse, and (b) related graph of curvature against time. The fully printed structure is represented in blue color, while the interlocked structure is in orange color. The interlocked structure showing curvature at an earlier stage compared to the fully printed structure. In the interlocked structure, hot water can easily access the interfaces, allowing the entire structure to be heated rapidly above the transition material T_g . This results in the assembled structure relieving stored stress and bending more quickly. The fully printed structure takes longer to achieve a temperature higher than the T_g of the VeroWhite™ material, thus explaining the slower deformation. All scale bars: 10 mm.

Besides the time spent by both structures to bend, Figure 60a,b compares the theoretical curvatures radius measurements resulting from the simulations and the radius of the experimental curvature. The results turned out quite favorable, both theoretical and experimental presented comparable results either for the assembled or the fully printed structure. We note that the curvature radii in Figure 60a were measured after immersion in the cold-water bath. Images were captured in Figure 60c,d,e to illustrate these similarities.

4.3.4.3. Demonstration of reversibility

To demonstrate the reversibility of the physical behavior of the samples, the latter had to complete multiple cycles of actuation and shape recovery phases. Besides the necessary stages mentioned in the previous section to carry out the actuation phase of the samples, the shape recovery phase takes place in two main steps. One can consider that it is mandatory for samples to dry after the actuation phase. In such a way, ethanol molecules diffuse out of the Agilus30™ material, and the latter recovers its elasticity and initial volume. While the Agilus30™ decreases in volume, compression energy is stored again in the structure. However, this energy is insufficient to return the sample to its original shape. It is here where the recovery shape phase will take place. First, we heat the structure above the T_g of the transition material one more time, to soften the VeroWhite™ material. Thus, the stored energy can once again pull the structure to its original shape. Last, and to complete a cycle, the samples are newly immersed in cold water. Figure 61 and 62 illustrate four completed cycles by each assembled and fully printed structure. Photos were taken after actuation and shape recovery stages. The figures demonstrate that from the first to fourth programming cycle, the samples kept pace and the curvature radii remained alike. In addition, the samples were also able to return to the initial shape, after the shape recovery phase.

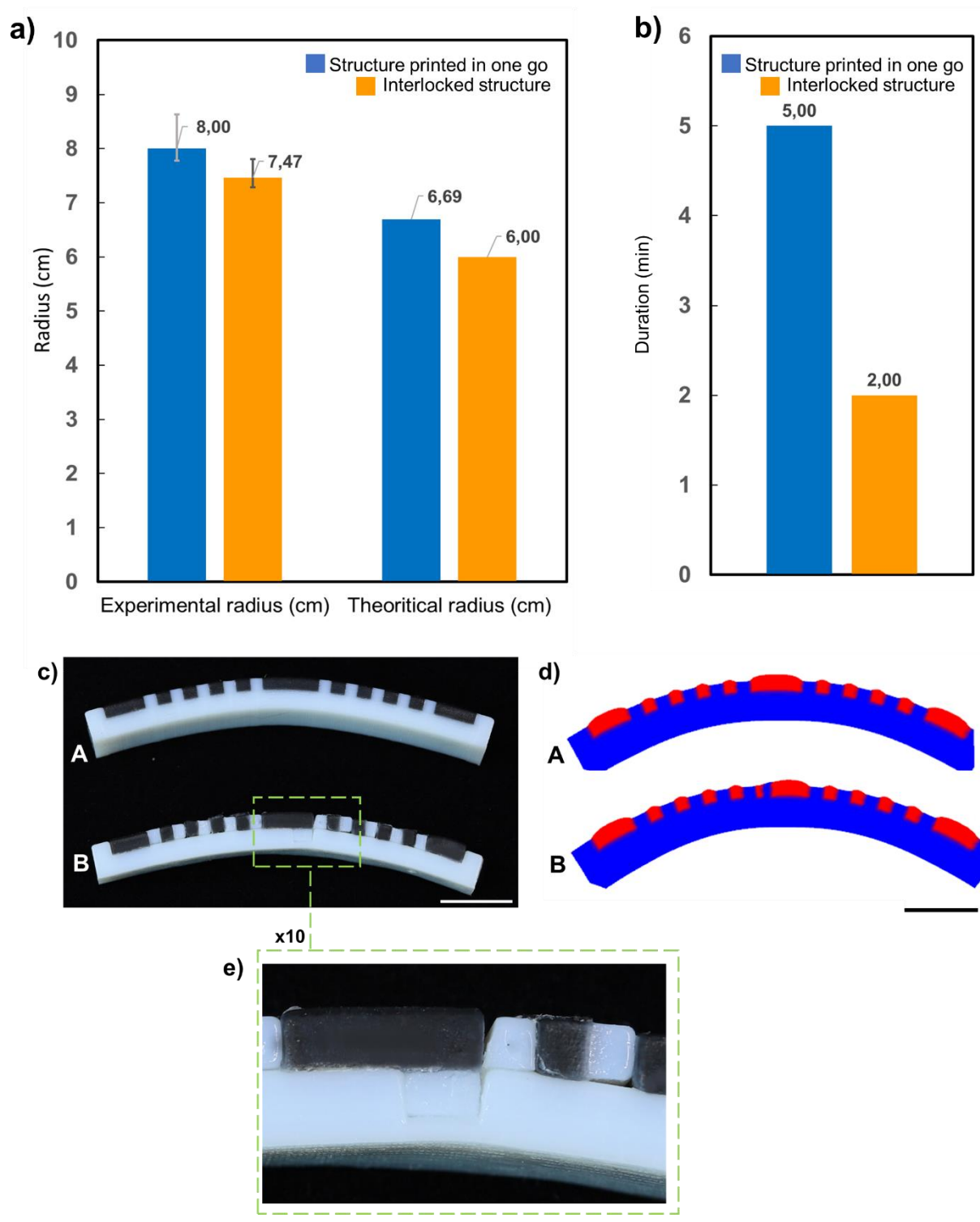


Figure 60: Comparison of the samples performance: (a) experimental curvature radius (experiments outcome) vs. the theoretical curvature radius (from simulation results), (b) time spent to achieve the experimental curvature by both interlocked and fully printed structures, (c) experimental stimulated structures once cooled down in water bath, (d) voxel-based simulations, and (e) local view of the interlocked structure after actuation. All scale bars: 10 mm.

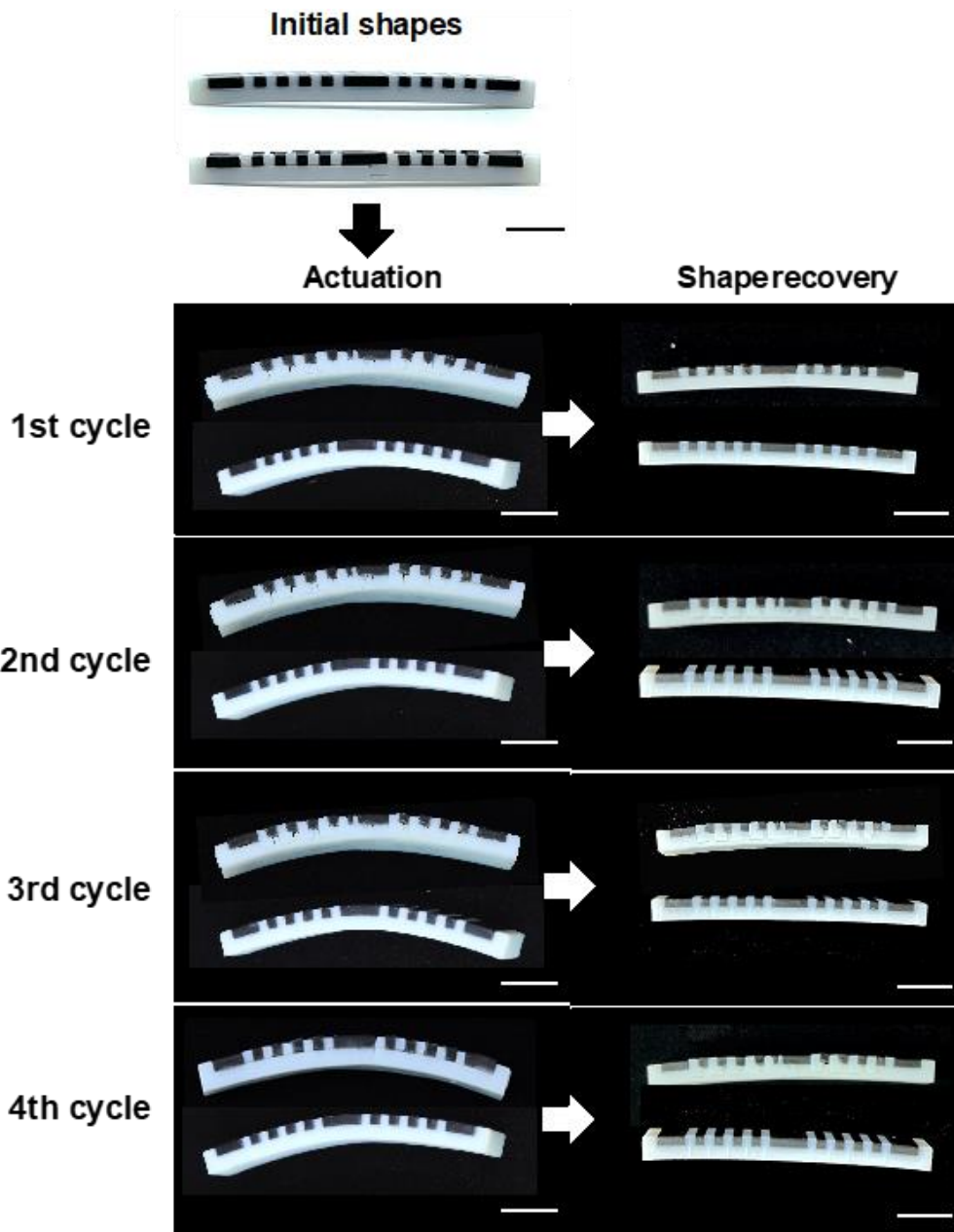


Figure 61: Reversibility cycles of both interlocked structure samples and fully printed ones. The samples bend in the programming phase, then return to their straight shape after the shape recovery phase. Four completed cycles are presented. All scale bars: 10 mm.

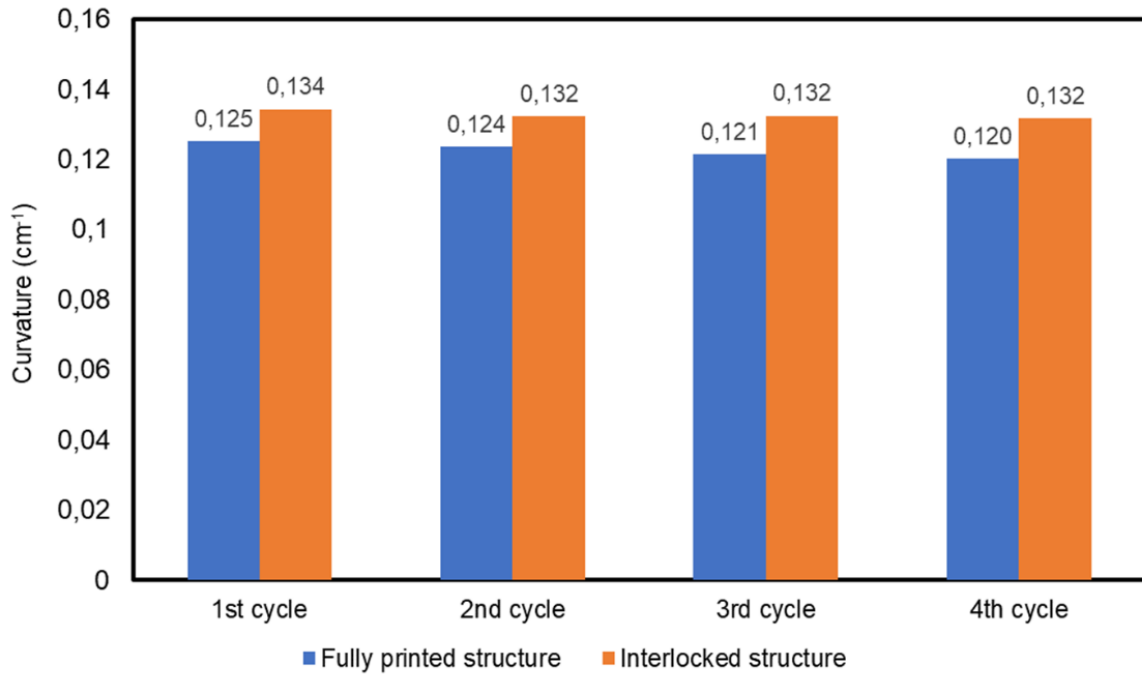


Figure 62: Curvature measurements of four completed reversibility cycles of both interlocked structure samples and fully printed ones.

Besides, to expose the load-bearing ability of the structures, we placed a weight of 200 g on the samples whenever the structures are cooled down after an actuation phase (see Figure 63). Both interlocked and fully printed structures carried the weight evenly, which is important for load-bearing purposes after shape-changing, where structures must bear the weight of the load without deforming or collapsing.

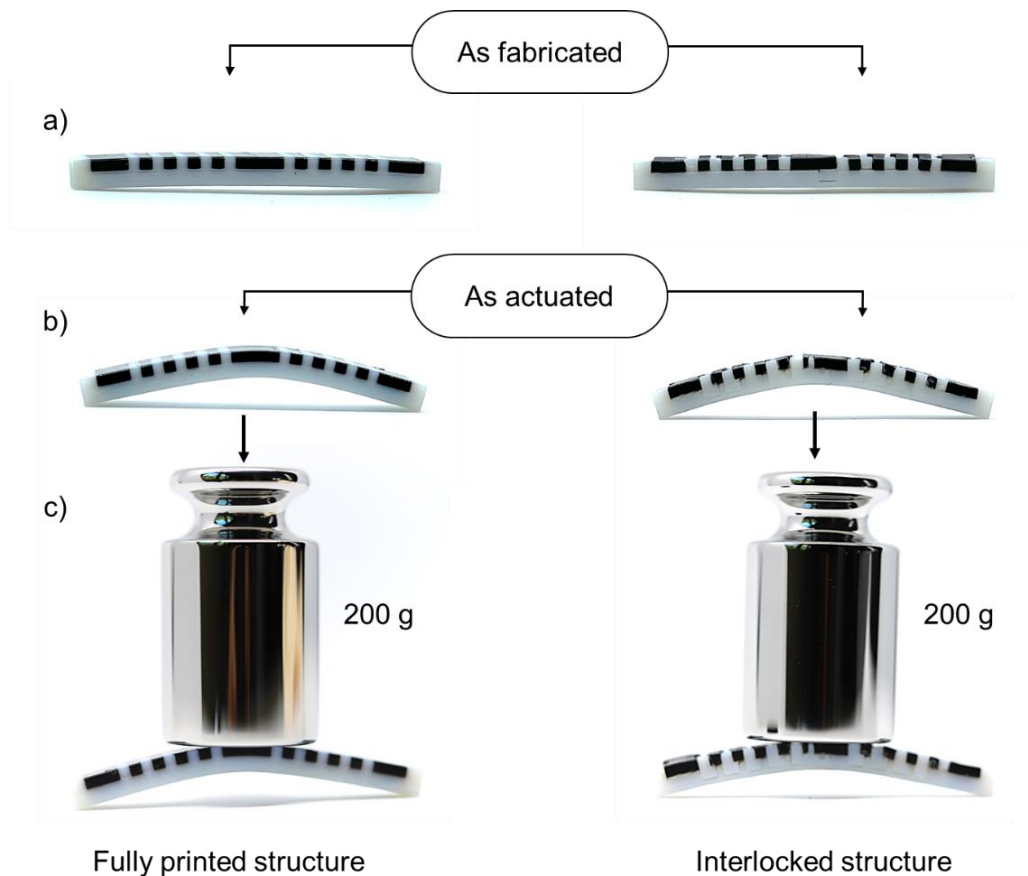


Figure 63: The stimulated samples of both interlocked and fully printed structures are bearing weight once are cooled down and the transition material gains its glassy state after the actuation phase. (a) the specimens as fabricated, (b) the specimens as actuated, (c) the actuated specimens bearing a load of 200 g.

4.4. Conclusion

In this chapter, we have studied the manufacturing strategy of multi-material interlocking blocks in greater depth, by investigating their effect on the behavior of 4D printed structures. As a first step, results from a computational design approach were used to obtain a multi-material 4D interlocking assembly. This process was carried out by an algorithm that considers materials distribution in a voxel-based 4D structure, to iteratively generate puzzle-like blocks intended to be printed separately and then assembled to the target shape. A comparison between both assembled 4D structures and multi-material structures printed in one go was made in terms of actuation response time, shape change and reversibility, through a combination of experimental tests and numerical simulations. The related results were presented and discussed to demonstrate the relevance and added value to the multi-material 4D printing via interlocked blocks. The study shows that on one hand, an interlocked multi-material structure achieved comparable performance to a simple printed structure, from the cited criteria. On the other hand, this study adds

value to the multi-material interlocking assembly approach, which offers an efficient way to build complex assemblies that can couple metals/polymers or solid voxels/lattices in the same assembly. Such assemblies are actually impossible to be manufactured by the current AM technologies in a single run.

Under these conditions, one can notice that our experiments were meant to execute one limited shape-changing configuration. Relaxation of these limitations will be attempted in the next chapter to generalize the present strategy. Thus, it is necessary to consider other case studies presenting other shape-changing configurations such as curling, and twisting to name a few, as well as adapting the proper interlocking models and assembly sequence planning.

Chapter 5: A Customized Interlocking Assembly blocks for Improved Multi-Material 4D Printing Structures Performances

”من لم يذق مر التعلم ساعة تجرع ذل الجهل
طول حياته“

*"He who has not tasted the bitterness
of learning for an hour will gulp the
humiliation of ignorance for
eternity."*

Arabic saying

Chapter 5: A Customized Interlocking Assembly blocks for Improved Multi-Material 4D Printing Structures Performances	105
5.1. Introduction	107
5.2. Materials & Methods.....	109
5.2.1. Materials.....	109
5.2.2. Printing parameters.....	110
5.2.3. Interlocking assembly generation approaches	110
5.2.4. Assembly stability	114
5.2.5. Actuation simulation	114
5.2.6. Actuation process	114
5.3. Results & Discussion.....	115
5.3.1. Interlocking assembly generation with customized interlocking blocks results	115
5.3.2. Assembly stability	117
5.3.3. Actuation simulation	120
5.3.4. Actuation process	124
5.4. Conclusion.....	126

5.1. Introduction

The contributions of this thesis are structured into three chapters that progressively build upon each other. The first chapter proposes a novel computational design approach for multi-material 4D printing after meticulously analyzing the distribution of digital materials on a voxel basis within a given structure. By understanding the spatial arrangement of materials at the voxel level, we can achieve precise control over the interlocking generation, enabling the creation of complex and functional assemblies. What makes this approach particularly significant is its generality and efficiency. It opens up new possibilities for exploring intricate assemblies that were previously unattainable using a single AM technique in a single run. For instance, we can seamlessly combine solid voxels or lattices with different materials, such as metals and polymers, within the same 4D printed structure. This approach expands freedom in design and allows for the creation of innovative and customized objects with varying material properties in a single print. The second chapter delves deeper into the exploration of interlocking block assemblies and their impact on the behavior of multi-material 4D printed structures. In this investigation, comprehensive analyses of various critical parameters were conducted, including actuation time, shape change, and reversibility of the 4D printed structures, through a combination of mechanical tests, stimulation experiments, and numerical simulations. These insights aimed to validate the practical relevance and effectiveness of the proposed computational design approach, showcasing its potential to create functional objects with dynamic properties.

Arriving at this chapter of our study, we will introduce the concept of customized interlocking blocks generation, in order to significantly enhance our research endeavors. This particular concept is explored in the literature and can bring with it a multitude of advantages. For instance, customizing the shapes of the interlocking blocks grants the ability to perfectly suit specific utilization requirements and optimize their functionality and performances [209,223-224]. One other key advantage of utilizing the customized interlocking blocks concept is the simplification it offers in the assembly process [225-226]. Since the blocks are already predefined and standardly designed, the streamlining of the assembly workflow saves valuable time and effort by avoiding additional computation of the interlocking blocks. Additionally, such types of interlocking blocks add the advantage of not only being recyclable but also versatile in their assembly [223,227-229]. These blocks possess the capability of being assembled into multiple shapes and designs, further enhancing their usability and adaptability. The sustainability and versatility aspects of customized interlocking blocks align perfectly with the commitment to reducing waste and promoting environmentally friendly manufacturing practices. Furthermore, leveraging such a concept enables us to advance toward the automation of robot-guided assembly [226]. This is due to the predefined and standard nature of the blocks. By incorporating robot-guided assembly techniques, higher levels of accuracy, repeatability, and efficiency in constructing interlocked structures, can be achieved. Moreover, customized interlocking blocks concept opens up exciting possibilities for multi-

scale interlocking assembly since voxel sizes can be controlled [228]. It is to say that interconnected systems and structures at various levels of detail can be created, allowing for the development of complex and adaptable architectures.

However, in our study, we will harness the potential of the customized interlocking blocks concept from a different perspective. As we are aware, the algorithm developed in Chapter 3 generates interlocking blocks to construct 4D multi-material structures capable of undergoing shape/property transformations through the application of energy stimulation. However, in some cases of shape transformations (see Figure 64a), particularly when using certain SMs, the interfaces within the assembly may not keep up with the overall deformation of the structure. This can lead to a lack of contact and deformation continuity, which hinders the uniformity of the overall deformation.

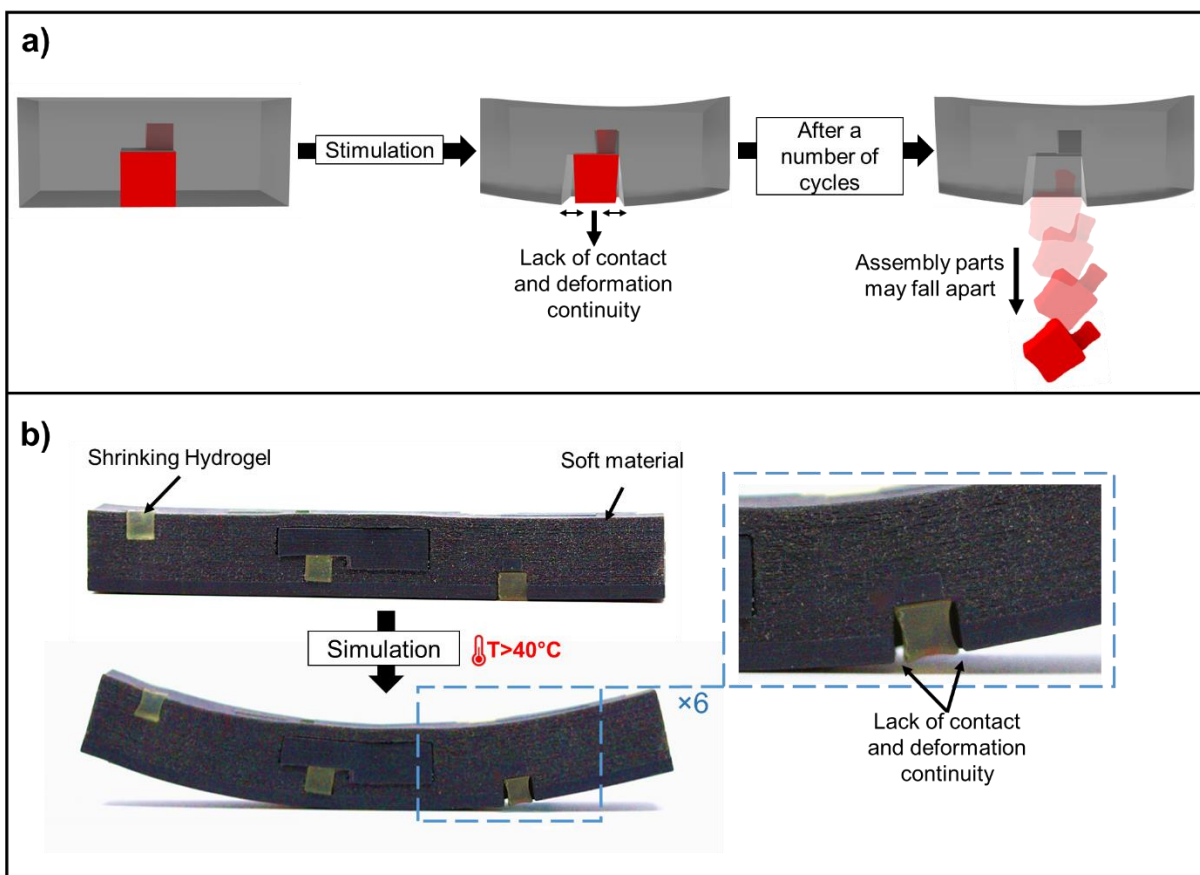


Figure 64: illustrating limitations of interlocking blocks assembly concerning the contact and deformation continuity, a) illustration scheme after multiple cycles of stimulation, b) case of a shrinking hydrogel demonstrating the un-uniform overall deformation of the structure.

For instance, as illustrated in Figure 64b, even though the assembly remains intact after the stimulation, the external interfaces surrounding the shrinking hydrogel may not adhere properly. The shrinking hydrogel block fails to drive the neighboring interfaces, resulting in non-uniform or interrupted deformation in other terms. To overcome these challenges and generalize the applicability of the computational design approach, we will rely on the customized interlocking blocks concept.

Therefore, the main idea of this chapter is to customize the shapes of the interlocking blocks during the early stages of assembly generation, taking into account the specific SMs at our disposal and their potential transformations (isotropic or anisotropic behavior). By tailoring the block shapes to accommodate the behavior of the SMs, we aim to improve the uniformity of shape/property changes within the 4D multi-material interlocked assembly. Additionally, we will address the limitations associated with the interfaces between blocks, ensuring both contact continuity and deformation continuity which are two critical factors in achieving successful 4D printed structures. To assess the effectiveness of utilizing customized interlocking blocks, we will compare the physical behavior and the stability of two assemblies (see B and C in Figure 65): Assembly B derived from the previous interlocking assembly approach developed in Chapter 3 (without using a customized interlocking blocks), and the second assembly (Assembly C) is generated using the customized interlocking blocks concept.

The structure of this chapter will be organized as follows: The subsequent sections will initially describe the materials and methods involved in this study. Following that, comprehensive results and discussions will be presented, incorporating mechanical test results, simulations, and stimulations performed on illustrative cases. Lastly, the chapter will conclude with a concise summary and closing remarks.

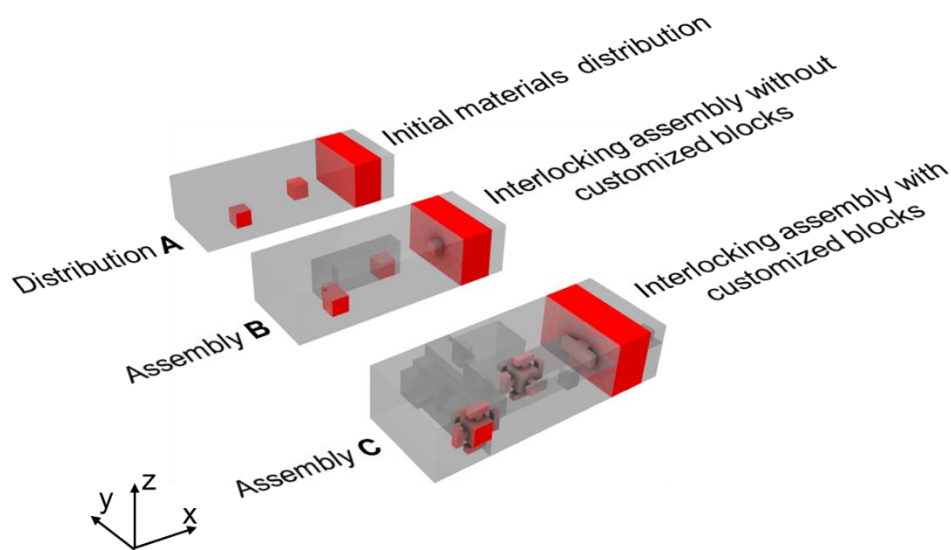


Figure 65: Illustrative case studies. Starting from (A) as an initial digital materials distribution, (B) is the interlocking assembly generated from the previous interlocking approach developed in chapter 3 (without customized interlocking blocks), and (C) is the interlocking assembly generated using customized interlocking blocks.

5.2. Materials & Methods

5.2.1. Materials

Two materials were used to undertake this study. As an inert material we used a PolyJet™ Objet260 Connex3 printer (Stratasys®, Ltd., USA) to print Agilus30™ parts. This machine combines Inkjet technology and the use of photopolymers. The Agilus30™ is a soft and rubber-like material with a T_g of -10°C . Its liquid resin contains a photoinitiator, exo-1,7,7-trimethylbicyclo(2.2.1)hept-2-yl acrylate, urethane acrylate oligomer, methacrylate oligomer, and polyurethane resin [221]. As an active material we printed hydrogel parts using DLP [230-231]. The formulation is prepared by mixing the N-isopropylacrylamide monomers (50 wt% relative to the formulation) with PEG700-diacrylate crosslinker (2.5 wt% relative to the formulation) in ethylene glycol (50 wt%) as a non-reactive diluent. Irgacure TPO (3 wt% relative to the NIPAM and crosslinker) was added as photo-initiator.

5.2.2. Printing Parameters

On one hand, the Agilus30™ parts were printed using the digital material mode at a resolution of 118 dpi. cm^{-1} along the x - and y -directions and a layer thickness of 30 μm and up to 85 μm for the x - and y -axes. The resins are polymerized by the ultraviolet light with a spectral range of 300-450 nm.

On the other hand, the hydrogel parts were fabricated using a DLP machine (Max X43, Asiga Australia). The parts were constructed by photocrosslinking successive 100 μm thick resin layers. Each layer was irradiated at an intensity of 2.5 mW/cm^2 for 3 seconds. After construction, the hydrogel parts were first washed in ethanol then several times with distilled water for 3 days.

5.2.3. Interlocking Assembly Generation Approaches

To thoroughly evaluate the efficiency of incorporating a customized interlocking blocks based on SMs behavior, our investigation focuses on comparing the behavior and the stability of two distinct assemblies. The first assembly (labeled as assembly B in Figure 65) is derived from the previously established interlocking assembly approach outlined in Chapter 3. This approach served as the foundation for constructing an interlocking assembly without the utilization of a customized interlocking blocks. In contrast, the second assembly (labeled as assembly C in Figure 65) will be generated using a customized interlocking blocks. By conducting a detailed analysis of both assemblies, we aim to evaluate the comparative performance of the first interlocking approach (assembly B) versus the implementation of the customized blocks (assembly C).

5.2.3.1. Interlocking Assembly Generation Without Customized Interlocking Blocks

To generate assembly B, we will employ the conventional approach. Initially, a 3D/4D structure is established through machine learning or genetic algorithms, with a digital multi-material distribution

(see Figure 66,a). This computational design approach, facilitated by software tools like Rhinoceros3D/Grasshopper® and the VoxSmart add-on, determines homogeneous interlocking blocks of voxels. These blocks are designed to be printed separately using various AM processes and materials, and subsequently assembled. hereby, we will apply this computational procedure to an $80 \times 18 \times 30 \text{ mm}^3$ strip sample comprising 5400 voxels, with each voxel having a volume of 2 mm^3 .

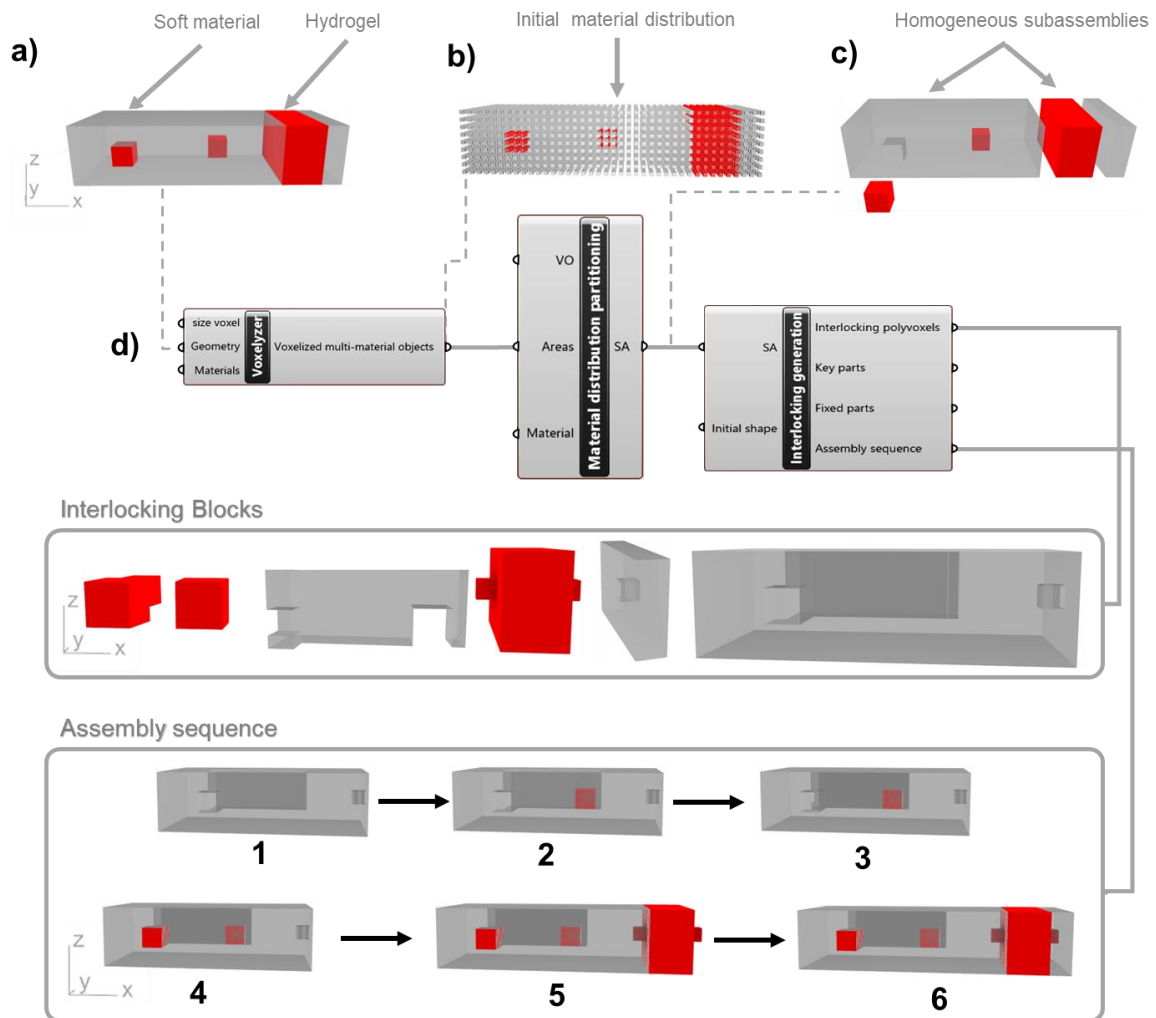


Figure 66: Rhinoceros3D/Grasshopper® program flow to determine the interlocked blocks assembly of an $80 \times 30 \times 18 \text{ mm}^3$ multi-material sample: (a) initial geometric structure highlighting the distribution of active/inert materials, (b) voxelization of the materials distribution, (c) homogeneous subassemblies after material distribution partitioning, (d) design program flow dedicated to the interlocking computation.

The process involves the three usual components: (i) the 'Voxelyzer' component, which obtains a voxel-based representation of the materials distribution within the 3D/4D structure (see Figure 66,b); (ii) the 'Material distribution partitioning' component, which divides the structure into homogeneous parts based on material composition (see Figure 66,c); and (iii) the 'Interlocking generation' component, which generates interlocking blocks and determines the appropriate assembly sequence. These components are illustrated in Figure 66d.

5.2.3.2. Interlocking Assembly Generation With Customized Interlocking Blocks

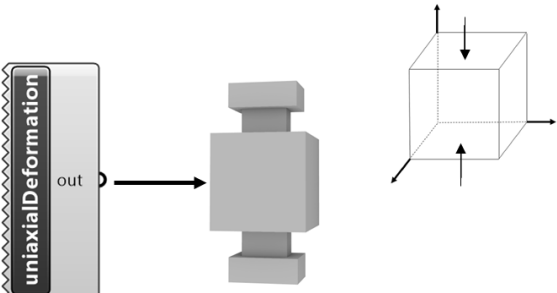
The primary goal of this chapter is to generate a 4D multi-material interlocking assembly after the customization of the interlocking blocks during the initial stages of the assembly computation. A crucial consideration in this process is understanding the specific SMs' potential transformations, whether they exhibit isotropic or anisotropic behavior. By incorporating this knowledge, we can optimize the shapes of the interlocking blocks to align with the anticipated deformations. For instance, let's compare the behavior of hydrogels and liquid crystal elastomers (LCEs) in this context. Hydrogels are known for their remarkable ability to absorb and retain water, resulting in significant swelling and softening. When subjected to external stimuli, such as changes in temperature or pH, hydrogels can undergo isotropic (uniform) swelling or shrinking in all directions due to their homogeneous network structure [57,231].

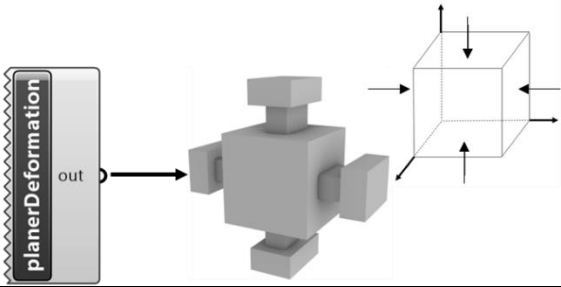
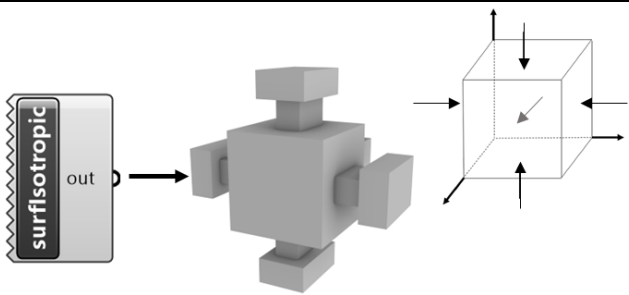
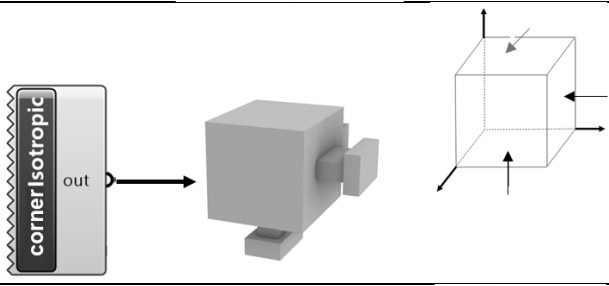
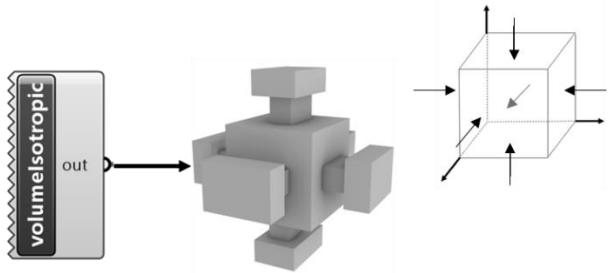
On the other hand, LCEs exhibit anisotropic behavior. LCEs are a class of soft materials that combine both the long-range orientational order of liquid crystals and the mechanical flexibility of elastomers. The anisotropic behavior of LCEs arises from the alignment of their liquid crystal domains, leading to a directional-dependent behavior when subjected to external stimuli i.e., a reconfiguration of the material's properties along specific directions [231-235].

By introducing interlocking blocks' designs with T-hinge-like shapes aligned with the expected deformation direction (see Table 10), we aim to maximize the functionality and effectiveness of interlocking structures, leverage the behavior of the SMs to achieve controlled and directional actuation, and ensure both contact continuity and deformation continuity at the assembly interfaces.

The T-hinges are added according to the digital materials distribution, the (isotropic/anisotropic) behavior and the location of the SM in a structure. Table hereafter gathers examples of components that were developed in Rhinoceros3D/Grasshopper® to add T-hinges to the interlocking blocks taking into account the aforementioned points.

Table 10: Customized interlocking blocks (examples of blocks according to SM Iso/anisotropic behavior and SMs location)

SM deformation	Grasshopper components and generated interlocking blocks
Uniaxial deformation	

<p style="text-align: center;">Planar deformation</p>		
	<p style="text-align: center;">Surface distribution</p>	
<p style="text-align: center;">Isotropic deformation</p>	<p style="text-align: center;">Corner distribution</p>	
	<p style="text-align: center;">Volume distribution</p>	

After incorporating T-hinges based on the digital materials distribution, the behavior (isotropic or anisotropic), and the location of the SMs within the structure, additional interlocking blocks will be generated to ease the overall assembly of the customized one. The interlocking assembly conditions involved in the development of the algorithm remain consistent with those discussed in the first approach presented in Chapter 3:

- 1- Only one translation direction is permitted for inserting each part into the assembly.
- 2- Each inserted part in the assembly effectively blocks the entire group of previously inserted parts, continuing until the key part(s) is ultimately inserted to secure the entire assembly.
- 3- Disassembly follows a single translation direction, with the key part(s) being the first to be disassembled.
- 4- Key parts are the only components that possess mobility within the assembly.

5.2.4. Assembly Stability

In order to compare the structural integrity and the assembly stability of both assemblies: Assembly B (an interlocking assembly that was generated without using customized interlocking blocks) and Assembly C (an interlocking assembly that was generated using customized blocks), a shaking test was performed. Also known as a vibration test, which is a destructive testing that can be undergone to assess stability and performance of component under simulated dynamic conditions. The purpose of the test is to subject both assemblies to a frequency of mechanical vibrations to compare their ability to withstand vibration environments. The vibrations can be applied in different directions and axes to cater to specific testing requirements. Test parameters such as amplitude and duration can be adjusted to simulate particular vibration scenarios or adhere to industry standards like DIN EN ISO 9000f [236].

In our study, the RETSCH® Type 3-D machine vibrating mode was employed, with an amplitude of 70 mm (representing the vertical vibration height). During the shaking test, both assemblies were mounted on a vibration platform and subjected to three-dimensional movements, including circular motion combined with vertical throwing motion. As a result, the samples were uniformly dispersed throughout the entire vibration area while undergoing reorientations. The time taken for both assemblies to experience their first separation of interlocking parts was then measured. In order to ensure repeatability and consistency of the findings, five samples of each assembly underwent the shaking test using the same procedure.

5.2.5. Actuation Simulation

To assess and compare the physical behavior of both assemblies, a comprehensive analysis is conducted using simulation and change calculation of physical deformations at multiple temperatures. This analysis is performed utilizing the VoxSmart add-on simulator within the Rhinoceros3D/Grasshopper® environment. The VoxSmart add-on also enables the generation of a computational predictive model of shape changing in both assemblies when subjected to stimulation energy. The simulation temperatures will be set at 25, 30, 35, 38, and 40°C, then a quantification of the voxel displacements will follow.

5.2.6. Actuation Process

As mentioned in Section 5.2.1, hydrogel was incorporated as an active material in both multi-material assemblies B and C. In these assemblies, the hydrogel acts as an actuator. It undergoes a shrinkage phenomenon when exposed to high temperatures due to the gradual evaporation of water initially absorbed within the PNIPAM hydrogel. Thus, the hydrogel parts will shrink leading to an overall

deformation of both assemblies. To evaluate the extent of contact continuity and compare between the two assemblies, the samples were heated at 40°C for a duration of 30 minutes. Following the heating process, gap measurements were conducted on captured images of the samples to assess the deformation visually and quantify the contact continuity. Again, to ensure repeatability and reliability of the results, five samples of each assembly were tested using the same procedure.

It is worth noting that the samples can recover their initial shape when immersed in distilled water at room temperature for at least two days. This recovery process demonstrates the reversible behavior of the hydrogel actuation. Figure 67 provides a visual representation of the actuation and recovery procedures involved in the testing process.

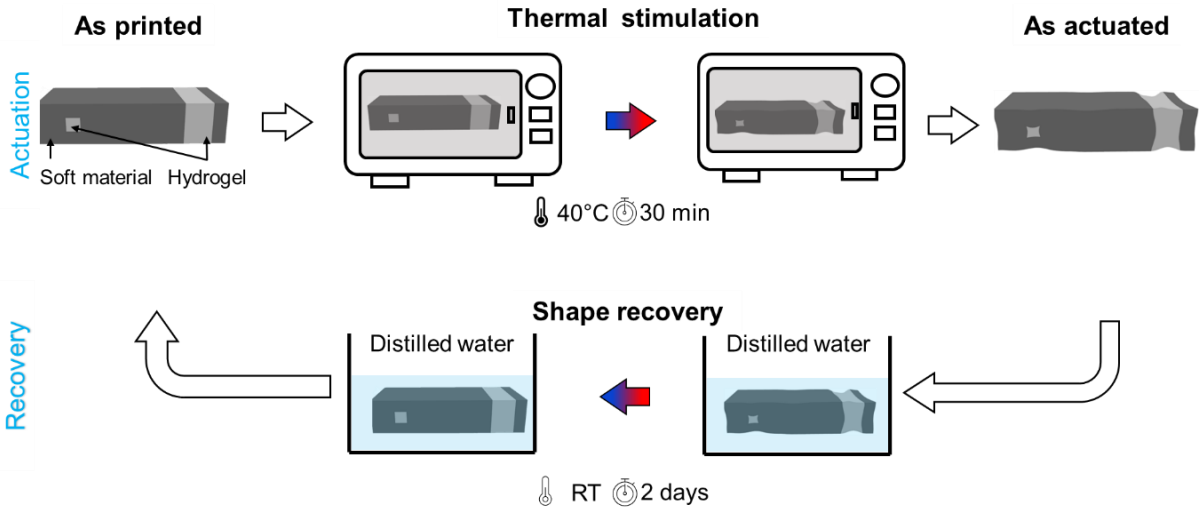


Figure 67: Actuation and recovery procedures of the interlocking assembly case studies.

5.3. Results & Discussion

5.3.1. Interlocking Assembly Generation With Customized Interlocking Blocks Results

After customizing the SMs interlocking shapes based on the digital materials distribution, the behavior (isotropic or anisotropic), and their location within the structure, the algorithm proceeds by voxelizing the remaining inert space that encapsulates the SMs using the 'voxelizer left space' component (refer to Figure 68a,c). This component generates a list of points which, with the assistance of mathematical models such as DBGs and adjacency matrices, will be utilized to generate the interlocking assembly. To do so, another component, labeled as the "interlocking generator," is developed. This component computes the interlocking blocks assembly and determines the suitable assembly sequence (as depicted in Figure 68,b).

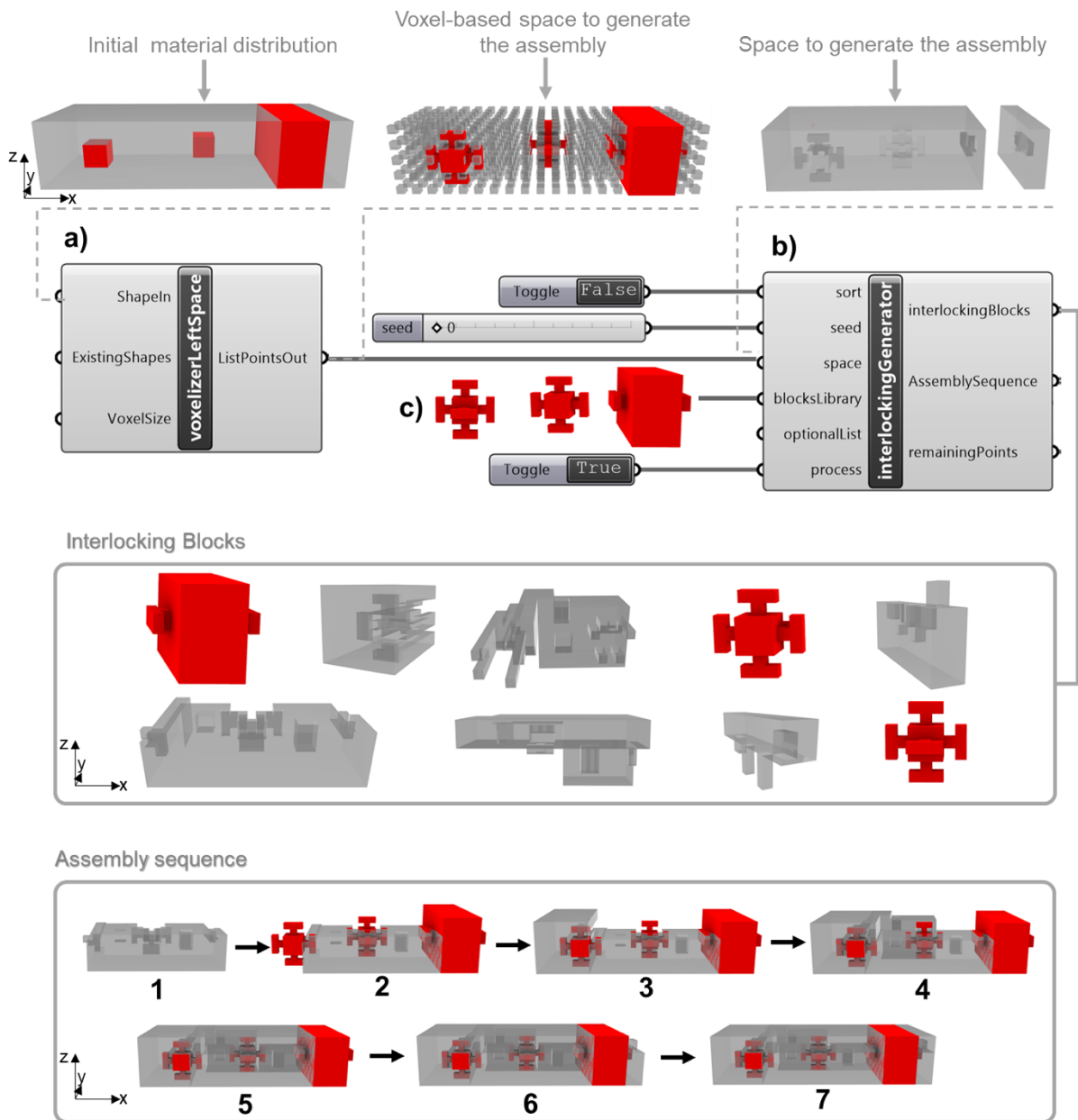


Figure 68: Rhinoceros3D/Grasshopper® program flow to determine the interlocked blocks assembly of the $80 \times 30 \times 18 \text{ mm}^3$ multi-material sample, the red color refers to the hydrogel and the grey color to the inert material: (a) voxelization of the remaining space component initial geometric structure highlighting the distribution of active/inert materials, (b) the interlocking assembly generator component, at the end of the process, it generates the interlocking blocks as well as their related assembly sequence, (c) the customized interlocking blocks involved in this case of study.

The algorithm generates numerous interlocking assemblies based on the chosen seed (as shown in Figure 69b), which governs the selection of voxel candidates during the assembly computation. Figure 69 provides one possible interlocking assembly generated by the tool, accompanied by the corresponding DBGs and adjacency matrices.

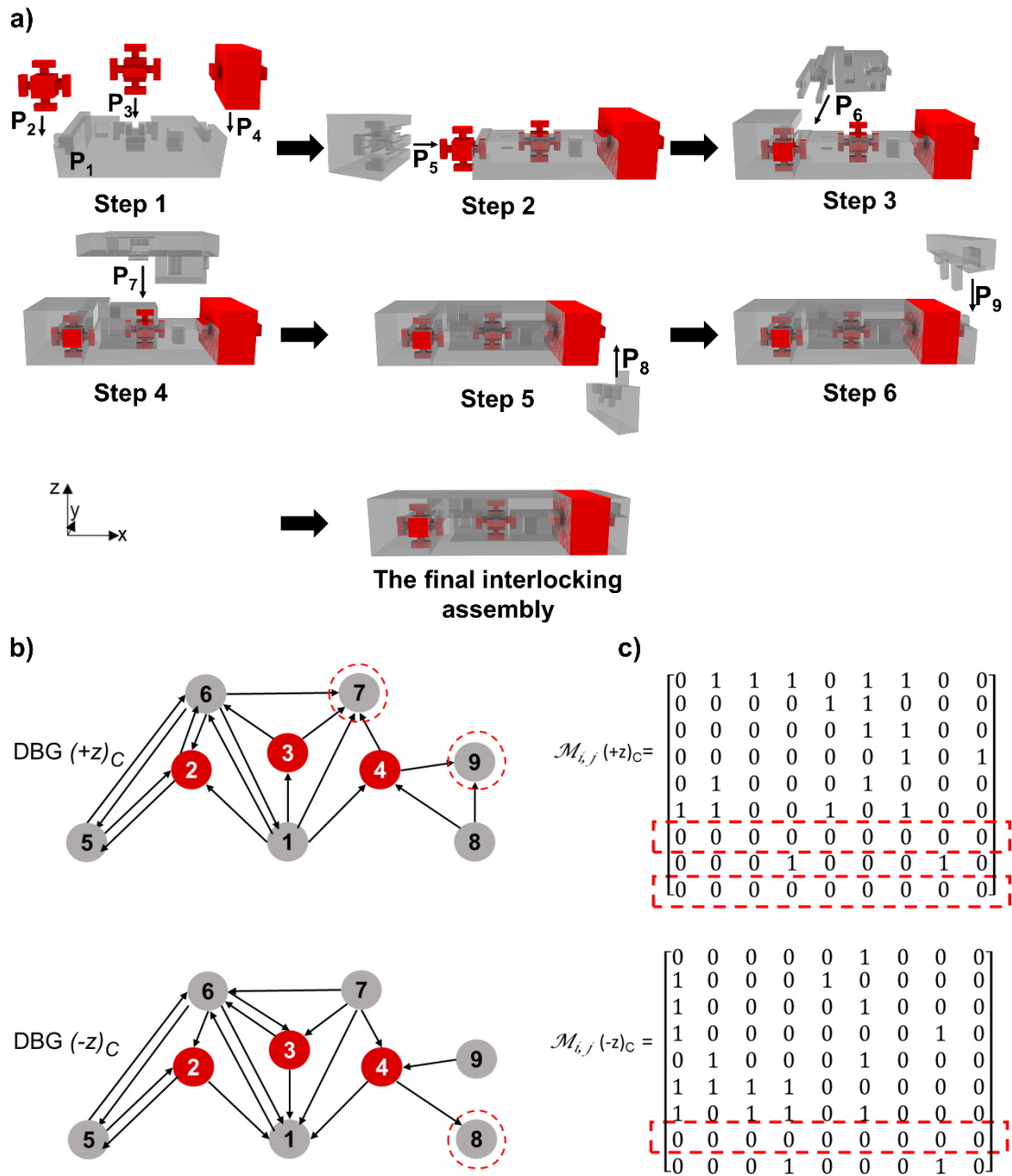
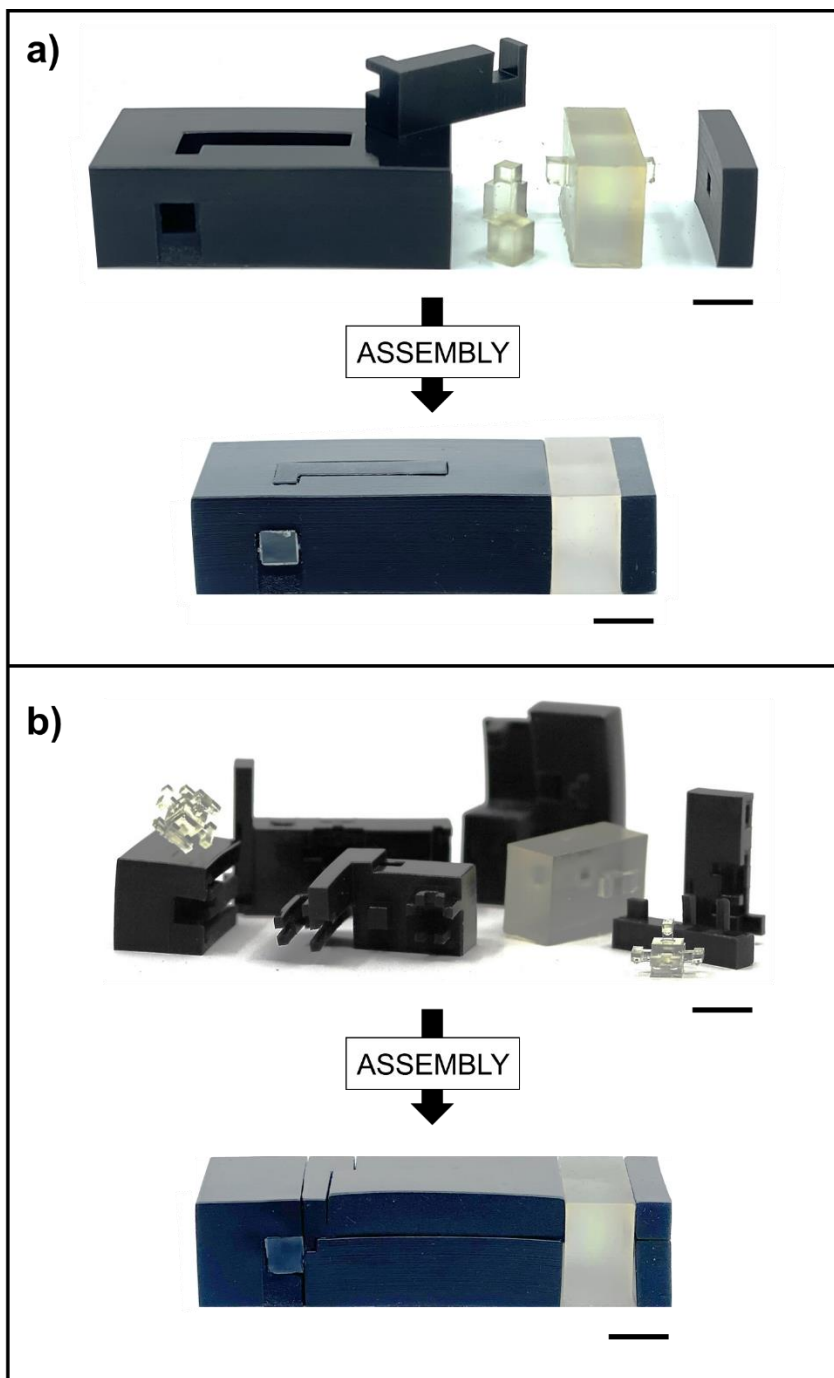


Figure 69: Multi-material interlocking assembly generated using a customized interlocking blocks. (a) description of the assembly sequence of the multi-material 4D printed sample, 6 blocks have been determined by the software tool in addition to the customized blocks, (b) the direct blocking graph of the final interlocking assembly, the nodes represent the 9 blocks of the assembly, an ordered pair (arrow) between P_1 and P_2 means that P_1 is blocked by P_2 along a direction d , the dashed red circles illustrate the key parts in the direction d , and (c) related adjacency matrices.

5.3.2. Assembly Stability

After physically printing the hydrogel and the Agilus30™ interlocking blocks (Figure 70), Assembly B and Assembly C were manually constructed, as depicted in Figure 70. Subsequently, both assemblies were mounted onto the vibration platform of the RETSCH® Type 3-D machine (as illustrated in the Figure 71).



Thermo-responsive hydrogel blocks
 Inert elastomer blocks

Figure 70: Printed interlocking blocks and related assemblies. (a) Assembly B, (b) Assembly C

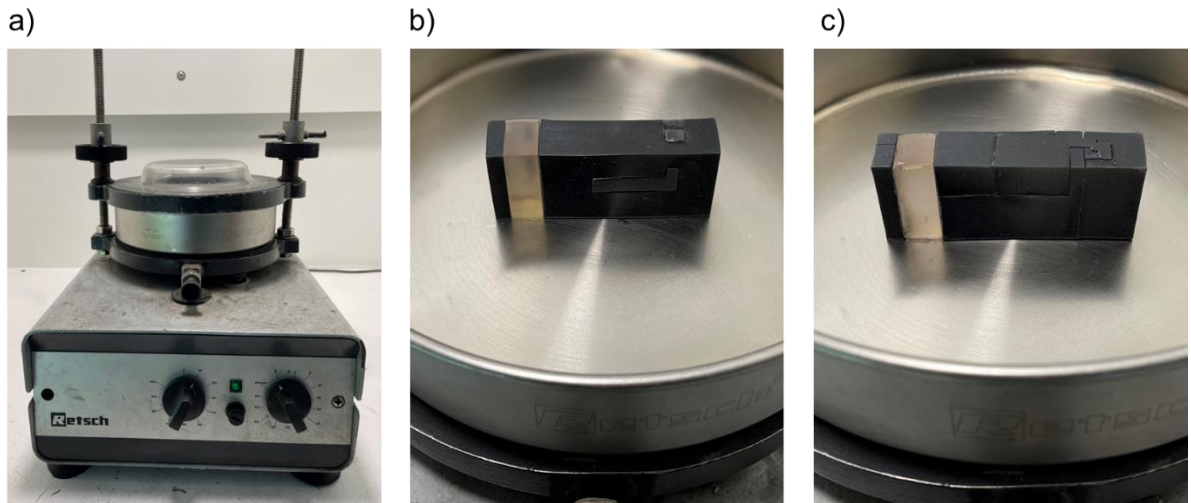


Figure 71: Shaking test protocol. (a) the shaking test machine, (b) Assembly B and (c) Assembly C on the vibration tray.

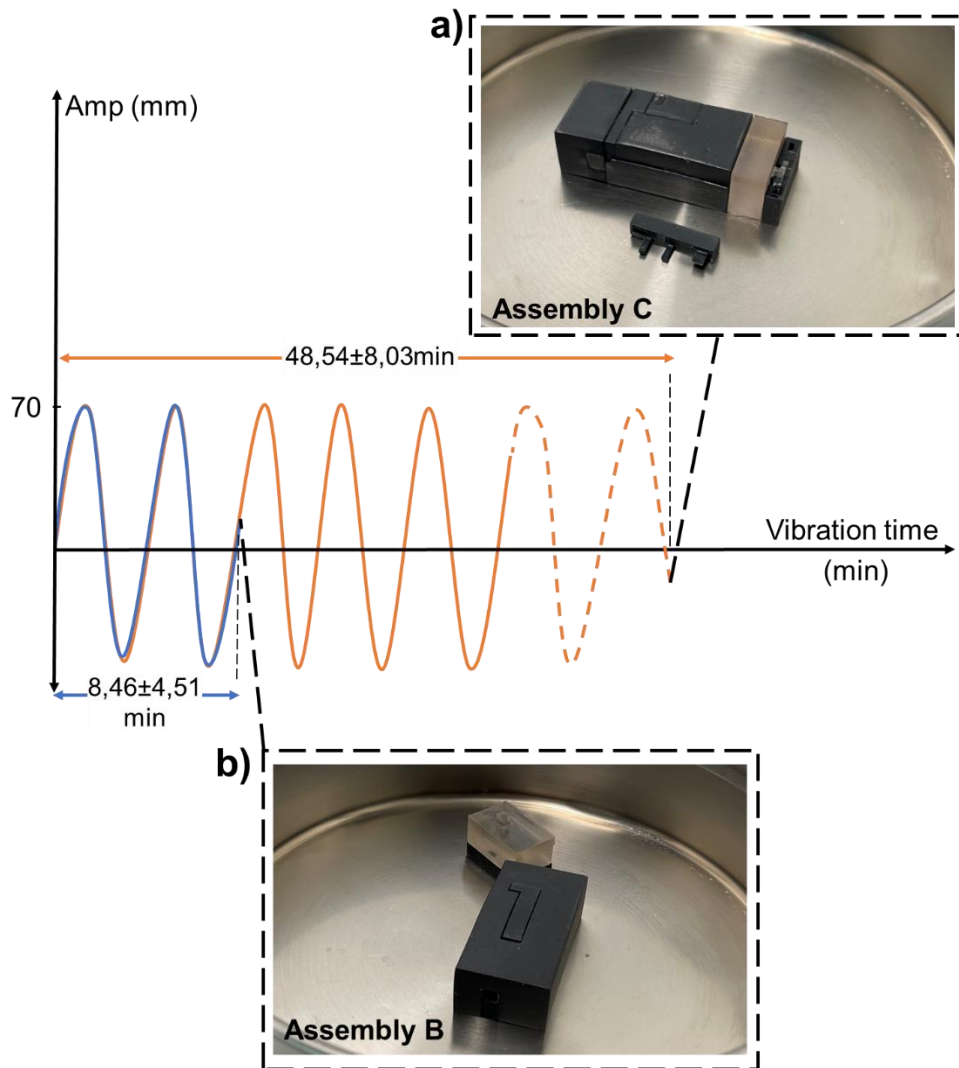


Figure 72: Shaking test results summary. The blue graph refers to the Assembly B performance and the orange graph refers to the Assembly C performance. (a) first Assembly C part separation, (b) first Assembly B part separation.

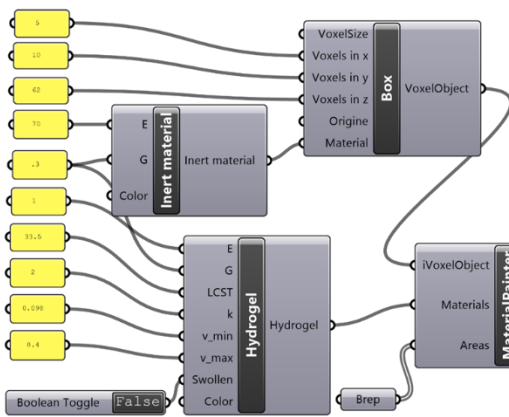
A uniform amplitude of vibration, set at 70 mm, was applied to both assemblies until the initial disassembly of the interlocking parts occurred. The duration required for this disassembly event was carefully measured for each assembly, as displayed in the Figure 72. This experimental setup allowed for a comparative assessment of the stability and durability of the interlocking structures in Assembly B and Assembly C, shedding light on their respective performance under the applied vibrations.

The results obtained from the measurement of the time until the first break-up event in the assemblies, as illustrated in Figure 72, revealed an interesting observation. Assembly B exhibited a relatively short period of 8 minutes before experiencing the first interlocking block separation. On the other hand, Assembly C, which had customized interlocking blocks, displayed a significantly longer duration of 48 minutes before encountering its initial block detachment. This discrepancy highlights the substantial impact that the customization of interlocking blocks can have on the stability of the overall assembly. By tailoring the interlocking blocks to suit the specific requirements and characteristics of the materials used, Assembly C demonstrated enhanced resistance to separation, ensuring a more robust and durable interlocking multi-material structure. These results validate the effectiveness of the customization approach in improving the stability and integrity of interlocking assemblies.

5.3.3. Actuation Simulation

Through simulation, the response of each assembly is evaluated under various temperature conditions using the VoxSmart add-on simulator within the Rhinoceros3D/Grasshopper® environment (see Figure 73). This allows for a thorough understanding and comparison of how temperature influences the structural integrity and deformation patterns of the two assemblies.

Voxelization and material assignment



Simulation

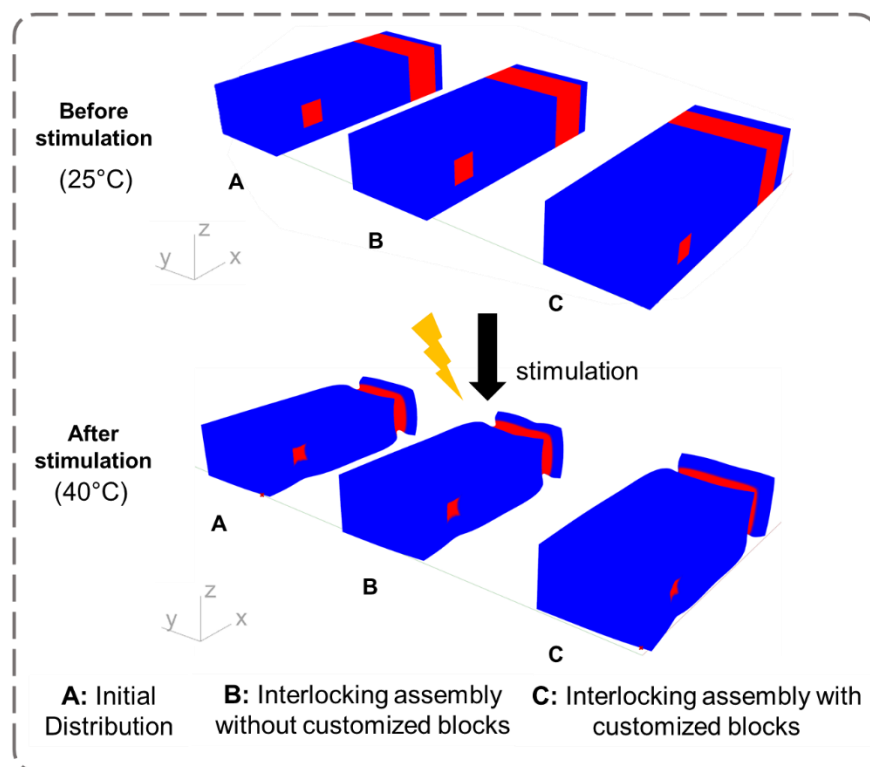
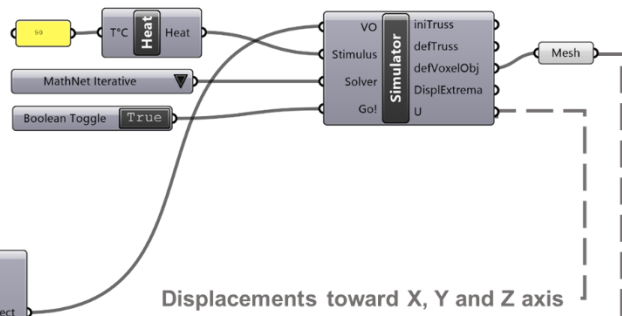


Figure 73: Simulation of multi-material 4D printed structures using the VoxSmart add-on simulator within the Rhinoceros3D/Grasshopper® environment, (A) initial distribution, (B) the interlocking assembly without using customized blocks, distribution (C) the interlocking assembly using a customized blocks. The different structures are represented before stimulation (at 25°C) and after stimulation at 40°C.

Furthermore, voxels displacements along the X, Y, and Z in the two assemblies are obtained after a stimulation at 25, 30, 35, 38, and 40°C (U output as highlighted in Figure 74). The computed displacements are then used to compare both assemblies B and C regarding their physical behavior in a presence of stimulation energy.

To do so, we measure vector moduli, representing the distance between the position of a voxel (v_B) in Assembly B and its position (v_C) in Assembly C. The vector moduli are given as follows (Equation 7):

$$\| \overrightarrow{v_C v_B} \| = \sqrt{(U_{x_C} - U_{x_B})^2 + (U_{y_C} - U_{y_B})^2 + (U_{z_C} - U_{z_B})^2} \quad (7)$$

where $v_B = (U_{x_B}, U_{y_B}, U_{z_B})$ and $v_C = (U_{x_C}, U_{y_C}, U_{z_C})$ are displacements vectors of the voxels in Assembly B (interlocking assembly generated without using customized blocks) and Assembly C (interlocking assembly generated using customized blocks) respectively.

Based on the results obtained from the simulations and distance calculations, Figure 74 and Table 11 provide evidence that the differences in deformation between the two structures are negligible. This holds true across various temperatures: 30°C, 35°C, 38°C, and 40°C. For example, in Table 11 that outlines the maximum and average distances between the positions of voxels in the two assemblies, the average distance between a voxel in Assembly B and its corresponding position in Assembly C at 40°C is found to be 0.223 mm. This distance is relatively small compared to the overall length of the 80 mm sample. These findings indicate that the use of customized interlocking blocks for assembly generation does not compromise the shape-change properties of the 4D structure. The implementation of the customized blocks has been successful in maintaining the physical properties of the assembly throughout its deformations from a simulation perspective.

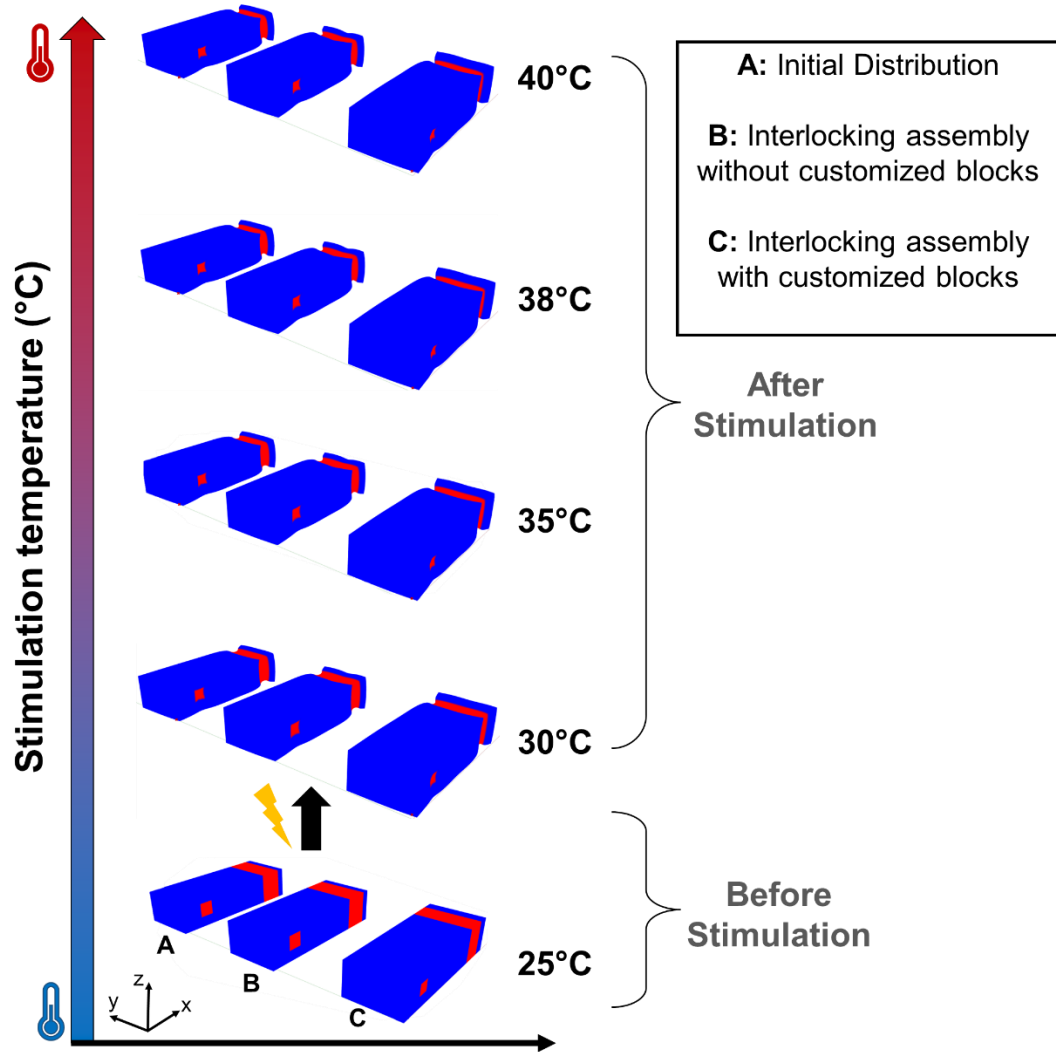


Figure 74: Shape-changing simulation of (A) initial distribution, (B) the interlocking assembly without using a customized blocks, distribution (C) the interlocking assembly using a customized blocks. Simulations were performed before stimulation at 25°C and after stimulation at 30°C, 35°C, 38°C, and 40°C.

Table 11: Calculation of the maximum and average distances between voxels' positions in (B) the interlocking assembly without using a customized blocks, distribution (C) the interlocking assembly using a customized blocks at 25°C, 30°C, 35°C, 38°C, and 40°C.

	Maximum distance [mm ±0.01]	Average distance [mm ±0.01]
25°C	0	0
30°C	0,326	0,273
35°C	0,388	0,244
38°C	0,481	0,192
40°C	0,356	0,223

5.3.4. Actuation Process

To evaluate the level of contact continuity and facilitate a comparative analysis between the two assemblies, the following testing protocol was implemented. The samples were subjected to a controlled heating process at a temperature of 40°C for a duration of 30 minutes. This thermal treatment aimed to induce deformation within the assemblies due to the presence of a thermo-sensitive hydrogel. After the heating process, high-resolution images of the samples were captured, and gap measurements were conducted using the ImageJ software tool. The focus of the analysis was on the interfaces between the hydrogel blocks, indicated by the red arrows in Figures 75 and 76. It is important to note that due to time constraints, the investigation was limited to the interfaces of the appearing hydrogel blocks, and the internal volume interfaces were not examined. (see c and d in Figures 75 and 76).

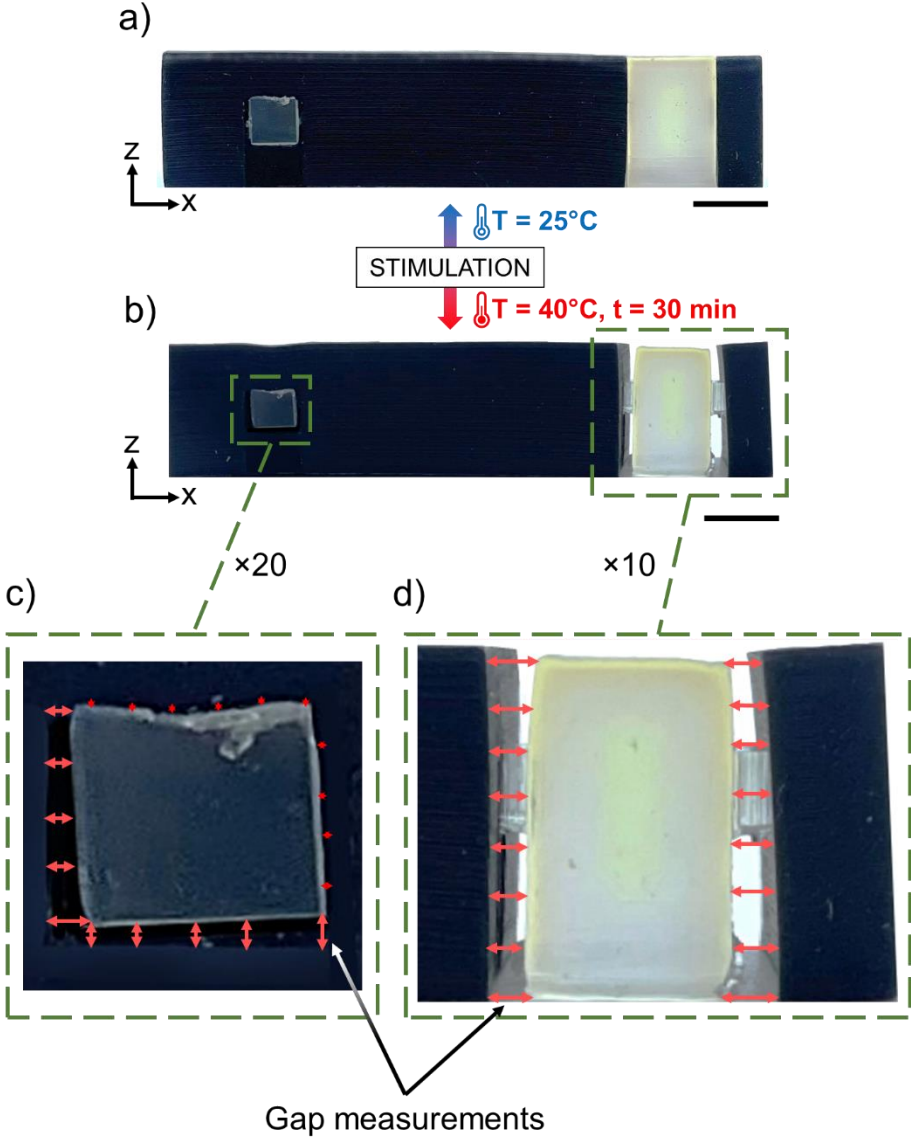


Figure 75: Multi-material 4D printed interlocking assembly without customized blocks (Assembly B): (a) manual assembly of the interlocking blocks by following the assembly sequence generated by the developed VoxSmart component, (b) deformed structure after stimulation at 40°C for 30 min, (c)

Hydrogel Block 1 deformation zooming in (Focus x20), (d) Hydrogel Block 2 deformation zooming in (Focus x10). Scale bars: 10 mm.

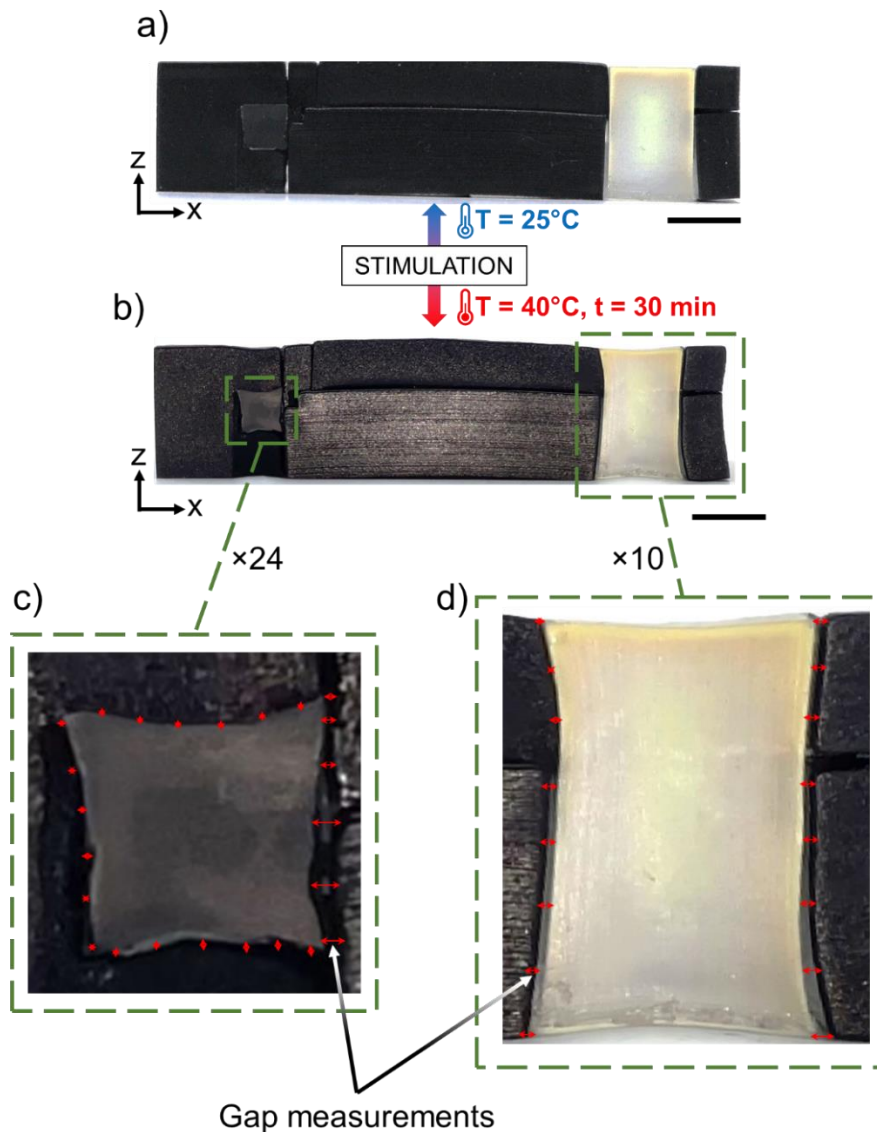


Figure 76: Multi-material 4D printed interlocking assembly with customized blocks (Assembly C) : (a) manual assembly of the interlocking blocks by following the assembly sequence generated by the developed VoxSmart component , (b) deformed structure after stimulation at 40°C for 30 min, (c) hydrogel block 1 deformation zooming in (Focus x24), (d) Hydrogel block 2 deformation zooming in (Focus x10). Scale bars: 10 mm.

A total of five samples from each assembly were tested using the same procedure to ensure repeatability and reliability of the results. The measured gap data were compiled and presented in Figure, providing valuable insights into the contact continuity between the hydrogel and inert materials within the interlocking assemblies. In terms of contact and deformation continuity, the analysis presented in Figure 77 clearly demonstrates the superior performance of Assembly C, which incorporates customized interlocking blocks, compared to Assembly B (interlocking assembly without customized blocks). For instance, the measured gaps at the interfaces of hydrogel block 1 in Assembly C are significantly smaller, with a measurement of 0.05 mm, in contrast to Assembly B where the measurement reaches 0.55 mm

(approximately 10 times larger). This observation holds true in the gap measurements at the interfaces of hydrogel block 2. The introduction of T-hinges to the hydrogel blocks, based on their deformations, has played a crucial role in enabling the neighboring blocks to adapt to the deformations of the hydrogel material. This implementation has resulted in improved stability and enhanced contact continuity within the interlocking assembly.

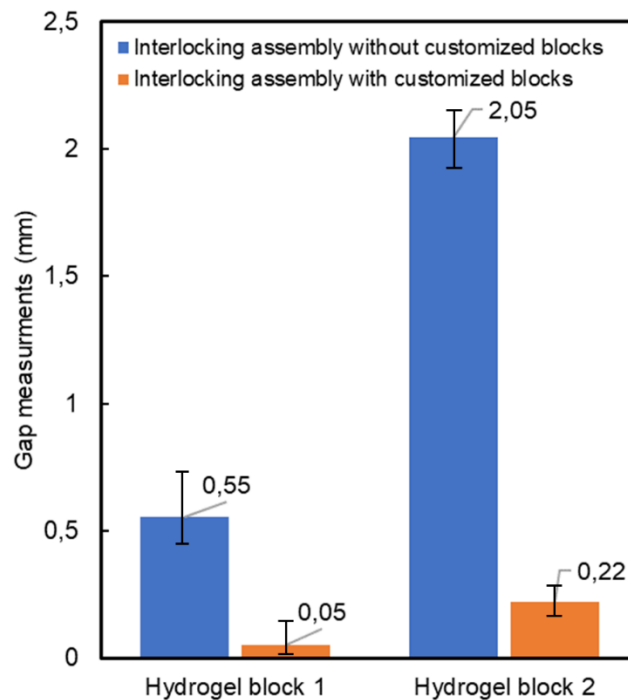


Figure 77: Gap measurements at hydrogel block 1 and 2 interfaces results. Blue color refers to Assembly B while the orange color refers to Assembly C.

However, when considering the overall deformation, Assembly C, which employed customized interlocking blocks, did not achieve the anticipated level of deformation compared to the simulation results. The mechanical deformation exhibited by the formulated PNIPAM hydrogel was not robust enough to induce the desired deformation in practice. This limitation was even more pronounced in Assembly B (interlocking assembly without customized blocks), where minimal to no observable deformation was observed. While it is evident that the customized blocks contributed to improved contact continuity and deformation, it is important to explore alternative smart materials with enhanced mechanical properties to fully demonstrate the efficacy of this approach. Further research and experimentation with such materials will add value and strengthen the potential of the interlocking assembly with customized blocks concept.

5.4. Conclusion

In conclusion, the main objective of this chapter was to introduce a customization approach for the shapes of interlocking blocks during the initial stages of assembly generation. This approach takes into consideration SMs properties and their potential transformations, whether they exhibit isotropic or anisotropic behavior. The aim is to optimize the interlocking block shapes to accommodate the behavior of the SMs, thereby enhancing the uniformity of shape and property changes within the 4D multi-material interlocked assembly. By customizing the interlocking block shapes, we address the limitations associated with the interfaces between blocks, focusing on two critical factors: contact continuity and deformation continuity. Ensuring seamless contact between blocks is essential for maintaining the structural integrity and stability of the interlocked assembly. Simultaneously, achieving smooth deformation transitions between blocks is crucial for achieving the desired shape-changing properties of the 4D printed structures. To evaluate the effectiveness of utilizing customized interlocking blocks, we compared the physical behavior and stability of two assemblies: one based on the previous interlocking assembly approach developed in Chapter 3, which did not employ customized blocks, and the other generated using the customized interlocking blocks.

Through experimental testing and analysis, we observed notable improvements in both contact continuity and deformation continuity in the assembly utilizing the customized interlocking blocks (Assembly C) compared to the assembly without customized blocks (Assembly B). The customized block design, tailored to the specific behavior of the SMs, facilitated better contact between blocks and enhanced the overall stability of the assembly.

However, it is important to note that the overall deformation achieved in Assembly C did not fully align with the simulation results. The mechanical deformation exhibited by the formulated PNIPAM hydrogel fell short of the anticipated level of deformation. This suggests the need for further exploration and testing of SMs with greater mechanical properties to fully harness the potential of this approach and achieve optimal deformation in practice.

Chapter 6: Conclusions and Perspectives

"There is no real ending. It's just the place where you stop the story."

Frank Herbert

"...and there are many things that don't really end, anyway, they just begin again in a new way..."

C. JoyBell C.

Chapter 6: Conclusions and Perspectives	129
6.1. Conclusions	131
6.2. Perspectives	132

The focus of research on 4D printing has primarily been centered around manufacturing and material aspects. As identified in the literature review, there has been a noticeable absence of design for 4D printing approaches and methodologies that cater specifically to this groundbreaking manufacturing technique. To the best of our knowledge, this thesis stands as one of the few encountered endeavors that examines 4D printing from a design and assembly perspectives. The overarching objective of this PhD project was to develop a design approach for multi-material 4D printed voxel-based structures.

This concluding chapter serves to summarize the contributions made towards achieving the aforementioned objective and highlights the areas that require further attention to establish multi-material 4D printing more broadly within the realm of design and, consequently, the industry.

6.1. Conclusions

The primary focus of the research questions outlined in the introductory chapters revolved around understanding how to achieve voxel-based hybrid structures that incorporate both passive and active materials using the currently available AM techniques and processes, and overcome the challenge of the limited compatibility of existing printers with SMs that possess the necessary properties for realizing such structures?

The thesis contributions were divided into three interconnected chapters, each building upon the other. The initial contribution chapter introduces an original computational design approach for multi-material 4D printing, which involves a meticulous analysis of voxel-based digital material distribution within a given structure. This level of understanding enables precise control over the generation of interlocking components, facilitating the creation of intricate and functional assemblies. Notably, this approach stands out for its versatility and efficiency, offering new possibilities for exploring complex assemblies that were previously unattainable using a single AM technique in a single process. By seamlessly integrating different materials, such as metals and polymers, within the same 4D printed structure, the design freedom is expanded, allowing for the fabrication of customized objects with varying material properties in a single print.

The subsequent chapter delved deeper into the investigation of interlocking block assemblies and their influence on the behavior of multi-material 4D printed structures. Different analyses were conducted on critical parameters including actuation time, shape change, and reversibility of the printed structures. This comprehensive examination involved a combination of mechanical tests, stimulation experiments, and numerical simulations. The objective was to validate the practical relevance and effectiveness of the proposed computational design approach, demonstrating its potential in creating functional objects with dynamic properties. These insights contributed to advancing the understanding of interlocking assemblies and their role in achieving desired structural transformations and functionalities in the context of multi-material 4D printing.

The third contribution chapter has highlighted the importance of customizing interlocking block shapes to enhance the uniformity of shape/property changes in 4D multi-material interlocked assemblies. It has also emphasized the significance of ensuring contact continuity and deformation continuity in achieving successful 4D printed structures. The utilization of customized interlocking blocks has demonstrated promising results in terms of improved contact continuity and stability. However, further advancements in smart materials are required to fully realize the envisioned deformation capabilities. This research opens avenues for future investigations and advancements in the field of 4D printing and interlocking assemblies.

6.2. Perspectives

The proposed research work has particular limitations that can open up captivating directions for future studies. First, to ensure better structural performances of the structure, a complimentary algorithm to generate a multi-scale interlocking blocks will be developed. This strategy will also allow the authors to better control the multi-material distribution interlocking when adjustment is required, so the impact on the physical properties of the structure can be further minimized. It would be also significant to optimize another essential aspect not yet covered in the proposed research work, i.e., the consideration of geometric deviation related to AM processes/techniques capabilities. Modifications in blocks geometries can be caused by AM inaccuracies, that in the context of multiple parts assembly can be magnified, therefore leading to assembly issues. As such, handling the geometric deviation to overcome the potential limitation, would be an exciting future research problem. This point can also be addressed and solved by using microfabrication technologies like two-photon polymerization.

From a simulation point of view, we adopted Euler-Bernoulli beam theory (as successfully addressed in [21,26]) to simulate the behavior of the materials in the structure where voxel materials are considered as tied. This hypothesis is usually applied in the modeling of active composites (see [20,22,26]). In this research work, interlocking blocks are assumed to follow the same modeling scheme. However, it would be more realistic to integrate the mechanical behavior at the interfaces of the interlocking blocks. Extensive research should cover this avenue to predict the functional fatigue of the interlocking blocks assembly under the effect of multiple cycles of stimulation.

Future work should also be focused on the improvement of the computational procedure to determine interlocking blocks. The use of AI-based techniques may be relevant to solve such combinatorial and time-consuming optimization problem. Further work will investigate the combination of deep reinforced learning and 3D convolutional neural networks. The latter, which leverage spatiotemporal information, are suitable to classify materials distribution and/or interlocking blocks through voxel-based simulation or FEM. It is also expected to consider other conditions for the interlocking blocks assembly

computation such as minimizing printing support, minimizing the variety of blocks depending on the voxels number (i.e., using standard blocks). Last, additional effort will be dedicated to the development of a robotic platform to which blocks can be handling and assembled at various scales.

One can also notice that our experiments were meant to execute limited shape-changing configurations. Relaxation of these limitations should be attempted in future work to generalize the present strategy. Thus, it is necessary to consider other case studies presenting other shape-changing configurations such as curling, and twisting to name a few, as well as adapting the proper interlocking models and assembly sequence planning. It would be also promising to utilize in the future other SMs that can be activated through other stimuli, as well as cellular structures like metamaterials in order to take a step closer to everyday-life applications.

In conclusion, the above work presents various perspectives and possibilities for future research and development:

- Developing a complementary algorithm to generate multi-scale interlocking blocks for better structural performance and control over multi-material distribution.
- Optimization of geometric deviation caused by AM inaccuracies.
- Integrating mechanical behavior at the interfaces of interlocking blocks to provide a more realistic modeling scheme and allow prediction of functional fatigue.
- Improvement of computational procedures for determining interlocking blocks using AI-based techniques.
- Consideration of additional conditions in interlocking block assembly computation
- Development of a robotic platform for handling and assembling blocks at various scales.
- Expansion of experiments to include different shape-changing configurations and other stimuli-activated SMs

Research Work Publications

Peer-review Journal Articles

- K. Benyahia, H. Seriket, R. Prod'hon, S. Gomes, J. C. André, H. J. Qi, F. Demoly. A computational design approach for multi-material 4D printing based on interlocking blocks assembly. *Additive Manufacturing* 58: 102993, 2022.
- K. Benyahia, S. Gomes, André J.C., Qi H.J., F. Demoly. Influence of interlocking blocks assembly on the actuation time, shape change, and reversibility of voxel-based multi-material 4D structures. *Smart Materials and Structures* 32.6 (2023): 065011.
- K. Benyahia, S. Gomes, André J.C., Qi H.J., F. Demoly. A customized interlocking assembly blocks for improved multi-material 4D printing structures performances. *Additive Manufacturing*, (in preparation).

Conference Papers

- K. Benyahia S. Gomes, André J.C., Qi H.J., F Demoly. Conception pour l'impression 4D multi-matériaux: Développement d'un algorithme pour la génération d'assemblages de blocs entremêlés, Colloque Smart 2023 : 445323
- K. Benyahia S. Gomes, André J.C., Qi H.J., F Demoly. Design for multi-material 4D printing: Development of an algorithm for interlocking blocks assembly generation, *Procedia CIRP*, 119, 2023, 396-401..

Promotion of this thesis' works in other international events

- Summer schools: 2021 Interactive Training for PhD Researchers in Integrated Product Development. University of Malta, May 2021. (Online)
- 4ème colloque des Assemblages Mécaniques: Evolutions récentes et perspectives. Saint-Ouen, 1-2 juillet (Online).
- Presentation of thesis subject: Animate Materials Workshop: 4D Printing and Metamaterials, Birmingham, UK. June 2022.
- Presentation of thesis subject: 18ème colloque national S.mart 2023, 4-6 Avril 2023, Carry le Rouet, France.
- Presentation of thesis subject: CIRP Design Conference2023, May 2023, Sydney, AUS. (Online)

References

- [1] L. Putre, "The Evolution of Manufacturing: What's Next?", 2019, IndustryWeek.
- [2] S. Dimassi. "Knowledge formalization and recommendation in computational design synthesis for 4D printing". Université Bourgogne Franche-Comté, 2022.
- [3] Z. Cohen, "The Evolution of Manufacturing Technology: From the Industrial Revolution to Today and Beyond", Zacks Investment Research, 2021.
- [4] J.C. André, A. Le Méhauté, O. De Witte, Dispositif pour réaliser un modèle de pièce industrielle, French Patent n° 84 11 241, 16.07.1984, 1984.
- [5] J. C., André, Industrie 4.0: paradoxes et conflits. ISTE Group, 2019.
- [6] L. Jiewu, W. Sha, B. Wang, P. Zheng, C. Zhuang, Q. Liu, T. Wuest, D. Mourtzis, L. Wang. "Industry 5.0: Prospect and retrospect." Journal of Manufacturing Systems 65: 279-295. 2022. DOI: <https://doi.org/10.1016/j.jmsy.2022.09.017>
- [7] Customising the future – The next industrial revolution: <https://nickelinstitute.org/en/blog/2020/november/customising-the-future-the-next-industrial-revolution/>
- [8] F. Demoly, O. Dutartre, X. T. Yan, B. Eynard, D. Kiritsis, and S. Gomes, "Product relationships management enabler for concurrent engineering and product lifecycle management," Comput. Ind., vol. 64, no. 7, pp. 833–848, 2013.
- [9] D. Kiritsis, "Closed-loop PLM for intelligent products in the era of the internet of things," CAD Comput. Aided Des., vol. 43, no. 5, pp. 479–501, 2011.
- [10] M. L. Thomas, "The Transformable Sofa in Classical Antiquity," the Society of Architectural Historians, 1991.
- [11] Ö. Harmansah, "Triclinia and Dining Culture in the Roman East", Roman Archaeology, 2011.
- [12] M. Dillon and L. Garland, "Furniture and Furnishing in the Ancient World," 2009.
- [13] R. Armstrong, "Adaptive Transformable Structures in Architecture", Architectural Design, 2010.
- [14] H. Liu and C. Peng, "Transformable Design: A Survey of Transformable Design Techniques and Materials in Contemporary Design Practice", the International Journal of Design, 2013.
- [15] S. Tibbits, "Transformable Materials and Structures: From Active Matter to Self-Formation", the IEEE, 2015.
- [16] Z. X. Khoo, J. E. M. Teoh, Y. Liu, C. K. Chua, S. Yang, J. An, K. F. Leong & W. Y. Yeong (2015) 3D printing of smart materials: A review on recent progresses in 4D printing, Virtual and Physical Prototyping, 10:3, 103-122, DOI: [10.1080/17452759.2015.1097054](https://doi.org/10.1080/17452759.2015.1097054)
- [17] D. Manfredi, F. Calignano, E. P. Ambrosio, M. Krishnan, R. Canali, S. Biamino, M. Pavese, E. Atzeni, L. Iuliano, P. Fino, C. Badini., "Direct metal laser sintering: an additive manufacturing

- technology ready to produce lightweight structural parts for robotic applications memories,” *Sinterizzazione LA Met. Ital.*, vol. 10, pp. 15–24, 2013.
- [18] F. Rengier, A. Mehndiratta, H. von Tengg-Kobligk, C. M. Zechmann, R. Unterhinninghofen, H.-U. Kauczor & F. L. Giesel., “3D printing based on imaging data: Review of medical applications,” *Int. J. Comput. Assist. Radiol. Surg.*, vol. 5, no. 4, pp. 335–341, 2010.
- [19] F. Demoly, J.C. André, Research strategy in 4D printing: Disruptive vs incremental?, *Journal of Integrated Design and Process Science* 24 (2020), 53-73, <https://doi.org/10.3233/JID200020>.
- [20] “Standard ASTM. (2012). F2792.2012 standard terminology for additive manufacturing technologies.”
- [21] J.C. André, From additive manufacturing to 3D/4D printing. Breakthrough innovations: programmable material, 4D printing and Bio-printing, ISTE-Wiley, London, UK, 2017.
- [22] S. Dimassi, F. Demoly, C. Cruz, H.J. Qi, K.Y. Kim, J.C. André, S. Gomes, An ontology-based framework to formalize and represent 4D printing knowledge in design, *Computers in Industry* 126 (2021) 103374, <https://doi.org/10.1016/j.compind.2020.103374>.
- [23] M. D. Hager, S. Bode, C. Weber, and U. S. Schubert, “Shape memory polymers: past , present and future developments,” *Prog. Polym. Sci.*, vol. 49–50, pp. 3–33, 2015.
- [24] T. van Manen, S. Janbaz, and A. A. Zadpoor, “Programming the shape-shifting of flat soft matter,” *Mater. Today*, vol. 21, no. 2, pp. 144–163, 2018.
- [25] Y. Xu, X. Li, M. Hu, L. Li, & H. Wang, “4D printing and its biomedical applications”. *Journal of Medical Imaging and Health Informatics*, 8(4), 744-752. doi: 10.1166/jmihi.2018.2453, 2018.
- [26] S. J. Garcia, “4D printing of reversible shape changing hydrogel structures”. *Macromolecular Rapid Communications*, 36(12), 1211-1217. doi: 10.1002/marc.201500053, 2015.
- [27] Y. Lu. 4D printing of shape memory polymer for functional applications. *Materials Science and Engineering: C*, 94, 1056-1070. doi: 10.1016/j.msec.2018.10.010, 2019.
- [28] Y. Yao, “A review of 4D printing”. *Journal of Intelligent Material Systems and Structures*, 29(5), 797-826. doi: 10.1177/1045389X17740460, 2018.
- [29] Q. Ge, C. K. Dunn, H. J. Qi, and M. L. Dunn, “Active origami by 4D printing,” *IOP Sci.*, vol. 094007, 2014.
- [30] S. E. Bakarich, R. G. Iii, and G. M. Spinks, “4D printing with mechanically robust, thermally actuating hydrogels,” *Macromol. Rapid Commun.*, pp. 1–7, 2015. Knowledge Formalization and Recommendation in CDS for 4D printing
- [31] Y. Zhou, W. M. Huang, S. F. Kang, X. L. Wu, H. B. Lu, J. Fu & H. Cui, “From 3D to 4D printing: approaches and typical applications,” *J. Mech. Des. Technol.*, vol. 29, no. 10, pp. 4281–4288, 2015.
- [32] R. Niiyama, X. Sun, L. Yao, H. Ishii, D. Rus, and S. Kim, “Sticky actuator: free-form planar actuators for animated objects,” *TEI 2015 - Proc. 9th Int. Conf. Tangible, Embed. Embodied Interact.*, pp. 77–84, 2015.

- [33] S. Tibbits, “4D Printing: multi material shape change,” pp. 116–121, 2013.
- [34] S. Tibbits, C. McKnelly, C. Olguin, D. Dikovsky, and S. Hirsch, “4D printing and universal transformation,” Proc. 34th Annu. Conf. Assoc. Comput. Aided Des. Archit., pp. 539–548, 2014.
- [35] M. Vaezi, S. Chianrabutra, B. Mellor, and S. Yang, “Multiple material additive manufacturing part1: a review,” Virtual Phys. Prototyp., vol. 8, no. 1, pp. 19–50, 2013.
- [36] F. Heibeck, B. Tome, C. Della, and S. Hiroshi, “uniMorph - fabricating thin-film composites for shape-changing interfaces,” in UIST ’15 Proceedings of the 28th Annual ACM Symposium on User Interface Software & Technology, 2015.
- [37] Z. Ding, Z. Ding, C. Yuan, X. Peng, T. Wang, H.J. Qi, M.L. Dunn, “Direct 4D printing via active composite materials”. Science advances, 3(4), e1602890. 2017.
- [38] 3D printed stent example: <https://3dprintingindustry.com/news/tu-eindhoven-demonstrates-3d-vprinted-stents-paediatric-heart-surgery-113291/>
- [39] F. Demoly, M. L. Dunn, K. L. Wood, H. Jerry Qi, and J.-C. André, “The status, barriers, challenges, and future in design for 4D printing,” Mater. Des., vol. 212, p. 110193, 2021.
- [40] Gartner, “Gartner’s 2017 Hype cycle highlight digital business ecosystems,” 2017.
- [41] E. Gruhier, F. Demoly, O. Dutartre, S. Abboudi, and S. Gomes, “A formal ontology-based spatiotemporal mereotopology for integrated product design and assembly sequence planning,” Adv. Eng. Informatics, vol. 29, no. 3, pp. 495–512, 2015.
- [42] Airbus: "Airbus is Betting on 4D Printing to Revolutionize the Aviation Industry," Digital Trends, June 11, 2018.
- [43] BMW CONCEIVES OF 4D PRINTING HYPER-FUTURISTIC CONCEPT CAR: <https://3dprintingindustry.com/news/bmw-conceives-of-4d-printing-hyper-futuristic-concept-car-67921/>.
- [44] M. Zarek , “4D printing shape memory polymers for dynamic jewellery and fashionwear,” Virtual Phys. Prototyp., vol. 11, no. 4, pp. 263–270, 2016.
- [45] B. C. M. Yakacki, R. Shandas, D. Safranski, A. M. Ortega, K. Sassaman, and K. Gall, “Strong, tailored , biocompatible shape-memory polymer networks,” Adv. Funct. Mater., vol. 18, pp. 2428–2435, 2008.
- [46] A. Haleem, M. Javaid, R. P. Singh, and R. Suman, “Significant roles of 4D printing using smart materials in the field of manufacturing,” Adv. Ind. Eng. Polym. Res., 2021.
- [47] F. Demoly and J. André, “Impression 4D : promesses ou futur opérationnel ?” Tech. l’Ingénieur, vol. 33, 2021.
- [48] F. E. Azhar and E. Pei, “A conceptual framework to improve the symbol implementation of 4D printing communication between designers and engineers,” 2022.
- [49] Y. Tao et al., “Demonstrating thermorph,” pp. 1–4, 2018.
- [50] F.K. Aldawood, “A Comprehensive Review of 4D Printing: State of the Arts, Opportunities, and Challenges”. Actuators 2023, 12, 101. <https://doi.org/10.3390/act12030101>

- [51] TedX Tibbits talk: https://www.ted.com/talks/skylar_tibbits_the_emergence_of_4d_printing
- [52] Z. Ding, C. Yuan, X. Peng, T. Wang, H. J. Qi, and M. L. Dunn, "Direct 4D printing via active composite materials," *Sci. Adv.*, vol. 3, no. 4, 2017.
- [53] K. Benyahia, H. Seriket, R. Prod'hon, S. Gomes, J. C. André, H. J. Qi, F. Demoly, "A computational design approach for multi-material 4D printing based on interlocking blocks assembly." *Additive Manufacturing* 58: 102993, 2022.
- [54] B. Subeshan, Y. Baddam, and E. Asmatulu. "Current progress of 4D-printing technology." *Progress in Additive Manufacturing* 6: 495-516, 2021.
- [55] McAlpine K 4D-printed structure changes shape when placed in water | Harvard Gazette. <http://news.harvard.edu/gazette/story/2016/01/4d-printed-structure-changes-shape-when-placed-in-water/>.
- [56] F. Momeni, M. Mehdi, N. S.Hassani, X. Liu, J. Ni. "A review of 4D printing". *Mater Des* 122:42–79,2017. <https://doi.org/10.1016/j.matdes.2017.02.068>
- [57] A. Gladman. "Biomimetic 4D printing". *Nat Mater* 15:413–418. <https://doi.org/10.1038/nmat4544>
- [58] Additive manufacturing and 3D printing slides: <https://www.slideshare.net/Shamoonrw/additive-manufacturing-and-3-d-printing>
- [59] G. Sossou, "Une approche globale de la conception pour l'impression 4D", Université Bourgogne Franche-Comté, 2019.
- [60] M. Zarek , "4D printing shape memory polymers for dynamic jewellery and fashionwear," *Virtual Phys. Prototyp.*, vol. 11, no. 4, pp. 263–270, 2016.
- [61] D. Kokkinis, M. Schaffner, and A. R. Studart, "Multimaterial magnetically assisted 3D printing of composite materials," *Nat. Commun.*, 2015.
- [62] B. Gao, Q. Yang, X. Zhao, G. Jin, Y. Ma, and F. Xu, "4D bioprinting for biomedical applications," *Trends Biotechnol.*, vol. 34, no. 9, pp. 746–756, 2016.
- [63] S. Miao, W. Zhu, N. J. Castro, M. Nowicki, X. Zhou, H. Cui, J. P. Fisher & L. G. Zhang, "4D printing smart biomedical scaffolds with novel soybean oil epoxidized acrylate," *Nat. Publ. Gr.*, no. March, pp. 1–10, 2016.
- [64] X.-L. Gong, Y.-Y. Xiao, M. Pan, Y. Kang, B.-J. Li, and S. Zhang, "pH- and thermal-responsive multi-shape memory hydrogel," *Appl. Mater. Interfaces*, pp. 1–21, 2016.
- [65] C.M. Hamel, D.J. Roach, K.N. Long, F. Demoly, M.L. Dunn, H.J. Qi, Machine-learning based design of active composite structures for 4D printing, *Smart Materials and Structures* 28 (2019) 065005, <https://doi.org/10.1088/1361-665X/ab1439>.
- [66] G. Sossou, F. Demoly, H. Belkebir, H. J. Qi, S. Gomes, G. Montavon, Design for 4D printing: Modeling and computation of smart materials distributions, *Materials & Design* 181 (2019) 108074, <https://doi.org/10.1016/j.matdes.2019.108074>.

- [67] X. Sun, L. Yue, L. Yu, H. Shao, X. Peng, K. Zhou, F. Demoly, R. Zhao, H.J. Qi, Machine learning-evolutionary algorithm enabled design for 4D-printed active composite structures, *Advanced Functional Materials* 32 (2022) 2109805, <https://doi.org/10.1002/adfm.202109805>.
- [68] J. Hiller, H. Lipson, Design and analysis of digital materials for physical 3D voxel printing, *Rapid Prototyping Journal* 15 (2009) 137-149, <https://doi.org/10.1108/13552540910943441>.
- [69] E.L. Doubrovski, E.Y. Tsai, D. Dikovskiy, J.M. Geraedts, H. Herr, N. Oxman, Voxel-based fabrication through material property mapping: A design method for bitmap printing, *Computer-Aided Design* 60 (2015) 3-13, <https://doi.org/10.1016/j.cad.2014.05.010>.
- [70] G. Sossou, F. Demoly, H. Belkebir, H.J. Qi, S. Gomes, G. Montavon, Design for 4D printing: A voxel-based modeling and simulation of smart materials, *Materials & Design* 175 (2019) 107798, <https://doi.org/10.1016/j.matdes.2019.107798>.
- [71] G. Sossou, F. Demoly, H.J. Qi, S. Gomes, G. Montavon, An additive manufacturing-oriented design approach to mechanical assemblies, *J. of Comput. Des. Eng.* 5 (2018) 3-18, <https://doi.org/10.1016/j.jcde.2017.11.005>.
- [72] I. Q. Vu, L. B. Bass, C. B. Williams, and D. A. Dillard, "Characterizing the effect of print orientation on interface integrity of multi-material jetting additive manufacturing," *Addit. Manuf.*, vol. 22, no. February, pp. 447–461, 2018.
- [73] L. D. Sturm, M. I. Albakri, P. A. Tarazaga, and C. B. Williams, "In situ monitoring of material jetting additive manufacturing process via impedance-based measurements," *Addit. Manuf.*, vol. 28, no. February, pp. 456–463, 2019.
- [74] V. Mechtcherine, F. P. Bos, A. Perrot, W. R. Leal da Silva, V. N. Nerella, S. Fataei, R. J. M. Wolfs, M. Sonebi, N. Roussel, "Extrusion-based additive manufacturing with cement-based materials – Production steps, processes, and their underlying physics: A review," *Cem. Concr. Res.*, vol. 132, no. March, p. 106037, 2020.
- [75] G. Wang, Y. Tao, O. B. Capunaman, H. Yang, and L. Yao, "A-line: 4D printing morphing linear composite structures," *Conf. Hum. Factors Comput. Syst. - Proc.*, pp. 1–12, 2019.
- [76] R. J. M. Wolfs and A. S. J. Suiker, "Structural failure during extrusion-based 3D printing processes," *Int. J. Adv. Manuf. Technol.*, vol. 104, no. 1–4, pp. 565–584, 2019.
- [77] L. Morawska, "A review on stereolithography and its applications in biomedical engineering," *Biomaterials*, vol. 44, no. 24, pp. 6121–6130, 2010.
- [78] B. An, "Thermorph: Democratizing 4D Printing of Self-Folding Materials and Interfaces," 2018.
- [79] A. Bagheri and J. Jin, "Photopolymerization in 3D Printing," *ACS Appl. Polym. Mater.*, vol. 1, no. 4, pp. 593–611, 2019.
- [80] I. N. Qader. "A review of smart materials: research and applications." *El-Cezeri* 6.3: 755-788. 2019.
- [81] R. Bogue, "Smart materials: a review of recent developments. *Automation*, 32(1), 3-7. 2014.

- [82] M. A. Woodruff and D. W. Hutmacher, "The return of a forgotten polymer polycaprolactone in the 21st century," *Prog. Polym. Sci.*, vol. 35, pp. 1217–1256, 2010.
- [83] A. Ölander, "An electrochemical investigation of solid cadmium-gold alloys". *Journal of the American Chemical Society*. 54(10): p. 3819-3833. 1932.
- [84] S Bahl, H Nagar, I Singh, S Sehgal. "Smart materials types, properties and applications: A review." *Materials Today: Proceedings* 28: 1302-1306. 2020.
- [85] ZX Khoo, JEM Teoh, Y Liu, CK Chua. "3D printing of smart materials: A review on recent progresses in 4D printing." *Virtual and Physical Prototyping* 10.3: 103-122, 2015.
- [86] G. Sossou, F. Demoly, G. Montavon, and S. Gomes, Design for 4D printing: rapidly exploring the design space around smart materials. *Procedia CIRP*, 2018. 70: p. 120-125.
- [87] M. Behl, K. Kratz, J. Zotzmann, U. Nochel, and A. Lendlein, Reversible bidirectional shape-memory polymers. *Adv Mater*, 2013. 25(32): p. 4466-9.
- [88] M.I. Khan, A. Pequegnat, and Y.N. Zhou, Multiple Memory Shape Memory Alloys. *Advanced Engineering Materials*, 2013. 15(5): p. 386-393.
- [89] Z. Suo, Theory of dielectric elastomers. *Acta Mechanica Solida Sinica*, 2010. 23(6): p. 549-578
- [90] T. Xie, Tunable polymer multi-shape memory effect. *Nature*, 2010. 464(7286): p. 267-70.
- [91] J.Tellinen, I. Suorsa, A. Jääskeläinen, I. Aaltio, and K. Ullakko, Basic properties of magnetic shape memory actuators, in 8th international conference ACTUATOR2002: Bremen, Germany.
- [92] K. Asaka, and H. Okuzaki, *Soft actuators: Materials, modeling, applications, and future perspectives*. 1 ed. 2014: Springer Japan. 1-507.
- [93] J. Zhou and S. S. Sheiko, "Reversible Shape-Shifting in Polymeric Materials," vol. 1, no. c, pp. 1–16, 2016.
- [94] U. S. S. M.D. Hager, S. Bode, C.Weber, "Shape memory polymers: past, present and future developments," *Prog. Polym. Sci.* 49 3–33.
- [95] L. Sun and W. Min W., "Mechanisms of the multi-shape memory effect and temperature memory effect in shape memory polymers," *Soft Matter*, vol. 6, no. 65, pp. 4403–4406, 2010.
- [96] J. Wu et al., "Multi-shape active composites by 3D printing of digital shape memory polymers," *Sci. Rep.*, vol. 6, no. April, pp. 1–11, 2016.
- [97] H. Ding, X. Zhang, Y. Liu Review of mechanisms and deformation behaviors in 4D printing. *Int J Adv Manuf Technol* 105, 4633–4649 (2019). <https://doi.org/10.1007/s00170-019-03871-3>
- [98] He H, Guan J, Lee JL (2006) An oral delivery device based on self-folding hydrogels. *J Control Release Official Journal of the Controlled Release Society* 110:339–346. <https://doi.org/10.1016/j.jconrel.2005.10.017>
- [99] Sun L, Huang WM (2010) Thermo/moisture responsive shape-memory polymer for possible surgery/operation inside living cells in future. *Materials & Design (1980–2015)* 31:2684–2689. <https://doi.org/10.1016/j.matdes.2009.11.036>

- [100] Anand LAME, Ames NM, Srivastava V, Chester SA (2009) A thermo-mechanically coupled theory for large deformations of amorphous polymers. Part I: formulation. *Int. J. Plasticity* 25:1474–1494. <https://doi.org/10.1016/j.ijplas.2008.11.004>
- [101] Yakacki CM, Shandas R, Safranski D, Ortega AM, Sassaman K, Gall K (2008) Strong, tailored, biocompatible shape-memory polymer networks. *Adv. Funct. Mater.* 18:2428–2435. <https://doi.org/10.1002/adfm.200701049>
- [102] Yakacki CM, Shandas R, Lanning C, Rech B, Eckstein A, Gall K (2007) Unconstrained recovery characterization of shape-memory polymer networks for cardiovascular applications. *Biomaterials* 28:2255–2263. <https://doi.org/10.1016/j.biomaterials.2007.01.030>
- [103] G Qi, SA Hosein, L Howon, CK Dunn, NX Fang, ML Dunn (2016) Multimaterial 4D printing with tailorable shape memory polymers. *Sci. Rep.-UK* 6: 31110. doi: <https://doi.org/10.1038/srep31110>
- [104] duig M, Damanpack AR, Liao WH (2016) Self-expanding/shrinking structures by 4D printing. *Smart Mater Struct* 25. <https://doi.org/10.1088/0964-1726/25/10/105034>
- [105] Zarek M, Mansour N, Shapira S, Cohn D (2017) 4D printing of shape memory-based personalized endoluminal medical devices. *Macromol. Rapid Comm.* 38:1600628. <https://doi.org/10.1002/marc.201600628>
- [106] Welp, E.G. and J. Breidert, Knowledge and Method Base for Shape Memory Alloys. *Materialwissenschaft und Werkstofftechnik*, 2004. 35(5): p. 294-299.
- [107] Burman, Å., E. Møster, and P. Abrahamsson, On the Influence of Functional Materials on Engineering Design. *Research in Engineering Design*, 2000. 12(1): p. 39-47.
- [108] Park, J.-K. and G. Washington. Advanced development of a smart material design, modeling, and selection tool. in *ASME 2011 Conference on Smart Materials, Adaptive Structures and Intelligent Systems*. 2011. American Society of Mechanical Engineers.
- [109] Park, J.-K. and G. Washington. Smart material database compilation and material selection tool development. 2010.
- [110] Yu, K., A. Ritchie, Y. Mao, M.L. Dunn, and H.J. Qi, Controlled Sequential Shape Changing Components by 3D Printing of Shape Memory Polymer Multimaterials. *Procedia IUTAM*, 2015. 12: p. 193-203.
- [111] Kuksenok, O. and A.C. Balazs, Stimuli-responsive behavior of composites integrating thermo-responsive gels with photo-responsive fibers. *Materials Horizons*, 2016. 3(1): p. 53-62.
- [112] Thomas, D., *The Development of Design Rules for Selective Laser Melting*, 2009, University of Wales.
- [113] Zimmer, D. and G. Adam, Direct Manufacturing Design Rules, in *Innovative Developments in Virtual and Physical Prototyping 2011*, CRC Press. p. 545-551.

- [114] Adam, G.A.O. and D. Zimmer, Design for Additive Manufacturing—Element transitions and aggregated structures. *CIRP Journal of Manufacturing Science and Technology*, 2014. 7(1): p. 20-28.
- [115] S.M. Montgomery, X. Kuang, C.D. Armstrong, H.J. Qi, Recent advances in additive manufacturing of active mechanical metamaterials, *Current Opinion in Solid State & Materials Science* 24 (2020) 100869, <https://doi.org/10.1016/j.cossms.2020.100869>.
- [116] M. Baniasadi, E. Yarali, M. Bodaghi, A. Zolfagharian, M. Baghani, Constitutive modeling of multi-stimuli-responsive shape memory polymers with multi-functional capabilities, *International Journal of Mechanical Sciences*, 192 (2021) 106082, <https://doi.org/10.1016/j.ijmecsci.2020.106082>.
- [117] D.J. Roach, C.M. Hamel, C.K. Dunn, M.V. Johnson, X. Kuang, H.J. Qi, The m4 3D printer: A multi-material multi- method additive manufacturing platform for future 3D printed structures, *Additive Manufacturing* 29 (2019) 100819, <https://doi.org/10.1016/j.addma.2019.100819>.
- [118] D. Roy, J.N. Cambre, B.S. Sumerlin, Future perspectives and recent advances in stimuli-responsive materials, *Progress in Polymer Science* 35 (2010) 278-301, <https://doi.org/10.1016/j.progpolymsci.2009.10.008>.
- [119] A. Kafle, E. Luis, R. Silwal, H.M. Pan, P.L. Shrestha, A.K. Bastola, 3D/4D printing of polymers: Fused deposition modeling (FDM), selective laser sintering (SLS), and stereolithography (SLA), *Polymers* 13 (2021) 3101, <https://doi.org/10.3390/polym13183101>.
- [120] A.B. Baker, D.F. Wass, R.S. Trask, 4D sequential actuation : combining ionoprinting and redox chemistry in hydrogels, *Smart Materials and Structures* 25 (2016) 10LT02, <https://doi.org/10.1088/0964-1726/25/10/10LT02>.
- [121] P. Boyraz, G. Runge, A. Raatz, An overview of novel actuators for soft robotics, *Actuators* 7 (2018) 48, <https://doi.org/10.3390/act7030048>.
- [122] G. Scalet, Two-way and multiple-way shape memory polymers for soft robotics: An overview, *Actuators* 9 (2020) 10, <https://doi.org/10.3390/act9010010>.
- [123] N. An, M. Li, J. Zhou, Modeling SMA-enabled soft deployable structures for kirigami/origami reflectors, *International Journal of Mechanical Sciences* 180 (2020) 105753, <https://doi.org/10.1016/j.ijmecsci.2020.105753>.
- [124] Y.L. Yap, S.L. Sing, W.Y. Yeong, A review of 3D printing processes and materials for soft robotics, *Rapid Prototyping Journal* 26 (2020) 1345-1361, <https://doi.org/10.1108/RPJ-11-2019-0302>.
- [125] G. Decroly, A. Toncheva, L. Blanc, J.M. Raquez, T. Lessinnes, A. Delchambre, P. Lambert, Programmable stimuli-responsive actuators for complex motions in soft robotics: concept, design and challenges, *Actuators* 9 (2020) 131, <https://doi.org/10.3390/act9040131>.
- [126] J. Mohd, A. Haleem, 4D printing applications in medical field: A brief review, *Clinical Epidemiology and Global Health* 7 (2019) 317–321, <https://doi.org/10.1016/j.cegh.2018.09.007>.

- [127] M.Y. Shie, Y.F. Shen, S.D. Astuti, A.K.X. Lee, S.H. Lin, N.L.B. Dwijaksana, Y.W. Chen, Review of polymeric materials in 4D printing biomedical applications, *Polymers* 11 (2019) 1864, <https://doi.org/10.3390/polym11111864>.
- [128] A. Mitchell, U. Lafont, M. Hołyńska, C. Semprimoschnig, Additive manufacturing — A review of 4D printing and future applications, *Additive Manufacturing* 24 (2018) 606-626, <https://doi.org/10.1016/j.addma.2018.10.038>.
- [129] Q. Ge, C.K. Dunn, H.J. Qi, M.L. Dunn, Active origami by 4D printing, *Smart Materials and structures* 23 (2014) 094007, <https://doi.org/10.1088/0964-1726/23/9/094007>
- [130] K. K. Westbrook, H. J. Qi, *J. Intel. Mater. Syst. Struct.* 2008, 19, 597-607.
- [131] N. Oxman, Structuring materiality: Design fabrication of heterogeneous materials, *Architectural Design* 80 (2010) 78-85, <https://doi.org/10.1002/ad.1110>.
- [132] Q. Ge, A. H.Sakhaei, H. Lee, C.K. Dunn, N. Fang, M.L. Dunn, Multimaterial 4D printing with tailorable shape memory polymers, *Scientific Reports* 6 (2016) 31110, <https://doi.org/10.1038/srep31110>.
- [133] S.T. Ly, J.Y. Ki, 4D printing – fused deposition modeling printing with thermal- responsive shape memory polymers, *Int. J. Precis. Eng. Manuf. - Green Technol.* 4 (2017) 267–272, <https://doi.org/10.1007/s40684-017-0032-z>.
- [134] M. Rafiee, R.D. Farahani, D. Therriault, Multi-material 3D and 4D printing: a survey, *Adv. Sci.* 7 (2020) 1902307, <https://doi.org/10.1002/advs.201902307>.
- [135] A. Costa, A. Abdel-Rahman, B. Jenett, N. Gershenfeld, I. Kostitsyna, K. Cheung. Algorithmic approaches to reconfigurable assembly systems, *IEEE Aerospace Conference* (2019), 2-9 March, Big Sky, MT, USA, <https://doi.org/10.1109/AERO.2019.8741572> .
- [136] H. Medellín, T. Lim, J. Corney, J.M. Ritchie, J.B.C. Davies, Rapid prototyping through octree decomposition of 3D geometric models, *ASME Design Engineering Technical Conference* (2004) 843-852, <https://doi.org/10.1115/DETC2004-57769>.
- [137] M. Delmans, J. Haseloff, μ Cube: A framework for 3D printable optomechanics, *Journal of Open Hardware* 2 (2018), <http://doi.org/10.5334/joh.8>.
- [138] D. Wang, M. Hermes, R. Kotni, Y. Wu, N. Tasios, Y. Liu, B. de Nijs, E.B. van der Wee, C.B. Murray, M. Dijkstra, A. van Blaaderen, Interplay between spherical confinement and particle shape on the self-assembly of rounded cubes, *Nature Communications* 9 (2018) 2228, <https://doi.org/10.1038/s41467-018-04644-4>
- [139] K. Benyahia, S Gomes, J. C. André, H. J. Qi, F. Demoly. "Influence of interlocking blocks assembly on the actuation time, shape change, and reversibility of voxel-based multi-material 4D structures." *Smart Materials and Structures* 32.6 (2023): 065011.

- [140] G. Villar, A. D. Graham, and H. Bayley, "A tissue-like printed material," *Science* (80-.), vol. 340, no. 6128, pp. 48–53, 2017.
- [141] A. B. Baker, D. F. Wass, and R. S. Trask, "4D sequential actuation: combining ionoprinting and redox chemistry in hydrogels," *Smart Mater. Struct.*, vol. 25, no. 10, pp. 1–9, 2016.
- [142] J. Wu et al., "Multi-shape active composites by 3D printing of digital shape memory polymers," *Sci. Rep.*, vol. 6, no. April, pp. 1–11, 2016.
- [143] Q., K. Zhang, and G. Hu, "Smart three-dimensional lightweight structure triggered from a thin composite sheet via 3D printing technique," *Nat. Publ. Gr.*, no. February, pp. 1–8, 2016.
- [144] W He, D Zhou, H Gu, R Qu, C Cui. "A biocompatible 4D printing shape memory polymer as emerging strategy for fabrication of deployable medical devices." *Macromolecular Rapid Communications* 44.2 (2023): 2200553.
- [145] K. McLellan, S. Yu-Chen, and H. E. Naguib. "A review of 4D printing: Materials, structures, and designs towards the printing of biomedical wearable devices." *Bioprinting* 27 (2022): e00217.
- [146] W. Zhao, C. Yue, L. Liu, Y. Liu, "Research progress of shape memory polymer and 4D printing in biomedical application." *Advanced Healthcare Materials* 12.16 (2023): 2201975.
- [147] Y. Wang, H. Cui, T. Esworthy, D. Mei, Y. Wang. "Emerging 4D printing strategies for next-generation tissue regeneration and medical devices." *Advanced Materials* 34.20 (2022): 2109198.
- [148] C. Li, G. C. Lau, H. Yuan, A. Aggarwal, V. L. Dominguez., Fast and programmable locomotion of hydrogel-metal hybrids under light and magnetic fields. *Sci. Robot.* 5eabb9822(2020). DOI:[10.1126/scirobotics.abb9822](https://doi.org/10.1126/scirobotics.abb9822)
- [149] Bhattacharyya, A., Kim, J. Y., Alacoque, L. R., & James, K. A. Bio-Inspired 4D-Printed Mechanisms with Programmable Morphology. arXiv preprint arXiv:2306.00233. (2023).
- [150] Li, S. Review on development and application of 4D-printing technology in smart textiles. *Journal of Engineered Fibers and Fabrics*, 18, 15589250231177448. (2023).
- [151] L. Aaron, N. Michelson, B. Minevich, Y. Flegler, M. Stern, A. Shaulov, Y. Yeshurun, O. Gang, DNA-assembled superconducting 3D nanoscale architectures, *Nature Communications* 11 (2020) 5697, <https://doi.org/10.1038/s41467-020-19439-9>.
- [152] L. Yuan, S. Zhuo, Y. Xiao, G. Zheng, G. Dong, F.Z. Yaoyao, Rapid modeling and design optimization of multi-topology lattice structure based on unit-cell library, *Journal of Mechanical Design*, 142 (2020) 091705, <https://doi.org/10.1115/1.4046812>
- [153] B. Jenett, N. Gershenfeld, M. Carney, S. Calisch, W. Spencer, Digital morphing wing: active wing shaping concept using composite lattice-based cellular structures, *Soft Robotics* 4 (2017) 33-48, <https://doi.org/10.1089/soro.2016.0032>.
- [154] J. Zhu, H. Zhou, C. Wang, L. Zhou, S. Yuan, W. Zhang, A review of topology optimization for additive manufacturing: status and challenges, *Chinese Journal of Aeronautics* 34 (2021) 91–110, <https://doi.org/10.1016/j.cja.2020.09.020>.

- [155] A. Ion, L. Wall, R. Kovacs, P. Baudisch, Digital mechanical metamaterials, Conference on Human Factors in Computing Systems (2017) 977–88, <https://doi.org/10.1145/3025453.3025624>.
- [156] V. Hahn, P. Kiefer, T. Frenzel, J. Qu, E. Blasco, C. Barner-Kowollik, M. Wegener, Rapid assembly of small materials building blocks (voxels) into large functional 3D metamaterials, *Advanced Functional Materials* 30 (2020) 1907795, <https://doi.org/10.1002/adfm.201907795>.
- [157] Osouli-Bostanabad, K., Masalehdan, T., Kapsa, R. M., Quigley, A., Lalatsa, A., Bruggeman, K. F., & Nisbet, D. R. Traction of 3D and 4D printing in the healthcare industry: From drug delivery and analysis to regenerative medicine. *ACS Biomaterials Science & Engineering*, 8(7), 2764-2797. (2022).
- [158] M. Orlov, “pH-Responsive Thin Film Membranes from Poly (2-vinylpyridine): Water Vapor-Induced Formation of a Microporous Structure,” pp. 2086–2091, 2007.
- [159] M. Nadgorny, Z. Xiao, C. Chen, and L. A. Connal, “Three-dimensional printing of pH-responsive and functional polymers on an affordable desktop printer,” *Appl. Mater. Interfaces*, pp. 28946–28954, 2016.
- [160] Egan, P. F.. Design for Additive Manufacturing: Recent Innovations and Future Directions. *Designs*, 7(4), 83. (2023)
- [161] Guertler, M. R., Clemon, L. M., Bennett, N. S., & Deuse, J. "Design for Additive Manufacturing (DfAM): Analysing and Mapping Research Trends and Industry Needs." 2022 Portland International Conference on Management of Engineering and Technology (PICMET). IEEE, 2022.
- [162] Borgianni, Y., Pradel, P., Berni, A., Obi, M., & Bibb, R. "An investigation into the current state of education in Design for Additive Manufacturing." *Journal of Engineering Design* 33.7 (2022): 461-490.
- [163] Vinodh, S. "Prioritization and deployment of design for additive manufacturing strategies to an automotive component." *Rapid Prototyping Journal* ahead-of-print (2023).
- [164] S. K. Mangla, Y. Kazancoglu, M. D Sezer, N. Top, & I. Sahin, "Optimizing fused deposition modelling parameters based on the design for additive manufacturing to enhance product sustainability." *Computers in Industry* 145 (2023): 103833.
- [165] Chinchankar, Satish, and Avez A. Shaikh. "A review on machine learning, big data analytics, and design for additive manufacturing for aerospace applications." *Journal of Materials Engineering and Performance* 31.8 (2022): 6112-6130.
- [166] F. Veiga, T. Bhujangrao, A. Suárez, E. Aldalur, I. Goenaga. "Validation of the Mechanical Behavior of an Aeronautical Fixing Turret Produced by a Design for Additive Manufacturing (DfAM)." *Polymers* 14.11 (2022): 2177.
- [167] S. H. Mian, K. Moiduddin, S. M. Elseufy, H. Alkhalefah . "Adaptive mechanism for designing a personalized cranial implant and its 3D printing using PEEK." *Polymers* 14.6 (2022): 1266.

- [168] Lee, Young-A. "Trends of emerging technologies in the fashion product design and development process." *Leading edge technologies in fashion innovation: Product design and development process from materials to the end products to consumers* (2022): 1-16.
- [169] Yuan, Chao, Tongqing Lu, and T. J. Wang. "Mechanics-based design strategies for 4D printing: A review." *Forces in Mechanics* 7 (2022): 100081.
- [170] X. Sun, L. Yue, L. Yu, H. Shao, X. Peng, K. Zhou, F. Demoly, R. Zhao, H. J. Qi. "Machine Learning-Evolutionary Algorithm Enabled Design for 4D-Printed Active Composite Structures." *Advanced Functional Materials* 32.10 (2022): 2109805.
- [171] S. Dimassi, F Demoly, H Belkebir, C Cruz, KY Kim, S. Gomes, H. J. Qi, J. C. André, "A knowledge recommendation approach in design for multi-material 4D printing based on semantic similarity vector space model and case-based reasoning." *Computers in Industry* 145 (2023): 103824.
- [172] S. Shinde, R. Mane, A.Vardikar, A. Dhumal, & A. Rajput. "4D printing: From emergence to innovation over 3D printing." *European Polymer Journal* (2023): 112356.
- [173] Y. Tao, S. Wang, J. Ji, L. Cai, H. Xia, Z. Wang, "4Doodle: 4D Printing Artifacts Without 3D Printers." *Proceedings of the 2023 CHI Conference on Human Factors in Computing Systems*. 2023.
- [174] Pingale, P., Dawre, S., Dhapte-Pawar, V., Dhas, N., & Rajput, A., "Advances in 4D printing: From stimulation to simulation." *Drug Delivery and Translational Research* 13.1 (2023): 164-188.
- [175] C. Guo, M. Zhang, B. Bhandari, S. Devahastin. "Investigation on simultaneous change of deformation, color and aroma of 4D printed starch-based pastes from fruit and vegetable as induced by microwave." *Food Research International* 157 (2022): 111214.
- [176] Park, J.-K., *Advanced Development of a Smart Material Design, Modeling, and Selection Tool with an Emphasis on Liquid Crystal Elastomers*, 2012, The Ohio State University.
- [177] Welp, E.G. and J. Breidert, *Knowledge and Method Base for Shape Memory Alloys*. *Materialwissenschaft und Werkstofftechnik*, 2004. 35(5): p. 294-299.
- [178] A. Zolfagharian, M. Denk, M. Bodaghi, A. Z. Kouzani, and A. Kaynak, "Topology-optimised 4D printing of a soft actuator," *Acta Mech. Solida Sin*, vol. 33, pp. 418–430, 2020.
- [179] A. Zolfagharian, A. Kouzani, A. A. A. Moghadam, S. Y. Khoo, S. Nahavandi, and A. Kaynak, "Rigid elements dynamics modeling of a 3D printed soft actuator," *Smart Mater. Struct.*, vol. 28, no. 2, 2019.
- [180] A. Zolfagharian, A. Kaynak, S. Y. Khoo, J. Zhang, S. Nahavandi, and A. Kouzani, "Control-oriented modelling of a 3D-printed soft actuator," *Materials (Basel)*, vol. 12, no. 1, 2018.
- [181] Athinarayanarao, D., Prod'hon, R., Chamoret, D., Qi, H. J., Bodaghi, M., André, J. C., & Demoly, F. (2023). Computational design for 4D printing of topology optimized multi-material active composites. *npj Computational Materials*, 9(1), 1.

- [182] Dalgleish, G. F., Jared, G. E. M., & Swift, K. G. (2000). Design for assembly: influencing the design process. *Journal of Engineering Design*, 11(1), 17-29.
- [183] Boothroyd, G., & Alting, L. (1992). Design for assembly and disassembly. *CIRP annals*, 41(2), 625-636.
- [184] F. Demoly. *Conception intégrée et gestion d'informations techniques: application à l'ingénierie du produit et de sa séquence d'assemblage*. Sciences de l'ingénieur [physics]. Université de Technologie de Belfort-Montbéliard, 2010.
- [185] Moultrie, J., & Maier, A. M. (2014). A simplified approach to design for assembly. *Journal of Engineering Design*, 25(1-3), 44-63.
- [186] Gualtieri, L., Monizza, G. P., Rauch, E., Vidoni, R., & Matt, D. T. (2020). From design for assembly to design for collaborative assembly-product design principles for enhancing safety, ergonomics and efficiency in human-robot collaboration. *Procedia CIRP*, 91, 546-552.
- [187] Spencer, A. J. (2023). *Brick architecture in ancient Egypt (Vol. 16)*. Oxbow Books.
- [188] Hsieh, C. T., & Rossi-Hansberg, E. (2023). The industrial revolution in services. *Journal of Political Economy Macroeconomics*, 1(1), 3-42.
- [189] Q. Zhang, X. Liu, L. Duan, G. Gao, Ultra-stretchable wearable strain sensors based on skin-inspired adhesive, tough and conductive hydrogels, *Chemical Engineering Journal* 365 (2019) 10–19, <https://doi.org/10.1016/j.cej.2019.02.014>.
- [190] M. Zhu, F. Zhang, X. Chen, Bioinspired mechanically interlocking structures, *Small Structures* 1 (2020), 2000045, <https://doi.org/10.1002/sstr.202000045>.
- [191] Djumas, L., Molotnikov, A., Simon, G. P., & Estrin, Y. (2016). Enhanced mechanical performance of bio-inspired hybrid structures utilising topological interlocking geometry. *Scientific reports*, 6(1), 26706.
- [192] C. Shaokang, Z. Lu, Z. Yang, Effect of interlocking structure on mechanical properties of bio-inspired nacreous composites, *Composite Structures* 226 (2019) 111260, <https://doi.org/10.1016/j.compstruct.2019.111260>.
- [193] Z. Yuming, Y. Haimin, C. Ortiz, J. Xu, M. Dao, Bio-inspired interfacial strengthening strategy through geometrically interlocking designs, *Journal of the Mechanical Behavior of Biomedical Materials* 15 (2012) 70–77, <https://doi.org/10.1016/j.jmbbm.2012.07.006>.
- [194] Alsheghri, A. A., Alageel, O., Mezour, M. A., Sun, B., Yue, S., Tamimi, F., & Song, J. (2018). Bio-inspired and optimized interlocking features for strengthening metal/polymer interfaces in additively manufactured prostheses. *Acta biomaterialia*, 80, 425-434.
- [195] S.A. Morin, Y. Shevchenko, J. Lessing, S.W. Kwok, R.F. Shepherd, A.A. Stokes, G.M. Whitesides, Using 'Click-e-Bricks' to make 3D elastomeric structures, *Advanced Materials* 26 (2014) 5991–5999, <https://doi.org/10.1002/adma.201401642>.

- [196] L.J. Young, J. Eom, W.Y. Choi, K.J. Cho, Soft LEGO: Bottom-up design platform for soft robotics, IEEE International Conference on Intelligent Robots and Systems (2018): 7513–7520, <https://doi.org/10.1109/IROS.2018.8593546>.
- [197] L.J. Young, W.B. Kim, J. Eom, W.Y. Choi, and K.J. Cho, Soft robotic blocks: Introducing SoBL, a fast-build modularized design block, IEEE Robotics and Automation Magazine 23 (2016) 30-41, <https://doi.org/10.1109/MRA.2016.2580479>.
- [198] X. Yang, S. Druga, Legoons: Inflatable construction kit for children, Annual Symposium on Computer-Human Interaction in Play (2019), 139-146, <https://doi.org/10.1145/3341215.3356980>.
- [199] AROK, O., & MYTHS, K. D. DESIGN ACTION FIGURE 1/6 WITH SNAP-FIT JOINT SYSTEM BASED. 2016.
- [200] L. Luo, I. Baran, S. Rusinkiewicz, W. Matusik, Chopper: partitioning models into 3D-printable parts, ACM Trans. Graph.
- [201] X. Jiang, X. Cheng, Q. Peng, L. Liang, N. Dai, M. Wei, C. Cheng, Models partition for 3D printing objects using skeleton, Rapid Prototyp. J. 23 (2017) 54-64, <https://doi.org/10.1108/RPJ-07-2015-0091>.
- [202] M. Yao, Z. Chen, L. Luo, R. Wang, H. Wang, Level-set-based partitioning and packing optimization of a printable model, ACM Trans. Graph. 34 (2015) 1-11, <https://doi.org/10.1145/2816795.2818064>.
- [203] P. Song, B. Deng, Z. Wang, Z. Dong, W. Li, C.W. Fu, L. Liu, CofiFab: coarse-to-fine fabrication of large 3D objects, ACM Trans. Graph. 35 (2016), 1-11, <https://doi.org/10.1145/2897824.2925876>.
- [204] A.K. Jadoon, C. Wu, Y.J. Liu, Y. He, C.C.L. Wang, Interactive partitioning of 3D models into printable parts, IEEE Computer Graphics and Applications 38 (2018) 38-53, <https://doi.org/10.1109/MCG.2018.042731658>.
- [205] A. Deka, S. Behdad, Part separation technique for assembly-based design in additive manufacturing using genetic algorithm, Procedia Manuf. 34 (2019) 764-771, 10.1016/j.promfg.2019.06.208.
- [206] Y. Oh, Part decomposition and evaluation based on standard design guidelines for additive manufacturability and assemblability, Addit. Manuf. 37 (2021) 101702, <https://doi.org/10.1016/j.addma.2020.101702>.
- [207] S.J. Luo, Y. Yue, C.K. Huang, Y.H. Chung, S. Imai, T. Nishita, B.Y. Chen, Legolization: optimizing LEGO designs, ACM Transactions on Graphics 34 (2015), 1-12, <https://doi.org/10.1145/2816795.2818091>.
- [208] Z. Wang, P. Song, M. Pauly, State of the art on computational design of assemblies with rigid Parts, Computer Graphics Forum 40 (2021) 633-657, <https://doi.org/10.1111/cgf.142660>.

- [209] S.G. Shih, The art and mathematics of self-interlocking SL blocks, Bridges Conference Proceedings, Tesselations Publishing (2018) 107-114.
- [210] D. Qi, N. Milef, S. De, Divided voxels: An efficient algorithm for interactive cutting of deformable objects, Visual Computer 37 (2021), 1113-1127, <https://doi.org/10.1007/s00371-020-01856-y>.
- [211] P. Song, C.W. Fu, D. Cohen-Or, Recursive interlocking puzzles, ACM Transactions on Graphics 31 (2012), 1–10, <https://doi.org/10.1145/2366145.2366147>.
- [212] Z.Wang, P. Song, M. Pauly, Desia: A general framework for designing interlocking assemblies, ACM Transactions on Graphics 37 (2018) 1–14, <https://doi.org/10.1145/3272127.3275034>.
- [213] D. Roach. Developing intelligent structures and devices using smart materials and multi-material multi-method (M 4) 3D printing, PhD Dissertation, Georgia Institute of technology, 2021.
- [214] Q. Ge, H.J. Qi, M.L. Dunn, Active materials by four dimensions printing, Appl. Phys. Lett. 103 (2013) 131901, <https://doi.org/10.1063/1.4819837>.
- [215] P. Rastogi, K. Balasubramanian, Breakthrough in the printing tactics for stimuli-responsive materials: 4D printing, Chemical Engineering Journal 366 (2019), 264-304, <https://doi.org/10.1016/j.cej.2019.02.085>.
- [216] P. Song, Z. Fu, L. Liu, C.W. Fu, Printing 3D objects with interlocking parts, Computer Aided Geometric Design 35-36 (2015) 137-148, <https://doi.org/10.1016/j.cagd.2015.03.020>.
- [217] J. Lai, X. Ye, J. Liu, C. Wang, J. Li, X. Wang, M. Ma, M. Wang, 4D printing of highly printable and shape morphing hydrogels composed of alginate and methylcellulose, Materials & Design 205 (2021) 109699, <https://doi.org/10.1016/j.matdes.2021.109699>.
- [218] Lee, A. Y., An, J., Chua, C. K., & Zhang, Y. (2019). Preliminary investigation of the reversible 4D printing of a dual-layer component. Engineering, 5(6), 1159-1170.
- [219] Le Duigou, A., Castro, M., Bevan, R., & Martin, N. (2016). 3D printing of wood fibre biocomposites: From mechanical to actuation functionality. Materials & Design, 96, 106-114.
- [220] Fullcure material. Vero family [Internet]. Utah: GoEngineer; c2019 [cited 2019 Jan 31]. Available from: <https://www.goengineer.com/products/vero-family/>.
- [221] Stratasys."Agilus30 Material Datasheet.": <https://support.stratasys.com/en/materials/material-datasheets/agilus30/>.
- [222] Digital materials Data Sheet: https://www.stratasys.com/siteassets/materials/materials-catalog/mds_pj_digitalmaterialsdatasheet_0122a-1.pdf?v=49c186
- [223] Shih, S. G. Grammars of Interlocking SL Blocks. 2018.
- [224] Shih, S. (2016). Advances in Architectural Geometry 2016, Chapter On the Hierarchical Construction of SL Blocks – A Generative System that Builds Self-Interlocking structures. Hochschulverlag AG an der ETH Zürich.

- [225] Fu, C., X. Yan, L. Yang, P. Jayaraman, and D. Cohen-Or (2015). Computational interlocking furniture assembly. *Journal of ACM Transactions on Graphics (TOG)*, Proceeding of ACM SIGGRAPH 2015.
- [226] Kanel-Belov, A., A. Dyskin, Y. Estrin, E. Pasternak, and I. Ivanov-Pogodaev (2010). Interlocking of convex polyhedra: towards a geometric theory of fragmented solids. *Moscow Mathematical Journal* 10(2), 337–342.
- [227] Lo, K.-Y., C.-W. Fu, and H. Li (2009). 3d polyomino puzzle. *ACM Trans. Graph.* 28(5).
- [228] Weizmann, M., O. Amir, and Y. J. Grobman (2017). Topological interlocking in architecture: A new design method and computational tool for designing building floors. *International Journal of Architectural Computing* 15(2), 107–118.
- [229] Yong, H. (2011). Utilisation of topologically-interlocking osteomorphic blocks for multi-purpose civil construction. Ph. D. thesis, University of Western Australia.
- [230] Haq, M. A., Su, Y., & Wang, D. Mechanical properties of PNIPAM based hydrogels: A review. *Materials Science and Engineering: C*, 70, 842-855. 2017.
- [231] Zheng, W. J., An, N., Yang, J. H., Zhou, J., & Chen, Y. M., Tough Al-alginate/poly (N-isopropylacrylamide) hydrogel with tunable LCST for soft robotics. *ACS applied materials & interfaces*, 7(3), 1758-1764, 2015.
- [232] Roach, D. J., Yuan, C., Kuang, X., Li, V. C. F., Blake, P., Romero, M. L., ... & Qi, H. J., Long liquid crystal elastomer fibers with large reversible actuation strains for smart textiles and artificial muscles. *ACS applied materials & interfaces*, 11(21), 19514-19521, 2019
- [233] Chen, M., Hou, Y., An, R., Qi, H. J., & Zhou, K.. 4d printing of Reprogrammable Liquid Crystal Elastomers with Synergistic Photochromism And Photo-Actuation. *Advanced Materials*, 2303969, 2023.
- [234] Leanza, S., Wu, S., Sun, X., Qi, H. J., & Zhao, R. R., Active Materials for Functional Origami. *Advanced Materials*, 2302066, 2023.
- [235] Chen, M., Gao, M., Bai, L., Zheng, H., Qi, H. J., & Zhou, K., Recent Advances in 4D Printing of Liquid Crystal Elastomers. *Advanced Materials*, 2209566, 2023
- [236] Retsch general catalogue: <https://www.retsch.fr/files/14586/general-catalogue.pdf>